FROM THE ARCHIVES

Rapid Inexpensive Tests for Determining Fracture Toughness (1976)

Pages
247

Size
8.5 x 11

ISBN
0309025370

Committee on Rapid Inexpensive Tests for Determining Fracture Toughness; National Materials Advisory Board; Commission on Sociotechnical Systems; National Research Council

🔍 **Find Similar Titles**   📄 **More Information**

Visit the National Academies Press online and register for...

✔ Instant access to free PDF downloads of titles from the

- NATIONAL ACADEMY OF SCIENCES
- NATIONAL ACADEMY OF ENGINEERING
- INSTITUTE OF MEDICINE
- NATIONAL RESEARCH COUNCIL

✔ 10% off print titles

✔ Custom notification of new releases in your field of interest

✔ Special offers and discounts

NATIONAL ACADEMY OF SCIENCES

1863-2013
Celebrating 150 Years of Service to the Nation

Rapid Inexpensive Tests for Determining Fracture Toughness

Report of
The Committee on Rapid Inexpensive Tests
for Determining Fracture Toughness

·NATIONAL MATERIALS ADVISORY BOARD
·Commission on Sociotechnical Systems
National Research Council

NATIONAL ACADEMY OF SCIENCES
Washington, D.C.   1976

PREFACE

The National Materials Advisory Board (NMAB) Committee on Rapid, Inexpensive Tests for Determining Fracture Toughness was established in response to the recommendation of the NMAB Committee on the Application of Fracture Prevention Principles to Aircraft that ". . . standardized, low-cost methods of fracture toughness characterization of aerospace materials in the thickness range of their application" (Report NMAB-302, February 1973) be developed. Because interest in this problem was broad, the Committee was charged to consider other than aerospace materials as well.

One major drawback to complete acceptance and use of the American Society for Testing and Materials (ASTM) E399-20 test for plane strain fracture toughness is the cost of performing the test. The machining quality and large size of the specimen required and the intricate (by production quality-control standards) test procedures tend to keep the ASTM E399-20 fracture test a laboratory operation. The quality-control tests discussed in this report are aimed specifically at material acceptance usage and should not be considered replacements for any of the fracture design data specimen requirements.

During its study, the Committee concluded it could not select a single fracture toughness test method that would be useful for all materials or even for a single material over the full range of possible strength levels. The ideal basis of comparison would be the predictability of satisfactory service performance, but information available is far from sufficient to provide useful comparisons of this nature. Consequently, the ASTM Standard Method of Test for Plane Strain Fracture Toughness of Metallic Materials (currently designated ASTM E399-74) was selected as the most practicable basis of comparison. It is recognized that the fracture behavior of a material cannot be characterized fully by any single quantity, such as K_{Ic}. The complexity of the fracture phenomenon requires several independent quantities to characterize a material completely in this respect. However, a complete characterization is unattainable by any test method that must be rapid and inexpensive. The Committee therefore decided to assess the most promising test methods to determine their possible correlation with plane-strain fracture toughness (K_{Ic}) measurements and to recommend that further experimental investigations be made to establish the precise quantitative correlation that might be used for quality control of material in a given application.

v

CONTENTS

ix

TABLES

xiv

Chapter 1

CONCLUSIONS AND RECOMMENDATIONS

1.1 GENERAL CONCLUSIONS

No single, rapid, inexpensive test method is expected to yield a universally applicable correlation with valid plane-strain fracture toughness (K_{Ic}) measurements (American Society for Testing and Materials Standard Method of Test E 399) for all materials, material strengths, temperatures, and strain rates considered. Although correlations sufficiently precise for quality-control purposes appear possible, such correlations must be established experimentally for each material specification and contemplated condition of use. In any given application, this restriction should not place a severe limitation on the use of rapid, inexpensive test methods to assure a satisfactory level of fracture toughness for a given lot of material.

The specific test methods offering promise in establishing such correlations are discussed in section 1.2. All other suggested test methods considered by the Committee were deemed unsatisfactory on the basis of data available.

The various correlations noted below are general in nature and show considerable promise for establishing less expensive and more rapid test methods for measuring fracture toughness. To apply these test methods, however, will require systematic programs of investigation to establish detailed correlation curves and quality-control procedures. Despite the initial cost of such programs, substantial savings should result within a relatively short time.

1.2 SPECIFIC CONCLUSIONS AND RECOMMENDATIONS

1.2.1   Conclusion -- Slow-bend test results of fatigue-precracked Charpy-size specimens correlate well with plane-strain fracture toughness values for a number of materials. Correlations are possible between K_{Ic} and the ratio of the total energy for fracture to the net uncracked area of the specimen (W/A). However, a much simpler and less expensive method is to correlate K_{Ic} with the ratio of the specimen strength to yield strength or ultimate tensile strength of the material,

1

$(R_{sb} - CV)/\sigma_{ys}$. Because of the specimen's small size, such correlations are restricted to materials for which the ratio of plane-strain fracture toughness to yield strength is less than $0.75\sqrt{}$ in. $(K_{Ic}/\sigma_{ys} < 0.75\sqrt{}$ in.). Correlation based on W/A values have a somewhat higher limit at present of $K_{Ic}/\sigma_{ys} = 1.0\sqrt{}$ in. or above; the limit is not clearly defined by the available data. The advantages offered by this specimen type are its low preparation cost and small size; in addition, it permits toughness to be measured in several directions and facilitates the measurement of toughness as a function of temperature (see section 3.1.3 and appendix D).

Recommendation -- It is recommended that the fatigue-precracked Charpy-size specimen, tested in slow bending to measure the ratio of specimen strength to either the yield strength or the ultimate tensile strength of the material (ASTM E399-74) be utilized, when applicable, for establishing correlation with plane-strain fracture toughness and minimum acceptance standards in quality-control programs (see section 3.1.3 and appendix D). To foster implementation of this recommendation, the Committee urges that the test method be standardized as soon as practicable (standardization of this test method is currently under investigation by Task Group E-24.03.03 under Subcommittee E-24.03.03 of ASTM Committee E-24). It is recommended that investigations be initiated to determine whether the correlation between specimen-strength ratio for a precracked Charpy-size specimen and plane-strain fracture toughness may be valid to higher levels of the ratio (K_{Ic}/σ_{ys}) than the limit of $0.75\sqrt{}$ in. set for the Charpy-size specimen if larger specimen sizes are used.

1.2.2   Conclusion -- Based on a limited number of tests, the energy to fracture a material in the dynamic tear (DT) test developed by the U.S. Naval Research Laboratory correlates reasonably well with valid K_{Ic} measurements for aluminum and titanium alloys and some higher-strength steels. This test method (Military Standard No. 1601) generally requires a somewhat larger amount of material and more specialized test apparatus than does the precracked Charpy test method; however, there are indications that this method is capable of providing correlation with K_{Ic} for materials having a K_{Ic}/σ_{ys} ratio somewhat higher than the Charpy specimen limit ($0.75\sqrt{}$in.).

Recommendation -- It is recommended that the investigation of the correlation between valid K_{Ic} measurements and DT energy be extended to establish a larger data base for predicting K_{Ic} or minimum acceptance standards for quality control (see section 3.1.4 and appendix E-1). A proposed standard for the DT test has been prepared and published (ASTM Standards, Part 10, pp. 826-33). It is

recommended that support be provided for a more extensive investigation of the correlation between DT test results and plane-strain fracture toughness to generate sufficient data for the establishment of quality-control procedures using this test method.

1.2.3 <u>Conclusion</u> -- It is sometimes possible to use the <u>standard</u> (not pre-cracked) Charpy-V test to indicate large differences in, or to make rough estimates of, plane-strain fracture toughness for a limited number of low- and medium-strength steel grades (see section 3.1.3 and appendix D).

1.2.4 <u>Conclusion</u> -- When it is possible to machine a sufficiently small radius notch without eccentricity with respect to the loading axis, the notched-round bar test can establish lower-bound levels of K_{Ic} for quality-control purposes. Because of machining problems, use of this test method appears practicable only for aluminum and magnesium alloys (see section 3.1.2 and appendix C).

<u>Recommendation</u> -- It is recommended that the notched-round-bar test be considered for correlating the fracture toughness, particularly minimum levels for quality-control programs, of those materials to which it is applicable, e.g., aluminum and magnesium (see appendixes B and C).

1.2.5 <u>Conclusion</u> -- Some materials, notably low- and medium-strength steels, exhibit a drastic decrease in fracture toughness in a narrow temperature range. For such materials, it is more appropriate to determine the nil-ductility transition temperature using the drop-weight test (ASTM Standard Method of Test E208) than the plane-strain fracture toughness. The fatigue-precracked Charpy-size specimen test can be used as an alternate to ASTM E208 for determining the nil-ductility transition temperature of structural grades of steel but, although the two tests usually give nearly identical measures of the nil-ductility temperature, occasional exceptions exist and must be recognized (appendix D).

1.2.6 <u>Conclusion</u> -- In dealing with high-toughness materials, the crack-opening-displacement (COD) and J-integral methods may correlate with plane-strain fracture toughness but the tests require simplification to be useful.

<u>Recommendation</u> -- It is recommended that a variety of materials be tested using the COD and J-integral test methods to assess their potential for correlating tests.

Chapter 2

INTRODUCTION

While the inclusion in the structural design process of damage-tolerance design methods based on fracture mechanics methodology offers improvements in reliability and safety, the special damage-tolerance-design data requirements, including crack growth rate and fracture toughness information, are considered expensive to develop. The major recommendation of a previous NMAB study committee (National Materials Advisory Board, 1973) was that an indicator test of fracture toughness be developed that would reduce the cost of applying fracture mechanics methodology to design. The study described in this report was mounted by the NMAB in response to the Department of Defense request that this recommendation be pursued through a review and evaluation of test specimens and methods that could apply to materials quality control.

2.1 OBJECTIVES

The NMAB Committee on Rapid Inexpensive Tests for Determining Fracture Toughness appointed to conduct the study was charged to "identify rapid, inexpensive tests which will correlate to plane-strain fracture toughness (K_{Ic}) and be amenable for use by quality-control personnel." A secondary goal was to identify similar correlations to the nil-ductility transition temperature in the drop-weight test (ASTM E208).

2.2 APPROACH

The Committee reviewed the existing data on all specimens that could be used in a fracture test. Accordingly, test methods that were neither rapid nor inexpensive were considered to cover special applications. Correlations to K_{Ic} values obtained using ASTM E399 and to nil-ductility transition temperature using ASTM E208-69 were reviewed.

ASTM E399-74 was selected as the basis for comparison because it is the only quantitative test for fracture toughness available and a considerable amount of data is available. In addition, the validity of the method is continuously assessed by ASTM Committee E-24. (Appendix A discusses this test method as well as other analytical techniques currently under investigation.)

ASTM E208-69 prescribes use of a drop-weight test machine and appropriate procedures to define the highest critical temperature at which fracture occurs in a limited deflection bend specimen as a result of the dropped weight. Above this critical temperature, termed the nil-ductility transition temperature, the specimen bends but does not fracture across the tensile loaded surface of the specimen. This test method can be used only on ferritic steels at least 5/8 in. thick. (Discussion of this specimen and test method is included as section 3.1.5).

The evaluation of the various candidate specimens and test methods for correlation with K_{Ic} values was hampered in many cases by the lack of usable correlation data (i.e., supporting data usually were available for various alloys and heat treatments while, for quality-control purposes, the comparison data must be for a specific alloy and condition), and these additional data are necessary before any of the specimens and correlations are committed to quality-control purposes. As an aid in comparing the relative expense of specimens, machining and testing costs obtained from available sources were analyzed (see section 3.2).

2.3   PRESENT USES OF FRACTURE METHODOLOGY

A fracture mechanics design methodology evolved when adequate strength in the presence of defects was recognized as the key to structural reliability. This design procedure has evolved rapidly since the late 1950s when the ASTM Special Committee on Fracture Testing of High Strength Materials was formed to assist in solving the Polaris missile failures. This committee subsequently became ASTM Committee E-24, Fracture Testing of Metallic Materials, and has served as a focal point for fracture mechanics technology development. Four areas of fracture mechanics applications are presented below.

2.3.1   Aircraft Structures

At the present time, fracture mechanics principles are being used in designing the airframes and propulsion systems for almost all military and commercial aircraft. Army aircraft design methods are similar to those used for commercial aircraft to prevent premature structural fatigue failure. Both the Navy and the Air Force require airframe contractors to conform to Aircraft Structural Integrity Programs (ASIP) that specify critical airframe components

to be designed using fracture mechanics considerations to ensure adequate structural life. Confidence in the ASIP approach is enhanced by rigid control of materials properties, and the material property presently used for quality control from a fracture mechanics standpoint is the plane-strain fracture toughness of the material.

2.3.2 Ship Hull Structures

The Liberty ship failures during and following World War II led to considerable study of the fracture resistance of lower-strength steels. The Charpy V-notch impact test was selected by the American Bureau of Shipping (ABS) to qualify hull materials, and a 15 foot-pound energy requirement was established as the minimum needed to "arrest" a propagating crack based on tests conducted by the ABS and the Naval Research Laboratory (NRL).

The Navy presently is incorporating the dynamic tear test in its materials specifications as the fracture quality measurement. The temperature specified for tests of hull material is either 0° F or 30° F (-18° C or -1° C), depending on the materials and proposed usage. The main concern is whether the material has sufficient ductility at the lowest expected operating temperature to ensure yielding in the presence of a flaw or crack.

2.3.3 Ordnance Structures

Military requirements for lightweight, air-transportable, highly mobile weapons require the use of very-high-strength material and more sophisticated design methods (Adachi, 1969). A requisite for using such materials properly is the need for more meaningful and usable measures of toughness in materials since very high and obviously safe toughness values cannot always be provided. However, the current trend is to incorporate linear elastic fracture mechanics techniques in design approaches wherever possible (e.g., to aid in preventing fracture in armor, controlling fracture in projectiles, and predicting the life of cannon tubes and mounts).

Unfortunately, the high procurement costs of fracture toughness measurements (as defined by ASTM E399) usually preclude their inclusion in material specifications. However, the desired fracture toughness in a given material may be attained indirectly by requiring mechanical property data such as yield strength, tensile strength, percent elongation, and Charpy V-notch.

2.3.4 Nuclear Power Plants

Pressure vessels and associated pressure-retaining components of light, water-cooled nuclear reactors are designed, fabricated, and operated in accordance with sections III and XI of the American Society of Mechanical

Engineers (ASME) Boiler and Pressure Vessel Code. Procedures based on fracture mechanics are included in the current editions of these sections of the Code for defining material fracture toughness requirements and for evaluating structural integrity.

The materials used (steels) are generally in the high-toughness and low- to medium-yield-strength category, which requires that large specimens be used to fully characterize fracture toughness. However, fracture toughness must be monitored for degradation over the life of the facility, due to the radiation environment, and because of the space limitations in the high-neutron-flux sections of reactors, only small specimens are feasible for monitoring changes. At present, standard V-notch Charpy specimens are used most commonly for this purpose.

2.4   CLASSIFICATION OF SPECIMEN TYPES AND TEST METHODS

The various test methods and specimen types used in measuring and estimating fracture toughness that were reviewed by the Committee for useful- ness and potential have been grouped into five general categories:

- Methods that are elastic-plastic extensions of the K_{Ic} toughness measurement procedures -- These include the J-integral, crack- opening-displacement, and crack-extension resistance (R-curve) concepts; the specimen strength ratio (R_s) parameter also falls within this category when it is used in an empirical correlation to K_{Ic} values (see appendix A).

- Tensile loaded specimens -- Included in this category are the notched-round tensile and the double-edge-notched specimens that have been used in either sharp machined notch or the fatigue precracked versions. (Testing details and correlation data for these specimens are presented in appendix C.) Also in this category are double cantilever beam (DCB) that have been used on high toughness steels, and surface flaw specimens that have proven useful in develop- ing design data and in failure analysis (see appendix C).

- The Charpy-size specimen -- This specimen has been treated as a single category since it has been the basis of a considerable amount of work on estimating or correlating K_{Ic} values; considered are both the standard machined notch and the fatigue precracked versions of the basic Charpy-size specimen tested in either the impact or the slow- bending loading modes. (Testing details and correlation data are presented in appendix D.)

- The dynamic tear test -- This test, used primarily by the Navy (MIL-STD-1601) for those materials exhibiting elastic-plastic and plastic fracture behavior, was reviewed in a more restricted sense in this report to determine its applicability for correlation with K_{Ic} values. (See appendix E which also includes a description of the drop-weight test for nil-ductility transition temperature determination for steels, since temperature has been used as an alternative to K_{Ic} value as a correlation basis in this report.)

- Methods that relate K_{Ic} to other conventionally or specially measured mechanical properties -- This category includes correlations with properties such as strain hardening exponent and tensile, plane-strain, and bulge ductilities (see appendix G).

2.5 MATERIALS CONSIDERED

Materials for which data were reviewed include 2000, 6000, and 7000 series aluminum, titanium alloys, and low- to high-strength steel alloys. Applications for these alloys include airframes, spacecraft and booster rocket propulsion systems, Naval and ordnance structures, nuclear pressure vessels, and bridges. The materials exhibited a large range of fracture toughness (K_{Ic}) and yield strength (σ_{ys}) values as illustrated in Figure 1.

2.6 STATISTICAL TREATMENT OF CORRELATIONS

The use of any rapid, inexpensive test in lieu of the standard K_{Ic} test raises the question of data correlation and the confidence that can be placed in the results. Since both the K_{Ic} test and the alternate test to be used for quality-control purposes will produce variable results even under the most stringent test conditions, the method for correlating the data should take this variability into account. Because of the random nature of the inputs, statistical analysis techniques may be required. (Appendix B presents some basic points to be considered in using correlated variables to establish a quality-control procedure. An example of the use of such a correlation is given by evaluating available sharp notch round tensile specimen data for high-strength aluminum alloys.)

If a quality-control specimen is to serve as the basis for acceptance or rejection of incoming materials, the criteria and test methods to be used must be agreed upon by both the producer and the user. Adequate procedures for retests or substantiation by a standard K_{Ic} test also should be agreed upon.
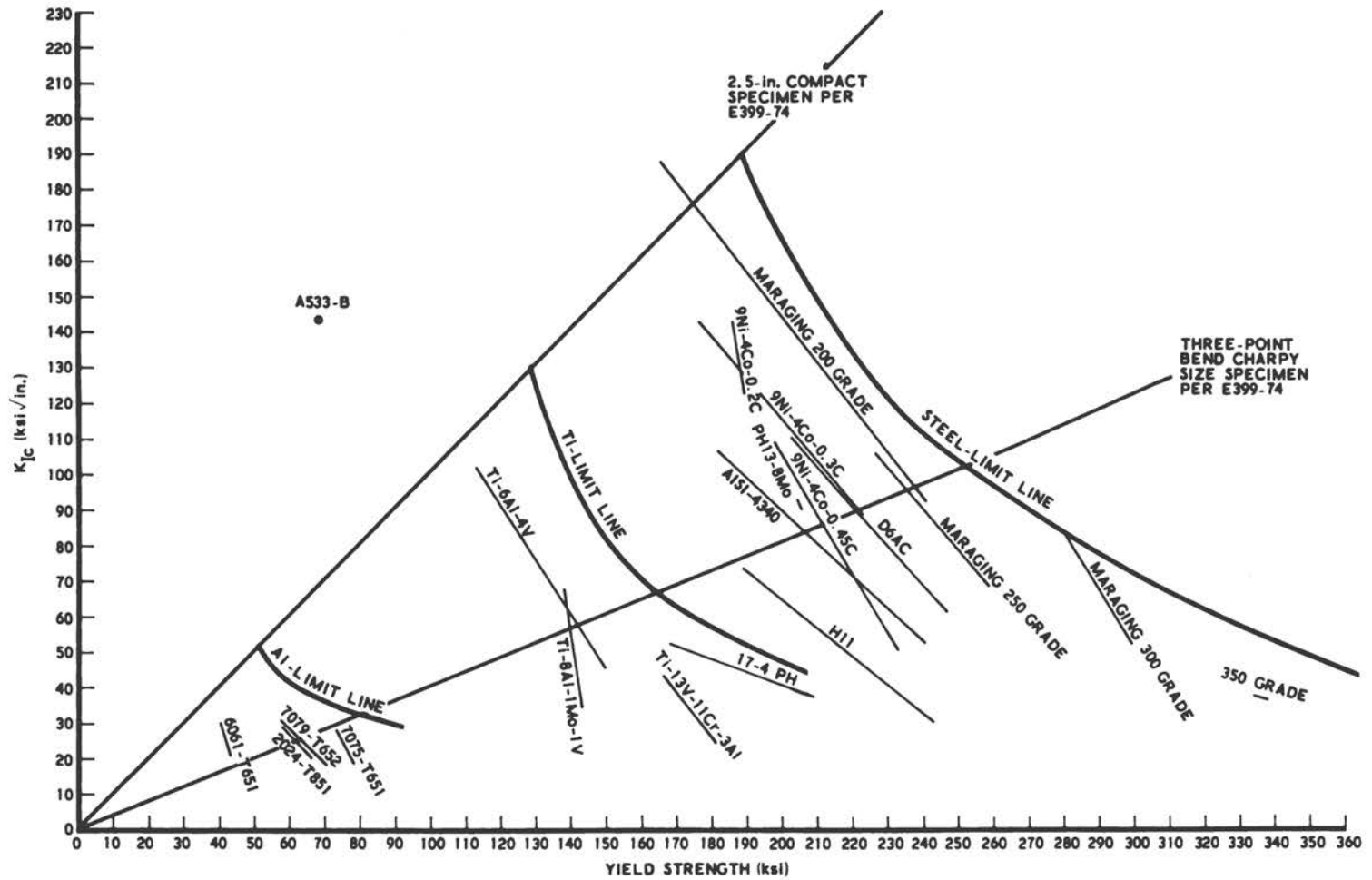
NOTE: The limit lines represent the loci of combinations of maximum values of K_{Ic} and σ_{ys} obtainable from state-of-the-art materials. The radial lines are upper bounds for regions where ASTM E399-74 thickness (B) requirements, i.e., $B \geq 2.5 (K_{Ic}/\sigma_{ys})^2$, are satisfied by the indicated specimens. For example, a three-point bend Charpy size specimen meets the ASTM thickness requirements for 17-4 PH steels but not for 9Ni-4Co-0.2C steels.

FIGURE 1   Range of Toughness and Yield Strength Properties for a Variety of Materials at Room Temperature.

Chapter 3

CLASSIFICATION OF TEST METHODS AND RELATIVE COSTS

3.1 TEST METHOD EVALUATION

3.1.1 General Considerations

A number of general topics, concepts, and terms are mentioned in the body of this report without detailed explanation. Since all readers will not be equally familiar with such matters, they are discussed in detail in appendix A and are summarized below.

3.1.1.1 Basis of Comparison of Test Effectiveness: ASTM E399-74 and E208-69. The most practical basis currently available for comparing test effectiveness is plane-strain fracture toughness (K_{Ic}) as defined by ASTM Standard Method of Test E399. Therefore, it was adopted by the Committee as the primary reference test method.* In order that the comparison data should be as great as possible, the Committee decided that any K_{Ic} value would be considered valid if it met the requirements of any earlier version of the current standard, ASTM E399-74, including the method originally proposed in 1968. (The significant features of ASTM E399 are discussed in appendix A.)

The K_{Ic} test is neither rapid nor inexpensive for two reasons: (a) the minimum necessary specimen dimensions are proportional to the ratio (K_{Ic}/yield strength)^2 and can be prohibitively large for high-toughness, low-strength materials, and (b) the specimen must be instrumented so that an accurate record of load versus displacement can be obtained for analysis. However, ASTM E399-72 and E399-74 do provide for a rapid, inexpensive test method in the form of an alternative result, the specimen strength ratio.

It must be noted that comparing K_{Ic} values is not always the most appropriate method for assessing the effectiveness of rapid, inexpensive tests. In particular, many structural steels suffer a drastic decrease in toughness when

---

* Ideally, in assessing candidate test methods for rapid, inexpensive quality control of the fracture toughness of materials, the predictability of satisfactory service performance should be compared, but existing information is insufficient to permit a useful comparison to be made on that basis.

the temperature is reduced over a narrow range, and the lower bound of this temperature range, the nil-ductility transition temperature, is of great practical importance in the application of such materials. The determination of the nil-ductility transition temperature by the drop weight test, in itself a rapid, inexpensive test, is specified in ASTM Standard Method of Test E208-69 (see appendix F) and wherever appropriate in this report, the reliable predictability of the nil-ductility transition temperature is employed as a complementary basis of comparison.

3.1.1.2 Specimen Strength Ratio as Defined in ASTM E399 as a Basis for Rapid Inexpensive Test Methods. The need for rapid, inexpensive tests has been recognized for many years by ASTM Committee E-24, and to meet the need for high-strength sheet materials, the ASTM Committee developed Standard Method E338-68 on sharp notch tension testing of high-strength sheet materials. Originally issued in 1967, revision of this method is currently under consideration (see appendix C). The concept of specimen strength ratio, which is of more general applicability because there is no limitation on specimen thickness, was incorporated into ASTM E399-72 to provide an alternative test result when specimen dimensions are too small to result in a valid K_{Ic} value.* This concept also permits a radical simplification of the ASTM E399 procedure to result in a rapid, inexpensive test for measuring specimen strength ratio (but not, of course, K_{Ic}). The specimen can be of any standardized size (e.g., Charpy size) but, as with any fracture toughness specimen, the larger it is, the wider the range of applicability. The specimen also must be fatigue cracked so that the severity of the damaging effect of an actual crack is realized. No instrumentation is needed since the only measurements to be made are the maximum load sustained in the test and the specimen dimensions. The specimen strength ratio (for any form of specimen) is the ratio of the specimen strength to the yield strength of the material, and the specimen strength is the sum of the ratio of maximum load to net section area and the ratio of maximum bending moment to net section modulus. (Specimen strength ratio is discussed further in appendixes A, C, and D.)

3.1.1.3 J_I and J_{Ic}, R Curves, and Crack Opening Displacement. The concepts of J_I and J_{Ic}, R curves, and crack opening displacement are each, in a different but related manner, extensions of linear elastic fracture mechanics and form the bases of proposed test methods that go well beyond the scope of the standard plane-strain fracture toughness test method. The associated test

---

* No such provision was made in earlier versions of ASTM E399. The provisional value K_Q often has been mistaken as an approximation to K_{Ic} when the specified dimensional requirements are not met, but, in fact, there is no necessary relation between an invalid K_Q and K_{Ic}.

methods are not intended to be rapid or inexpensive; rather, they are intended to fill needs not met by measurement of K_{Ic} or nil-ductility transition temperature.

The quantity J_I (Rice, 1968) is essentially a nonlinear generalization of $\mathscr{G}_I$ (Irwin, 1956), which was formulated for the linear elastic regime of material behavior (in the gross). $\mathscr{G}_I$ is proportional to the square of K_I (Irwin, 1957), the quantity more commonly used in this report, and evidence that the property J_{Ic} (analogous to K_{Ic}) applies to material behavior in the predominantly plastic-strain-hardening regime as well as in the nonlinear elastic regime is accumulating rapidly. In fact, J_{Ic} values obtained with small specimens are generally consistent with K_{Ic} values obtained from much larger specimens required for valid K_{Ic} measurement. (J_I and J_{Ic} are discussed further in appendix A.)

The crack extension resistance of a material is a quantity that continually increases to balance the increase of applied crack extension force, J_I or $\mathscr{G}_I$, up to some point of instability, which depends on the form of the cracked body as well as on the nature of the material. It is possible to measure crack extension resistance, R, as a function of the increase in crack area, and the corresponding curve is commonly called an R curve. Such curves vary considerably in form and magnitude with factors such as material, thickness and temperature. They provide much more information about the crack extension behavior of materials than do any other single quantity such as K_{Ic}, which, in fact, corresponds to a single point on the R curve (not generally a distinctive point). (An understanding of this topic is important to adequate comprehension of crack extension behavior and fracture instability; it is discussed further in appendix A.)

Crack opening displacement (COD) can be considered as the amount of inelastic stretching of the material immediately ahead of the crack tip and is linked to linear elastic fracture mechanics by the recognition that the crack tip in any real material has a surrounding "plastic zone" that necessitates modification of the purely linear model (Wells, 1961 and 1963). Unfortunately, there is not yet any accepted operational definition of COD that would provide a basis of homogeneity among the sets of data (obtained in a variety of ways, and therefore somewhat subjective) reported by various investigators. However, the British have prepared a Standard Draft for Development (DD 19:1972) that focuses on tests of three-point bend specimens and that depends on a formal relation between crack mouth opening and COD for inferring the reported result. While COD is little used in the United States, it is used widely in Great Britain; therefore, it is advisable to have a clear understanding of the concept and its interpretation (see appendix A).

3.1.2 Tensile-Loaded Specimens

Tensile-loaded specimens considered in this study include the notched-round bar (NRB) specimen, the surface-flawed (SF) plate specimen, the double-edge-notch (DEN) specimen and the double cantilever beam (DCB) specimen. Currently, only the notched-round bar is being investigated regarding

a correlation with K_{Ic}/YS. The ratio of notched tensile strength to smooth bar yield strength (called the notched strength ratio [NSR]) is the parameter being measured, but its usefulness is limited to aluminum and possibly magnesium. The machined root radius of the notch is specified to be less than 0.0007 in. The correlation to K_{Ic} must be based on an appropriate statistical analysis (see appendix B), and proper precautions must be taken to avoid eccentricity in loading.

The DEN specimen also has been used in a similar manner to measure the notched strength ratio as an index of toughness for sheet materials less than 0.25-in. thick. Again, the machined root radius of the notches is specified to be less than 0.0007 in. K_{Ic} correlation data do not exist because the materials are normally too thin to permit K_{Ic} to be measured. The machined notch again appears to limit the application of the DEN specimen to aluminum and possibly magnesium.

High fabrication costs and large specimen size requirements hinder the usefulness of the SF plate specimen in a quality-control test. The SF specimen is used primarily to develop design data. The DCB specimen is a load-efficient specimen requiring much less load than an SF plate specimen to produce the same stress intensity; however, because of material and machining costs, it cannot compete economically unless one specimen can be used to generate several data points. A fatigue-cracked NRB specimen becomes impractical because of the difficulty involved in obtaining a uniform circumferential crack. Currently, the DEN specimen is being modified by ASTM Committee E-24 to include a fatigue crack located at the root of one edge of the notch (DENF).

3.1.3 Charpy Size Specimen

The standard Charpy specimen with the 0.010-in. radius V-notch, as covered in ASTM E23, represents well-known specimen geometry. In the past, the specimen has been used most widely in the impact mode of loading for testing lower- and intermediate-strength grades of steel. Using the Charpy specimen as a quality-control test for correlating with or estimating the fracture toughness of materials offers several advantages that derive primarily from the small overall size of the specimen (which means a small test material volume requirement), the flexibility it offers in examining various test orientations, the relatively low specimen-preparation cost, and the ease it offers in testing at various temperatures. In addition, its long use history means that testing personnel generally are familiar with the specimen and the test.

Given these factors, it is natural that a number of methods have been proposed to correlate one or another of the parameters derived from the standard Charpy test with plane-strain fracture toughness, K_{Ic}. However, these correlation methods had to contend with the relatively blunt machined notch of the standard Charpy specimen while K_{Ic} testing requires a specimen with a sharp precrack. Recently, considerable effort has been devoted to testing a precracked modification of the Charpy specimen wherein the basic overall size is retained but the machined notch is replaced by a fatigue precrack.

The precracked specimen can be, and has been, tested in either the slow-bend or impact mode of loading.

The simplest method of slow-bend testing the precracked Charpy specimen involves a three-point loaded bend specimen and, without any deflection or displacement instrumentation, recording only the applied load. From this test, a specimen-strength ratio (denoted as R_{sb-CV} in this report) can be obtained for correlation with K_{Ic}. R_{sb-CV} is the ratio of the nominal stress, (σ_N) at maximum load to the material yield strength (σ_y).

By including suitable instrumentation in a slow-bend test, the following additional correlation parameters can be obtained:

- A P_Q load value, per ASTM E399 procedures, from which K_Q can be calculated for comparison with K_{Ic} values.

- Energy absorbed by the specimen per unit uncracked ligament area (W/A) that can be correlated with K_{Ic}^2/E (E = elastic modulus).

- Crack opening displacement (COD) or J-integral values that can be used in conjunction with elastic-plastic fracture mechanics concepts to derive a calculated K_{Ic}.

For the impact method of testing precracked Charpy specimen, the dial readings of the total energy absorbed can be converted to W/A values. Another procedure is the instrumented impact test in which load-time data that can be converted to load-displacement information are obtained. Several possible correlation parameters can be derived by treating the information in a manner analogous to a slow-bend load-displacement record. These various quantities obtainable from an impact mode of testing can be compared with either K_{Ic} or the dynamic fracture toughness (K_{Id}) of the material.

Impact tests on precracked specimens also have been used to correlate with the drop-weight nil-ductility transition temperature as defined in ASTM E208. For this purpose, the temperature at which a marked inflection occurs in the energy absorbed versus temperature curve is compared with the nil-ductility transition temperature.

An assessment of the available data pertaining to the various methods of testing the precracked specimen and correlating with K_{Ic} (or K_{Id}) does not show a clear-cut superiority of any one of them over all others. Each has some limitations in terms of range of applicability, degree of correlation, or convenience of testing.

Up to moderate levels of toughness-to-yield-strength ratio $(K_{Ic}/\sigma_y = 0.75 \sqrt{in.})$, the strength ratio procedure in a slow-bend test offers the best combination of predictive capability and ease of testing. The test data for a group of aluminum, steel, and titanium alloys in the higher strength grades and conditions indicate an overall correlation between R_{sb-CV} and K_{Ic}/σ_y within a total scatter of about ± 20 percent from a relation derived from linear elastic fracture mechanics (LEFM) concepts. The data also indicate that the

correlation could be improved if each specific alloy type or grade were considered on an individual basis. However, a more comprehensive and systematic set of data for each material category is required to verify this conclusion.

Given these features, the strength ratio method of correlation should be pursued actively to permit its eventual use as a simple quality-control test. One means of doing this is to require that a slow-bend precracked Charpy specimen test be conducted and the resulted reported for each K_{Ic} test conducted on materials of interest. Note that available data indicate no major dependence on crack size for this method within a crack depth/width (a/W) ratio range of about 0.3 to 0.45.

Although the strength ratio method has several desirable features, it is limited at higher toughness-to-yield-strength levels due primarily to the limit load phenomenon. At R_{sb-CV} values greater than about 1.8, the correlation departs from the LEFM-based relation and R_{sb-CV} becomes a less sensitive index of K_{Ic}. The exact limit of applicability varies depending upon the material involved and must be established empirically from additional tests.

Slow-bend test W/A values offer similar potential for correlation with K_{Ic}. The data show an advantageous feature in that W/A versus K_{Ic}^2/E has a generally linear relation up to $K_{Ic}/\sigma_y = 1$ √in., the upper limit of the available data. It remains to be determined, however, whether this linear dependence will continue at higher toughness levels. The data available for a W/A correlation include a variety of materials primarily in the higher strength grades and conditions. The data show a correlation generally within about ± 15 percent when expressed in terms of K_{Ic}, although larger deviations up to ± 25 percent sometimes occur.

From a quality-control test viewpoint, the slow-bend W/A determination requires more care in testing and data reduction than the determination of the specimen-strength ratio. Also, no standardized test procedure for conducting a W/A test currently exists. Thus, the slow-bend W/A method should be considered for use primarily in testing high-relative-toughness materials since in such cases the increased testing complexity is compensated for by a wider range of potential applicability. To do this, a standardized procedure for slow-bend W/A testing should be developed as rapidly as possible.

The COD and the J-integral based methods also are potential correlation bases in the higher toughness range. Data available for evaluating these methods on precracked Charpy specimens are very limited, but they do indicate a correlation potential within ± 10 percent for predicting K_{Ic}. In general, these tests require considerable expertise, and although simplified techniques have been proposed, additional developmental studies on a variety of materials are needed to assess their potential.

Methods based on impact testing precracked Charpy specimens result in correlations with K_{Ic} that are often erratic and variable, primarily because of the loading-rate sensitivity of fracture toughness among materials. The precracked Charpy impact test, therefore, is not recommended for correlation with K_{Ic} (the slow-bend test is much more suitable for this purpose). It is possible that impact test data may correlate better with K_{Id} but this is a complex problem which currently is being investigated at the developmental level. The principal

application of impact testing the precracked specimen is probably for low- and medium-strength steels since the K_{Id} value is often of interest. In this connection, impact test results generally show good correlation with drop-weight nil-ductility transition temperature test results for these materials. However, since the drop-weight test (ASTM E208-69) is a fairly simple test, the use of precracked Charpy specimens for this purpose appears justified primarily when test material is limited or additional information is desired.

Although the precracked specimen is recommended as being most generally suitable for correlation with K_{Ic}, empirical correlations based on results from the standard machined-notch Charpy specimen will continue to be useful for some specific materials, particularly the low- to intermediate-strength grades of steels (a number of these applicable areas are described in appendix D). When considered in an overall sense, these empirical correlations appear to have a rather large scatter; however, in specific circumstances when limited to a narrow range of grades, strength levels, test regimes, etc., the correlations can provide a useful guide to estimating the fracture toughness of these materials. One problem with these empirical correlations based on the standard V-notched specimen is the occasional instances when the steel may exhibit good fracture toughness with a 0.010 in. radius notch but a low toughness with a sharp precrack notch. Also, the loading-rate-dependent character of the toughness of low- and medium-strength steels indicates that the correlations should be made at similar loading rates, that is, K_{Ic} should be correlated with values measured in slow-bend tests of V-notched Charpy specimens. The principal problem with empirical correlations based on the standard V-notched specimen is that occasionally a steel may exhibit good fracture toughness with a 0.010-in. radius notch while a sharp precrack shows low toughness.

3.1.4 Dynamic Tear Test

The dynamic tear (DT) test developed by the U.S. Navy for characterizing the fracture resistance of steels, titanium alloys, and aluminum alloys has been correlated with K_{Ic} results for these materials in the high-strength range. Early correlation efforts conducted in the late 1960s were based primarily on K_{Ic} data obtained with single-edge-notch (SEN) tension specimens, which do not conform to current ASTM standard K_{Ic} test methods, and 1-in. DT test results; however, more recent data gathered in conformance with ASTM E399 generally confirm the accuracy of the earlier results.

The 5/8-in. DT test is covered by a military specification (MIL-STD-1601), and a Proposed Method has been published for information purposes in the gray pages of the 1975 Annual ASTM Standards (Part 10).

3.1.5 The Drop-Weight (Nil-Ductility Transition Temperature) Test

The drop-weight test (DWT) is a widely used ASTM standard method (E208) developed specifically for the determination of the nil-ductility transition

temperature (the temperature above which structural steels undergo a transition from brittle to ductile fracture behavior). From the nil-ductility transition temperature determination, interpretations to dynamic fracture initiation conditions can be made using fracture analysis diagram (FAD) procedures. The DWT-nil-ductility transition temperature concept and FAD procedures have been validated by correlation with a wide variety of tests involving initiation of fractures as well as numerous service failures.

3.1.6 Special Ductility Tests

A number of relations between K_{Ic} and more fundamental flow and fracture properties derived from detailed analyses of the crack extension process have been proposed. Involved in these relations are measured mechanical properties including the tensile flow properties (yield stress, strain hardening exponent, etc.) and some measure of ductility derived from standard or special test specimens, such as:

- Reduction-in-area/ordinary (round bar) tensile test.

- Plane strain ductility/plane strain tension or bend specimen.

- Bulge ductility/bulge specimen.

- Triaxial stress-plane strain ductility/special notched specimen.

Various K_{Ic} property relations and correlations are the nucleus for several possible quality-control procedures. The plane-strain tensile specimen and the triaxial-stress/plane-strain ductility specimen appear impractical since they involve costs comparable to the standard fracture toughness specimen. However, the ordinary tensile specimen, the plane-strain bend specimen, and the bulge specimen could be relatively cheap to produce and test. It remains to be established whether these tests really reflect the kinds of K_{Ic} variations encountered in practice, particularly those associated with undesirable inclusions. Alternatively, the mechanical test could be combined with a measure of the chemical composition to give a more complete picture of toughness behavior.

Extensions of analytical capabilities of the crack tip fracture processes and measurements of K_{Ic} ductility relations that underlie potentially useful quality-control methods should be supported.

3.1.7 Range of Applicability

Valid fracture toughness data (per ASTM E399) generally have been limited to materials with a $(K_{Ic}/YS) \leq 1$, with the exception of A533B steel, which has a $(K_{Ic}/YS) \cong 2 \sqrt{\text{in}}$. at 50° F. Other tests of material with $K_{Ic}/\sigma_y > 1$ have

been conducted on heavy sections used in electrical-power-generating equipment; however, the data from tests of large specimens are limited due to the large test machine requirements involved in measuring K_{Ic} with a specimen whose thickness (B) must satisfy $B \geq 2.5 (K_{Ic}/YS)^2$. Thus, valid K_{Ic} data exist primarily for high-strength materials. The data plotted in Figure 2 for aluminum alloys, titanium alloys, and various steel alloys, represent a variety of heats, heat treatments, product forms and test orientations (relative to the grain flow).

3.1.8 Conclusions and Recommendations

Tensile-Loaded Specimens

Conclusions

1. The only tensile-loaded specimen that might qualify as a rapid, inexpensive test is the < 0.0007-in. machined notch round for
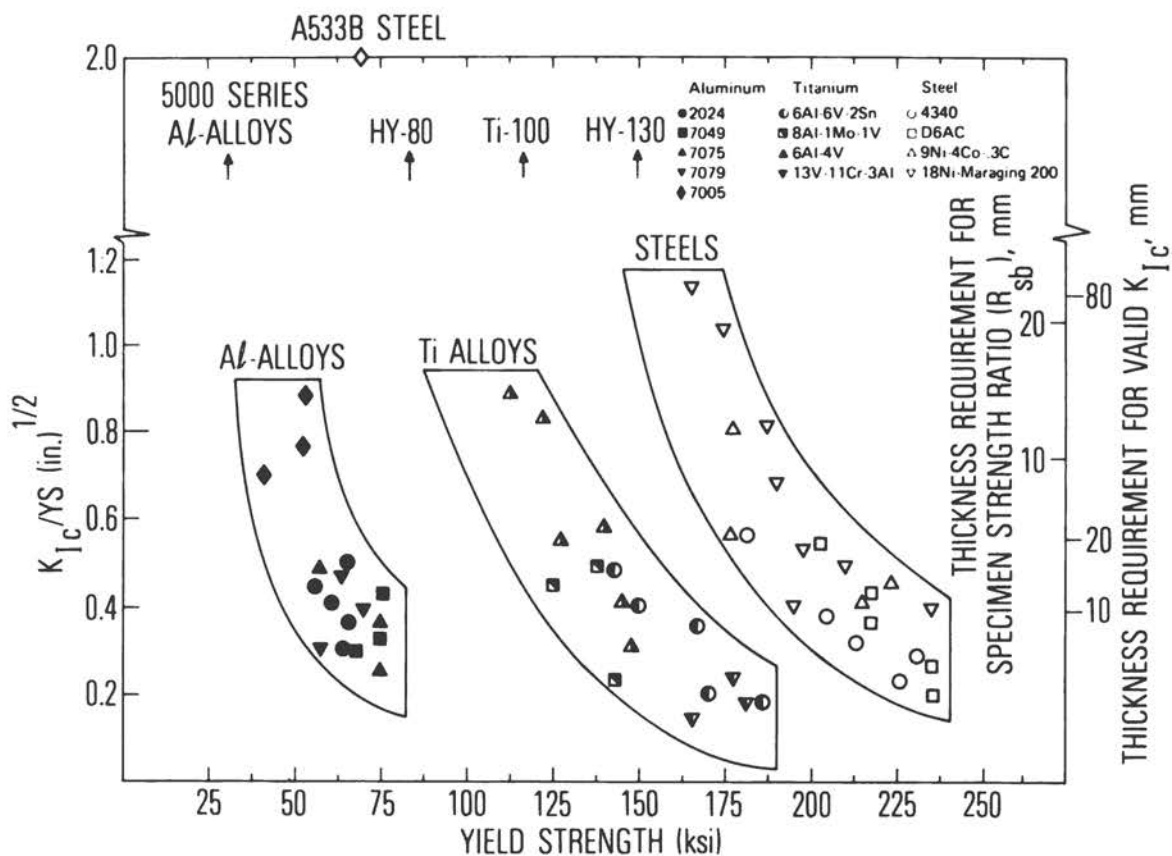
NOTE: The vertical axis on the right side of the figure indicates the thickness requirements for valid K_{Ic} tests per ASTM E399 (i.e., $t = 2.5 (K_{Ic}/\sigma_{ys})^2$.

FIGURE 2   Valid K_{Ic} Data for High-Strength Materials (Matthews, 1973).

aluminum alloys and possibly magnesium alloys. According to information supplied to the Committee, it is less expensive to machine a V-notch in a round bar than in a rectangular specimen. The notch-round bar does not require a fatigue precrack, but special aligning fixtures are necessary to eliminate eccentricity problems.

2. Compared to the compact K_{Ic} specimen, most other tensile-loaded specimens do not represent a significant cost savings and, therefore, do not compete as a rapid, low-cost method for determining fracture toughness. In general, the load requirements are higher, the required instrumentation is comparable, the material requirements are greater, and fatigue precracking is a necessity to have one test procedure for all materials.

Charpy Size Specimens

Based on overall considerations of the optimum combinations of testing simplicity and range of applicability, the following conclusions and recommendations summarize the situation concerning Charpy size size specimens:

Conclusions

1. The precracked specimen tested in slow-bending is the most promising for correlation with K_{Ic}.

2. For toughness levels up to about $K_{Ic}/\sigma_y = 0.75 \sqrt{in.}$, the slow-bend (W/A) and the strength ratio (R_{sb-CV}) both provide good indices to K_{Ic}; however, the strength ratio is easier to measure.

3. For toughness levels (K_{Ic}/σ_y) above $0.75 \sqrt{in.}$ and up to $1.0 \sqrt{in.}$ or possibly higher, the slow-bend W/A shows the best correlation potential.

4. Precracked specimen impact test results show poor general correlation with K_{Ic}; however, limited correlation for specific materials may be possible.

5. Precracked specimen impact tests can be used to determine the drop-weight nil-ductility transition temperature for low- to medium-strength steels; the correlation is usually quite good and would be useful in circumstances where material and testing space considerations apply.

6. Several empirical correlations are available for estimating K_{Ic} values of steels from standard V-notch Charpy test data; however, the specific nature and limitations of each such correlation always

must be recognized, including the fact that a 0.010-in. radius notch is quite different from a sharp precrack.

Recommendations

1. A standardized procedure for precracked Charpy slow-bend W/A test is needed and Task Group E24.03.03 of ASTM Committee E-24 currently is working on this. It is recommended that this work be extended to include evaluation of specimen strength ratio data that will be obtained during the course of the effort.

2. A precracked Charpy slow-bend test should be included, to the extent possible, in K_{Ic} testing programs to obtain a larger data base for improved correlations.

3. Further studies are needed to determine the usefulness of precracked Charpy impact for correlation with dynamic fracture toughness (K_{Id}). However, no standard test exists for K_{Id}. ASTM E24.03.04 task group currently is addressing the problem of a standard test method for K_{Id}.

Dynamic Tear Test

Conclusion

1. The dynamic tear (DT) test has promise as a rapid, inexpensive quality control test for aircraft-grade metal alloys.

Recommendations

1. Further research is required to verify the accuracy of the DT-K_{Ic} correlations, to establish more exactly the precision for predicting K_{Ic} values from 5/8-in. DT test results, and to develop an improved method for introducing a sharp crack into DT specimens of hardness greater than Rockwell C of 36.

2. Consideration must be given to the effects of strain rate in the correlations for rate-sensitive materials.

Drop-Weight (Nil-Ductility Transition Temperature) Test

Recommendation

1. The drop-weight test is not recommended as a rapid, inexpensive quality-control fracture-toughness test (although it is both) for insuring minimum K_{Ic} values in quality control since it does not provide a direct measurement of energy to fracture a standard

specimen. Instead, it is a test to which several other fracture toughness tests, reviewed in this report, are correlated where accurate definition of nil-ductility transition temperature is of concern.

3.2   RELATIVE COSTS

Significant factors that affect the direct costs of testing specimens were identified from available sources and are summarized in Table 1. The information sources included independent, government, and industrial research laboratories. The cost elements included machining, precracking (if necessary), testing, and data analysis. All cost figures for the in-house laboratories are in direct charges and do not include any overhead rate or burden. Also, test machine charges or amortization costs are not included.

The cost figures were obtained during mid-1974 and reflect, as accurately as possible, the comparative costs of testing specimens at that time. A break-down between in-house and contract laboratories was deemed necessary, primarily because of the machining cost differences. For the cost summaries, government laboratories were classified as in-house.

The specimen machining cost has the most variability because of the ease or difficulty of machining various alloys. The following broad grouping based on machineability, ranging upward to the most difficult, was made: (a) aluminum alloys; (b) titanium and low- to medium-strength steels; (c) maraging steels, high nickel steels, and nickel-base alloys; (d) advanced super-alloys of nickel and cobalt bases. Machining estimates were made on 1/8-in. oversize blanks to normalize the material removal.

The comparative data are for single specimens of each type; some of the test methods require multiple specimens (i.e., drop weight nil-ductility transition temperature tests) and this was not taken into account in assembling Table 1. The data are presented only to indicate trends since different accounting methods, costing practices, and even machinist training programs tend to make precise cost comparisons difficult.

A general comparison of specimen testing costs, listed in the order of increasing cost, and the standard ASTM E399 test, is presented below:

Total Cost << E399	Tensile
	Sharp Notch Round
	Charpy Impact
	Dynamic Tear
	Drop Weight NDT*
Total Cost < E399	Precracked Charpy
	Instrumented Impact Charpy
Total Cost > E399	J_{Ic} Tests

* Nil-ductility transition temperature.

TABLE 1 Comparison of Specimen Testing Costs (in 1974 dollars).

	Aluminum Alloys	Low to Medium Strength Steels, Titanium	Maraging Steels, High-Nickel Steels, Nickel-Base Alloys	Advanced Super-alloys of Nickel and Cobalt Bases	Precracking	Special Preparation	Testing and Data Reduction
Tensile Test							
In-House	10*(15)**	12 (17)	--	--	--	--	5
Contract Laboratory	17 (23)	17 (23)	19 (25)	23 (29)	--	--	6
Sharp Notch Round Test							
In-House	10 (15)	--	--	--	--	--	5
Contract Laboratory	17 (23)	--	--	--	--	--	6
Compact K_{Ic} Test (ASTM E-399)							
In-House							
1T (specimen thickness)	--	70 (180)	--	--	66	--	44
2T (specimen thickness)	--	105 (215)	--	--	66	--	44
Contract Laboratory							
1T (specimen thickness)	46 (131)	65 (150)	75 (160)	84 (169)	50	--	35
2T (specimen thickness)	74 (179)	105 (210)	120 (225)	135 (240)	65	--	40
Charpy Specimen Tests							
Impact ASTM E-23							
In-House	--	7 (17)	--	--	--	--	10
Contract Laboratory	--	19 (29)	32 (42)	38 (48)	--	--	10
Precracked							
In-House	--	7 (42)	--	--	25	--	10
Contract Laboratory	--	19 (59)	32 (72)	38 (78)	30	--	10
Instrumented Impact							
In-House	--	7 (72)	--	--	25	--	40
Contract Laboratory	--	19 (74)	32 (87)	38 (93)	30	--	25
Dynamic Tear Test (MIL-STD-1601)							
In-House Only							
5/8 in. (specimen thickness)	6 (19)	8 (21)	--	--	--	3	10
1 in. (specimen thickness)	12 (25)	14 (27)	--	--	--	3	10
Drop Weight NDT⁺ Test (ASTM E-208)							
In-House Only	--	15 (33)	--	--	--	3	15
J_{Ic} Tests							
In-House Only							
1 in. Compact	--	90 (210)	--	--	72	--	48
1 in. Bend	--	60 (180)	--	--	72	--	48
Charpy	--	8 (78)	--	--	42	--	28

NOTE: All cost estimates are based on mid-1974 data.

* Specimen machining cost.   ** Total specimen testing cost.   ⁺ Nil-ductility transition temperature.

APPENDIX A

GENERAL CONSIDERATIONS

This appendix describes the significant features of existing standard test methods to provide readers with a common frame of reference; a summary of recent nonlinear fracture mechanics techniques also is included to permit a comprehensive evaluation and cover the concepts of the J-integral, crack opening displacement, and crack resistance or R curves. The Committee readily acknowledges, however, that the existing data base was not sufficient to permit these concepts to be included in its evaluation.

A.1   BASIS FOR COMPARISON OF TEST EFFECTIVENESS

The assessment of candidate test methods for rapid, inexpensive quality control of fracture toughness of materials requires that there be some common basis for comparing effectiveness. While the ideal basis for comparison would be the predictability of satisfactory service performance, information available is far from sufficient to permit useful comparisons of this nature; consequently, the Committee selected the ASTM Standard Method of Test for Plane-Strain Fracture Toughness of Metallic Materials (currently designated as ASTM E399-74) as the most practicable basis for comparison.

In order that the comparative data should be as extensive as possible, K_{Ic} plane-strain fracture toughness values were accepted as valid if they conformed to the requirements of any of the earlier versions of ASTM E399-74 (i.e., ASTM E399-72, E399-70T, and the Proposed Methods published in 1969 and 1968). In this report, all these versions are referred to collectively as ASTM E399.

It must be noted, however, that the K_{Ic} value determined by ASTM E399 is not always the most appropriate basis of comparison. In particular, many structural steels that are used in large quantities exhibit a marked decrease in toughness when the temperature is reduced over a narrow range which is characteristic of composition and metallurgical processing factors. For such steels, the nil-ductility transition (NDT) temperature, as determined by ASTM Standard Method of Test E208-69, may be the most important criterion of fracture behavior and, whenever appropriate, the ability to estimate the nil-ductility transition temperature reliably also should be considered in

24

assessing the effectiveness of candidate test methods. (This and related aspects of fracture avoidance technology are discussed in detail in appendix E.)

The complexity of the fracture phenomenon is such that several independent quantities are required to characterize a material completely in this respect; however, such a complete characterization obviously is unattainable by any test method that is required to be rapid and inexpensive. For this reason, the scope of the Committee's study was confined largely to the more commonly considered aspects of fracture testing. Furthermore, many practical applications exist for which a knowledge of the level of K_{Ic} is sufficient to determine the choice of material.

A.2 SIGNIFICANT FEATURES OF ASTM STANDARD METHOD OF TEST E399

In assessing candidate test methods by comparing results with corresponding ASTM E399 K_{Ic} values, the available data correlations were regarded primarily as purely empirical because of the disparate nature of some of the tests considered. Since some test methods are related to the ASTM E399 method in principle, in practice, or in both respects, knowing in which respects each method fails to conform to ASTM E399 requirements for valid K_{Ic} measurement should permit more critical scrutiny of the data correlations. The more important and relevant requirements, as detailed in the parenthetically indicated sections of ASTM E399-74, are as follows:

a. The specimen is precracked by controlled fatigue cycling (see section 7.4 of ASTM E399-74).

b. The relation of the stress intensity factor K_I to the applied force and the specimen dimensions must be known accurately (see section 9 of ASTM E399-74).

c. The effective crack length of the specimen must exceed the quantity $2.5 \, (K_{Ic}/\sigma_{YS})^2$, which itself has dimensions of length (see section 9.1.5 of ASTM E399-74). Also, the implication is that the effective width, and the difference between width and crack length, must exceed multiples of $(K_{Ic}/\sigma_{YS})^2$. These requirements ensure that the stress field near the crack tip sufficiently approximates that of a crack in a linear elastic body.

d. The specimen thickness (nominally equal to the length of crack front) also must exceed $2.5 \, (K_{Ic}/\sigma_{YS})^2$ so that the material near the crack front is under constraint that closely approaches tritensile plane strain (see section 9.1.5 of ASTM E399-74). It should be noted that items (c) and (d) are actually quite independent and serve entirely different purposes. The numerical factors were estimated

empirically and were chosen to have the same value of 2.5 for simplicity rather than for any more fundamental reason.*

e. A test record must be obtained of the applied load versus crack (notch) mouth opening (see section 8.5 of ASTM E399-74). (In principle a record of load versus displacement of the point of application of the load could serve the same purpose.)

f. The measurement point for K_{Ic} determination corresponds to an increase in effective crack length of 2 percent, defined in terms of a secant intercept point on the test record (see section 9.1 of ASTM E399). This is important because the result obtained depends strongly on the chosen measurement point (analogously to choice of definition of yield strength as determined from an ordinary tension test record -- ASTM E8-69). If the measurement point in the comparison test method is defined differently or ambiguously, the correlation is affected accordingly. This feature of ASTM E399 is recognized as a deficiency of the test method since it results in K_{Ic} values that are not entirely independent of specimen size. In general, for a given material, the larger the specimen the higher will be the K_{Ic} value even though all the results are valid (for invalid results, the K_Q value decreases towards zero as the specimen size is decreased.) The cognizant ASTM task group (E-24.01.01) considered this matter for several years but, so far, has been unable to find any simple alternative to the current method of defining the measurement point. The obvious but complicated approach would be to determine a crack extension resistance curve as described in section A.5.

g. The rate of load application during a test is restricted to a narrow range such that dynamic effects are negligible, and environmental effects are minimal. Test duration is of the order of 1 to 5 minutes.

h. It is worth noting that new varieties of K_{Ic} test specimens are currently under development. In particular, a proposed K_{Ic} test method for C-shaped specimens is expected to be issued shortly and should be of particular value for tests on tubular products, such as pipes and gun barrels. The C-shaped specimen, when notched and precracked internally, is tested under tensile load in a manner similar to the com-

---

* Any number of other specimen forms could be standardized for K_{Ic} determination. These must conform to equivalent dimensional requirements for the fundamental reasons mentioned in items (c) and (d). The significant dimensions depend on specimen form (e.g., the depth of the arms is the most significant in-plane dimension for long, slender double-cantilever-beam specimens).

pact specimen in ASTM E399, and when notched and precracked externally, is tested under compressive load. This alternative is applicable to products known to be subject to external cracking, such as certain welded pipes in unfavorable environments (Kendall, 1973).

A.3   SPECIMEN STRENGTH RATIO

ASTM E399 could be modified by omitting complicating requirements so that the resulting simplified test method could be used as a rapid, inexpensive quality-control test. The specimen should be fatigue cracked but can be of any standardized size (however, as with any kind of fracture test, the larger the specimen is, the wider is the range of applicability).

The simplified application depends on the provision of an alternative test result in ASTM E399 (i.e., the specimen strength ratio -- R_{sb} for a bend specimen, or R_{sc} for a compact specimen). (See sections 1.3, 9.1.6, and 9.1.7 of ASTM E399-74.) This ratio is a useful comparative measure of the toughness of materials when the specimens tested are all of the same form and size and when the size is sufficient to permit the maximum load to be determined by pronounced crack extension prior to plastic instability even though not sufficient to meet the requirements for a valid K_{Ic} test. If only the specimen strength ratio is to be determined, the test record and associated instrumentation can be omitted because only the maximum load and the specimen dimensions, including average crack length, are needed.

Data presented in appendix D show a good correlation between strength ratios for precracked Charpy-size specimens and K_{Ic}. This type of correlation can be based on strength ratios measured on specimens of various sizes. In further studies of this method, it would be advisable to use two standard types of specimen for strength ration determination: (a) the 1-cm-square (Charpy) specimen and (b) the 1-inch-thick ASTM E399 compact specimen.

A.4   THE CONCEPTS OF J_I AND J_{Ic} TEST TECHNIQUES

The quantity J_I (Rice, 1968) is essentially a generalization of $\mathscr{G}_I$ (Irwin, 1956). Whereas $\mathscr{G}_I$* was formulated for the linear elastic regime of material behavior (in the gross aspect), J_I applies equally to the nonlinear elastic regime; furthermore, it apparently is applicable to some kinds of inelastic behavior. The term "J integral" is used synonymously with J_I and derived from the original publication (Rice, 1968) that emphasized the path-independent integral form of J. The path-independent integral form of $\mathscr{G}$ was discussed earlier (Sanders, 1970)

---

* Note that $\mathscr{G}_I = K_I^2/E'$, where E' is the reduced modulus, equal to E (Young's modulus) for plane stress, or equal to $E/(1-\nu^2)$ for plane strain, where ν is Poisson's ratio.

but received little attention. Since $\mathscr{G}$ can be regarded as a specialization of J to apply only to linear elastic behavior, all further discussion of J applies equally to $\mathscr{G}$ within the constraints of the specialization. The aspect of J that is more intuitively comprehensible than its path-independent integral form is the partial derivative with respect to the increase of (projected) crack area of the energy available for dissipation in the region of crack growth.

In the remainder of this section, the subscript I (Roman numeral one) will be dropped as being understood in the present context. It indicates the first or opening mode of crack extension (Irwin, 1957). The other components of the vector J_k (Budiansky, 1971) are J_{II} for in-plane shear and J_{III} for antiplane shear modes of crack extension. These components are important in the general field of fracture mechanics, but are outside the scope of this report, which is restricted effectively to opening mode crack extension and fracture. Originally, J was formulated for a two-dimensional deformation field, and it currently is being exploited in that mode in practice. The generalization to three dimensions is straightforward mathematically, but its exploitation is vastly more complicated than the two-dimensional model, both computationally and experimentally.

The dimensions of J are: (ENERGY) (LENGTH) $^{-2}$ because J is basically a derivative of a component of energy with respect to an area; also: (FORCE) (LENGTH) $^{-1}$, or, fundamentally: (MASS) (TIME) $^{-2}$. These dimensions are the same as those of surface tension of a liquid; indeed, this is not coincidental but fundamental. The concept of surface tension of a crack was introduced by Griffith (1920) in his seminal paper on fracture mechanics.

> ". . . in a solid the bounding surfaces possess a surface tension
> which implies the existence of a corresponding amount of
> potential energy. If owing to the action of a stress a crack is
> formed, or a pre-existing crack is caused to extend, therefore,
> a quantity of energy proportional to the area of the new surface
> must be added, and the condition that this shall be possible is
> that such addition of energy shall take place without any increase
> in the total potential energy of the system. This means that the
> increase of potential energy due to the surface tension of the
> crack must be balanced by the decrease in the potential of the
> strain energy and the applied forces."

This lucid statement of the seminal conception should not be taken too simplistically because cracks in general do not have simple smooth surfaces and the dissipation of energy associated with crack extension is not confined to the immediate surface. Nevertheless, the statement is a good starting point for the comprehension of fracture mechanics.

The briefest satisfactory descriptive expression for J is "the crack extension force" (Irwin, 1957) that implies "per unit length of crack front." The material property that balances the applied crack extension force under quasistatic conditions is termed the "crack extension resistance." This crack extension resistance is not a single-valued quantity but increases to balance the increase of applied J up to some point of instability that depends on the form of the body which contains the crack and on the nature of the boundary

conditions. A simple crack extension resistance experiment provides a record of crack extension resistance (R) as a function of increase in crack area. This record is analogous to an ordinary tension test record of increase of resistance to deformation as a function of deformation (strain). The increase of R with increase of crack area is analogous to the increase of flow stress of a strain hardening material with increase of plastic strain in the tension test. The determination of crack extension resistance curves is discussed in more detail in section A.5.

The crack extension resistance derives physically from the various dissipative microprocesses associated with crack extension. These are: void formation, growth and coalescence; imperfect cleavage; and various forms of inelastic deformation, primarily slip and twinning in metals and some other materials, and viscous flow in other nonmetallics. The inelastic deformation is focused at the crack tip but may spread far from it when the material is relatively tough and/or low in strength and the cracked body is relatively small. This circumstance modifies the simple linear elastic size effect on fracture behavior in which fracture strength of a given material is inversely proportional to the square root of a characteristic dimension of a cracked body.*

The concept of J as the derivative of available energy with respect to crack area clearly is applicable to materials that behave elastically, whether linearly or nonlinearly, in the gross (i.e., everywhere except near the crack tip or regions of concentrated force). Although it initially might appear contradictory to expect J to be applicable to materials that behave substantially inelastically (since the energy required for the inelastic deformation elsewhere is not available to drive the dissipative microprocesses occurring near the tip of the extending crack), an alternative justification (Hutchinson, 1968) has been found for materials that strain harden according to a simple power law (Ramberg-Osgood materials) on the basis that the strength of the strain energy density singularity should have the constant value -1 (McClintock, 1972; Swedlow and Gerberich, 1964). Moreover, there is rapidly accumulating evidence that J_{Ic} values obtained from small specimens are consistent with valid ASTM E399 K_{Ic} values for much larger specimens.

A necessary but not sufficient condition for crack extension is that the available energy per unit projected area of crack extension should equal or exceed the energy required for the dissipative microprocesses. Apparently, a second condition to be met is some critical state of the elastic and plastic strain fields surrounding the fracture process region.

---

* Size effects are important in fracture. In principle, toughness could be measured in terms of the size of a proportionately cracked body -- standardized specimen form -- that could just sustain a nominal gross stress equal to some prescribed fraction of the material yield strength. Such an approach to toughness testing would be quite impracticable, however, even apart from cost, because the size of specimen required often would be much larger than could be obtained from available stock.

Irrespective of the theoretical justification for application of the J concept to fracture testing of materials which behave inelastically in the gross, there is sufficient encouraging experimental evidence to provide incentive for a major effort toward development of an ASTM standard test method for J_{Ic} measurement. This effort was started in March 1972 by the formation of Task Group E-24.01.09 of ASTM Subcommittee E-24.01, which currently is preparing a Proposed Recommended Practice for publication in 1976 or 1977 in Part 10 of the ASTM Book of Standards.

Assuming that this development is satisfactory, it is likely that ASTM E399 will be superceded by the J test method. During the interim, however, ASTM E399 is the reference method for evaluation of J test developments. Consequently, continuity will be maintained in the evaluation of plane-strain fracture toughness while the scope of testing will be markedly increased.

The major practical advantage of the J approach to toughness testing is that the size of specimen needed for a given material is much less (between 1/10 and 1/100) than that required by ASTM E399. In fact, if two specimens of exactly the same shape are each just large enough to give valid results in terms of J, on the one hand, and in terms of ASTM E399 on the other, the ratio of their linear dimensions currently is estimated to be 10 times the ratio of yield strength to Young's modulus.

A.4.1 Current J_{Ic} Test Techniques: Advantages and Disadvantages

As a fracture criterion, J permits a direct extension of linear elastic fracture mechanics (LEFM) into the realm of large-scale plasticity (Hutchinson, 1968; Rice and Rosengren, 1968; Begley and Landes, 1972; Landes and Begley, 1972) and allows many engineering problems outside the scope of LEFM to be treated. One interesting aspect of the J criterion is that the J values at crack initiation in plane strain (termed J_{Ic}) should be related directly to the K value for plane-strain crack initiation in the same material in an essentially elastically loaded body (Begley and Landes, 1972). Only minimal restrictions are placed on the scale of plasticity appropriate for a J integral characterization of crack tip processes (Landes and Begley, 1974). Hence, determination of the J_{Ic} level on small, reasonably sized specimens that may be loaded far into the plastic range can be used to evaluate K_{Ic} fracture toughness values.

The complexity of a single J_{Ic} test is about the same as a K_{Ic} test per ASTM E399. Also, any J_{Ic} test procedure can be used without modification to obtain a valid K_{Ic} result if the specimen dimensions are sufficient for that purpose per ASTM E399. However, since the necessary specimen size for J_{Ic} interpretation is much less than that required by ASTM E399, the cost of specimen material and machining is reduced and a smaller testing machine can be used. Also, there is less chance that the specimen size chosen will be insufficient.

—

It currently is necessary to approximate the crack extension resistance curve in terms of J_I to determine J_{Ic} and this involves tests of several specimens to obtain a single J_{Ic} result. However, the R-curve information is of much greater value than the single, arbitrarily defined point on it that corresponds to K_{Ic}.

For those materials with fairly flat R-curves, the correlation between J_{Ic} and K_{Ic} is good. When the R-curve is more rounded, the J_{Ic} value is less than the K_{Ic} value per ASTM E399; however, this is merely a consequence of the difference in definition of the two quantities. The operational definition of K_{Ic} in ASTM E399 is acknowledged to be unsatisfactory, and the advent of J_{Ic} provides an opportunity for improvement in this respect.

The J_{Ic} test can be accomplished most easily with deeply cracked $(a/w > 0.5)$ bend-type specimens, including the compact-type K_{Ic} specimen used in ASTM E399. For these geometries, a direct relationship exists between the applied J value and the work done on the sample (Rice et al., 1973):

$$J = \frac{2A}{B(W-a)}(1 - F),$$ \hfill (A-1)

where A is the area under the load deflection record up to the point of interest, B is specimen thickness, a is crack depth, W is specimen width, and F is negligible for sufficiently deeply cracked bend-type specimens. The deflection is that of the load points so that A represents the work done on the specimen.

The calculation of J is very simple, but the selection of a suitable measurement point is not. The analytical basis for J restricts the choice of a toughness measurement point to crack initiation or, at most, to some small amount of growth. An uncomplicated method of evaluating the onset of cracking consists of loading several specimens to various deflections. Following unloading, the extent of crack growth is marked by heat tinting, fatigue cracking, or chemical straining. A plot is made of the applied J versus the extent of cracking. Extrapolation of this curve leads to the J value at crack initiation or J_{Ic} (see Figure A-1, point 4).

The above technique requires three or more test specimens. The complexity of the specimen geometry, fatigue precracking, and instrumentation is the same as that involved in a K_{Ic} test, but the specimen size is much reduced and the chance of an invalid test result is lessened. A tentative size limit is given by Landes and Begley (1974):

$$a \text{ and } B \text{ and } (W-a) > 25\frac{J_{Ic}}{\sigma_{yield}}.$$ \hfill (A-2)

If this requirement is compared with the size requirements for valid K_{Ic} measurement per ASTM E399, using the equivalence $K_I^2 = E\, J_I / (1 - \nu^2)$, the ratio of similar linear dimensions is about 10 times the ratio of yield strength to Young's modulus of the material. This dimensional ratio is, therefore, between 1/10 and 1/100 for most structural materials.
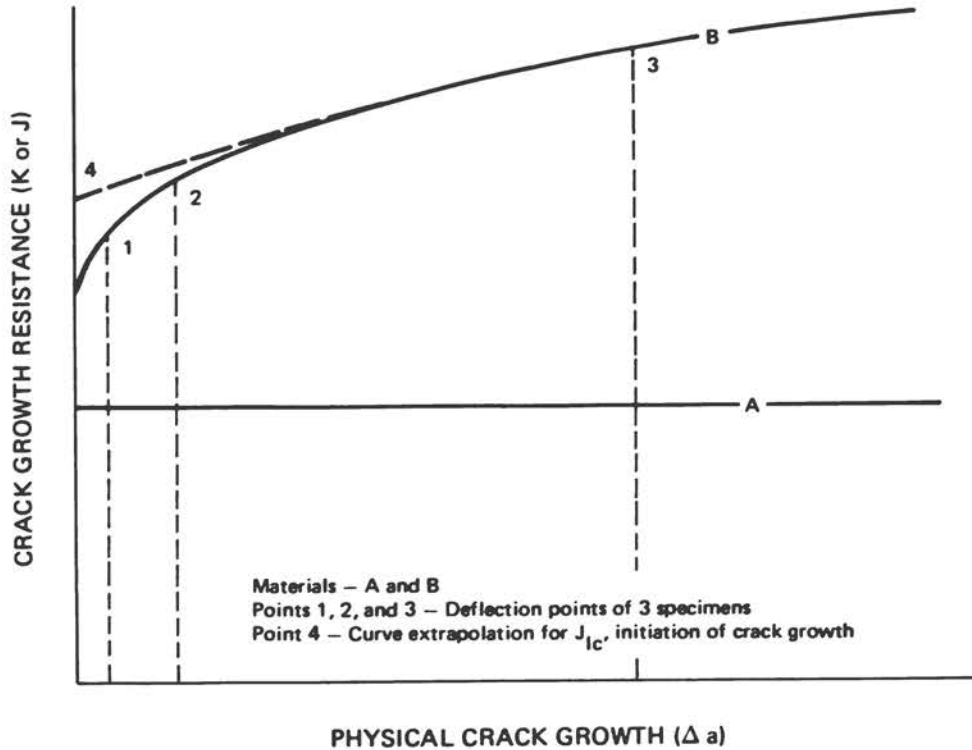
FIGURE A-1 Schematic Crack Growth Resistance Curves.

The requirement of multiple samples for a J_{Ic} test is apparently a disadvantage; however, one does not depend on a single K_{Ic} test value and several specimens generally are tested to obtain an average. In a sense, the extrapolation technique to obtain a J_{Ic} value also results in an average of toughness since the scatter in the plot of J versus crack growth can be used to infer a range of J_{Ic} values. Furthermore, the approximate R-curve obtained is basically of much greater value than the single arbitrary point which corresponds to K_{Ic}.

Various techniques have been used to obtain a J_{Ic} value from a single specimen test. Ultrasonics, elastic compliance, and electric potential have been used to determine the onset and extent of crack growth during a fracture toughness test. While these efforts have been successful, the instrumentation and experimental procedure is more complex than a K_{Ic} test.

A.4.2 Correlation of K_{Ic} and J_{Ic} Fracture Toughness Measurements

The rationale or theoretical basis for the use of the J integral as a fracture criterion reveals a direct relationship between J_{Ic} and K_{Ic} characterization of fracture toughness. This relationship is given by:

$$K_{Ic} = \sqrt{\frac{J_{Ic} E}{(1 - \nu^2)}} \quad , \qquad (A-3)$$

where E is Young's modulus and ν is Poisson's ratio. There is some controversy over the inclusion of the $(1 - \nu^2)$ term; however, the value is small and only changes the result by perhaps 5 percent.

A comparison of K_{Ic} and J_{Ic} toughness values is complicated by the choice of a measurement point. The ASTM definition of the K_{Ic} test places the measurement point at the K level required to cause up to 2 percent growth of the original crack. There is as yet no standard J_{Ic} measurement point, but recent publications tend to choose the initiation of crack growth as determined by an extrapolation technique. An illustration of difficulties involved in the selection of a suitable toughness measurement point is shown in Figure A-1, which presents schematic plots of the crack growth resistance (R curves) of two idealized materials. The toughness characterization may be K or J, and the abcissa is actual physical crack extension. The choice of a toughness characterization level for material A is obviously insensitive to any specified amount of crack growth, while the toughness of material B is sensitive to the absolute level of specified crack growth. Moreover, a relative specification of the measurement point, such as 2 percent growth for K_{Ic} testing, may lead to higher toughnesses as the specimen size increases. A systematic increase of "valid" ASTM E399 K_{Ic} values with increasing specimen size has, in fact, been noted for a titanium alloy (May, 1970). Fortunately, K_{Ic} testing is applied mainly to materials having shallow R curves and, consequently, routine specimen sizes lead to measurement points to the right of point 3 shown in Figure A-1. Beyond this point, specimen size has no significant effect on the K_{Ic} toughness value.

When comparing K_{Ic} and J_{Ic} toughness values, the relationship of Eq. A-3 is expected to be valid for materials having level or relatively shallow R curves. If this is not the case, then the initiation of crack growth (point 4 in Figure A-1) and perhaps determined by extrapolation, may occur at a toughness level substantially below that of 2 percent crack growth in a large specimen (point 3). Hence, in this case, J_{Ic} toughness values are expected to be lower than comparable K_{Ic} values.

An obvious solution to the latter problem would be to compare J_{Ic} and K_{Ic} toughness levels at the same amount of physical crack growth, but this procedure appears tenuous at present. If substantial crack growth (on the order of 10 percent) occurs, J calculations may be seriously in error. Additionally, the K_{Ic} compliance evaluation of 2 percent crack growth is complicated by plasticity effects. The actual physical crack growth at the K_{Ic} point may be 1 percent or less. While this procedure has its pitfalls, the concept is worthwhile and further research may provide practical results.

A comparison of K_{Ic} and J_{Ic} toughness measurements is shown in Figure A-2. The K_{Ic} values are valid according to ASTM E399 criteria and, for the most part, represent an average of several tests. The materials shown

have fairly level R curves; therefore, no ambiguity should exist between $\sqrt{\dfrac{J_{Ic}\,E}{(1-\nu^2)}}$
K_{Ic} and J_{Ic} measurement points. The correspondence of K_{Ic} and
is excellent, with most points falling within a ± 10 per cent
scatterband. Because of the scatter in normal fracture toughness
testing, this agreement is as good as can be reasonably expected.

For materials with distinctly rising R curves, the agreement of K_{Ic} and
J_{Ic} toughness levels will not be as good as shown in Figure A-2. The K_{Ic} measure-
ment point will be further out on the R curve and, thus, will be somewhat higher
than a J_{Ic} level that is based on crack initiation. Further research may
substantiate a choice of a common measurement point.

At the present time, K_{Ic} and J_{Ic} toughness characterizations agree quite
well for materials with level R curves. For materials with significantly rising
R curves (i.e., crack growth only under a rising driving force), the J_{Ic} toughness
is a lower bound of the K_{Ic} toughness.

Figure A-3 shows the effect of test temperature on K_{Ic} and J_{Ic} fracture
toughness characterizations.
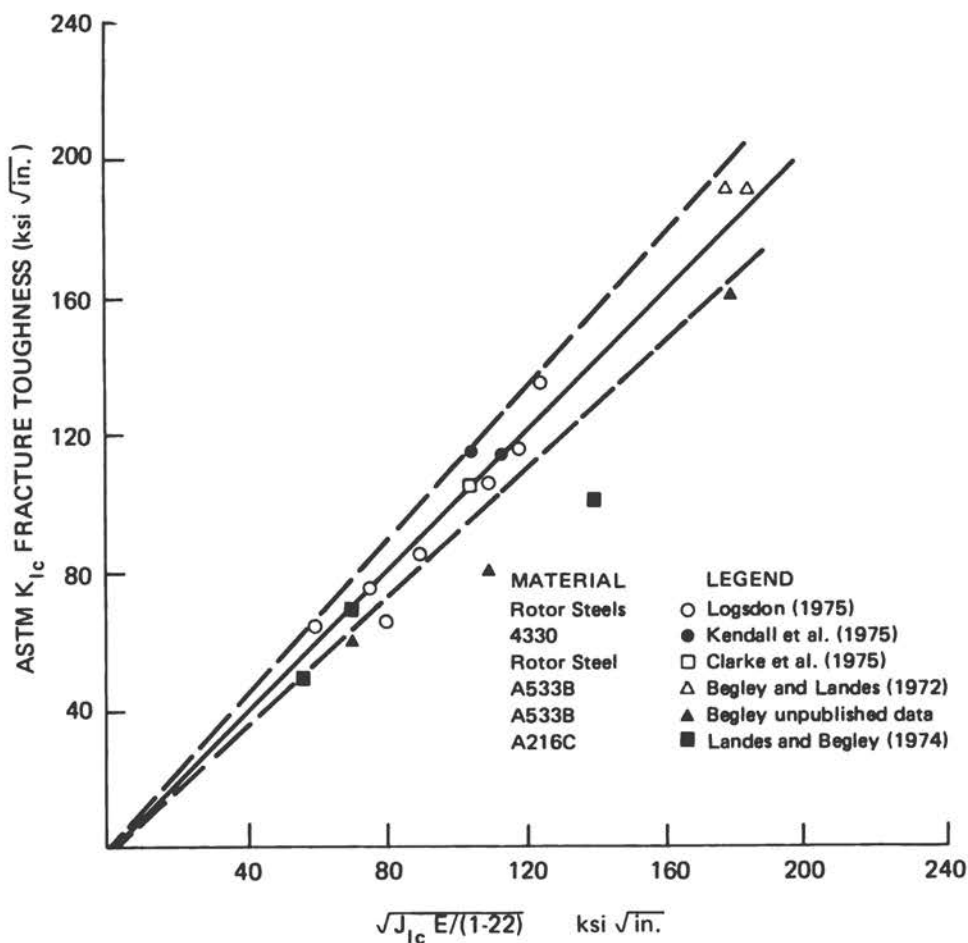
FIGURE A-2 Comparison of K_{Ic} and J_{Ic} Fracture Toughness Measurements.
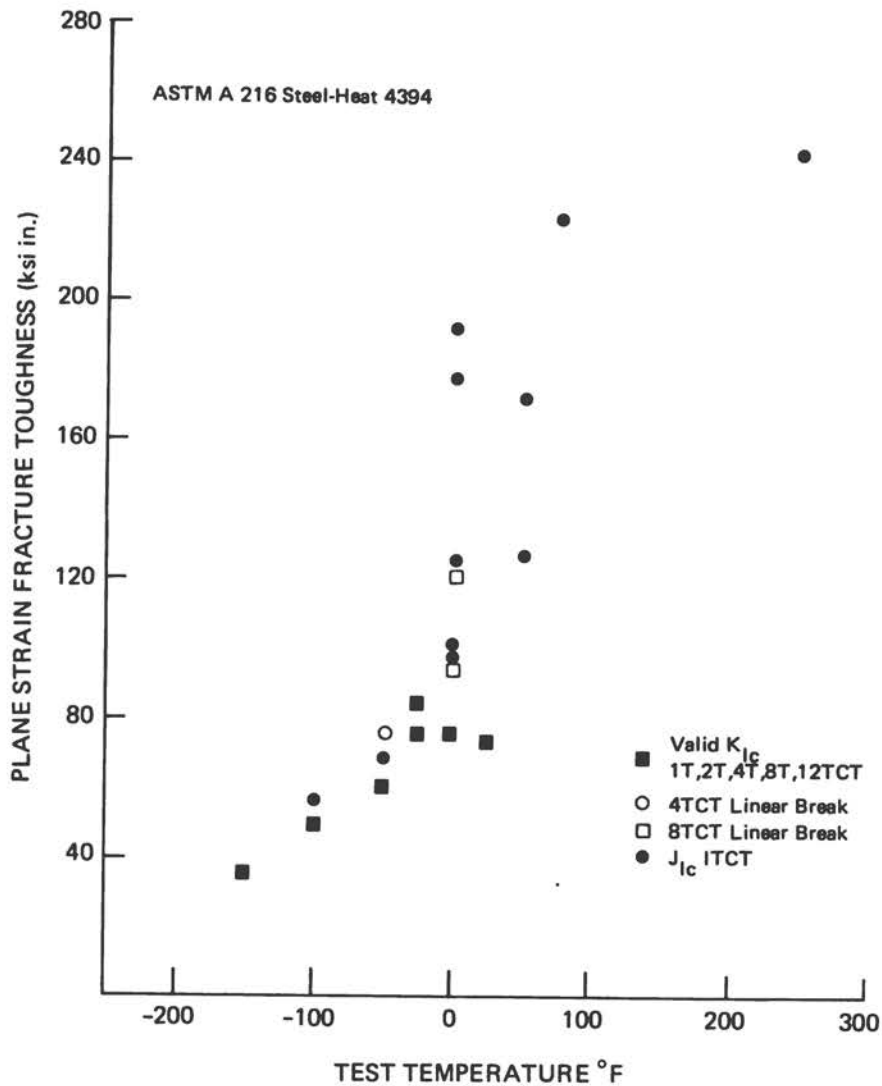
FIGURE A-3 Fracture Toughness versus Test Temperature.

A.5 PROGRESSIVE DEVELOPMENT OF CRACK EXTENSION RESISTANCE WITH CRACK GROWTH -- R CURVES

The crack extension resistance of a material is not a single-valued quantity; rather, it increases to balance the increase of applied crack extension force up to some point of instability that depends on the form of the cracked body and on the boundary conditions, as well as on the nature of the material. The crack growth that occurs before instability can vary from negligible to many times the original crack size, again depending on the circumstances.

This phenomenon and its quantitative treatment is illustrated below by describing a hypothetical experiment and the data reduction required to obtain an R curve. Descriptions of real experiments, such as can be found in ASTM STP 527 (1973), are not suited to the present didactic purpose because the essence of the matter is obscured by various practical considerations and limitations.

The hypothetical test specimen is a center-pin loaded single-edge cracked plate (shown inset in Figure A-4). Rotation at the pins is assumed to be unconstrained so that the cracked test section is subjected effectively to a combination of tension and bending rather than to tension only (such a configuration has a relation between compliance and crack length which is suited to the present purpose, as explained subsequently). The necessary linear elastic stress
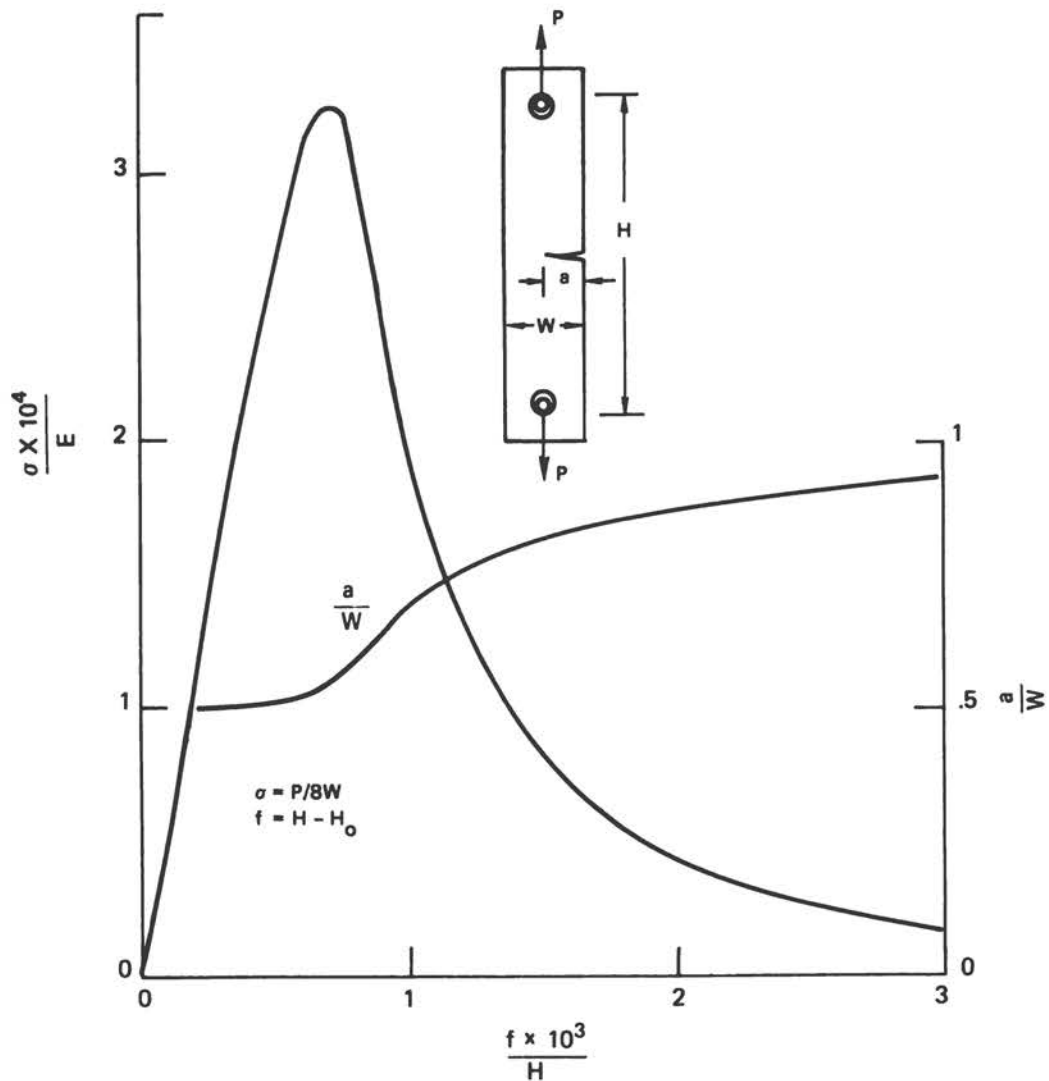
FIGURE A-4 Test Record for Determination of Crack Extension Resistance as a Function of Crack Growth for a Practically Linear Elastic Material (Srawley, 1975).

intensity factor and compliance relations are available for the entire range of
relative crack length (a/W) with adequate accuracy (Tada, 1973). The material
tested is assumed to behave in a practically linear elastic manner throughout
the entire course of the test and to have substantial resistance to crack extension.
Such a combination of behavior could be obtained in practice by using a specimen
of appropriate material and thickness with sufficiently large planar dimensions.

The variable controlled in the test is the relative displacement of the
points of load application ($f = H - H_0$) which is increased at some slow, steady
rate. If, alternatively, the test were to be conducted at a steady rate of increase
of force, no matter how slow, it would terminate abruptly at maximum load.
The load and the crack length are monitored continuously or at frequent intervals
during the test. Figure A-4 shows the most important part of the resulting record
-- i.e., from the start of the test to the point at which the crack has extended
from its initial value of 50 percent to 93 percent of the specimen width. The
remainder of the record would show the further increase of crack length and
corresponding decrease of load to zero at the point at which the specimen was
completely severed, but this occurs over a range of increase of displacement
10 times greater than that covered by Figure A-4.

In this and subsequent figures in this section, the variables employed
are in dimensionless form. Absolute magnitudes are not relevant because the
purpose is to illustrate the phenomenon and the procedure, not the behavior of
a particular material.

From the information on the test record the instantaneous
crack extension resistance can be calculated from the corresponding values of
f, the force P, and the crack length a. The basis of the calculation procedure
is shown in Figure A-5 for linear elastic materials considered here. Thus,
the crack extension resistance, R, corresponds to the crack extension force $\mathcal{G}$
rather than J. For materials that behave in a nonlinear but still practically
elastic manner, the crack extension force would be termed J, and the basis of
the calculation procedure would be a generalization of that presented in
Figure A-5 that would incorporate the appropriate nonlinear form of relation
between P and f with parameter a. For elastoplastic materials the matter is
more complicated.

On the basis of Figure A-5, the procedure for obtaining a set of values
of crack extension resistance, R, as a function of crack extension, ($a - a_0$),
from the test record (Figure A-4) is as follows:

Step 1 -- Obtain a suitable set of values of the work done by the force,
U_p, as a function of f, by numerical or other means of inte-
gration of the record of P versus f. The curve representing
U_p versus f for the present case is shown in Figure A-6.

Step 2 -- Calculate the corresponding set of values of the recoverable
stored energy, $U_S = Pf/2$, and also that of the energy absorbed
by the resistance to crack propogation, $U_A = U_p - U_S$. The
curve of U_A versus f is the lower curve in Figure A-6.
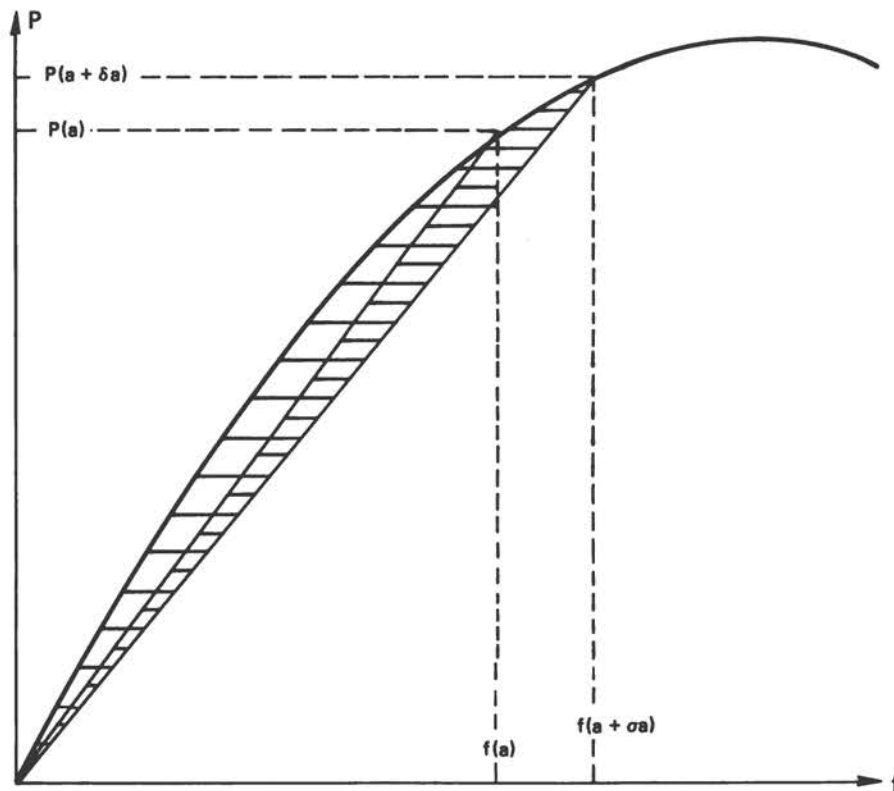
Energy U_A absorbed by crack extension resistance from the start (0,0) to the point (f, P) is the difference between the work done by the force, U_P, and the recoverable stored energy, U_S:

$$U_A = U_P - U_S = \int_o^f Pdf - \frac{Pf}{2}$$

$$\delta U_A = \int_{f(a)}^{f(a+\delta a)} Pdf - \frac{P(a+\delta a)f(a+\delta a) - P(a)f(a)}{2}$$

$$R = \underset{\delta a \to o}{\text{LIMIT}}\left(\frac{\delta U_A}{B\delta a}\right) = \frac{\partial}{B\delta a}\left(\int_o^f Pdf - \frac{Pf}{2}\right)$$

FIGURE A-5   Relation of Crack Extension Resistance R to f, P, and a (Srawley, 1975).
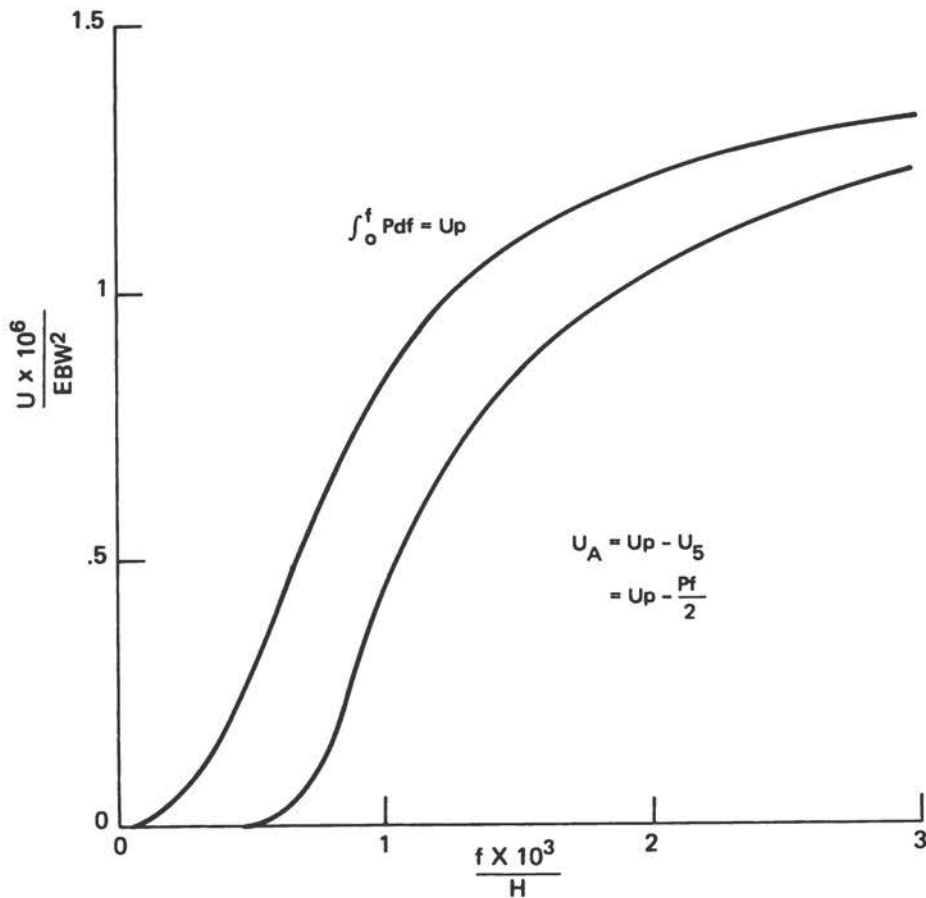
FIGURE A-6   Work Done on the Specimen (U_p) as a Function of Relative Displacement of the Load (f/H) Obtained by Integration of the Test Record (Figure A-4), and Energy Absorbed by Resistance to Crack Extension (U_A) (Srawley, 1975).

Step 3 -- Relate the values of U_A to the corresponding values of the crack length, a, as shown in the curve in Figure A-7, and determine the values of the slope $\partial U_A/\partial a = BR$, where B is the plate thickness, by numerical or other means of differentiation.

Step 4 -- The plot of R versus a, shown in dimensionless terms in Figure A-8, is the required R curve. It is usual, however, to plot R versus $(a - a_0)$ because it is expected that the R curve will be independent of a_0 (or, at least, largely so).
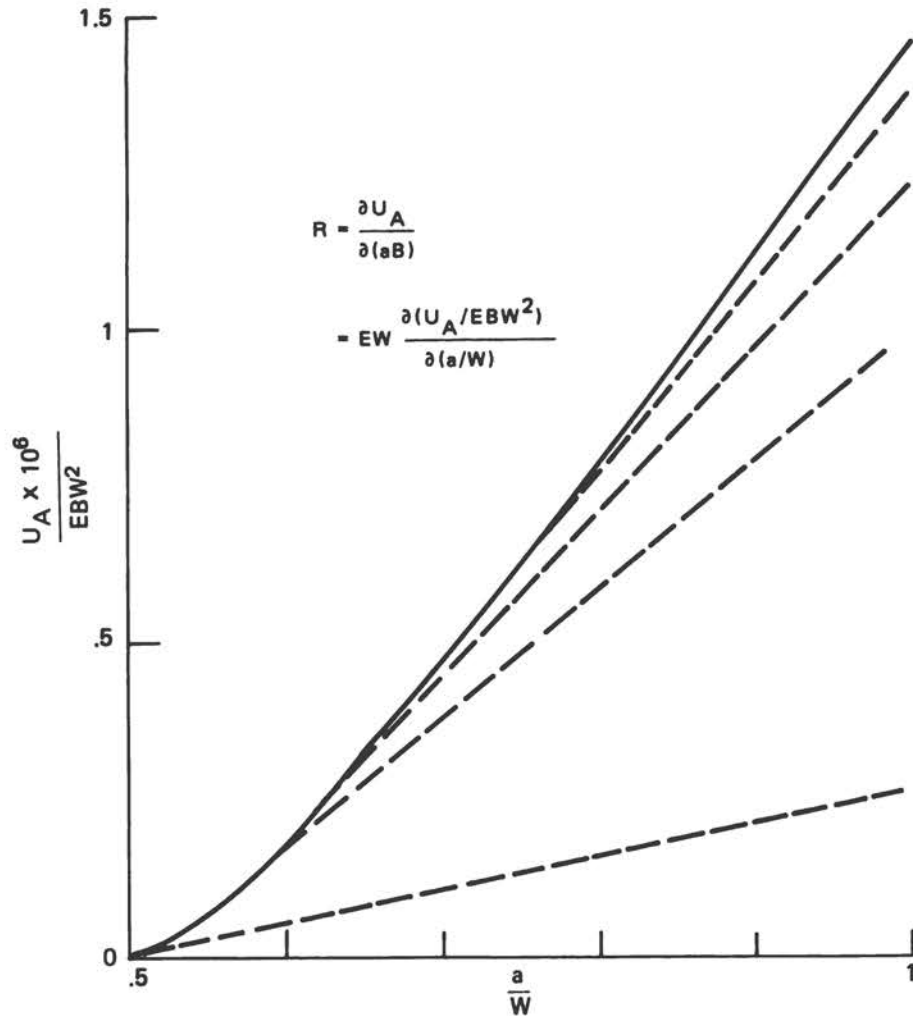
NOTE: The values of the crack extension resistance,
R, are proportional to the slopes of this curve.

FIGURE A-7   Energy Absorbed by the Resistance to Crack Extension (U_A)
as a Function of Crack Length (a/W) (Srawley, 1975).

While R curves are expected to vary considerably in form and magni-
tude with such factors as material, thickness and temperature, they should
conform to certain features of shape consistent with physical principles and
experimental observation. Thus:

a. The crack extension resistance should reach some value, R_0, before
   any crack growth occurs. The value of R_0 will depend on the
   characteristics of the initial precrack, which are determined by the
   way it is produced.
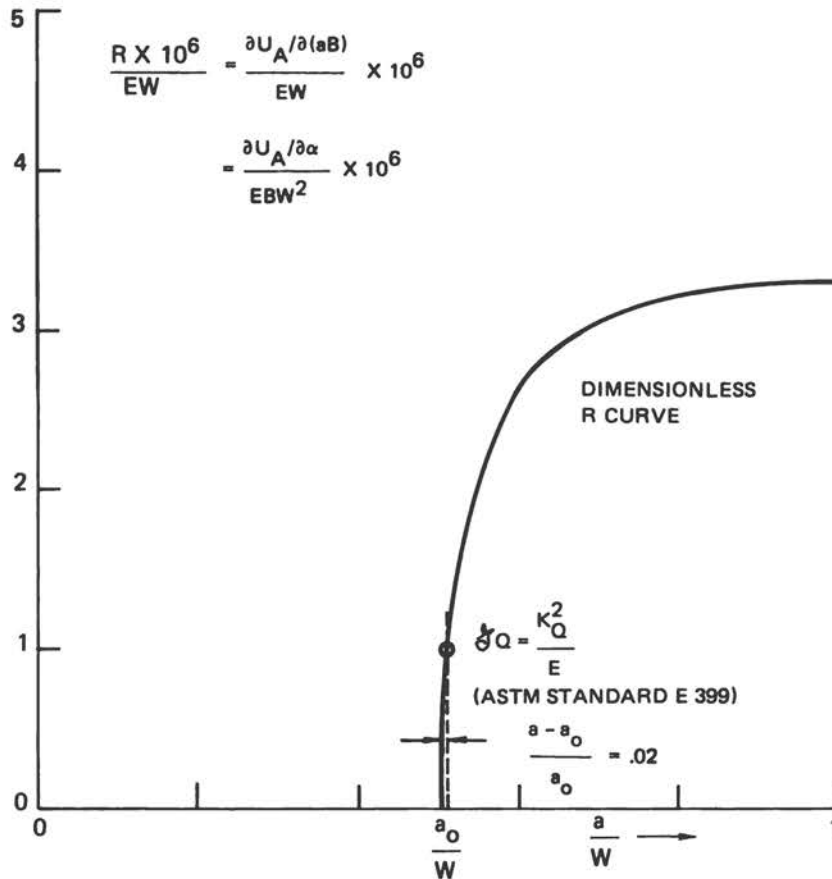
NOTE: The R curve results from the series of operations illustrated in Figures A-4 through A-7.

FIGURE A-8   Crack Extension Resistance as a Function of Crack Growth (Srawley, 1975).

   b. The resistance should not continue to increase indefinitely but should approach some asymptotic finite value, R_A.*

   c. The increase of R from R_0 should be practically completed when the crack length has increased by some finite amount, $(a_1 - a_0)$, which depends on the material and the thickness but is not more than about four times the thickness and may be negligible.

The hypothetical R curve in Figure A-8 was designed deliberately to exhibit these features of form, which can be incorporated into a fairly simple analytical expression. The shape parameters were chosen to illustrate a fully

_____

* Most R curves obtained in practice, however, are truncated at some value considerably lower than R_A because of the nature of the particular form of test that is conducted.

developed R curve for a material and thickness such that the initially square crack surface, free of shear lips, would transform through the transitional stage of shear lip growth to a finally fully oblique crack surface. The length over which this transition occurs is $(a_1 - a_0)$, as mentioned in item c above.

It is appropriate here to consider the connection between ASTM E399 and the R curve of Figure A-8. For this purpose, the value of $\mathscr{J}_Q$ that corresponds to K_Q, as defined in ASTM E399, section 9, is marked on the R curve: $\mathscr{J}_Q = K_Q^2/E$, where E is Young's modulus. At this point, the increase in crack length is 2 percent of the initial crack length. If the various requirements of ASTM E399 are satisfied, particularly sufficiency of specimen thickness and planar dimensions, the provisional values $\mathscr{J}_Q$ and K_Q are accepted as valid plane-strain fracture toughness values $\mathscr{J}_{Ic}$ and K_{Ic}; if the requirements are not satisfied, these values may bear no relation to the fracture toughness of the material and should not be regarded as approximate estimates. The value of $\mathscr{J}_Q$ in Figure A-8 is less than one-third of the asymptotic value, R_A, of the R curve, and this is quite consistent with what is known about the fracture toughness of materials in comparatively thin sections compared with plane-strain fracture toughness values obtained from tests of sufficiently thick sections. It should be appreciated, however, that it is not always possible to exploit a substantial part of the full potential toughness of a thin material because this is only developed when the crack becomes sufficiently long, whereas the crack length at which instability occurs could be comparatively short (see Figure A-10). One important consequence is that the application of K_{Ic} values to problems involving cracks in thin sections is not necessarily unduly cautious even though the proper justification is not immediately obvious.

The R curve of Figure A-8 is reproduced in Figures A-9 and A-10 -- in the first case with a set of dashed curves that represent crack extension force $\mathscr{J}$ as a function of relative crack length, a/W, for fixed values of the relative displacement, f/H; and in the second case with a contrasting set of dashed $\mathscr{J}$ curves for fixed values of the load parameter, σ/E. Each of these sets of dashed curves has a common shape since it represents the same functions of a/W, with magnitudes proportional to $(f/H)^2$ and $(\sigma/E)^2$, respectively. In Figure A-9 the intersections of the $\mathscr{J}$ curves with the R curve correspond to points on the original test record, Figure A-4. For form of these $\mathscr{J}$ (f/H) curves is such that they all intersect the R curve for all values of f/H. This means that quasistatic stability is maintained throughout the test when the controlled variable is f/H.* In contrast, the $\mathscr{J}(\sigma/E)$ curves in Figure A-10 do not intersect the R curve unless the value of the parameter σ/E is less than 3.25. This value represents the maximum load for the test, and the corresponding $\mathscr{J}$ curve is tangent to the R curve at the value of the crack length, which corresponds to maximum load in Figure A-4. If the test had been conducted at a steady rate of increase of load rather than displacement, instability would have occured at maximum load, the

---

* This is not true of some other configurations, such as a center-cracked plate stretched in the direction normal to the crack, and is one reason for the choice of a single-edge cracked plate for the present purpose.
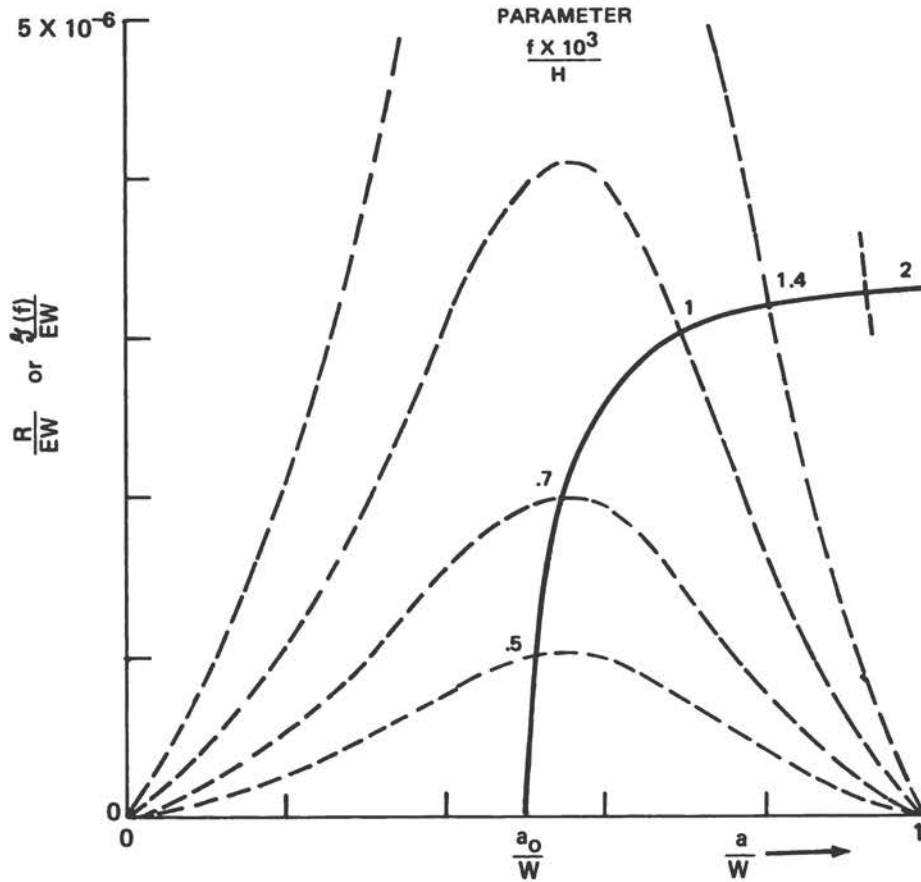
FIGURE A-9 R Curve with Superimposed Parametric Set of Crack Extension
Force (𝓖)Curves for Fixed Values of the Displacement Parameter
(f/H) (Srawley, 1975).

crack would have accelerated rapidly, and the test would have been terminated
almost immediately. Under these circumstances only that part of the R curve
up to the point of tangency could have been obtained.

Figure A-10 also can be regarded from a different point of view to
illustrate the application of R curves. Suppose that the R curve had already been
obtained by some other means (as, in fact, it was) and that the edge-cracked
specimen represents a cracked structural tension member. To determine the
maximum load that this member can sustain is simply a matter of finding the
value of the parameter σ/E at the point of tangency. In addition to the R curve,
this requires only a useful expression for the $\mathscr{Y}$ curves in terms of the two
variables a/W and σ/E.

The essential value of R curves depends upon a working hypothesis that
is commonly accepted but not yet thoroughly demonstrated. This hypothesis is
that the R curve for a given material in a given thickness is independent of the
configuration from which it was obtained and, consequently, is applicable to
any other configuration of the same material and thickness.
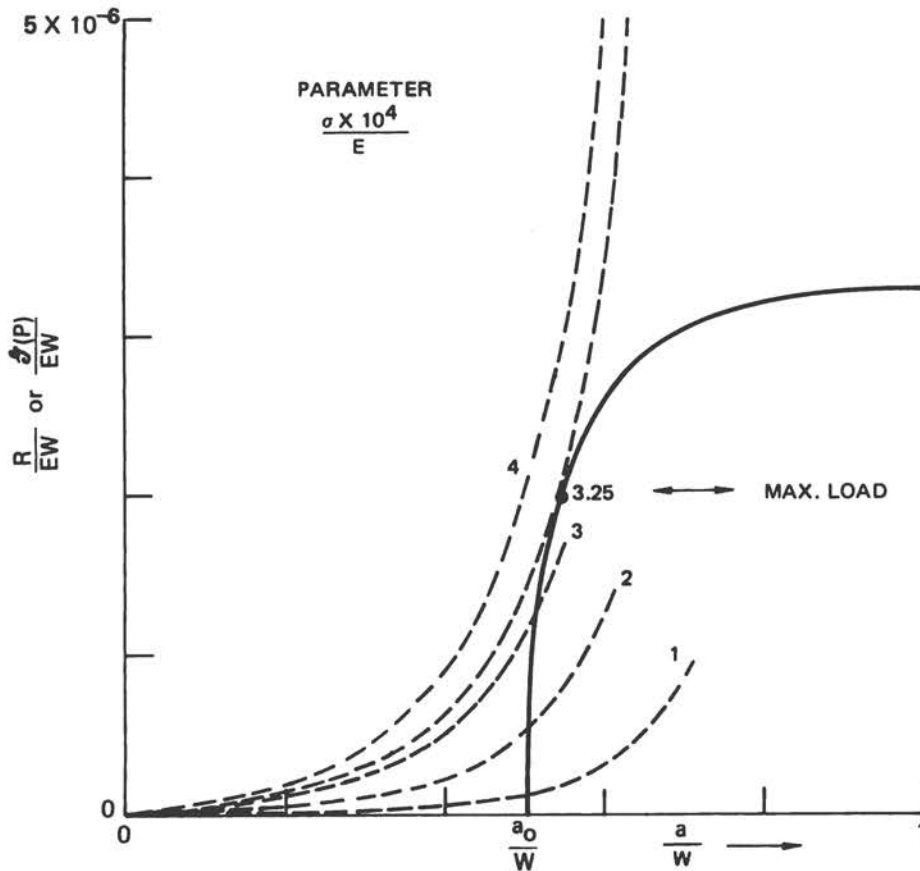
FIGURE A-10 R Curve with Superimposed Parametric Set of Crack Extension
Force (𝒢)Curves for Fixed Values of the Load Parameter (σ/E),
for Comparison with Figure A-9 (Srawley, 1975).

Understandably, the R curve will depend on temperature, which is
regarded as a material variable, and R applies only to quasistatic situations.
Since the R curve is known to be a function of thickness, any given R curve is a
plane section through an R surface at fixed thickness, but it appears that the
formidable task of determination of even part of an R surface has not yet been
attempted for any material.

The determination and application of R curves are very active areas of
current research from which a number of developments are expected in the next
few years. Currently, an ASTM Proposed Recommended Practice for R Curve
Determination (1974 Annual Book of ASTM Standards, Part 10) covers three
types of specimen and provides a framework for coordinated activity to develop
one or more standard test methods. The proposed calculation procedures are
equivalent to, but less fundamental than, that described here; they apply only to
practically linear elastic materials and this restriction permits the simplification.

A.6   THE CONCEPT OF CRACK OPENING DISPLACEMENT

Crack opening displacement (COD) originally termed "crack opening dislocation" (Wells, 1961 and 1963), is linked to linear elastic fracture mechanics through the recognition that in any real material there is a "plastic zone" around the crack tip which necessitates modification of the purely linear model. Qualitatively, the COD can be considered the amount of inelastic stretching of the material immediately ahead of the crack tip. It was the first quantity associated with linear elastic fracture mechanics to be proposed as a measure of fracture toughness in the predominantly inelastic regime of gross material behavior. The alternative expression, "crack opening stretch" (COS) (Irwin, 1972) also is encountered and was introduced because COD sometimes is used to denote the opening of the mouth of the crack notch.

The COD concept is appealing because it is superficially simple, plausible, and readily visualized in its ideal aspect. Unfortunately, no accepted operational definition of the COD exists to provide a basis for homogeneity among the sets of data reported by various investigators. It is very important to realize that the various sets of purported COD data were obtained in a variety of ways, mostly indirect, and are subjective to some degree. For this reason, COD measurements are considered only incidentally in this report, rather than on the same basis as standardized determinations of K_{Ic} or NDT temperature.

British Standard DD 19:1972 (British Standards Institution, 1972) is a step toward standardization of COD measurement, which is limited in scope to tests of three-point bend specimens. The COD value is not measured directly but is inferred from a measurement of the crack-notch mouth opening by a theoretical expression (Figure A-11). This British Standard states: "Although the crack opening displacement values inferred from the clip gauge measurements are not exact, they do provide an estimate of the true value which is sufficiently close for most applications of COD data." It is not explained what is meant by "true value," however.

To understand the COD concept, it is useful to consider an ideal line crack in a purely linearly elastic planar body. When forces are applied to the body so as to cause the crack to open, the crack profile will assume a form which is asymptotic at the tip to the vertex of a conic section (Figure A-12). The tip of the idealized open crack, therefore, has a definite radius of curvature exactly equal to $4\mathscr{J}/\pi E'$ (Williams, 1961). Thus, in ideal linear elastic fracture mechanics, the resistance to crack extension could be expressed just as well in terms of the crack tip radius as in terms of $\mathscr{J}$ or K.

The situation is changed considerably, however, if the linear elastic model is modified by introduction of a plastic zone around the crack tip. The crack then is deformed near the tip by plastic flow as well as elastically, and the radius of curvature at the tip becomes infinite (Figure A-13); consequently, the resistance to crack extension cannot be characterized usefully by this radius.
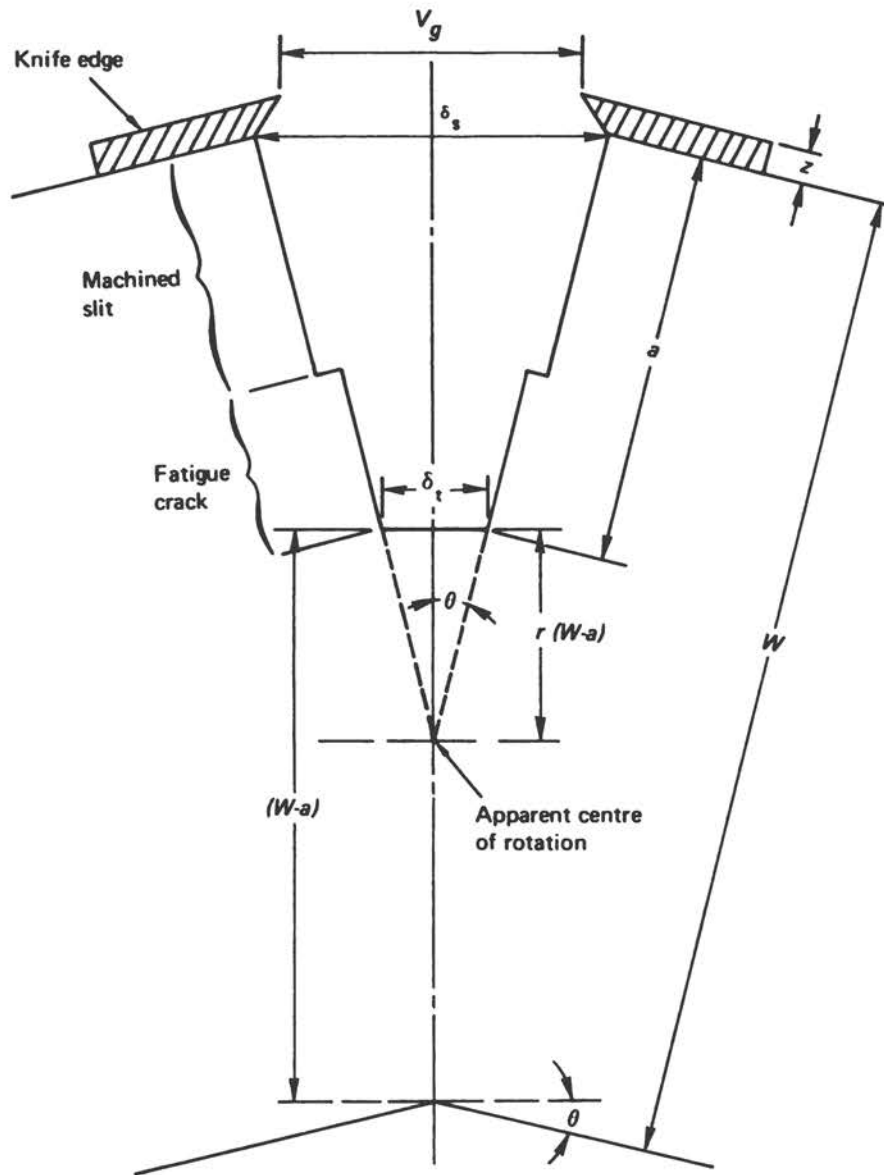
$$(1) \quad \delta_c = - \frac{0.45\,(W{-}a)}{0.45\,W + 0.55\,a + z} \left[V_c - \frac{\gamma\sigma_Y\,W(1{-}\nu^2)}{E} \right]$$

$$\text{for } V_c \geqslant \frac{2\gamma\sigma_Y\,W(1{-}\nu^2)}{E}$$

$$(2) \quad \delta_c = \frac{0.45\,(W{-}a)}{0.45\,W + 0.55\,a + z} \left[\frac{V_c^2 E}{4\gamma\sigma_Y\,W(1{-}\nu^2)} \right]$$

$$\text{for } V_c < \frac{2\gamma\sigma_Y\,W(1{-}\nu^2)}{E}$$

γ is a non-dimensionalized limiting value of elastic clip gauge displacement. $\gamma = V'E/\sigma_Y\,W(1{-}\nu^2)$ where $V' =$ limiting elastic clip gauge displacement, $\sigma_Y =$ material yield strength, $E =$ modulus of elasticity, $\nu =$ Poisson's ratio.

FIGURE A-11 Illustration of Basis of Calculation of COD (δ_t) from B.S. DD 19:1972 (British Standards Institution, 1972).
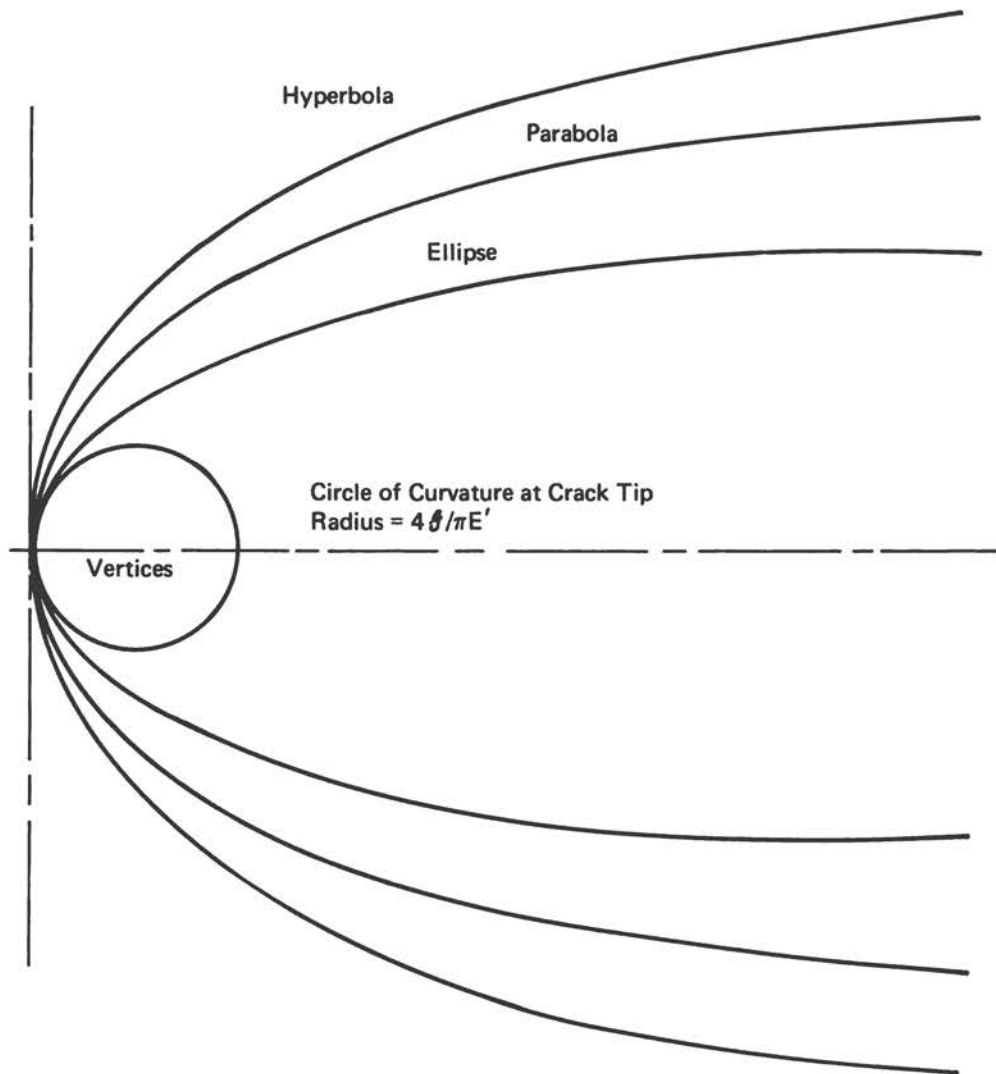
NOTE: The exact shape of a profile will depend on the loading
conditions of the cracked body.

FIGURE A-12   Conic-Section Asymptotes to Ideal Linear Elastic Crack Tip
Profiles (Srawley, 1975).

At the other extreme, an ideal line crack in a planar body that behaves
in an elastic/perfectly-plastic manner with constant flow stress σ can be con-
sidered. The appropriate model (Figure A-14) is the strip-yield model
(Dugdale, 1960), and the crack tip profile is definitely blunt with a well-defined
COD equal to J/σ_0 (Rice, 1968).

For more realistic materials in which flow stress is an increasing
function of strain, the shape of the crack tip should be intermediate, and the
value of the COD might be considered bound by the extremes $8J/\pi E'$ (the
diameter of the osculating circle at the tip of the linear elastic crack) and
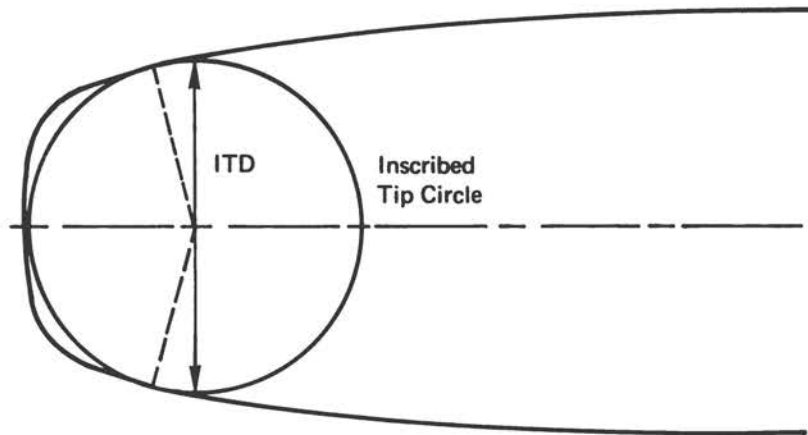
NOTE: The curvature is zero at the tip, but the diameter of the unique inscribed circle which is tangent at the tip is a well-defined characteristic dimension, ITD, of the crack tip.

FIGURE A-13   Crack Tip Profile in an Elastic-Plastic-Strainhardening Body (Srawley, 1975).
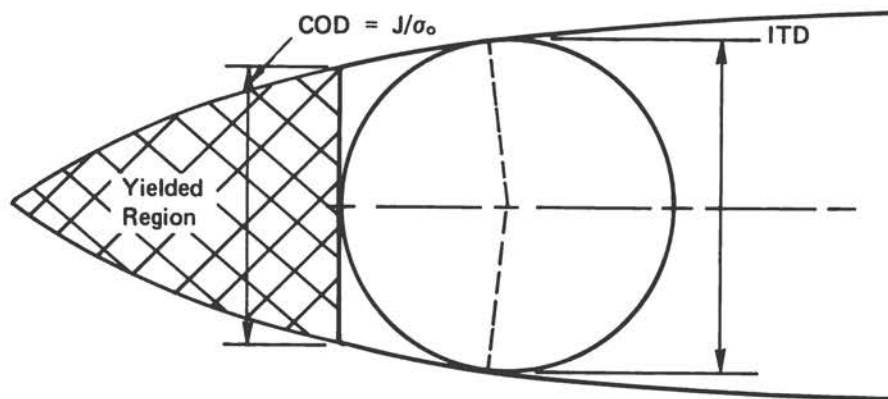
NOTE: Dugdale strip-yield model -- the ITD is well-defined, and somewhat larger than the COD, which is well-defined also for this model.

FIGURE A-14 Crack Tip Profile in an Elastic/Perfectly-Plastic Body (Srawley, 1975).

J/σ_0 (the COD for a nonhardening material). Since the ratio of these bounds is about $2.5\,\sigma_0/E'$ (typically of the order of 1/100), this information is not very specific. More definite information, obtained by numerical methods of analysis on large digital computing machines (Srawley, 1970 and 1971; Wells, 1971),

indicates that at any stage of loading where the nominal elastic and plastic strains are of comparable magnitude, the crack tip profile displays no obvious feature that might be used to define the COD precisely. However, there is one well-defined characteristic dimension of any (ideal) crack tip profile -- i.e., the diameter of the unique inscribed circle that is tangent at the crack tip and at two other symmetrically disposed points (Figures A-13 and A-14), or, in other words, the inscribed tip diameter (ITD) (Srawley, 1971). For linear elastic behavior, the ITD is identical with twice the radius of curvature at the tip; for nonhardening behavior it approaches the value of the COD as the ratio of plastic to elastic nominal strains is increased. Hence, the ITD could be considered a general measure of crack extension resistance. (To avoid further confusion of terminology, the ITD should not be called the COD.)

In essence, the ITD concept could provide a precise basis of an operational definition for one practical procedure that has been used for direct experimental measurement of what was referred to as the COD (Robinson, 1974). In this procedure, a crack in a specimen under steady boundary displacement is infiltrated with a rubbery or polymeric catalytic hardening liquid. After setting, the negative replica of the crack tip is removed so that sections of it can be examined and measured. This procedure for measuring COD is somewhat subjective, however, and a more objective operational procedure could be specified in terms of the ITD. This direct experimental approach to characterization of crack tip bluntness has so far been applied to only a few materials, and, although the approach is too tedious for routine use, it should be applied to many more materials to calibrate indirect methods that would be more suitable for routine use.

In summary of this section, the characterization of resistance to crack extension in terms of some measure of crack tip bluntness (usually called the COD) has received, and continues to receive, considerable attention. The direct method could prove economical of material -- COD measurements have been extracted from relatively small test pieces (Robinson and Tetelman, 1974) -- but is not inexpensive to perform. The main virtue of the indirect instrument test procedure of BS.DD 19:1972 is that it provides a measure of the full thickness toughness for non-plane-strain conditions. Neither procedure can be classed as rapid.

As a reference test concept, characterization in terms of crack tip bluntness would seem to have no advantage over characterization in terms of the J concept; indeed, it might have some disadvantages. The two concepts are formally connected, but not as simply as is sometimes suggested.

APPENDIX B

STATISTICAL TREATMENT OF CORRELATION DATA

Demonstrating an acceptable K_{Ic} level by means of measurements from a quality-control specimen requires that the relationship between the measurement and K_{Ic} be known for the specific alloy under consideration. Since both sets of data will exhibit variability, statistical analyses are required to correlate the variables. Such analysis also permits the risks of error to be expressed quantitatively in terms of probability and the strength of the correlation to be evaluated. Possible methods to be considered are discussed in this appendix and an example analysis on the sharp-notch round specimen is presented.

B.1   GENERAL

Implementing the usage of a quality-control test in lieu of the standard K_{Ic} test requires the correlation of data generated on the same material samples using the two methods. The number of data points required for a satisfactory correlation depends on the inherent variability of the test method involved, the material selected, and the accuracy needed in the estimation. The data from the standard K_{Ic} test are not fixed, firm numbers due to material and experimental variability. The problem of correlating two experimental variables dictates the use of a statistical approach.

B.2 K_{Ic} VARIABILITY

The standard K_{Ic} test method, ASTM E399, was evaluated under a round robin test program conducted by ASTM Committee E-24. A detailed accounting of the test results using the three-point bend specimen is presented in ASTM STP 463. To provide an indication of the magnitude of inherent scatter in the determination of K_{Ic} for aluminum, the data from this round robin K_{Ic} testing program among nine laboratories were reviewed. The pooled standard deviation of K_{Ic} values from replicate tests of 2219-T851 aluminum after removing a possible bias effect due to laboratories was 1.1 ksi √in. (this value excludes one

50

laboratory that had a significantly larger variation). Thus, under these idealized conditions, a single observed K_{Ic} value on this aluminum alloy can be expected to be within ±2.2 ksi √in. in 95 percent of the determinations. For a true mean K_{Ic} value of 30 ksi √in., this would represent an error of less than 7.5 percent in 95 percent of the single determinations.

To provide a material comparison, 4340 steel was tested in the same round robin, and the results exhibited a variation slightly less than that of the aluminum data on a percentage basis.

B.3   METHODS OF CORRELATION ANALYSIS

Several methods can be used to interpret the data from a quality-control test and to infer from these results a level of fracture toughness. Three methods are discussed and examples are given of their use.

B.3.1   Probability Distribution Analysis

The probability distribution method, which is presented in Military Handbook 5B (Department of Defense, 1966) for use in evaluating other mechanical properties, provides for the calculation of a one-sided lower tolerance limit above which subsequent data points will fall with a specified reliability and confidence level. An analysis of aluminum alloy data obtained using a sharp-notch round specimen was made to determine notch-yield strength ratios and K_{Ic} values that could be exceeded by subsequent test values with 90 percent probability* and 95 percent confidence.* Results are presented in Figure B-1 for each of the longitudinal-transverse (L-T), transverse-longitudinal (T-L), and short-longitudinal (S-L) crack propagation directions. This analysis assumes a correlation exists between the two variables; for an estimate of the degree of correlation, a regression analysis must be conducted.

---

* Military Handbook 5B (Department of Defense, 1966) defines probability as: "The ratio of the possible number of favorable events to the total possible number of equally likely events. For example, if a coin is tossed, the probability of heads is one-half (or 50%) because heads can occur one way and the total possible events are two, either heads or tails. Similarly, the probability of throwing a three or greater on a die is 4/6 or 66.7%. Probability, as related to design allowables, means the chances of a material-property measurement equalling or exceeding a certain value (the one-sided lower tolerance limit." Confidence is defined as: "A specified degree of certainty that at least a given proportion (P) of all future measurements can be expected to equal or exceed the lower tolerance limit. The degree of certainty is referred to as the confidence coefficient. The confidence level is a judgment of how well the sample reflects the larger population distribution."
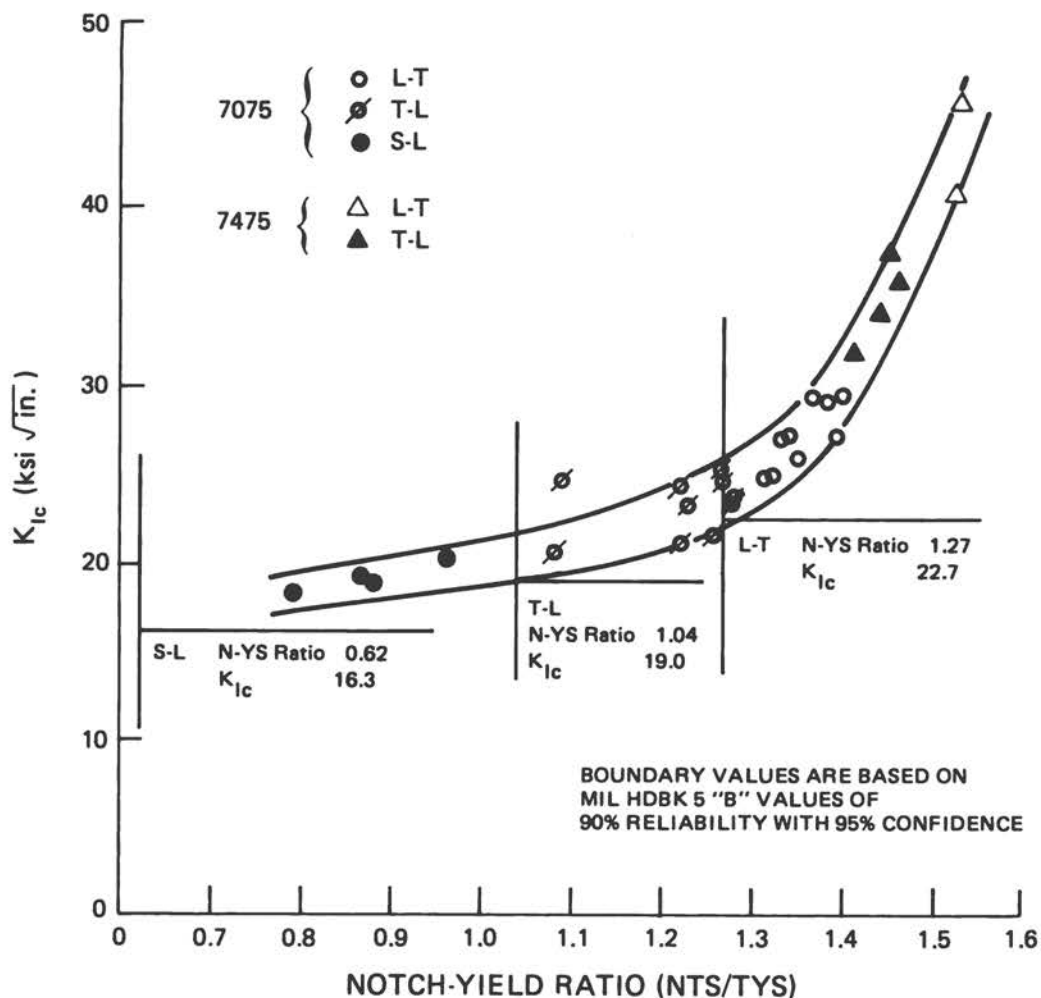
FIGURE B-1   One-Sided Tolerance Limits Applied to 1/2-in.-diameter
Sharp-Notch-Round Data (based on data from Kaufman, 1973).

B.3.2   Linear Regression Analysis

When two materials properties are known to be related functionally, a linear regression can be used to determine the degree of association or correlation between them. In this application, the quality-control test result (independent variable) is to be correlated to the fracture toughness indicator, K_{Ic} (dependent variable). From the matched data sets of each variable required for this correlation effort, an indication of the goodness of fit to the regression line also is obtained (see paragraph B.3.4).

B.3.3 Multiple Regression Analysis

Often the two functionally related variables to be correlated are masked by other product variables such as thickness, strength level, and specimen size and orientation. By use of the multiple regression techniques, the minor variables in a regression equation can be accommodated and, therefore, the fit to a regression line can be enhanced. The regression line also is not restricted to linear fitting but may be curvilinear to improve the goodness of fit (see paragraph B.3.4).

B.3.4 An Example of the Application of Regression Methods to Sharp-Notch - Round Specimen Data

A compilation of matched sets of K_{Ic} and sharp-notch round specimen data was provided by the Aluminum Company of America for Committee analysis efforts. These data, for aluminum alloy 2124-T851 heavy-plate sections, are plotted in Figure B-2 for three different crack propagation directions. Each point indicates a discrete K_{Ic} and 1.060-inch-diameter sharp-notch round specimen data set. One technique for quality-control purposes would be to separate the data for each material grain orientation. Using a bivariant linear regression method, a best fit linear line through each orientation group is illustrated in Figures B-3, B-4, and B-5. The limit lines shown define the band within which subsequent data would be expected to fall with 90 percent reliability and 95 percent confidence. As can be seen, the band is very wide and the goodness of fit is not very satisfactory.

By use of a multiple regression technique, an improvement in the fit can be made by considering other variables that affect the data. A model for multiple regression has been presented based on the general form:

$$\log K_{Ic} = A_0 \text{ (thickness in inches)} + A_2 \text{ (yield strength)} +$$
$$A_3 \text{ (notch-yield strength)}, \qquad \text{(Eq. B-1)}$$

for use with the sharp-notch round specimen results (Kaufman et al., 1975). Application of a specific form of this model,

$$\log K_{Ic} = A_0 + A_1 \text{ (thickness in inches)} + A_2 \text{ (thickness -- 3.8)}^2 +$$
$$A_3 \text{ (yield strength)} + A_4 \text{ (notch-to-yield-strength ratio)},$$

$$\text{(Eq. B-2)}$$

to the data described above results in the improvement in productive capability shown in Figures B-6, B-7, and B-8. The open points are the original data and the asterisks are calculated values. Relative to the bivariate analysis, considerable improvement can be noted in agreement between data and prediction.
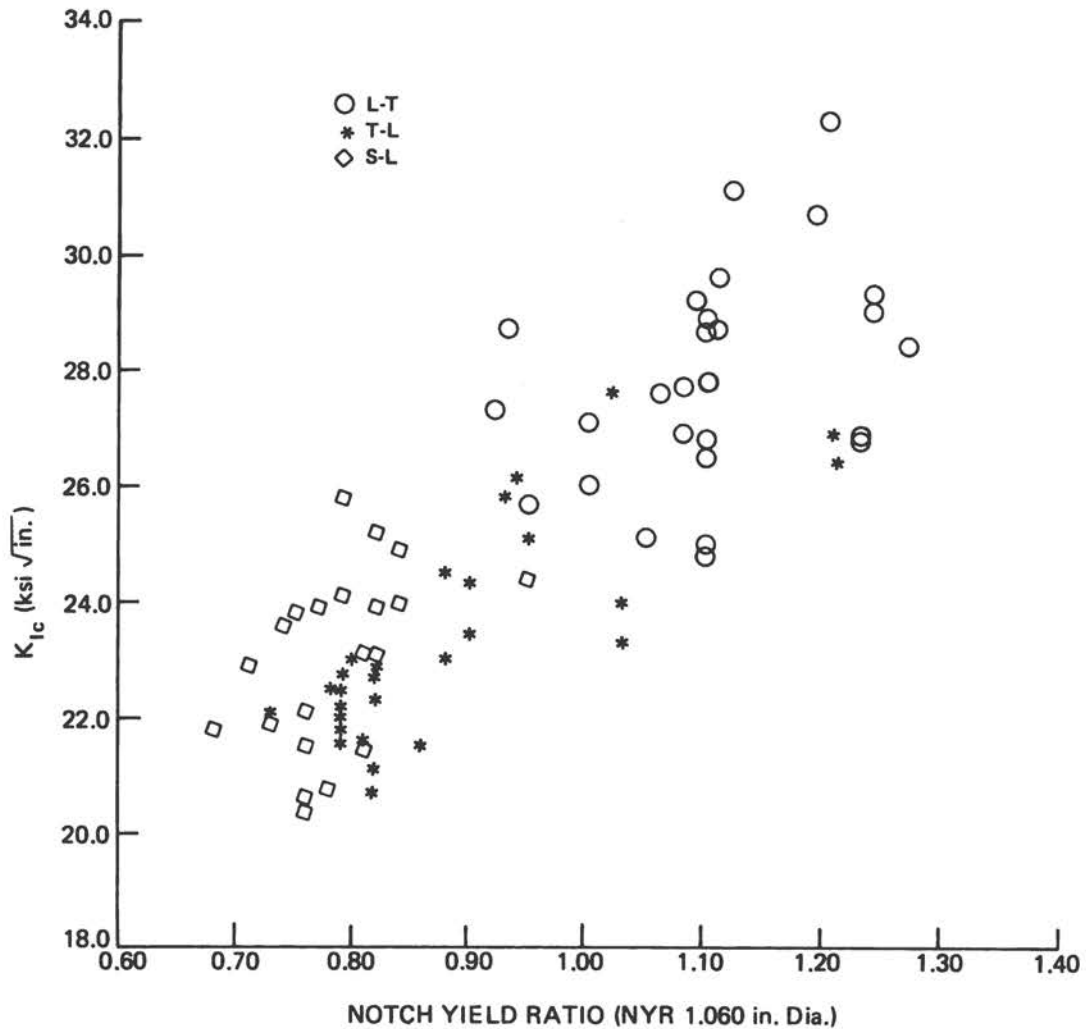
FIGURE B-2   Data Input Sets for Sharp-Notch-Round Analysis (based on data from Kaufman et al., 1975).

The specimen orientation effect drops out as a primary variable in this data group so the data from all orientations is presented in Figure B-9 with the curvilinear best-fit line.

B.3.4.1 <u>Data Presentation and Correlation</u>. The chosen method of presenting and correlating the data depends on the consistence of the input data and the end usage. A straightforward, simple approach would be the most desirable; however, as noted in the example, multiple variables often mask the
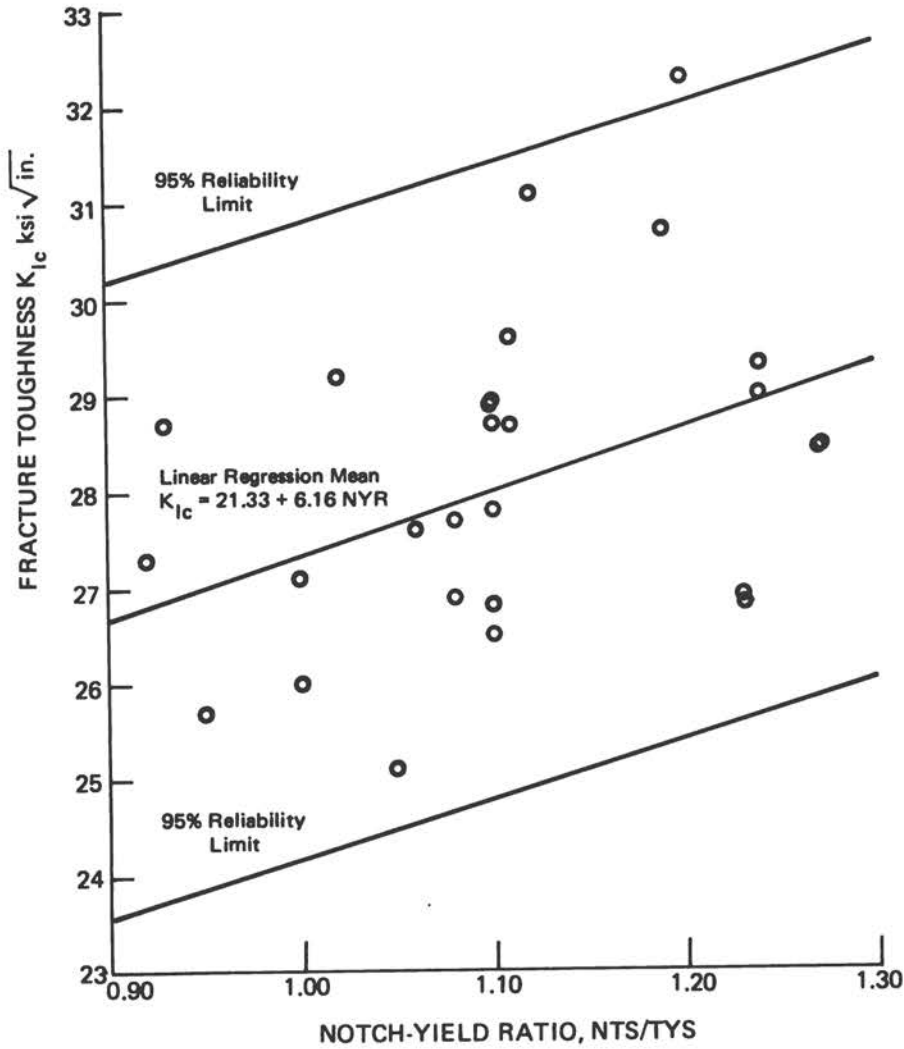
FIGURE B-3 Sharp-Notch-Round Analysis, Longitudinal Orientation.

relationship and a more complex procedure is required. A periodic updating of the correlation analysis is recommended to include more recently determined data to provide as wide a data base as possible and to make the correlation representative of current production material.
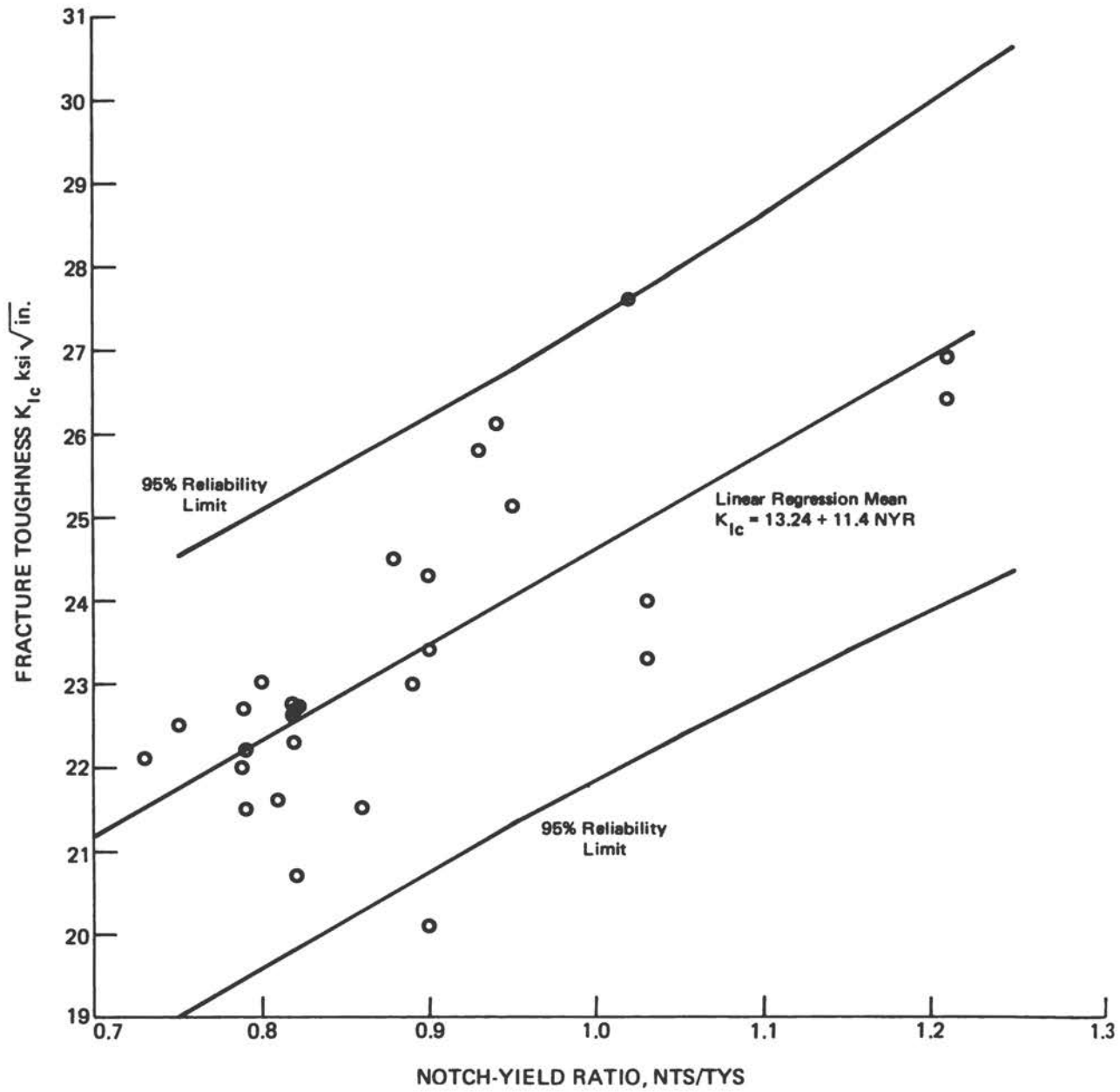
FIGURE B-4   Sharp-Notch-Round Analysis, Transverse Orientation.
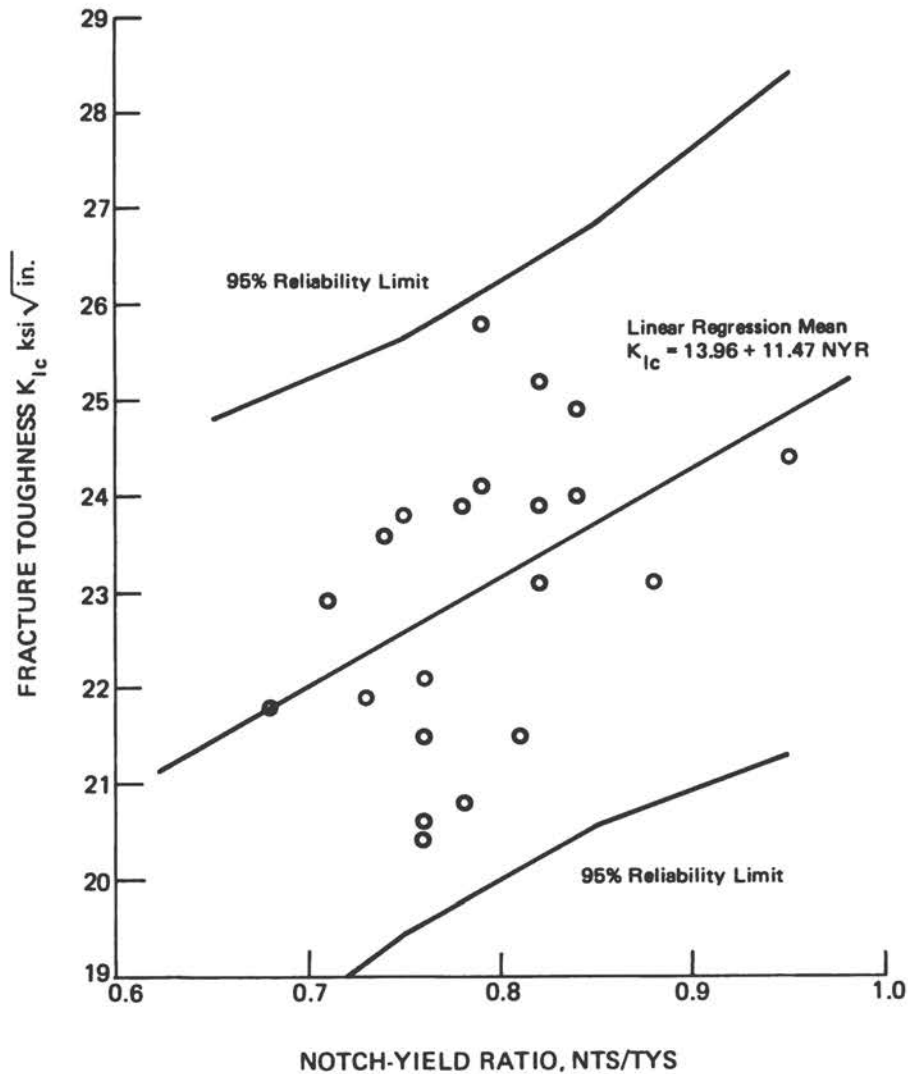
FIGURE B-5 Sharp-Notch-Round Analysis, Short-Transverse
Orientation.

B.4 ACCEPTANCE/REJECTION CRITERIA

If the quality-control test is to be used for a material, the criteria for
acceptance/rejection should be documented and mutually agreed upon by both
producer and consumer. How a quality-control specimen test can be used is
illustrated below by a procedure that proposes using the sharp-notch-round
tension specimen for aluminum alloys (Kaufman, 1973):

FIGURE B-6 Multiple Regression Analysis, Longitudinal
Orientation (based on data from Kaufman et al.,
1975).

a. Conduct a sharp-notch-round specimen test and divide the obtained
    notch tensile strength by the yield strength obtained per ASTM
    E8-69. This determination is called the notch-yield ratio (NYR).

b. If the NYR is greater than the acceptance level, the lot is accepted.
    If the NYR is less than the acceptance level, two additional notch
    tensile specimens will be tested. If both the retests exceed the

FIGURE B-7   Multiple Regression Analysis, Transverse Orientation (based
on data from Kaufman et al., 1975).

acceptance limit, the lot is accepted. If either of the retests fall below
the acceptance level, the lot is subject to K_{Ic} testing per ASTM E399-74.

c. If the K_{Ic} test passes the minimum K_{Ic} level, the lot is accepted. If it
falls below the minimum level, the lot is rejected.
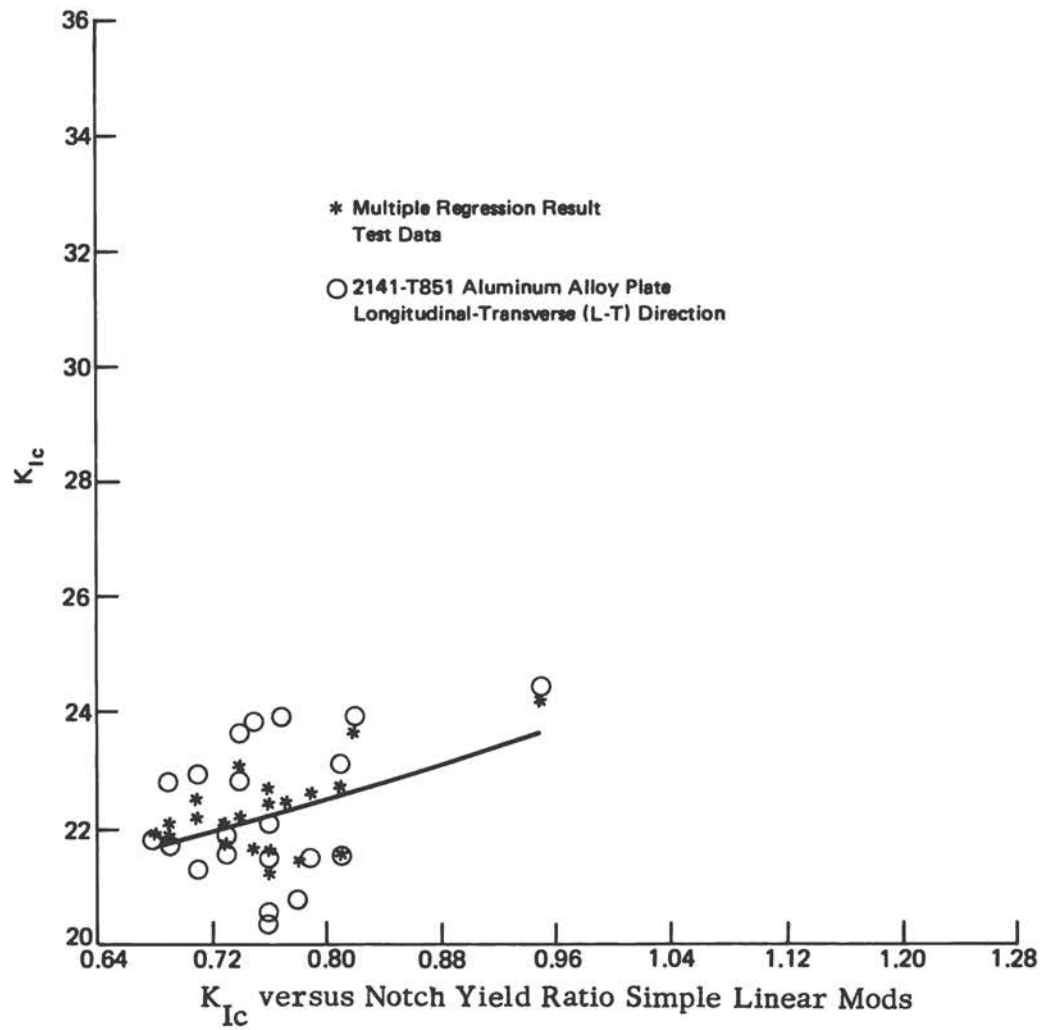
FIGURE B-8   Multiple Regression Analysis, Short-Transverse
Orientation (based on data from Kaufman, et al., 1975).
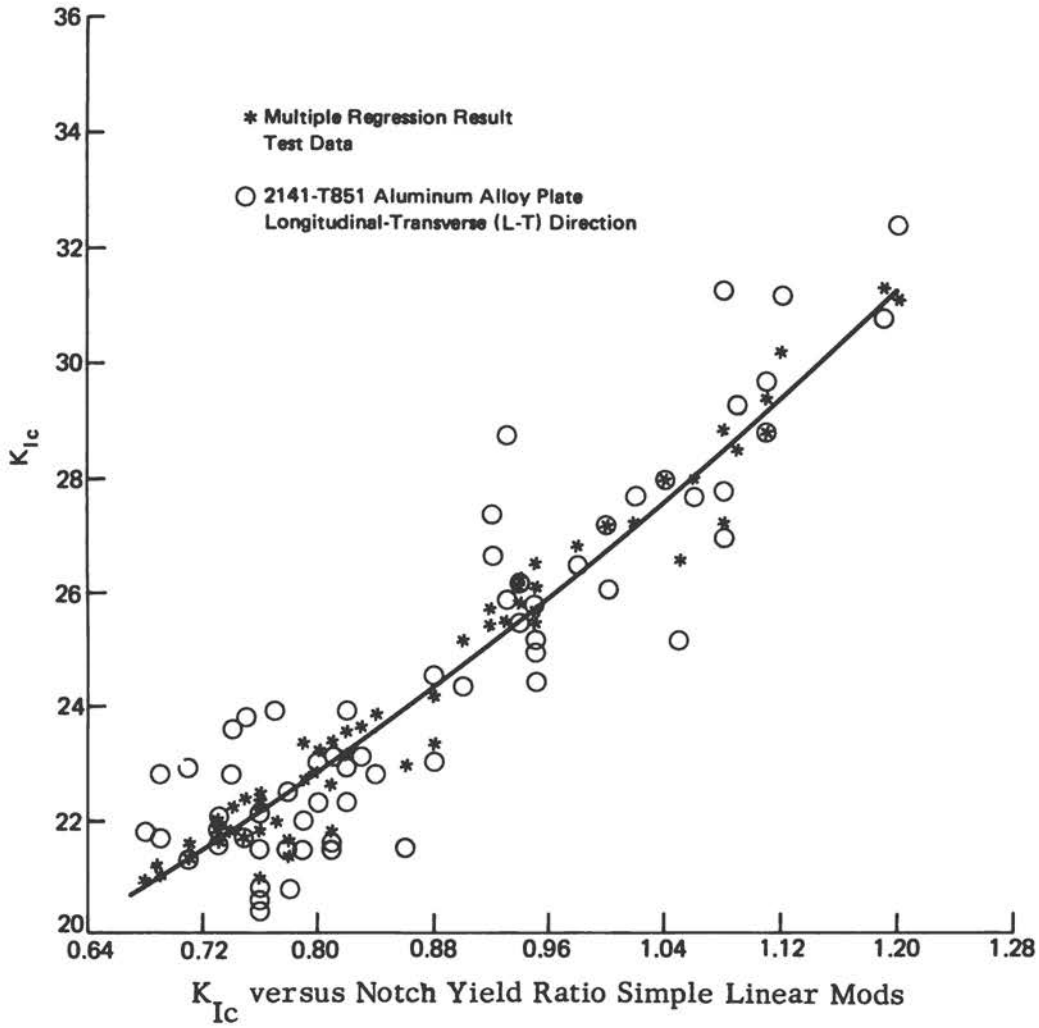
FIGURE B-9   Multiple Regression Analysis, All Orientations
(based on data from Kaufman et al., 1975).

APPENDIX C

TENSILE TESTS

C.1   NOTCH-ROUND TESTING

All specimens that can be tested on a tensile testing machine are discussed in this appendix. The variety of configurations under consideration include notch-round-bar specimens for plate and bar stock, double-cantilever-beam specimens for plate stock, surface-flawed specimens for plate stock or sheet materials, and double-edge-notch specimens for sheet materials.

Modern day fracture toughness testing has roots in the notch-round tensile test. The notch round has a rich history (Sachs, Lubahn, Ebert and Brown, 1944, 1945, 1947, 1948, and 1959; and Sachs, Weiss, and co-workers, 1956, 1960, 1961, and 1964). The early investigations emphasized the notch sensitivity of steels. The application of the sharp-notch-round bar test to aluminum and magnesium alloys has been advocated recently (Aluminum Association, 1972). Although there has not been a great deal of precracked round bar testing, its history starts with Irwin's (1956 and 1961) solutions for the stress intensity factor.

In the very early days of toughness testing, the investigators involved were familiar with smooth round bar tensile testing and used handbooks of stress concentration factors for simple configurations (Neuber, 1946; Peterson, 1953). Since notch rounds were the easiest specimens to machine, much of the pioneer work was done with this specimen type. The main reason for the continued use of notch-round bar testing in the 1950s and 1960s was that is provided a simple method for measuring notch sensitivity. The measure normally was taken as the ratio of the sharp-notch strength to either the yield or tensile strength. (Correlation of this measure to K_{Ic} will be discussed later.)

Direct measurement of K_{Ic} with precracked notch rounds is possible but probably will not be used extensively because of:

a. The large inherent loads* required (e.g., for notched to unnotched ratios of unity in a tough material, a 240,000 psi yield strength steel requires about 100,000 lb capacity for a 0.75-in.-diameter notch round).

---

* This is not a severe restriction on aluminum and magnesium alloys in medium section sizes since applied loads are generally less than 20,000 lb. Also, a test in bending, rather than tension, could reduce loads by a factor of five.

b. The difficulty in making uniform fatigue cracks since any deviation would promote eccentric loading.

c. The difficulty in obtaining reproducible results due to notch preparation and/or alignment problems.

Even though it is unlikely that K_{Ic} testing of precracked notch rounds will become widespread, it is useful to consider as background and will be discussed after considering sharp-notch-round tensile testing as a correlative measure.

C.1.1 Sharp-Notch-Round Tensile Screening Tests

The 1973 draft test method prepared by Task Group E-24.01.07 of ASTM Committee E-24 specifies the testing of cylindrical specimens with a major diameter, D, * of 0.500 or 1.06 inches. With a 60° notch and a d/D** of 0.707, the specimen configurations are shown in Figures C-1, C-2 and C-3. These figures require a machined notch root radius of $\rho \leq 0.0007$ in., a very difficult task in steels, but an attainable one in aluminum and magnesium alloys. The specimens are tested under a slowly rising tensile load to failure. The maximum load is measured and the initial net area is utilized to measure the notch tensile strength, σ_{NTS}. Although no extensometer is utilized, the test set-up must be carefully aligned prior to testing. Once the system has been aligned, it is a simple matter to test as in an ordinary tensile test with the speed of testing being maintained to less than 100,000 psi/min on the net section.

The only parameters reported are the notch tensile strength, σ_{NTS}, and the notch-strength-to-yield-strength ratio, σ_{NTS}/σ_{YS}. The notch tensile strength is determined by dividing the maximum load sustained in a slow tension test by the initial area of the supporting cross section in the plane of the notch.

Extensive studies of the 2000, 6000 and 7000 series of aluminum alloys (Kaufman, 1972 and 1973; Aluminum Association, 1972) demonstrated that the σ_{NTS}/σ_{YS} ratio may be used as a lower bound for qualification of fracture toughness. This conclusion was based upon correlations established by separately evaluating σ_{NTS}/σ_{YS} and K_{Ic} on the same heat of material. Such a correlation for 7075 and 7475 alloys is shown in Figure C-4. Data from 0.5-in.-diameter rounds having notch root radii ≤ 0.0007 inches were compared to K_{Ic} data conforming to ASTM E399 standards and, significantly, the correlation holds in both the notch-sensitive ($\sigma_{NTS} < \sigma_{YS}$) and notch-strengthening

---

* Terms are defined at the end of the section.

** d = diameter of notch.
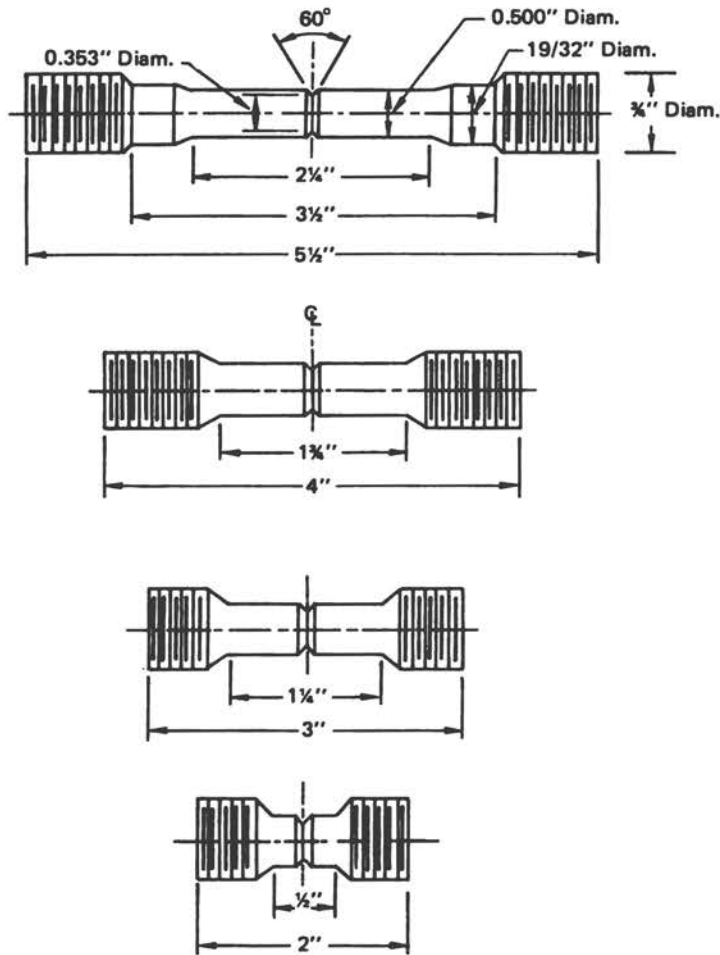
FIGURE C-1 Threaded End Notched 1/2-in.-diameter Tension Specimen (Kaufman, 1972).

FIGURE C-2 Tapered Seat Notched 1/2-in.-diameter Tension Specimen (Kaufman, 1972).

Notch-Tip Radius ≳ 0.0005"
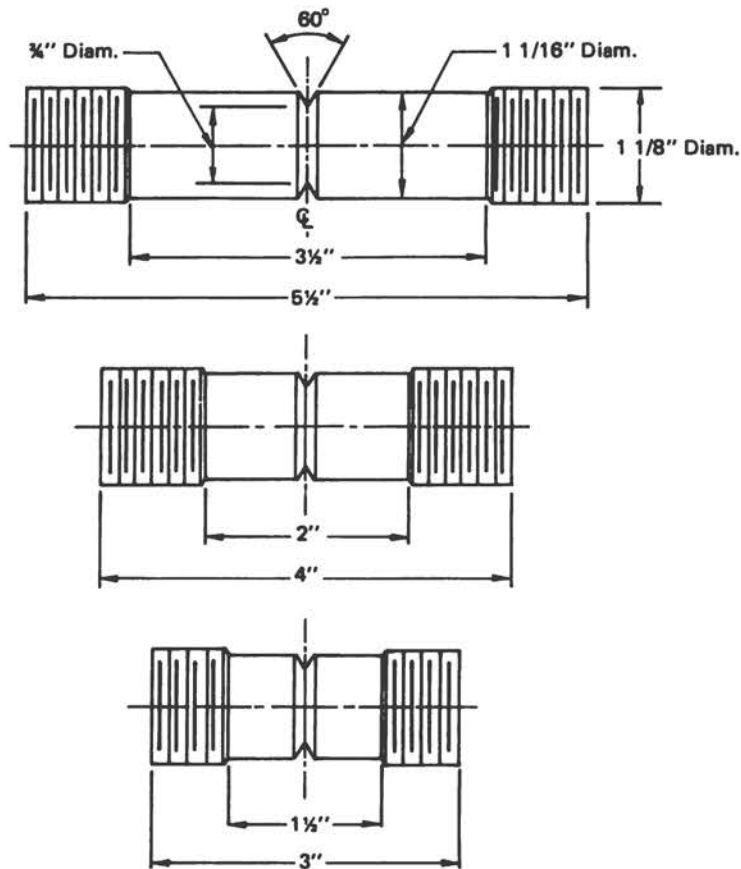
FIGURE C-3 Threaded End Notched
1-1/16-in.-diameter Tension
Specimen (Kaufman, 1972).

$(\sigma_{NTS}/\sigma_{YS} > 1)$ ranges. The contention is that such a correlation presents
an inexpensive and efficient method of quality control to assure that specified
minimum K_{Ic} fracture toughness levels are met at an agreed level of confidence
(Kaufman, 1973).

For example, if a $K_{Ic} \geq 30$ ksi $\sqrt{\text{in.}}$ is specified, a notch-bar and a
smooth-bar test are run on a new lot and compared to Figure C-4.

a. If $\sigma_{NTS}/\sigma_{YS} \geq 1.42$, the lot is accepted.

b. If $\sigma_{NTS}/\sigma_{YS} < 1.42$, two additional samples are run. If both give
ratios ≥ 1.42, the lot is accepted. If either ratio is < 1.42, K_{Ic}
testing per ASTM E399 is required.

c. Further acceptance or rejection is based on K_{Ic} testing.
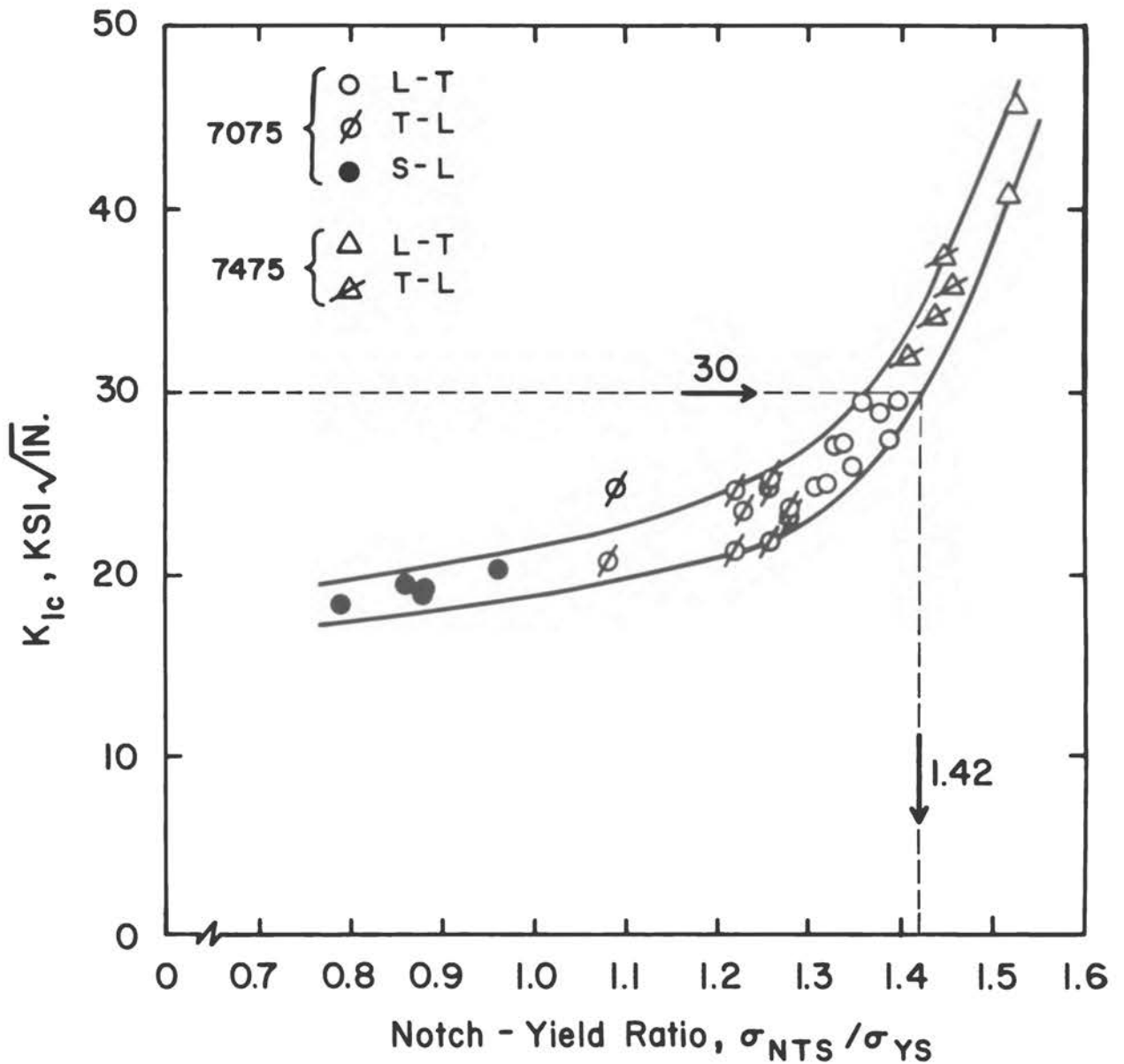
FIGURE C-4   Correlation of K_{Ic} to Notch-Yield Ratio for 7x75-T7651
             Aluminum (Kaufman, 1974).

Such a procedure has been adopted by the aluminum producers with regards to
fracture toughness for quality-control procedures (Aluminum Association,
1972). However, some questions remain concerning the statistical significance
of such an approach. For example, in Figure C-4, the envelope is based upon
two different grades and three different orientations, none of which give
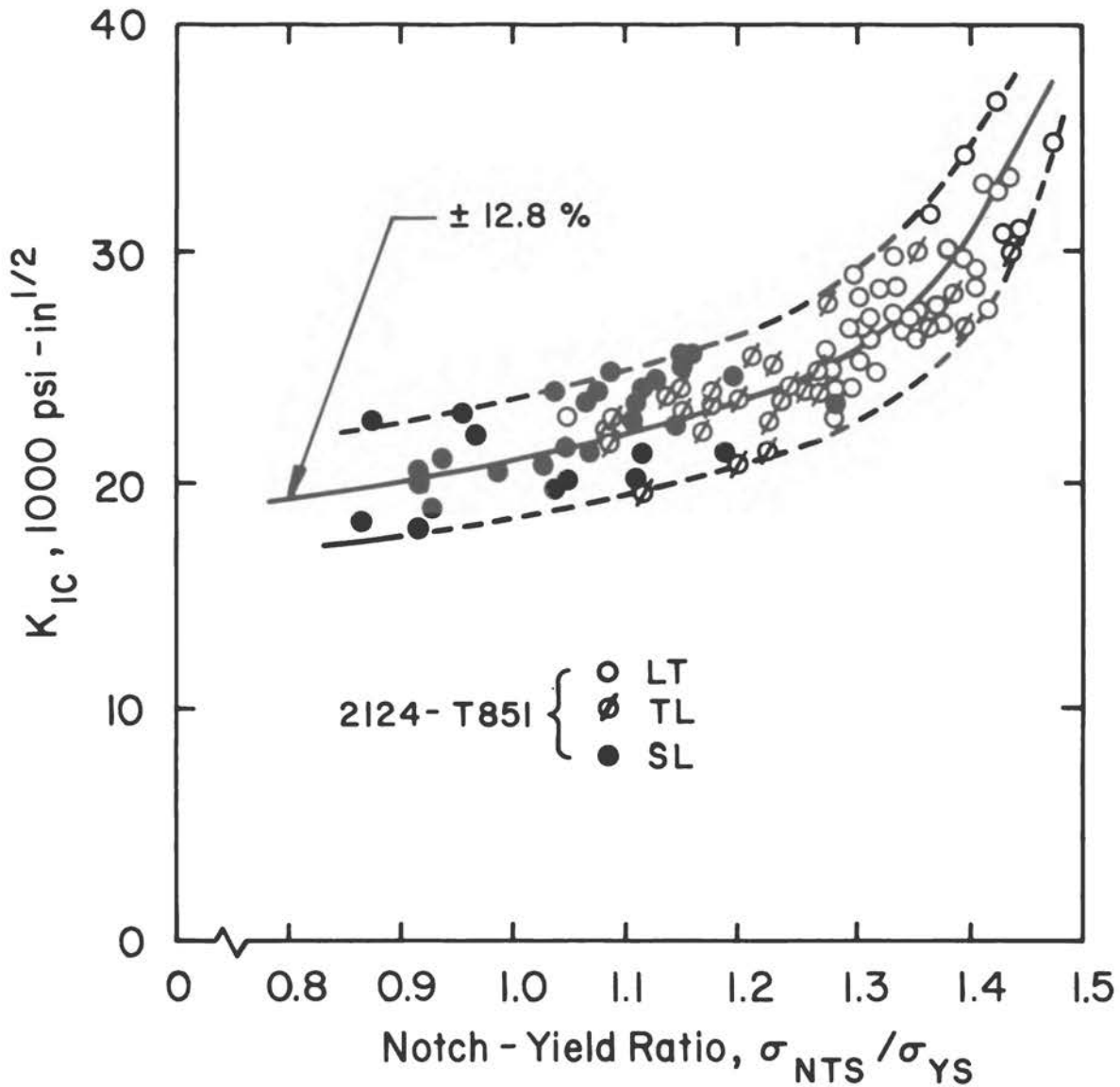
FIGURE C-5   Statistical Scatter in K_{Ic}-Notch-Round Correlations for 2124-T851 Aluminum Based upon Arbitrary Envelope (Kaufman, 1974).

overlapping data with respect to notch-yield ratio.* Although there are some overlapping data presented in Figures C-5 and C-6, this effect should be assessed thoroughly prior to using such envelopes as acceptance or rejection criteria.

---

* It is appropriate to point out here that different orientations should be treated as separate populations.
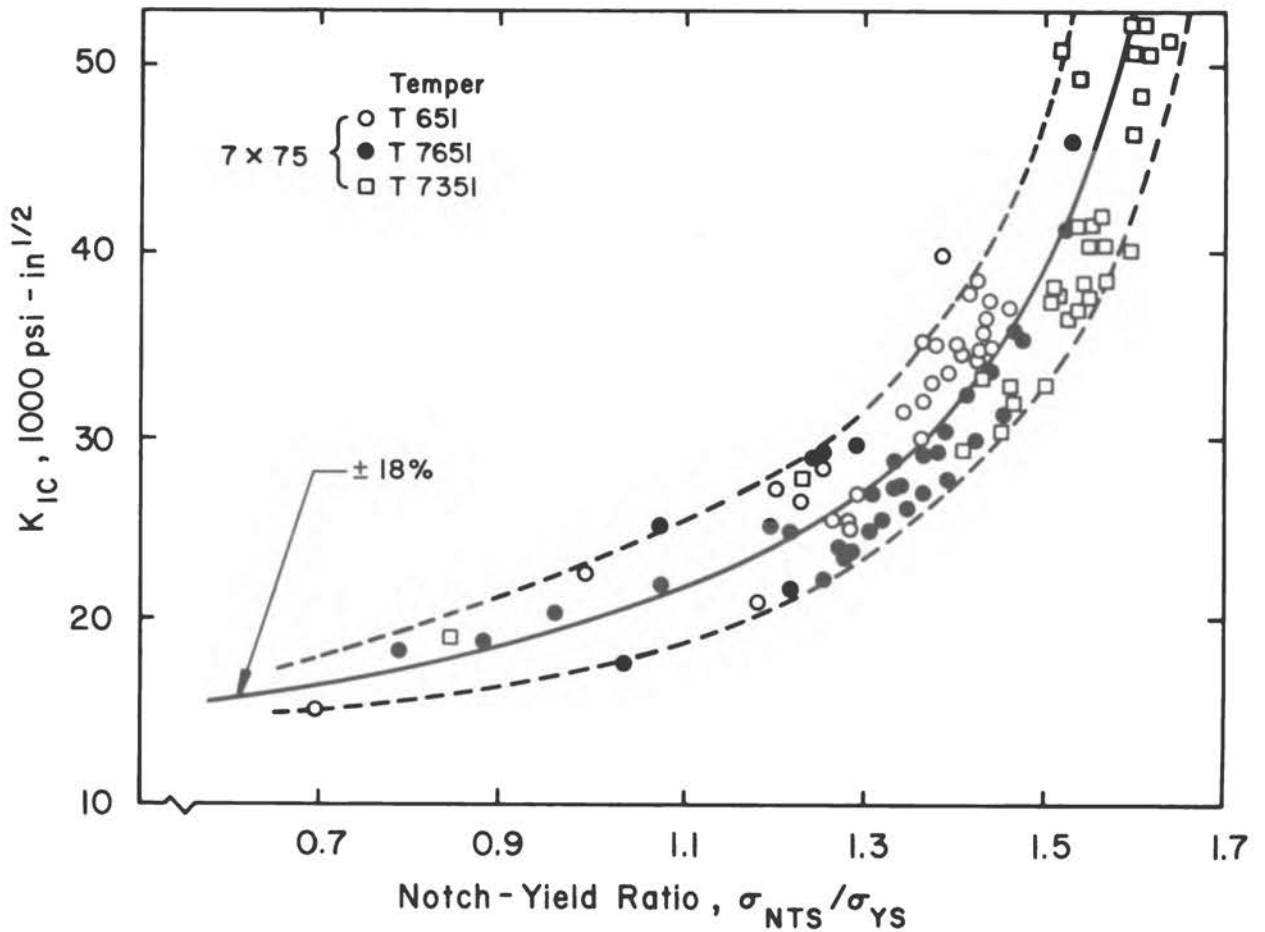
FIGURE C-6 Statistical Scatter in K_{Ic}-Notch-Round Correlation for 7x75 Aluminum Based upon Arbitrary Envelope (Kaufman, 1974).

Sufficient data exist to validate this approach for aluminum alloys. However, as noted above and as discussed in appendix B, the user should be extraordinarily careful with respect to the statistical aspects of such an approach. No such data were available with respect to magnesium alloys.

Two approaches were used to assess the precision of this method. The first involved applying the theoretical relationship, described at the end of this section, in Eq. C-2 as a trend line (Brown and Srawley, 1974). This suggests that a valid correlation should be based upon straight lines when $(K_{Ic}/\sigma_{YS})^2$ is plotted versus $D(\sigma_{NTS}/\sigma_{YS})^2$. This linear elastic fracture mechanics (LEFM) correlation is shown in Figure C-7 for about 100 data points (Kaufman, 1974) on 2124-T851 aluminum. The data purposely are split into groups as there was a small thickness variation. Taking the square root of the slopes and comparing it to a mean slope which went through zero gave a range of errors up to ± 18.5 percent.
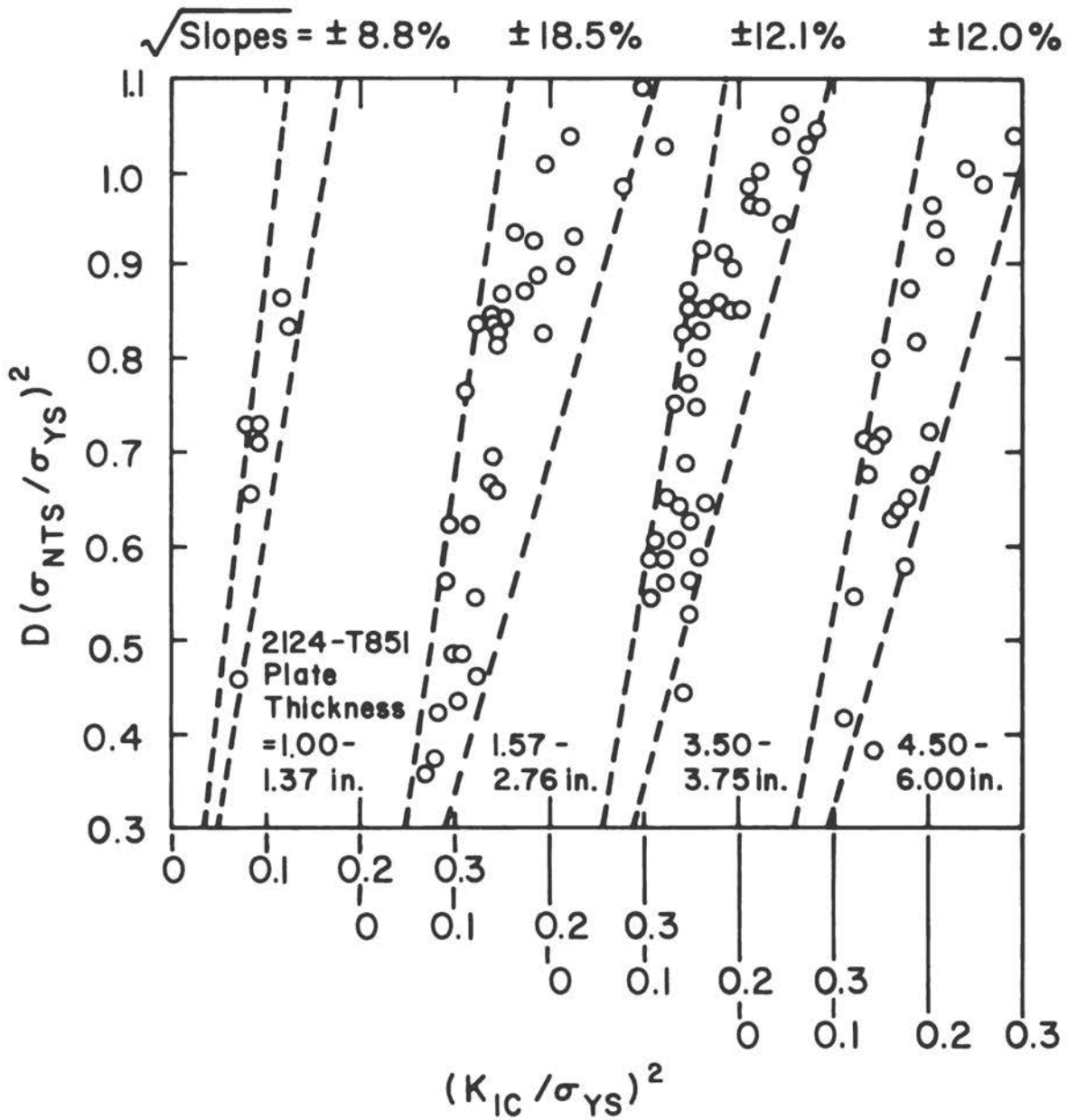
FIGURE C-7 Statistical Scatter in K_{Ic}-Notch-Round Correlation for 2124- T851 Aluminum Based upon LEFM Trend Lines (Kaufman, 1974).

A somewhat less theoretical, but nevertheless valid, approach is to plot K_{Ic} versus σ_{NTS}/σ_{YS} (Kaufman, 1973). Since it is only an empirical correlation, a curve representing this data is an equally valid approach even though it may lack the precise physical meaning of the former approach. A plot of the 2124 data from Figure C-7 (Kaufman's 1973 approach) was already shown in Figure C-5. The empirical envelope approach indicates a scatter of $\pm$ 12.8 percent. A similar plot for about 100 data points of 7075 with three different tempers is shown in Figure C-6. The scatter here is somewhat greater, being $\pm$ 18 percent. However, if σ_{NTS}/σ_{YS} levels were restricted to $\leq$ 1.5 and if each temper were treated individually, as was the case for Figure C-5, the scatter in Figure C-6 would be closer to $\pm$ 14 percent.

Although these values appear as unduly large statistical scatter, one could ask how much of the variation is due to the K_{Ic} test itself (i.e., K_{Ic} might vary because of either material variations or test scatter). Such statistical data generally are lacking but in one set of K_{Ic} data (Kaufman, 1974), six sequential plates of 7475-T651, 1.30 in. thick, were evaluated. The LT and TL orientations were virtually indistinguishable since $\overline{K}_{Ic}$ = 35.4 ksi $\sqrt{in}$. for LT and $\overline{K}_{Ic}$ = 35.5 ksi $\sqrt{in}$. for TL. This allowed a total of 20 tests to be examined and it was determined that K_{Ic} = 35.5 ksi $\sqrt{in}$. $\pm$ 8.2 percent for this "single lot." For the same lot, 20 tests of sharp-notch rounds gave σ_{NTS}/σ_{YS} = 1.41 $\pm$ 3.6 percent. The combined range of errors is just about what is noted as the overall deviation in Figures C-5, C-6 and C-7 if individual tempers are considered. Seemingly, there might be difficulty in obtaining any correlation that was much better than $\pm$ 10 percent, at least in aluminum alloys. If the quality-control method as proposed by Standard E-24.01.07 is followed, the width of the scatter band is not important. Using the lower bound on materials with wide scatter bands simply means one is being highly conservative.

Another important concern is the useability of the test. Here such factors as cost, experience, and simplicity as controlled by ease of preparation and testing become most important.

The notch-round-bar tension test as a simple means of quality-control testing for K_{Ic} has the following advantages:

a. It is simple in that a single parameter results (i.e., notch strength). No deflection or displacement readings are necessary. No load-displacement interpretation is required. Only load at fracture is measured.

b. It is inexpensive in that a single lathe set-up can be used for machining.

c. Tests can be carried out on the basic equipment available in most industrial laboratories.

d. Data are readily recorded and analyzed by personnel experienced in standard tensile testing procedures.

The test is not simple, however, primarily because of machining and test set-up precautions necessary to reduce eccentric loading:

a. Notches must be machined to have root radii $\leq$ 0.0007 inches.

b. The notch must be machined concentrically with the other features of the specimen within 0.0005 inches.

c. Use of tapered seat specimens with special grips are recommended to reduce eccentricity below 0.01 inches.

d. Alignment* must be further controlled to reduce eccentricity by using four-point aligners to provide positive alignment of precision-machined tension bolts and grips, or using crossed-knife edge clevises which are commercially available.

e. Bending stresses must be measured at regular intervals on instrumented, grooved 1/2-in.-diameter steel specimens. Four strain gauges, 90° apart around the circumference, used to measure percent bending as defined by 100 ($\Delta\sigma_m/\sigma_o$). Here, $\Delta\sigma_m$ is the difference between maximum outer fiber stress and the average stress, σ_o, on the specimen. The relationship is:

$$\Delta\sigma_m/\sigma_o = [(\Delta g_{1,3})^2 + (\Delta g_{4,2})^2]^{1/2}/g_o \qquad \text{(Eq. C-1)}$$

where g_i are the individual gauge readings and g_o is the average of g_i. The percent bending cannot exceed 10 percent at a 30,000 psi average tensile stress.

Besides a brief flurry of testing steels in the late 1940s and early 1950s, the notch round has been largely of theoretical interest (Schaeffer and Weiss, 1964) except for the Aluminum Association's experience. Here, the bulk of experimental evidence has come from Alcoa Research Laboratories (Kaufman, 1972, 1973, and 1974). More specifically, the experience has been limited almost exclusively to the 2000 and 7000 series aluminum alloys.

The minimum plate thickness that can be evaluated with the tapered-end notch round is 0.75 inches (19 mm). The draft prepared by ASTM E-24.01.07 specifies a minimum test section length of 1.0 inch (25.4 mm) for 1/2-in.-diameter specimens and 2-1/8 inches (54 mm) for 1-1/16-in.-diameter specimens. This L/D = 2 requirement simply satisfies the St. Venant principle

---

* Brown (1974) has discussed loading eccentricities in great detail and demonstrates a collet-rod assembly with cross-flexure aligners which reduces the eccentricity to "4 percent bending." This will be included in the forthcoming ASTM method on testing sharply notched cylindrical specimens.

and avoids superposition of stress states. However, this test section length does not include the tapered or threaded grip ends so that the overall specimen length would be 3 and 4 inches, respectively. These minimum lengths approximately correspond to the onset of the plateau regions in Figure C-8. Actually, some success has been obtained with 2-in.-long specimens of 1/2-in.-diameter rounds having tapered ends.

Because of this size limitation, it would not be possible to measure short transverse properties on plate less than 2 in. thick. The circumferential nature of the notch limits the orientations to longitudinal, transverse, and short transverse. For strongly anisotropic plates where the crack orientation might give large variations in K_{Ic}, it is only possible to get the minimum value of the
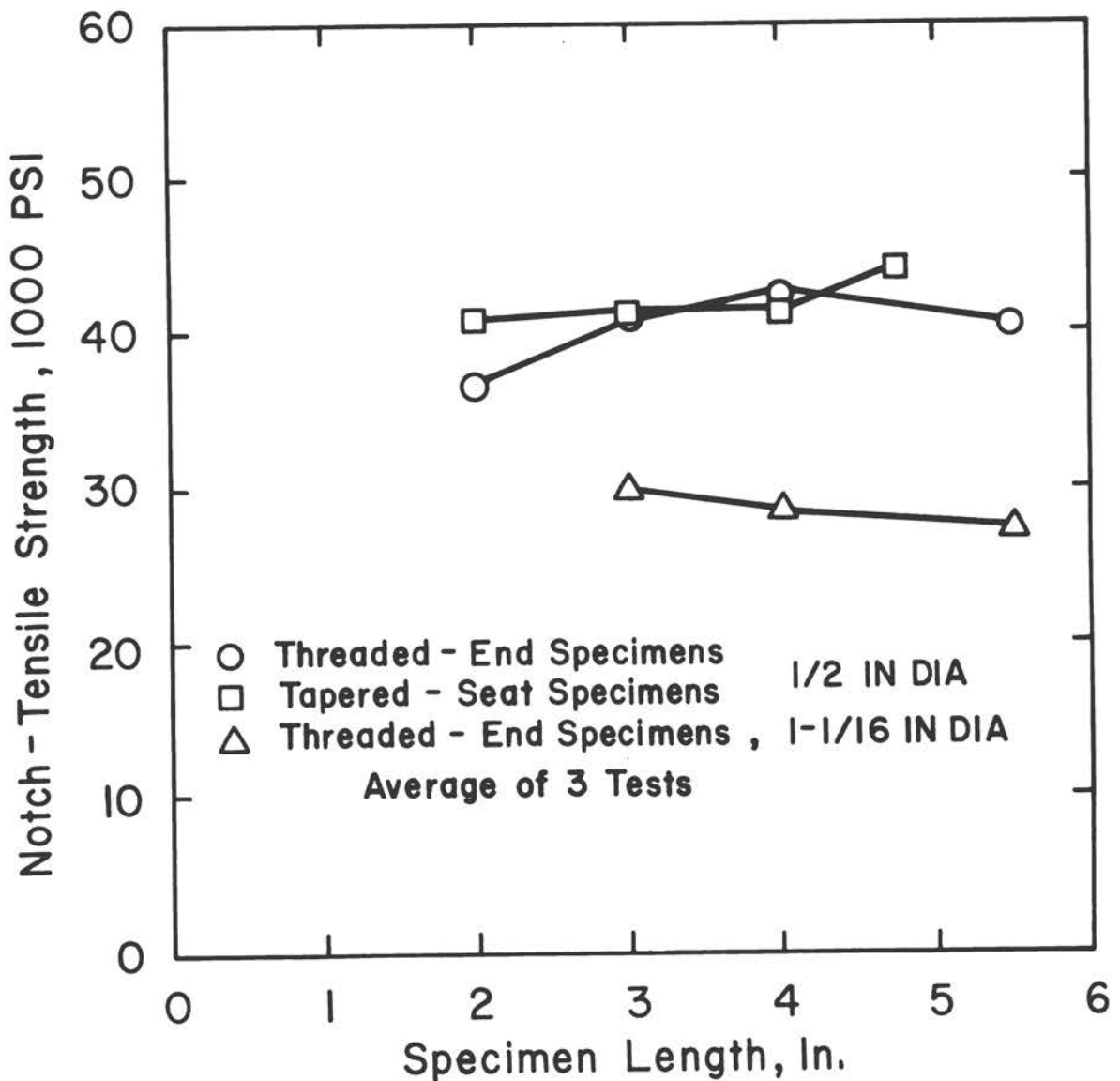
FIGURE C-8   Effect of Specimen Length on Notch-Tensile Strength (Kaufman, 1972).

two crack orientations possible in a bend test, for example (Figure C-9). It has been suggested (Kaufman, 1975) that this could be taken care of by establishing K_{Ic} values for the two orientations so that two correlations would result. This procedure seems less than satisfactory, however, since σ_{NTS} as based on one orientation would be used for quality control of a second orientation.

Cost estimates have been made for preparation and testing on an in-house bases and a commercial test lab as indicated in Table 1 of section 3.2 in the text. These costs are roughly equivalent to, or as much as, twice the cost of a tensile test. Still, they are as low as any other type of test and reflect the ease of machining and familiarity of testing that one associates with the smooth-bar tensile test.

Considering the difficulty in machining uniform, sharp, concentric notches in ferrous and titanium alloys, prospects for extending notch-round testing to other alloy systems are not good. For easily machineable materials such as aluminum and magnesium alloys, the aluminum industry currently is utilizing the lower limit of the K_{Ic} versus σ_{NTS}/σ_{YS} scatter band for quality control. The notch round in bending is a perfectly valid approach and could resolve the eccentricity problem. Furthermore, the maximum load in a bend test of a given size of specimen would be less than one half that for a tension test. With square ends or machined flats on loading surfaces for four-point bending and a turned center portion, a simple, inexpensive test without eccentricities could be accomplished.

(a) Two Orientations for   (b) Single Orientation for
    Notch Bend   Notch Round
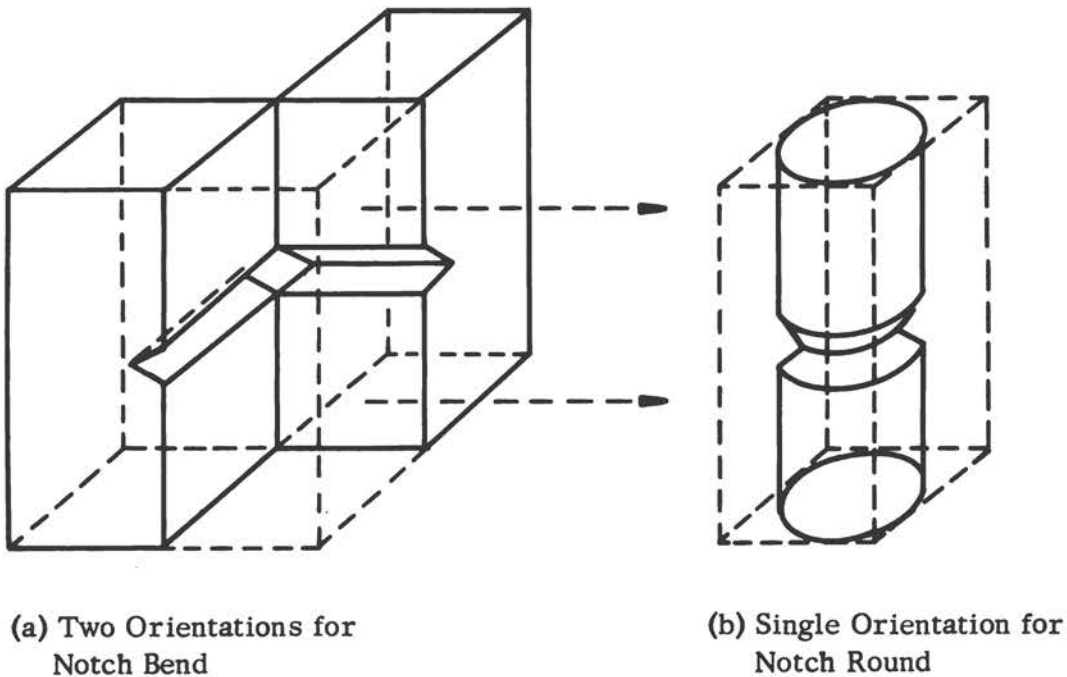
FIGURE C-9   Possible Orientations for Notch-Bend and Notch-Round Specimens.

C.1.2 Fracture Toughness Testing

The theoretical background for the notch round and some testing aspects are discussed at the end of this appendix. For K_{Ic} testing, there are no standards, but the procedures would be similar to those described above with the exception that the net area beyond the fatigue crack would be used to determine the notch strength at fracture. Also, the reported parameters would include notch strength, major and minor diameters, depth of fatigue crack, K level during precracking, and calculated K_{Ic} values.

The notch strength may be used as a direct measure of K_{Ic} for a material provided that:

a. The notch or precrack is sufficiently sharp so that any reduction in root radius will not affect the notch strength.

b. The notch-strength-to-yield-strength ratio ≤ 1.1.

c. Large amounts of slow crack growth do not precede instability.

d. Eccentricity of loading can be neglected.

If these conditions are achieved, the K_{Ic} value may be determined using existing solutions. The theoretical justification for using σ_{NTS}/σ_{YS} as a direct measure of K_{Ic} is discussed in the theoretical justification at the end of this section. As discussed there, it is shown why K_I values, as measured from precracked rounds, give results very close to those predicted directly from sharp-notch rounds. These results, as shown in Figure C-10, used σ_{NTS}/σ_{YS} ratios as determined on large-diameter samples with notch root radii ≤ 0.001 in. Again, only aluminum data indicate a good degree of agreement and only for cases where limited plasticity is involved (i.e., $\sigma_{NTS}/\sigma_{YS} \leq 1.1$). Even here, the data are very limited. Furthermore, the plastic zone correction, noted in the theoretical justification below, is very approximate. Thus, it is not appropriate to even consider σ_{NTS}/σ_{YS} as a direct measure of K_{Ic} for $\sigma_{NTS}/\sigma_{YS} > 1.1$, and it is best to use an empirical correlation.

Considering the direct measurement of K_{Ic}, there are extensive data only for aluminum alloys. Even in this case, additional testing must be accomplished before any such criteria could be used to give K_{Ic} directly from precracked notch rounds.

There are a number of difficulties -- such as maintaining concentricity, uniformity of the precrack, and minimizing the test set-up eccentricity -- and, as noted above, these can lead to considerable data scatter. For example, the most brittle alloy, H-11, in Table C-1 had a K_{Ic} variation of ± 16.4 percent. For the two toughest alloys, 2014 and 7075 T6 aluminum,* the scatter was

---

* Normally, 2014 T6 and 7075 T6 aluminum would not be this tough; these particular data represent samples taken from extruded bar.
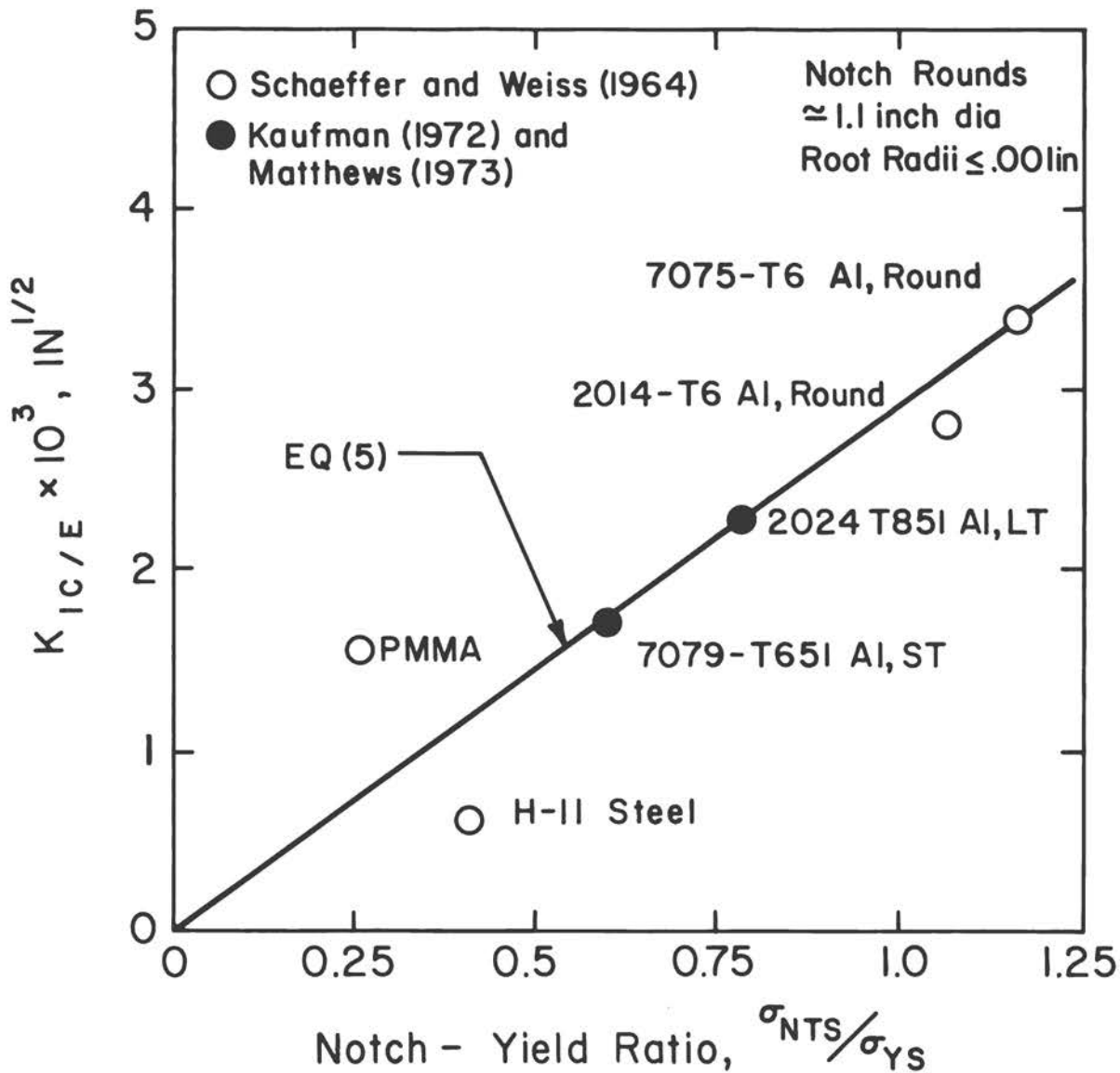
FIGURE C-10 Theoretical Relationship between K_{Ic} and Notch-Yield Ratio.

± 8.8 percent on K_{Ic}. Thus, the precision for using precracked rounds as a direct measure of K_{Ic} has not been established. This is particularly true for very ductile materials since the plastic zone correction has not been well defined. One should only rely on correlations of σ_{NTS}/σ_{YS} to K_{Ic} as indicators of fracture toughness.

Other factors that should be considered include:

Complexity -- All of the advantages enumerated earlier would disappear while all of the disadvantages would remain. There are no inexpensive methods to fatigue precrack notch rounds.

TABLE C-1   Yield, Notch-Round Tensile, and Plane-Strain Fracture Toughness Data.

Material	Material Condition	σ_{YS} (1000 psi)	σ_{NTS}* (1000 psi)	K_{Ic}** (1000 psi-$\sqrt{in.}$)	K_{Ic}/E ($10^{-3}\sqrt{in.}$)	σ_{NTS}/σ_{YS}
PMMA Polymer	Extruded Bar	7.0	1.79 ± 0.03	0.82	1.60	0.26
H-11 Steel	2 in. dia. rounds, quench & temper at 510° C	238	97.6 ± 17.7	18.4 ± 3	0.62	0.41
7079 Aluminum	6 in. plate (ST) T651	58.0	35 ± 6	18	1.72	0.60
2024 Aluminum	1-3/8 in. Plate (LT) T851	64.8	51 ± 3	24	2.30	0.78
2014 Aluminum	2 in. dia. rounds T6	66.3	71.0 ± 1.9	28.9 ± 2.5	2.76	1.07
7075 Aluminum	2 in. dia. rounds T6	76.0	89.2 ± 1.4	35.6 ± 3.2	3.40	1.17

* Test bars were either 1.16 in. (Schaeffer and Weiss, 1964) or 1-1/16 in. (Kaufman, 1972) diameter rounds with d = 0.707D and root radii ≤ 0.001 in.

** From precracked round or bend bars of same orientation (Schaeffer and Weiss, 1964).

Experience -- There has been very little experience in establishing K_{Ic} values with precracked notch rounds.

Size and Orientation -- A discussion on this topic also would parallel that made previously.

Cost -- Costs of preparing notch rounds would be large due to the difficulty in preparing uniform fatigue precrack depths. No quantitative estimate can be put on this procedure.

Prospects for Improvement -- This test probably will never be used for routinely determining plane-strain fracture toughness, K_{Ic}. Since some experienced investigators have reservations about notch-round testing due to eccentric loading problems, ASTM Committee E-24 has not recommended the notch round for K_{Ic} testing at this time (Brown, 1974).

C.1.3 Theoretical Justification for Obtaining K_{Ic} from Notch Tensile Testing

Irwin (1956, 1961) derived a relationship between notch tensile strength, σ_{NTS}, and K_{Ic} given by

$$K_{Ic} = \sigma_{NTS} [D]^{1/2} \left[2(\tfrac{d}{D})^4 (1 - \tfrac{d}{D}) + 0.364 (\tfrac{D}{d}) (1 - \tfrac{d}{D})^2 \right\} \right]^{1/2} \quad \text{(Eq. C-2)}$$

where D and d are the major and minor diameters of a cylindrical notched bar. This equation is for any notch depth whereas the preponderance of testing has been 50 percent notch area (d/D = 0.707). The equation for d/D = 0.707 reduces to (Paris and Sih, 1965)

$$K_{Ic} = 0.414 \, \sigma_{NTS} [D]^{1/2} \quad \text{(Eq. C-3)}$$

Since then, a summary (Tada, 1973) of the stress intensity solutions (Bueckner, 1965, 1972; Bentham, 1972) shows that a more appropriate constant for 50 percent notch area gives

$$K_{Ic} = 0.454 \, \sigma_{NTS} [D]^{1/2} \quad \text{(Eq. C-3a)}$$

This gives reasonable estimates of K_{Ic} (within 10 percent) for $\sigma_{NTS}/\sigma_{YS} \leq 1.1$ even without a plastic zone correction. If sufficient plasticity results so that the notch strength is much greater than the yield strength, one should use a plastic zone correction. A first order correction (Irwin, 1960) leads to

$$\sigma_{NTS}/\sigma_{YS} = \frac{X}{0.233} (1 - 1/2 \, X^2)^2 \quad \text{(Eq. C-4)}$$

with $\quad X = \dfrac{K_{Ic}}{\sigma_{YS}} [\pi D]^{-1/2}$

As applied to a later, more accurate solution (Tada, 1973), a similar plasticity correction would give

$$\sigma_{NTS}/\sigma_{YS} = 4X (1 - 1/2 \, X^2)^2 \quad \text{(Eq. C-4a)}$$

with $\quad X = \dfrac{K_{Ic}}{\sigma_{YS}} [\pi D]^{-1/2}$

This plasticity correction only applies to 50 percent notch areas. The term in parentheses in Eq. C-4 and C-4a is the plastic zone correction and for small X, Eq. C-4 and C-4a reduce to the linear elastic result, Eq. C-3 and C-3a.

There has been no in-depth study for utilizing notch round bar testing for K_{Ic} determinations. For example, there has been no ASTM study on how to assess non-linear, load-displacement curves in materials where $\sigma_{NTS}/\sigma_{YS} \gg 1$. With this in mind we will calculate K_{Ic} values directly from Eqs. C-3 and C-3a using σ_{NTS} at maximum load. The data, as taken from fatigue–cracked samples will be compared to notch strength data as taken from sharply machined samples.

C.1.4 Direct Measure of K_{Ic}

Notch round results have been evaluated on aluminum alloys, one steel and one glassy polymer (Schaeffer and Weiss, 1964; Kaufman, 1972). In these studies, sufficient data exist for identical heats of material to compare sharp notch round data to K_{Ic}. The notch tensile strength was evaluated on specimens of the configuration shown in Figure C-3. Corresponding K_{Ic} values were obtained from similar notch round bars (Schaeffer and Weiss, 1964) or notch bends (Matthews, 1973) that had been prefatigue cracked. For six different materials, both sharp-notch round and K_{Ic} data are present in Table C-1.

The notch round tensile strength represents averages of triplicate tests in one case (Schaeffer and Weiss, 1964) and 10 tests in another case (Kaufman, 1972), while the K_{Ic} data are averages of 6 tests. For the aluminum alloys, an increase in notch strength parallels an increase in K_{Ic}. More importantly, the ratio of σ_{NTS}/σ_{YS} increases with K_{Ic}. Direct comparison of this ratio to K_{Ic} is not possible within different classes of materials where there is a large variation in modulus of elasticity. As an attempt to normalize the data, the ratios K_{Ic}/E and σ_{NTS}/σ_{YS} are shown in the last two colums of Table C-1. σ_{NTS}/σ_{YS} generally increases with K_{Ic}/E. This is more clearly seen in Figure C-4 where K_{Ic}/E versus σ_{NTS}/σ_{YS} results in a linear relationship.

The reason there is a good correlation between K_{Ic}/E and σ_{NTS}/σ_{YS} is that the yield-strength-to-modulus ratio was nearly constant for this class of materials. For the one steel and four aluminum alloys, it was found that σ_{YS}/E was $(0.67 \pm 0.12) \times 10^{-2}$. The largest apparent deviation was the glassy polymer (polymethylmethacrylate) which had a ratio of 0.014 or about double that of the metals. For those metals in Table C-1, one could estimate as a first approximation

$$\sigma_{YS} \simeq 0.0067E \qquad \text{(Eq. C-5)}$$

Combining this with Eq. C-3 and using an average test bar diameter of 1.11 in., one finds

$$K_{Ic}/E \simeq \alpha \, (\sigma_{NTS}/\sigma_{YS}) \qquad \text{(Eq. C-6)}$$

where $\alpha = 2.9 \times 10^{-3} \sqrt{in}$. It is seen that Eq. C-6 is a direct theoretical prediction based upon linear elastic theory and observed yield and modulus data.

Note that the constant α only applies to one specimen diameter and a class of
materials roughly obeying Eq. C-5. A reasonable prediction results in
Figure C-10 from comparing Eq. C-6 to the data from Table C-1. Furthermore,
if the factor of two difference in σ_{YS}/E for PMMA is considered, this would put
Eq. C-6 right through the PMMA data point since α would be doubled. The only
real deviation then is the H-11 steel.

Considering the earlier theoretical discussion, it is obvious that a
requirement for the theoretical fit shown in Figure C-10 is that the notch root
radius is sufficiently sharp to give valid K_{Ic} results. It is well known that crack-
tip radii blunt out as plastic deformation commences. If the radii blunt out
sufficiently prior to fracture, then even precracked samples will have "blunt tips"
at K_{Ic}. This blunted fatigue crack may be considered as having a critical root
radius, ρ_{CR}, at fracture. If a machined notch root radius is less than ρ_{CR}, then
it may be anticipated that an as-machined bar could give a result similar to a
precracked bar. For example, the lowest toughness aluminum alloy shown in
Table C-1 would have a critical crack-tip radius estimated by

(ASTM, 1960)
$$\rho_{CR} \simeq \frac{K^2}{20\pi\sigma_{YS}^2} \simeq 0.0015 \text{ in.}$$

(Eq. C-7)

(Tetelman and
McEvily, 1967)
$$\rho_{CR} \simeq \frac{2V_c}{\epsilon_c} \simeq \frac{K^2}{2\sigma_{YS}E\epsilon_c} \simeq 0.0009 \text{ in.}$$

where $2V_c$ is the crack tip displacement and ϵ_c is the strain at the crack tip.
Since all other aluminum data in Table C-1 would give larger ρ_{CR} values, it is
understandable why the good agreement in Figure C-10 resulted. That is, the
machined root radii were just as sharp as the blunted root radii that developed
from fatigue cracks. Similar calculations for the high-strength steel and
polymer indicate ρ_{CR} values near 0.0001 in. and 0.00025 in., both of which are
well below the machined root radius of 0.001 in. Clearly, both of these
relatively brittle materials would violate a critical root radius criterion.
Perhaps it is not surprising then that the steel data with the largest deviation,
$\rho_{CR} \ll 0.001$ in., did deviate from the theoretical curve in Figure C-4 by a
factor of two.

At this time, evidence is insufficient to demonstrate that a good pre-
dictive quality exists between σ_{NTS}/σ_{YS} values and K_{Ic} in other than aluminum
alloys. Furthermore, it was indicated above that Eq. C-3 could deviate as much
as 10 percent from the true K_{Ic} as σ_{NTS}/σ_{YS} approached 1.1. All the data in
Table C-1 were well within the scope of this limit. Beyond this ratio, however,
notch strengthening occurs and plasticity becomes widespread. It is significant
that $\sigma_{NTS}/\sigma_{YS} \leq 1.1$ for 1.11-in.-diameter samples corresponds to $K_{Ic}/\sigma_{YS} \leq 0.52$
from Eq. C-4. This is actually more conservative than the ASTM recommenda-
tion for restricted plasticity, since the present case would give $D \geq 4 (K/\sigma_{YS})^2$.

C.1.5 Summary

Because of ease of machining, simplicity of interpretation, and familiarity of industry with tensile testing, the notch-round bar specimen test for quality-control purposes has been rapid and inexpensive. However, problems with respect to notch uniformity and loading eccentricity can produce relatively large scatter bands, and a direct correlation between K_{Ic} and σ_{NTS}/σ_{YS} (notch-tensile-to-yield ratio) is still relatively unproven with respect to statistical significance. Hundreds of correlations between K_{Ic} and σ_{NTS}/σ_{YS} have been made for a series of aluminum alloys. As such, they provide a reasonable base for using the lower bound of the scatter band for quality control.

At this time, sufficient resolution of eccentricity problems has not been accomplished for the purpose of using precracked notch rounds for K_{Ic} testing.

C.1.6 Glossary of Terms

d	- minor diameter of a notch-round tensile bar
D	- major diameter of a notch-round tensile bar
E	- modulus of elasticity
g_i	- strain gauge readings around circumference of an instrumented tensile bar
g_o	- average of g_i
K	- applied stress intensity factor
K_{Ic}	- plane-strain fracture toughness
L	- length of a notch-round tensile bar
α	- proportionality constant
ε_c	- strain at the crack tip
$2V_c$	- crack tip displacement
ρ_{CR}	- crack tip radius at fracture
σ_{NTS}	- notch tensile strength
σ_{YS}	- tensile yield strength
$\Delta\sigma_m$	- difference between outer fiber bending stress and average stress in a tensile bar
σ_o	- average stress in tension

C.2   DOUBLE CANTILEVER BEAM (DCB) TESTING

Application of the double cantilever beam (DCB) specimen to fracture toughness testing began in the late 1960s (Hoagland, 1967; Van der Sluys, 1969) along with experimental studies to determine the effect of side grooving on measurements of K_{Ic} (Freed and Krafft, 1966). The stress intensity factors for a variety of DCB specimens with straight boundaries using boundary collocation techniques have been determined (Srawley and Gross, 1967). The mathematical basis for the DCB specimen geometry also was developed in the late 1960s and the concept of contouring the shape of the specimen to produce a specimen with a stress intensity independent of crack length and proportional only to the applied load was introduced (Mostovoy et al., 1967). Further studies demonstrated that the same effect was closely approximated with a tapered DCB specimen which simplified machining and thereby reduced costs (Gallagher, 1971).

Most of the work on evaluating the DCB specimen was done with aluminum alloys. Mostovoy et al. (1967) found B* = 0.25 in. to be adequate for heavily side-grooved, contoured DCB specimens of 7075-T651 (K_{Ic}/YS = 0.3, $B/B_n \leq 3.3$) but 1-in.-thick plate was required for 2024-T351 (K_{Ic}/YS = 0.6). Hoagland 1967), with rectangular DCB specimen, found B = 0.5 adequate to measure the fracture toughness of 7075-T6 (K_{Ic}/YS = 0.5), but side-grooving to depths in excess of $B/B_n > 4$ caused the crack initiation toughness to increase. This agrees with Ripling and Falkenstein's (1973) work on K_R measurements where K_{max} was measured to be 66 ksi $\sqrt{in.}$ for 7075-T6 sheet 0.016/0.032 in. thick, reinforced such that $(B/B_n) = 33/16$. These results imply that the thickness criterion set forth in ASTM E399 (i.e., $B \geq 2.5 (K_{Ic}/YS)^2$) must be satisfied by the gross-section thickness for the specimen to produce crack initiation fracture toughness numbers that agree with K_{Ic} measured with standard compact specimens. In addition, the net section (B_n) must exceed 0.25 the thickness of the gross thickness (B), i.e., $B/B_n \leq 4$.

For steels, Hoagland (1967) reports fracture toughness numbers with 1/2-in.-thick specimens that agree with measurements on thicker specimens for A302B (K_{Ic}/YS $\simeq$ 2) and a Ni-Mo-V rotor steel (K_{Ic}/YS $\simeq$ 0.7). He attempted to explain this behavior on the basis that side grooving with B/B_n = 2 and $\rho \leq 0.001$ causes sufficient constraint to ensure plain-strain conditions analogous to those found with surface-flawed specimens where pop-in has been observed. Raymond and Usell (1971) found similar behavior in steels at room temperature with contoured, face-grooved DCB as shown in Figure C-11. The plates were nominally 0.5 in. thick with B/B_n ranging from 1.25 to 3.5 for T-1 (K_{Ic}/YS = 1.5), HY 140 (K_{Ic}/YS = 1.8), HP-9-4-0.2 (K_{Ic}/YS $\simeq$ 1.0) and 18 Ni (200) Maraging (K_{Ic}/YS $\simeq$ 0.65). A typical load trace also is shown in Figure C-11 with an example calculation using the maximum load. Weld (GTA) metal properties also were determined. To evaluate the results tabulated in Table C-2, a ratio analysis diagram (RAD) taken from Pellini (1967) was used as a source of baseline data (Figure C-12). The agreement is exceptionally good, and the weld

---

* Terms are defined at the end of the section.

HY 140, Base Metal #3
$B/B_n = 0.500/.172 = 2.9$
$K = 17.1P$
$K_{max} = (17.1)(15.2 \text{ kips}) = 260.2 \text{ ksi } \sqrt{\text{in.}}$

$P_{max} = 15,200$

LOAD (lb X 1,000)

Dimensions and Configuration for DCB Specimen.

h	a
1 000	1 000
1 250	1 443
1 500	1 936
1 750	2 475
2 000	3 055
2 250	3 674
2 500	4 330

DEFLECTION (0.2 in./in.)
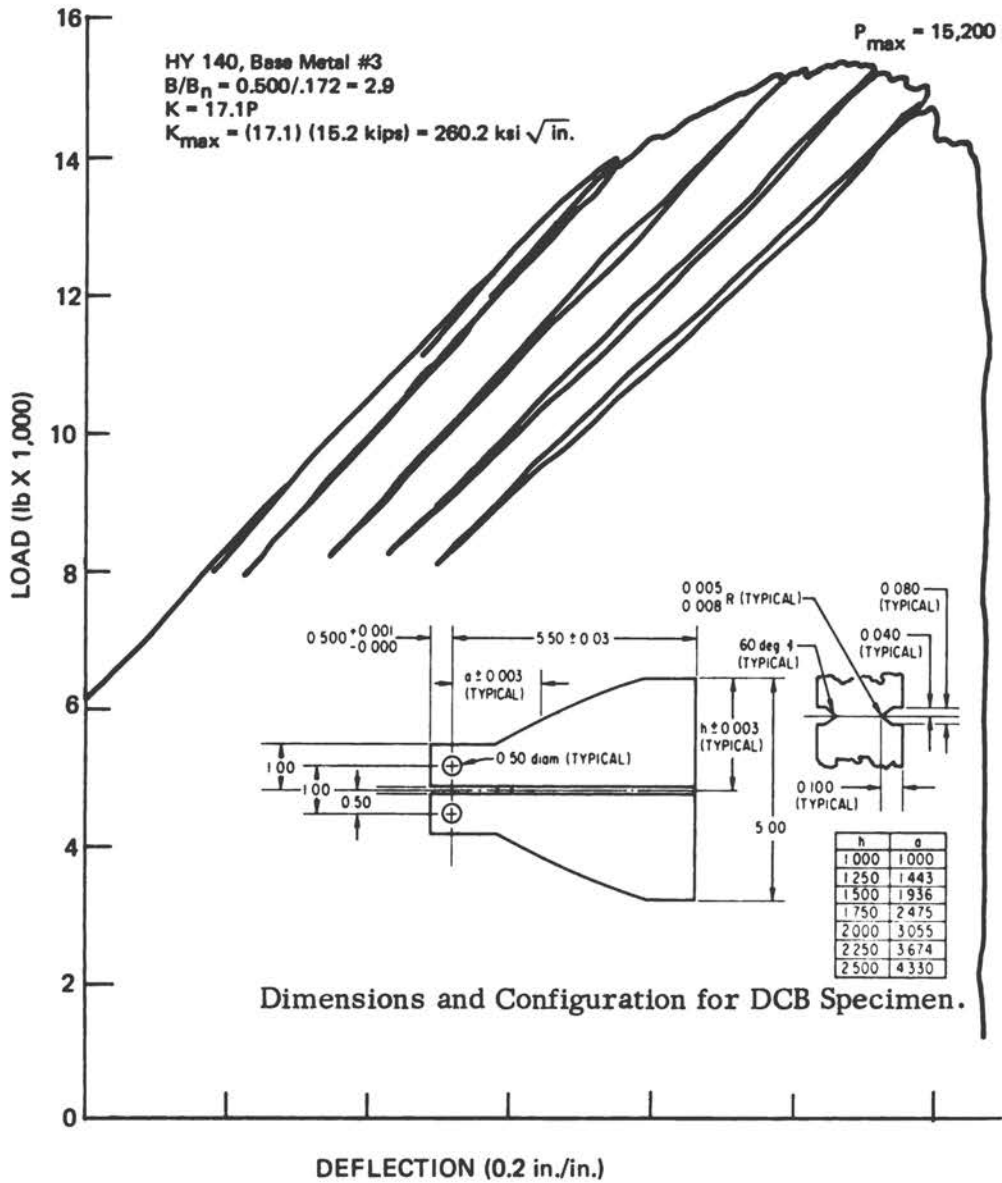
FIGURE C-11   Typical Load Deflection Curve for Contoured DCB.

properties are in the right direction for these alloys (i.e., lower yield strength and higher fracture toughness). The weld data are plotted separately on another diagram taken from the same report (Figure C-13). Again, the agreement is very good.

TABLE C-2 Data from SN-CDCB Steel Specimens.

Specimen	P_{max} (kips)	K_{max} (ksi √in.)	YS (ksi)	Dimension and Load Requirements per ASTM E399-74	
				$B=2.5(K_{max}/YS)^2$	$P_{critical}$ (kips) $a=B$ and $W=2B$
T-1					
Base #1	11.4	158			
Base #2	11.4	158			
Base #4	11.0	151			
Average		156	106	5.4	288
Weld #3	14.1	185	93	9.90	848
HY-140					
Base #1	16.5	276			
Base #2	16.0	268			
Base #3	15.2	260			
Average		268	144	8.65	1,004
Weld #1	17.8	391			
Weld #2	17.0	331			
Average		361	133	18.50	4,230
HP-9-4-20					
Base #1	14.2	191			
Base #2	12.5	168			
Base #3	13.3	179			
Average		179	185	2.35	95
Weld #1	14.2	202			
Weld #2	14.0	199			
Average		200	185	2.86	142
18 Ni (200) Maraging					
Base #2	14.0	146			
Base #5	13.4	141			
Average		144	207	1.07	23
Weld #3	14.6	154			
Weld #4	15.0	158			
Average		156	206	1.31	34

NOTE: Data from Raymond and Usell, 1971.
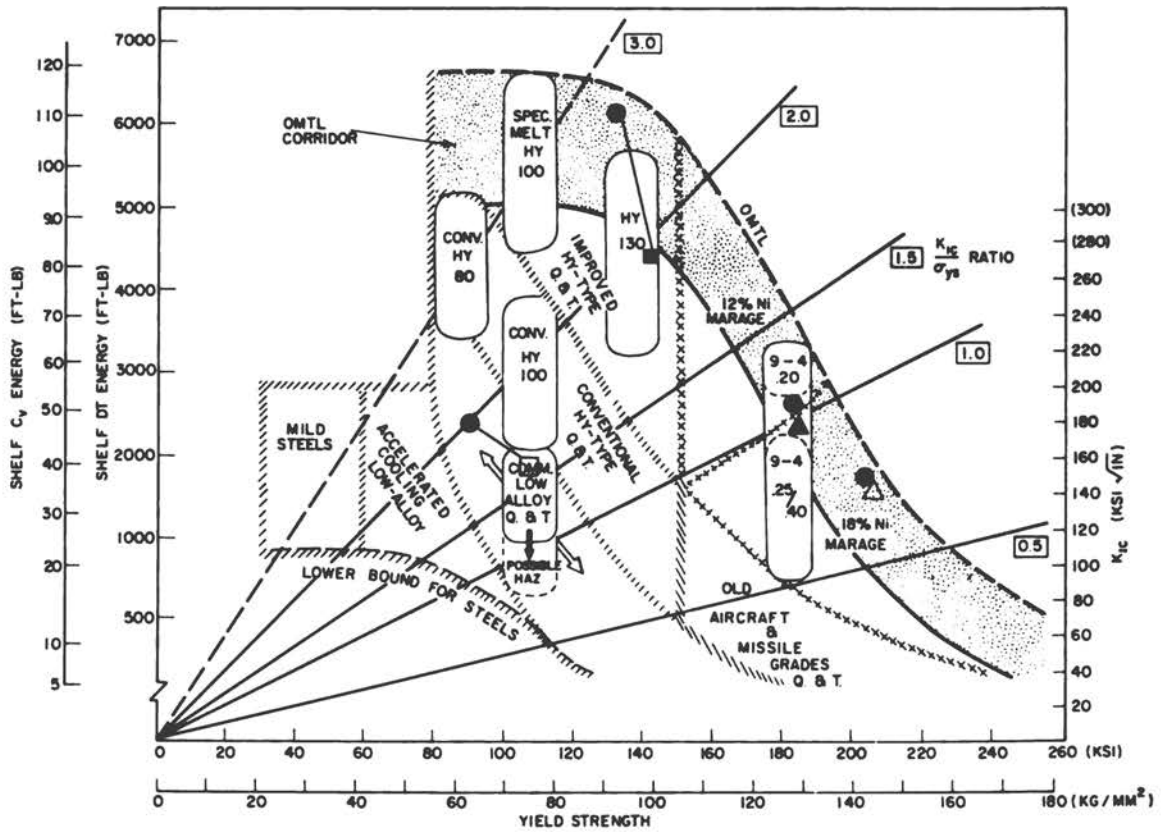
FIGURE C-12   Compendium RAD Indexing for Generic Classes of Steels (Pellini, 1967).

The fracture toughness numbers were calculated from:

$$K \text{ (ksi } \sqrt{\text{in.)}} = P_{max} \sqrt{\frac{E \, (dC/da)}{2B(1-v)^2}} \left(\frac{B}{B_n}\right)^m \simeq 20 \, P_{max} \text{ (kips),} \qquad \text{(Eq. C-8)}$$

for a 0.5-in. steel plate with $(B/B_n < 4)$. The gross thickness definitely violates ASTM E399 for at the extreme value the constant $B/K_{Ic}/YS)^2 = 0.15$, which is significantly less than the specified value of 2.5. The thickness requirement is
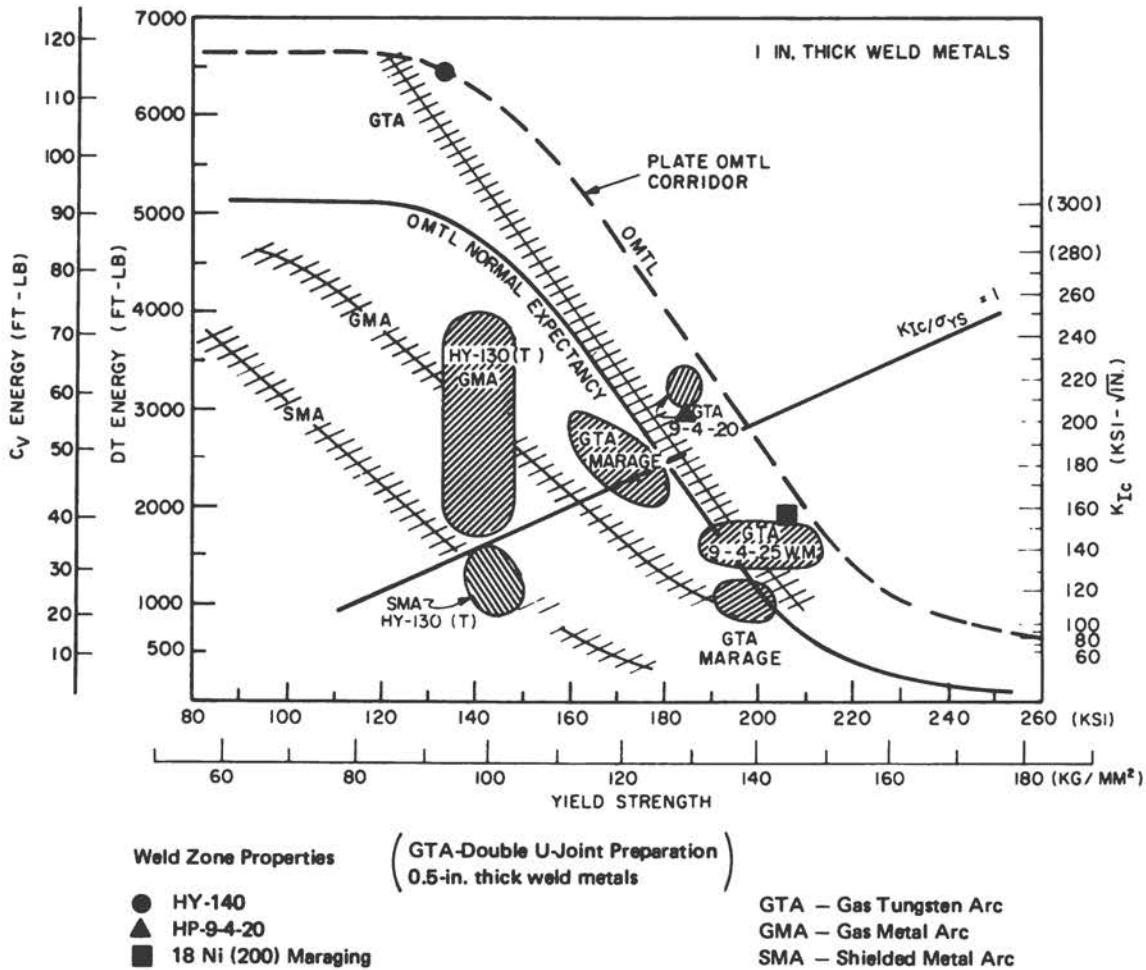
FIGURE C-13 Zonal Location of DT Test Data for Weld Metals Developed Specifically for Joining Various Steels of Primary Interest (Pellini, 1967).

actually closer to that required for J-integral measurements (appendix A). To further appreciate the significance of this number, Table C-2 also lists the dimension and machine load requirements to verify the toughness measurements with a standard compact specimen per E399-74. At an extreme, the difference in load requirements for testing HY 140 weld metal is 4213 kips or 4.2 million pounds with only 18 kips required to conduct the test with the contoured DCB.

Crosley and Ripling (1971) used a contoured DCB with $B/B_n = 1.3$ to 2 and $\rho = 0.01$ to measure the crack initiation and crack arrest fracture toughness of A533-A/B steel ($K_{Ic}/YS \simeq 2$ at RT). From their results, the root radius appears to play a significant role when an attempt is made

to correlate crack initiation measurements with subthickness DCB specimens to K_{Ic} measurements from compact specimens. When the root radius is 8 mil or less, a correlation seems possible, but for larger radii the thickness requirement rapidly approaches that specified by ASTM E399. Additional modifications have been made to add to the complexity of the DCB specimen in attempting to measure crack arrest in 4340 steel (Hahn et al., 1974).

The minimum size appears to be 0.5 by 6 by 6 in. overall dimensions. Face or side grooving to $B/B_n \approx 4$ and $\rho \leq 0.01$ is necessary to obtain critical fracture toughness values of the same value as valid fracture tests with compact specimens. This behavior appears to be occuring with steel. The compliance calibration needs to be performed only once for a given specimen geometry, and it then can be applied readily to other isotropic materials (Dull et al., 1972).

The specimen is extremely simple to use. After calibration, fracture toughness measurements reduce to load measurements since the stress intensity is proportional to the load for crack lengths up to 2.8 in. in a 6-in. specimen. Many different fracture resistance measurements could be made from one specimen. Conceivably, once specimen geometry has been standardized, the specimen could be used as a quality-control measure of the fracture toughness as a function of temperature using only P_{max}. If the latter were possible, cost could further be reduced through use of electrospark discharge machining from a master tool to produce the specified contour. Precracking and machining of side grooves also would be required.

The specimen is extremely versatile and can be adapted readily to studying rate effects because the cracking rate is related linearly to displacement rate (Ripling and Falkenstein, 1973) and has been used over a range of tem temperatures with a single specimen (Crosley and Ripling, 1971).

The most significant improvement would be to fix the specimen configuration for high-toughness steels, materials that apparently need not meet the full thickness plane-strain requirement.

C.2.1 Summary

The double cantilever beam (DCB) specimen encompasses a variety of geometrical shapes including rectangular, tapered (linear increase in height with length), and contoured to the equation $3a^2/h^3 + 1/h$ = constant [non-linear increase in height (h) with length (a)]. The constant, m, has ranged from 3 to 86 in.$^{-1}$. This is further complicated by face or side grooving by different amounts (B/B_n) and with different root radii.

Because of the complexity and variety of dimensions, machining costs appear to make the specimen prohibitive for use as a rapid, inexpensive test for quality control; but its advantage is the large number of fracture toughness data points that can be obtained over a range of temperatures with a single sample. Weld zone fracture properties are measured readily. In addition,

crack arrest toughness and subcritical crack growth studies can be measured with the same sample and the test method can be reduced to a simple load measurement because of the linear compliance change with crack extension. Therefore, the test procedure and equipment is relatively simple and if the shape were standardized, electro-spark discharge machining from a master tool could reduce significantly the cost per data point to a competitive position.

From the work done with aluminum alloys, the gross thickness dimension required for crack initiation measurements to agree with K_{Ic} measurements from a compact specimen, also must satisfy the criterion $B > 2.5 (K_{Ic}/YS)^2$ regardless of side groove depth for $B/B_n \leq 4$. For values greater than four, the crack initiation toughness value increases above K_{Ic}.

For steels, data exist that suggest that the thickness criterion can be relaxed. One-half-in.-thick plate with $B/B_n < 4$ was adequate to obtain fracture toughness numbers that correspond to K_{Ic} values measured on thicker specimens for steels ranging in properties from $0.7 < K_{Ic}/YS < 2.5$. This agreement might indicate that the amount of restraint developed in a side-grooved DCB is equivalent to that developed at pop-in in surface flawed specimens.

C.2.2 Conclusions and Recommendations

Conclusions

1. In high-toughness steels, side grooved, contoured DCB specimens have demonstrated the potential to justify further study regarding quality control testing as a function of temperature through the transition region with a single specimen.

2. For routine K_{Ic} correlations at room temperature, contoured DCB specimens are impractical due to high initial cost in machining them. They should be considered only when other variables, such as temperature and strain rate, are under study.

Recommendations

1. Because of experimental simplicity found in testing the contoured DCB, experimentation should be performed to achieve an optimum, standard design to minimize machining cost.

2. The strength ratio concept should be applied, as with compact specimens, to reduce the transition temperature fracture toughness determination in steels to a simple load-temperature measurement.

3. The thickness criterion for steels should be evaluated further using the face grooved contoured DCB specimen because existing data suggest $B > 0.1 (K_{Ic}/YS)^2$ which is similar to the minimum specimen thickness requirements for J-integral testing.

C.2.3 <u>Glossary of Terms</u>

a — Beam length (equivalent to crack length)

B — Thickness

B/B_n — Ratio of gross to net thickness of beam.

dC/da — Change in compliance with crack length.

E — Young's modulus.

h — Beam height.

P — Load, in kips.

v — Poisson's ratio.

YS — Yield strength, in ksi.

ρ — Root radius of face or side groove.

C.3　DOUBLE-EDGE NOTCHED FATIGUE (DENF) SPECIMEN TESTING

ASTM Standard Method of Test E338-68 prescribes a method for the sharp-notch tension of high-strength sheet materials where the ratio NTS/YS* is calculated. ASTM E338-68, although useful in screening sheet materials, has been, up to now, limited to thicknesses of 1/4-in. or less.

ASTM Task Group E24.01.02 may revise ASTM E388-68 and supplement it with another test method having essentially the same screening functions as E338-68 but possessing a greater applicability in terms of increased specimen thickness and reduced specimen size. ASTM E338 would retain the symmetrically loaded tension specimen (DEN specimen) shown in Figure 3 of E338-68 but, because of requirements for sharp machined double-edge notches, its use would be restricted to easily machined alloys. The new method could be applied to all materials and would use the double-edge notch specimen with one of the notches fatigue cracked (DENF specimen). In an analogous manner with ASTM E399-74, wherein a specimen strength ratio is computed for a compact tension (R_{sc}) and a bend (R_{sb}) specimen, the double-edge notch (fatigue) specimen will provide a specimen strength ratio which, for consistency, will be defined as $R_{st-DENF}$ and will be utilized as a basis for comparison to K_{Ic} whenever

---

* Terms are defined at the end of the section.

possible. The notch-yield ratio solicited from ASTM E338-68 is differentiated from the specimen strength ratio from the new ASTM E388 in that, for the former, data are procured from a specimen having a machined notch and, for the latter, from a fatigue-precracked specimen.

    The general features of the test should follow those specified for the sharp-edge notch (DEN) specimen in ASTM E338-68, Section 6. The test specimen differs in general configuration from the proposed DENF specimen in that knife edges are provided at the fatigue crack notch mouth. These knife edges would be used for the attachment of a clip-in displacement gauge to be used in securing plane-strain fracture toughness data and in providing supplemental information concerning crack growth characteristics. The displacement gauges, related instrumentation, and analysis of the load-displacement record should be in accordance with Method of Test E399-74, properly interpreted for the DENF specimen prescribed here (Figure C-14).
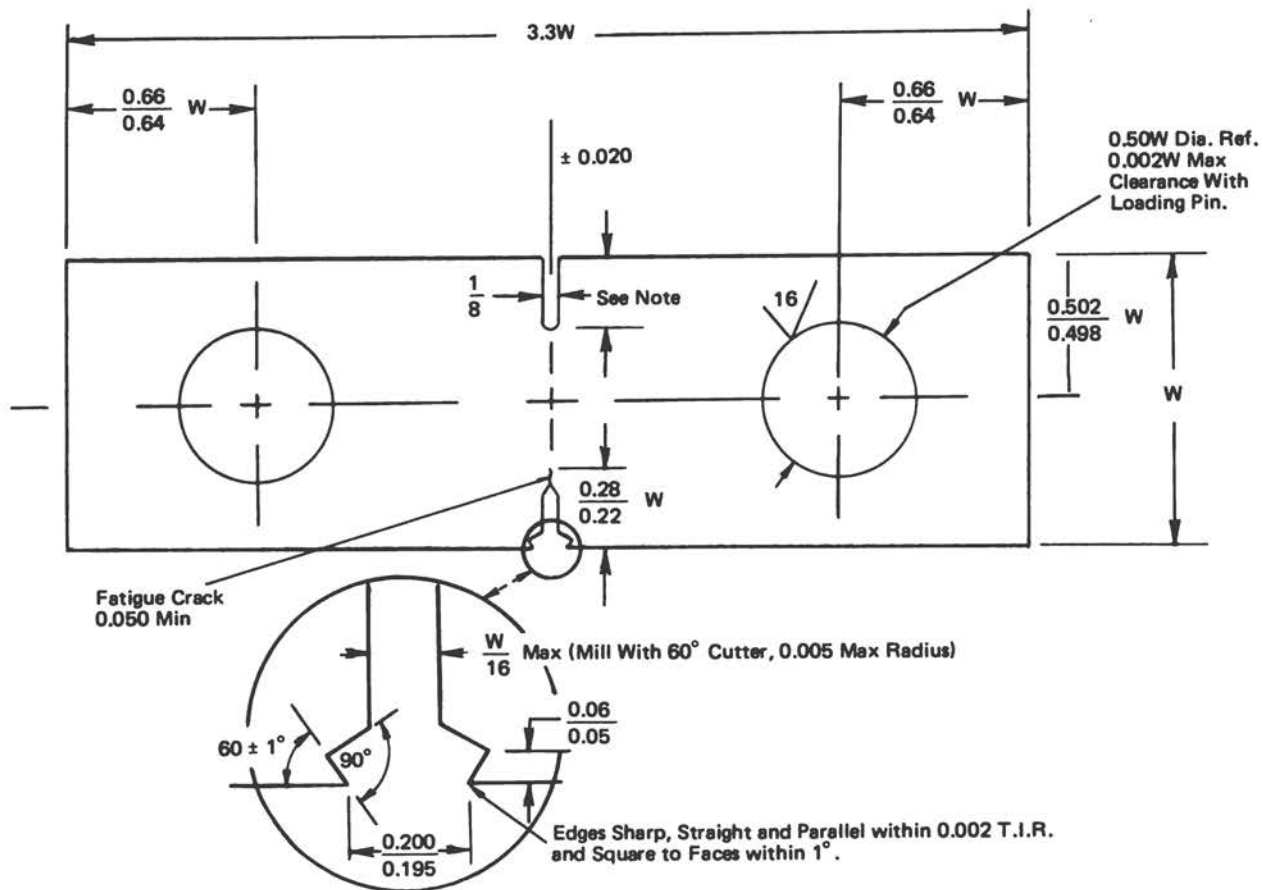
NOTE: The slot is to be machined after the opposing notch is fatigue cracked and is to match the average total length of the opposing notch plus fatigue crack to $\pm$ 0.002.

FIGURE C-14   DENF Test Specimen (Army Materials and Mechanics Research Center, 1974).

The proposed DENF specimen contains two symmetrically opposed notches, one of which is fatigue cracked and the other provided with an easily machined, relatively blunt tip. The blunt notch has the same maximum length as the notch plus fatigue crack and its purpose is to produce a balanced stress field. Fracture will run from the fatigue crack and the balanced stress state will not be maintained to fracture. However, the sharp double-edge notch (DEN) specimen of ASTM E338-68 generally exhibits this behavior, and experience shows that the consequent eccentricity in loading does not impair the usefulness of that test.

Formal calculations of apparent plane strain fracture toughness shall be made using an interpolation form, good to 0.5 percent (Tada, Paris, and Irwin, 1973). The tensile ultimate strength, yield strength, notch strength, maximum sustained load, and specimen strength ratio will be reported and a comparison of all test materials made as a function of specimen thickness, B, for each specimen width on the basis of both $B \geq (K_{Ic}/YS)^2$ and the specimen strength ratio. Triplicate notch specimen tests shall be made for each specimen thickness and width; test direction shall be RW.

Unfortunately, no existing data correlate the fracture toughness values (K_{Ic}) obtained per ASTM E399-74 and the specimen strength ratio ($R_{st-DENF}$) derived from the possible revision of ASTM E338. Data do exist from ASTM E338-68 specimen test programs in which the ratio NTS/YS was determined, but these data were acquired from materials whose K_{Ic} values were either unknown or unattainable because of product form (i.e., sheet materials), so no correlation was possible.

The length of the DENF specimen has been made as short as possible to avoid excessive interaction between the stress fields of the loading holes and the edge notches. The lower limit on specimen length was established by the results shown in Figure C-15 for tests on 300-grade maraging sheet steel specimens, heat treated to three different strength (toughness) levels. From these results it can be concluded that the crack-strength-to-yield-strength ratio (R_{s-DENF}) is nearly independent of the distance between the notch plane and the loading hole centers if this distance is greater than about 1W. Based on these results, the specimen total length has been set at 3.3W.

Furthermore, the total notch length (depth) was selected at 0.5W rather than 0.3W as specified in ASTM E338-68. This permits the use of a larger loading pin without increasing the possibility of specimen head failure and extends the thickness range that can be tested using a given width specimen. The pin diameter was taken equal to the net section width (0.5W) and, with these proportions, fracture always will occur at the notched section, providing the crack strength is less than the tensile strength.

Very little is known about the effects of varying the ratio of width to thickness of crack toughness specimens on the crack strength. Research is designed to explore the complex influence of specimen width and thickness on the fracture strength. For the time being, the lower limit of W/B = 12 prescribed in ASTM E338-68 will be used.
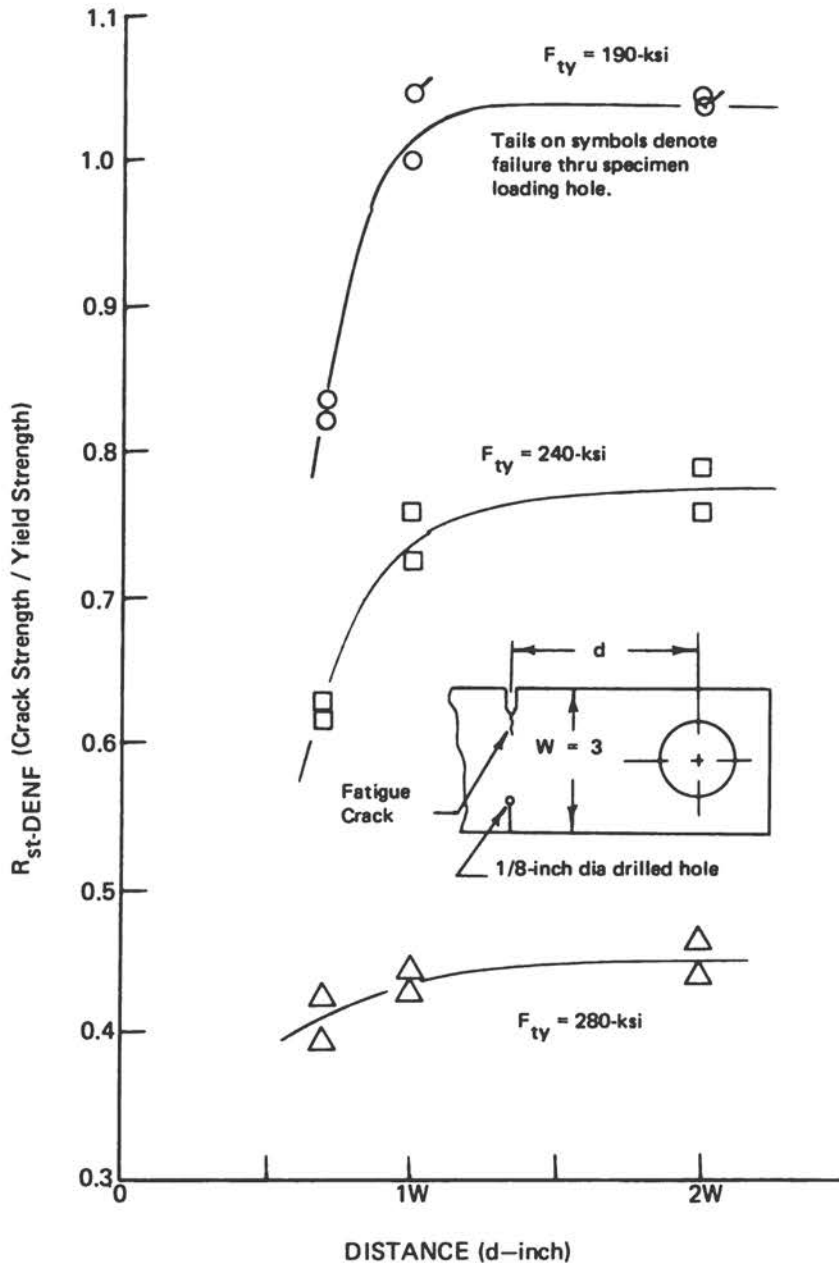
FIGURE C-15   Effect of Distance (d) from Loading Hole Centerline to Notch Plane on Crack-Strength-to-Yield-Strength Ratio for 1/8-in., 18 Ni (300) Maraging Steel Sheet at Three Strength (Toughness) Levels (Army Materials and Mechanics Research Center, 1974).

In addition, the maximum thickness that can be tested using a particular width is determined in part by the requirement that specimen failure occur before pin failure. In this regard, the lowest W/B ratio to be studied in this program (W/B = 2) is limiting and requires that the loading pin material have a yield strength at least 20 percent higher than that of the specimen. Therefore, the loading pins should be made of 18 Ni maraging steel with a yield strength of about 300 ksi, to ensure failure in the test section for test materials with yield strengths up to 83 percent of this value. Probably, stronger material would be brittle and fail in the cracked section well before the yield strength of the pin is reached.

With the exception of the fatigue crack, the preparation of the specimen involves only standard machine shop practices. The crack starter should be machined and fatigue cracked before the balancing notch. Fatigue cracking should follow complete heat treatment and conform to the practice outlined in ASTM Method of Test E399-72. The method of producing the balancing notch is optional; however, the dimensional tolerances on this notch should be observed strictly.

Very little experience exists with the DENF specimen in quality-control laboratories since it is seldom used. DENF specimens could be tested at a wide range of loading rates and test temperatures in a fully equipped test laboratory. However, equipment needed for such tests normally would not be found in a quality-control laboratory.

Research is currently under way to determine the influence of specimen width and thickness, separately and in combination, on the crack strength (net fracture strength) and, where possible, plane-strain fracture toughness of several alloys using the DENF specimen proposed by ASTM Subcommittee E24.01 for screening heavy section materials.

C.3.1 Summary

A test program at NASA-Lewis is currently underway to expand the use of ASTM E338-68 to measure the fracture toughness in specimens exceeding 1/4-in. with DENF specimens. The specimen has been used in the past to screen sheet materials based on the notch-tensile-strength-to-yield-strength ratio, but the data correlating this ratio to the fracture toughness is literally nonexistent because the material form was generally too thin to obtain valid K_{Ic} numbers.

The use of the DENF specimen as a rapid, inexpensive fracture toughness test only can be obtained once a larger amount of correlation data has been generated. The specimen strength ratio concept should be adapted for consistency since the notch sensitivity of the tensile strength is the index being correlated to the fracture toughness for all specimens being considered. This value is obtained readily from a maximum load measurement. Compliance gauge monitoring techniques are not necessary unless an attempt is made to measure

a valid fracture toughness number. Although existing methods of fracture toughness testing of the DENF specimen are used occasionally in quality control laboratories, tensile testing of notched specimens is commonplace.

C.3.2 Conclusion and Recommendations

Conclusion

1. The DENF specimen has been used as an index of fracture resistance but with no correlation to fracture toughness. The specimen is designed to provide the NTS/YS ratio for a given product form, i.e., sheet materials less than 0.25-in. thick, where valid K_{Ic} measurements are normally unattainable, except for very brittle materials.

Recommendations

1. For thicker sections, other more rapid, less expensive techniques, such as the Charpy or Notched Round Bar, should be used in quality control.

2. Data should be reported only in the context of $R_{st\text{-}DENF}$, even when the specimen is thick enough to measure the fracture toughness, in order to generate a data bank.

C.3.3 Glossary of Terms

B, W — Thickness, width of specimen (measured from load line in compact specimen and between load points in bend specimen).

DENF — Fatigue-cracked double-edge notch flat tensile specimen.

NRB — Notched round bar.

NTS/YS — Notch-tensile strength to yield-strength ratio of a round bar ≡ notch-yield ratio.

R_s-DENF — Maximum net section tensile-strength-to-yield-strength ratio of a DENF specimen ≡ specimen strength ratio of a tensile-loaded DENF specimen.

R_{sb} — Maximum net section tensile-strength-to-yield-strength ratio of a bend specimen ≡ specimen strength ratio of a bend specimen.

R_{sc} - Maximum net section tensile-strength-to-yield-strength ratio of a compact specimen ≡ specimen strength ratio of a compact specimen.

R_{st-NRB} - Specimen strength ratio of a tensile loaded NRB specimen = NTS/YS.

C.4 SURFACE-FLAW SPECIMEN

Surface-flaw specimens (Figure C-16) have been used since 1960 to quantitatively evaluate fracture, fatigue crack propagation, and stress corrosion cracking resistance of flawed metallic structures. In particular, considerable surface-flaw specimen testing has been performed within the aerospace industry since the surface flaw is a very good model of defects found in aerospace structures (Tiffany and Masters, 1965). Surface-flaw specimen data have been used to develop design methods to ensure that metallic pressure vessels will not undergo brittle fractures prior to meeting service life requirements (Tiffany, 1970). Notwithstanding considerable effort directed to the stress analysis and testing of surface-crack specimens, standardized test procedures and exact stress analyses have not yet been developed. However, variations in test procedures are not large and the latest solutions for stress intensity

SIZING

W ≥ 10C
G ≥ 2W
a/2c > 0.1
0.2 < a/t < 0.6

SECTION A-A
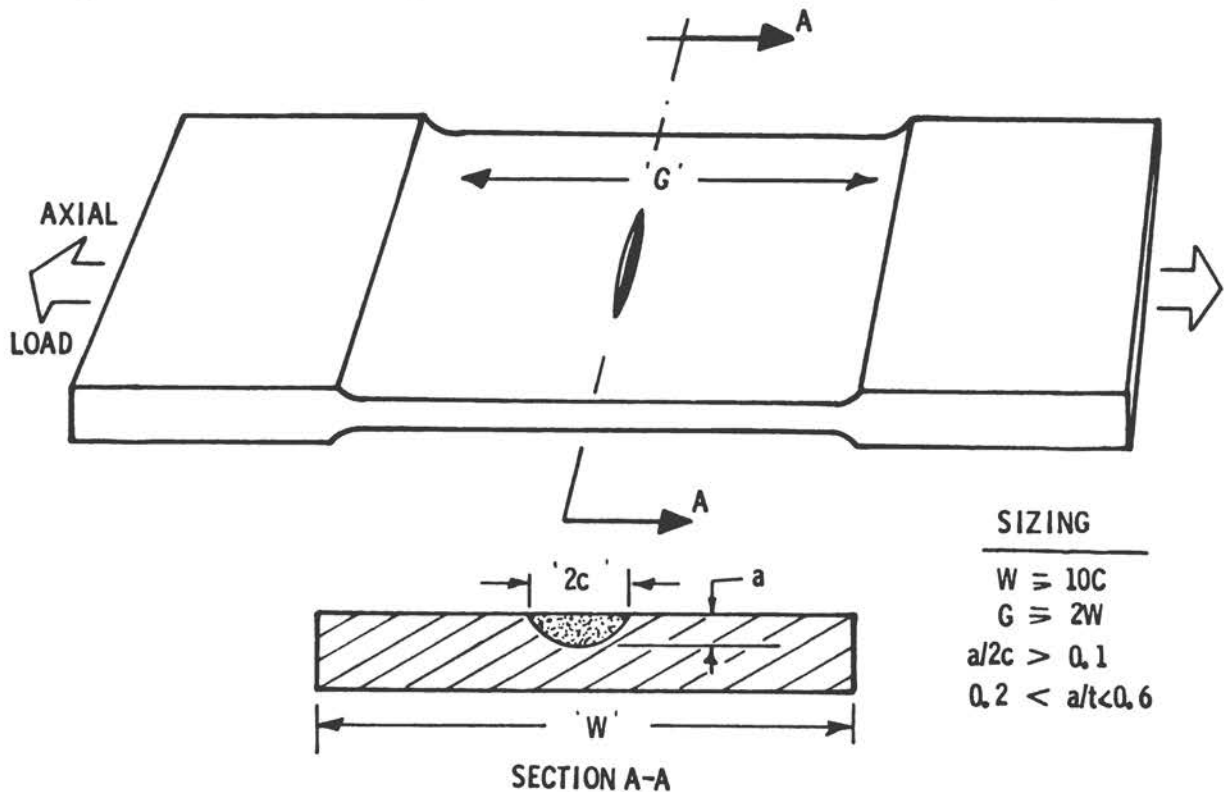
FIGURE C-16   Description and Sizing of Surface-Flaw Specimen.

factors are believed to be accurate within ± 5 percent for a wide range of geometries. Hence, surface-flaw specimens are characterized reasonably well and could be adapted to quality-control testing.

Surface-flaw specimens have a rectangular cross-section containing an approximately semielliptical-shaped flaw originating from one surface of the specimen. The flaws are prepared by growing fatigue cracks from starter slots. The most common method of producing starter slots is electrical discharge machining using thin, circular electrodes. Fatigue cracks are grown from the starter slot using axial tension or bending fatigue loadings. Stress levels used for precracking are kept to a minimum and are less than the subsequent test stress levels.

Most surface-flaw tests were conducted using uniaxial tensile loads acting perpendicular to the plane of the flaw. A few tests used either three- or four-point bending loads or combinations of tensile and bending loads. Continuously rising loads are used to investigate fracture strength of surface-cracked materials. Sustained loadings are used to study the stress corrosion cracking resistance of metallic alloys under the combined influence of stress and chemical environments. Fluctuating loads are used to study fatigue crack propagation characteristics of surface-cracked materials. Fracture tests are the only test type pertinent to the quality-control problem discussed in this report; accordingly, this discussion is restricted to a consideration of the static fracture behavior of surface-flaw specimens.

Fracture tests of surface-flaw specimens are conducted by applying a monotonically increasing uniaxial tensile load until the specimen fractures. Peak load is measured during the test and initial flaw dimensions are measured from the fracture surfaces of the specimen. Peak load and initial flaw dimensions are substituted into the appropriate stress intensity factor equation to calculate a fracture toughness value (often designated by the symbol K_{IE}). Clip gauge instrumentation (e.g., Figure C-17) is often used to continuously record crack

Flaw Depths, a > 0.050"   Flaw Depths, a < 0.050"
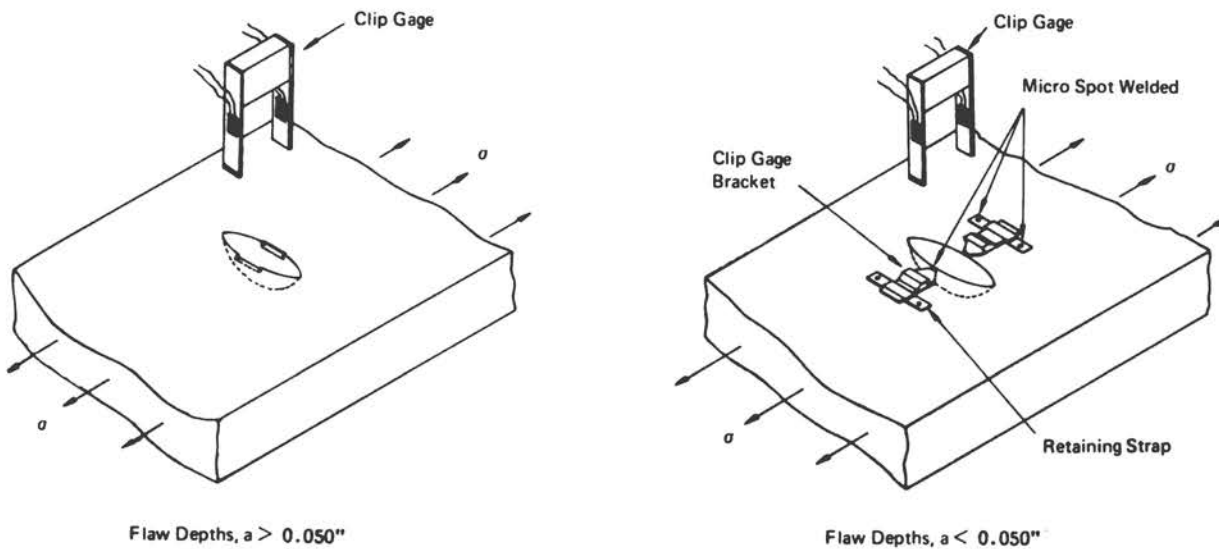
FIGURE C-17   Flaw Opening Measurement for Surface-Flaw Specimens.

displacement at the intersection of the semi-minor axis of the crack and the specimen surface from which the crack originates. Such records have served as qualitative indicators of fracture behavior but have not been used in quantitative evaluations of fracture toughness.

Since stress intensity factors for surface-flaw specimens usually are maximum at the point of maximum flaw depth, the resulting fracture toughness values normally are applicable to the crack propagation direction coinciding with the semi-minor flaw axis (usually the L-S or T-S direction). However, if the fracture toughness for the lateral direction is less than that for the depthwise direction, fractures can originate in the lateral direction and result in either complete fracture of the specimen (Masters, 1972) or in a "pop-in" (Hall, 1973). In such cases, apparent fracture toughness values calculated using peak or pop-in load, initial flaw dimensions, and stress intensity factor calibrations for the point of maximum flaw depth may not be equal to the actual fracture toughness for either the lateral or depthwise directions.

Testing experience has shown that, for given test conditions, fracture toughness values obtained from adequately designed surface flaw specimen tests are reasonably constant if the following conditions are met: (a) failure stress is less than 90 percent of the uniaxial tensile yield stress, (b) the distance between the tip and back specimen face is greater than $0.1 (K_{IE}/\sigma_{YS})^2$ * at the outset of the test (Masters, 1973), (c) flaw depth-to-length ratio is greater than 0.10, and (d) fractures originate at the point of maximum flaw depth. Violation of any of the above limitations can lead to wide variations in calculated fracture toughness values.

For many years, fracture toughness values obtained from tests of surface-crack specimens were designated as plane-strain fracture toughness values or K_{Ic} (during this time, K_{Ic} was defined simply as the lower limit of fracture toughness associated with conditions of plane strain crack tip deformations). This practice was based on the knowledge that surface cracks undergo plane-strain crack tip deformation (Irwin, 1962) and tend to yield lower bound fracture toughness values (Irwin, 1961). Plane-strain fracture toughness (K_{Ic}) subsequently has been defined more precisely by ASTM as the fracture toughness value corresponding to 2 percent crack extension in specimens and tests meeting specific requirements. Fracture toughness values for surface-flaw specimens (K_{IE}) are calculated presently by substituting peak load and initial flaw dimensions into the appropriate stress intensity factor equation and, hence, K_{IE} and K_{Ic} values may be numerically similar but should not be expected to be numerically equal.

Apparently, only one set of tests was conducted to compare K_{IE} and K_{Ic} values for a single crack propagation direction (Hall, 1971). Single-edge notched bend (SENB), single-edge notched tension (SENT), compact (CT), and surface-flaw specimens were cut from either one 2.5-in.-thick 2219-T87

---

* Terms are defined at the end of the section.

aluminum alloy plate or one 0.80-in.-thick 5Al-2.5Sn (ELI) titanium alloy plate (Figure C-18). Orientation of crack plane with respect to rolling direction was the same for all specimens of a given alloy (i.e., parallel to the rolling direction for the aluminum alloy and perpendicular to the rolling direction for the titanium alloy). All crack tips were located close to the mid-plane of the parent plates. Tests of each specimen type were conducted at 72° F, -320° F and -423° F in air, liquid nitrogen, and liquid hydrogen, respectively.

Results of the aluminum alloy tests are plotted on graphs of fracture toughness versus test temperature in Figure C-19. All of the SENB and CT specimens yielded valid plane-strain fracture toughness values per ASTM E399-72. The scatter band in Figure C-19 was drawn to include all SENB, SENT, and SF specimen fracture data. Plane-strain fracture toughness values obtained from the CT specimen tests fell consistently below the scatter band. Reasons for the disagreement could not be determined.

Results of the titanium alloy tests are illustrated in Figure C-20. At 72° F, specimen sizes were much too small to allow valid fracture toughness values to be measured. At -320° F and -423° F, most of the SENB and CT specimen tests yielded valid plane-strain fracture toughness values. At -423 °F, there was reasonable agreement between all data. At -320° F, however, fracture
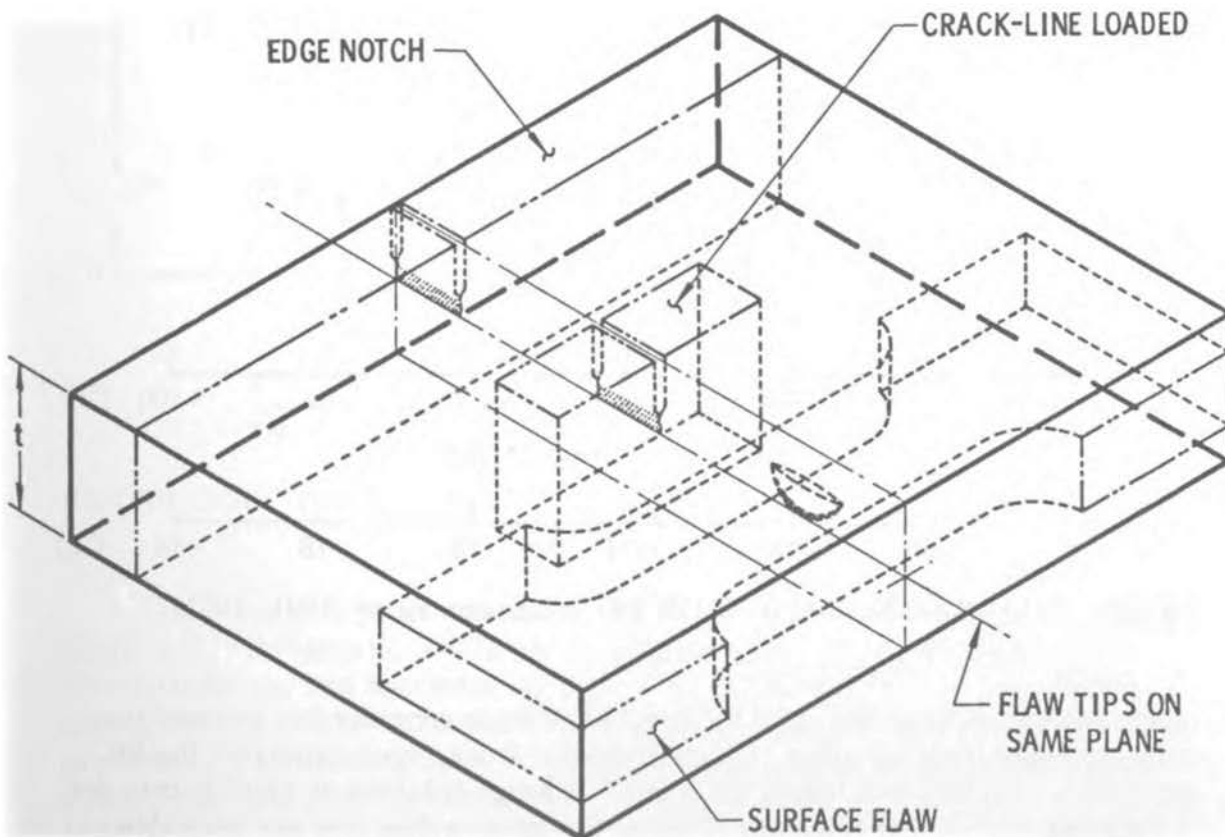
FIGURE C-18   Specimen Location within Plate.
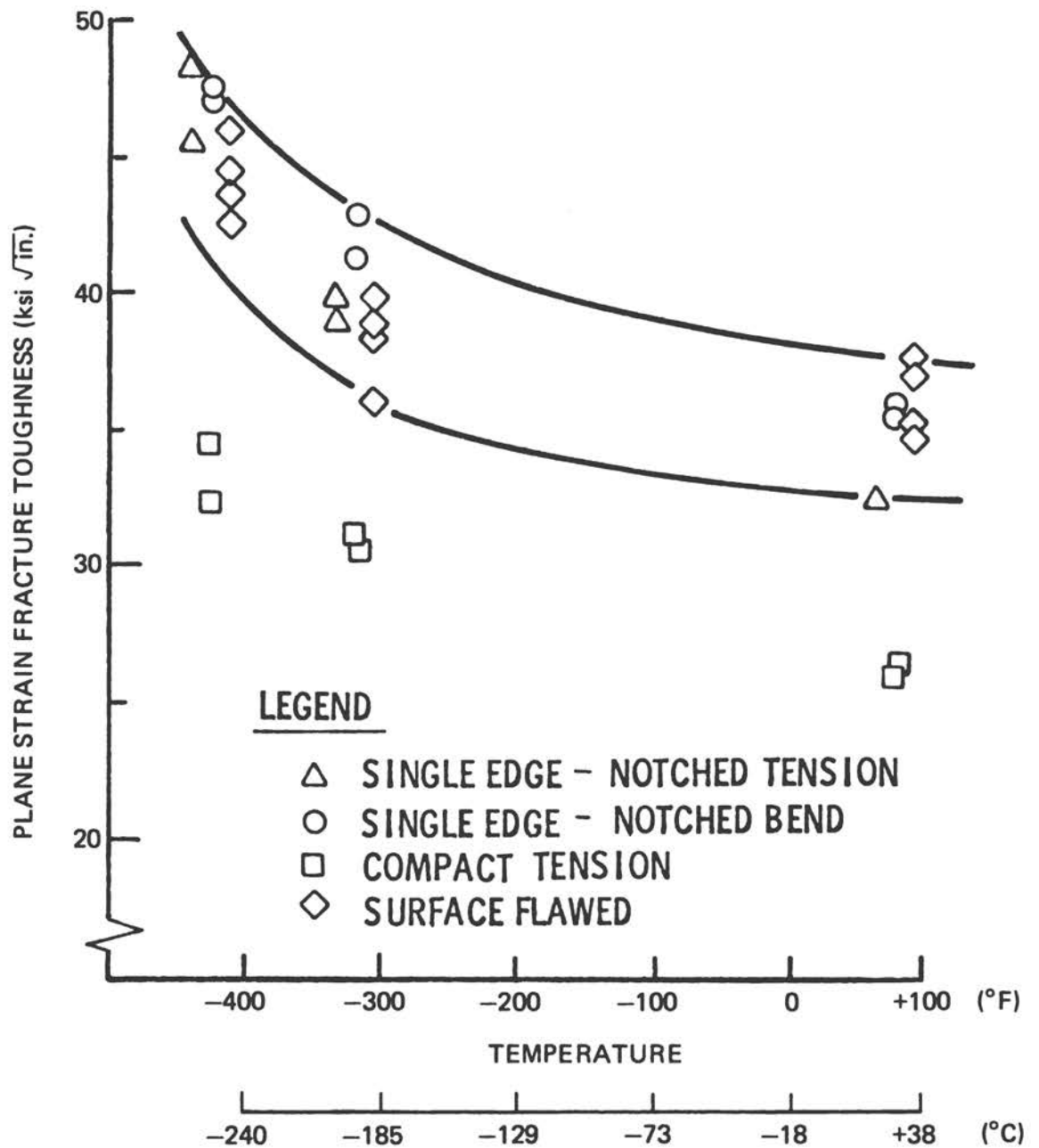
FIGURE C-19   Test Results for 2219-T87 Aluminum Alloy (Hall, 1971).

toughness values obtained from SF specimens were considerably greater than those obtained from all other specimen types. It was speculated that the SF specimens resulted in a lesser amount of cleavage fracture at -320° F than did the through-cracked specimens. Hence, the limited data that are available indicate that the relationship between fracture toughness values obtained from SF and CT specimens is dependent on alloy and test conditions and must be evaluated experimentally for each material/environment combination of concern.
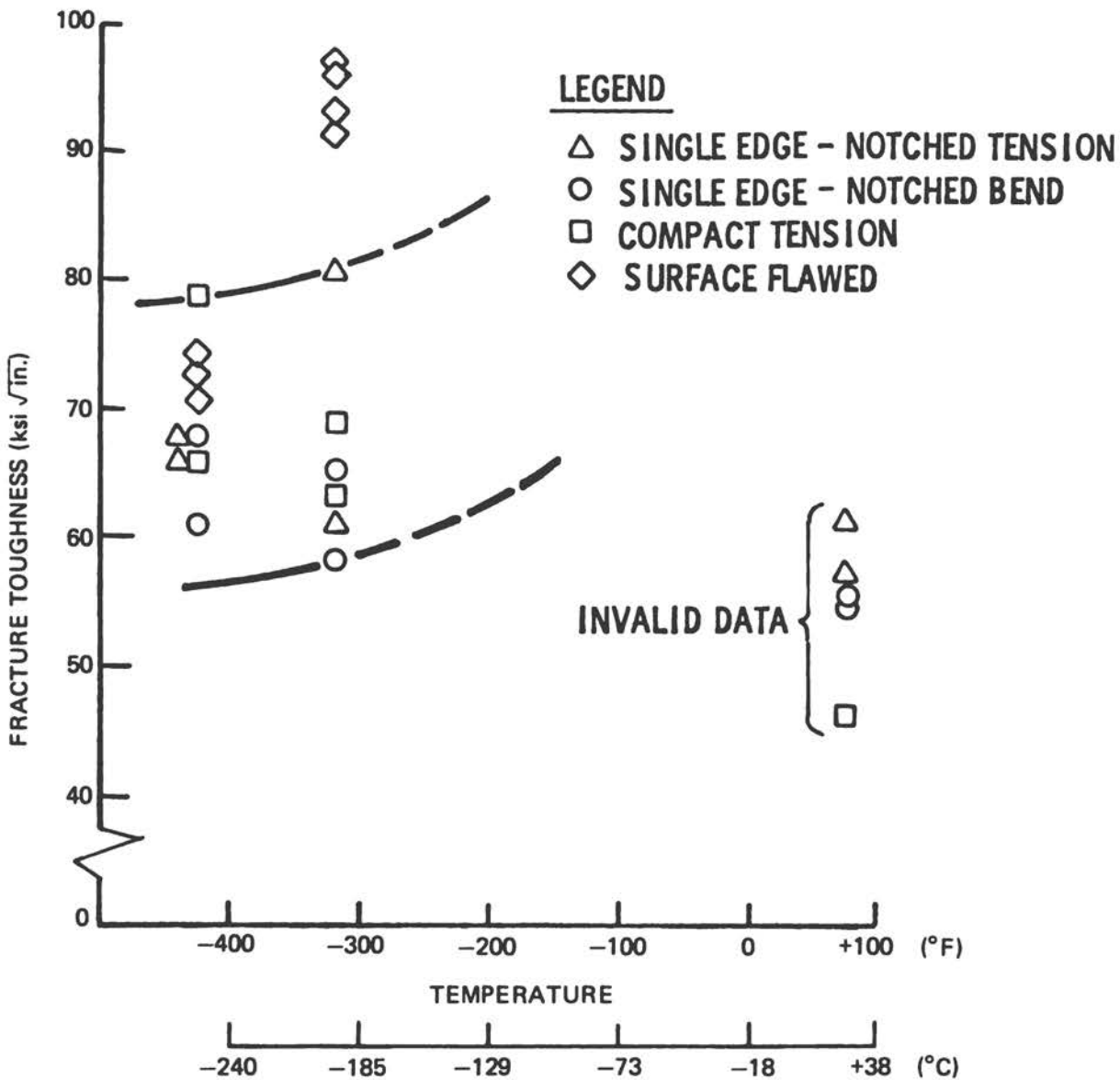
FIGURE C-20   Test Results for 5Al-2.5Sn (ELI) Titanium Alloy (Hall, 1971).

In other test programs in which both SF and CT specimens were tested (Hall, 1973; Fedderson, 1972), there were differences in crack propagation direction for the two specimen types. In some materials, fracture toughness undergoes little or no variation with crack propagation direction. In other materials, fracture toughness varies significantly with crack propagation direction. Some data showing variations in relationships between SF fracture toughness data for the T-S direction and CT fracture toughness data for the T-L direction are summarized in Table C-3. It is evident that the correspondence between the two different fracture toughness values varies with alloy and test temperature.

TABLE C-3 Summary of Some Fracture Toughness Data Obtained from Compact and Surface Flaw Specimens.

Alloy	Temperature (° F)	Fracture Toughness (ksi√in.)	
		T-L Direction*	T-S Direction**
Fe-9Ni-4Co-0.3C	-65	87	94
Hot Rolled Plate	72	107	107
(F_{ty} =208 ksi; F_{tu} = 244 ksi)	175	105	108
D6AC Steel		54	57
Forged Plate	72	66	63
(F_{ty} = 220 ksi; F_{tu} =240 ksi)		58	100
Ti-6Al-4V Ra	-65	84	103
Hot Rolled Plate	72	93	93
Al-7075-T651	-65	21.4	30.7
Hot Rolled Plate	72	22.7	32.6
	175	24.2	34.7

* Measured using ASTM compact specimens.
** Measured using surface-flaw specimens.

Relative values of estimated costs for conducting static fracture tests using surface-flaw, ASTM compact, and instrumented precracked Charpy specimens are shown in Figure C-21 for several airframe alloys. Surface-flaw specimens are consistently more expensive than either the ASTM compact or precracked Charpy specimens.

There are no standardized size requirements for SF specimens; however, SF specimens are larger than ASTM compact specimens and require considerably higher test machine capacities. It has been shown that fracture loads for SF specimens are about ten times those for ASTM compact specimens for four alloys including 7075-T651 aluminum, 9Ni-4Co-0.2C steel, Ti-6Al-4V βA, and Ti-6Al-4V RA (Hall, 1973).

Surface-flaw specimens are reasonably complex primarily because of the difficulties in producing flaws having regular peripheries and known sizes. A good crack starter having uniform sharpness is required.

Outside of the aerospace industry, there are few, if any, test laboratories that have had much experience in testing surface-flaw specimens. Surface-flaw specimens have never been used for quality-control purposes.

In its present state of development, the surface-flaw specimen can be used to test only the crack propagation direction coinciding with the semi-minor flaw axis. For most plate materials, this restricts the number of directions

ALLOY	ALUMINUM 7075-T651	TITANIUM 6Al-4V STA	STEEL 4340 (220-240)	ALUMINUM 2219-T87	TITANIUM 6Al- 4V RA
K_{IC}/σ_{ys}	MODERATE			HIGH	

INSTRUMENTED PRECRACKED CHARPY

ASTM COMPACT SPECIMEN

SURFACE FLAW SPECIMEN

(BASED ON COST DATA FROM R. WULLAERT)
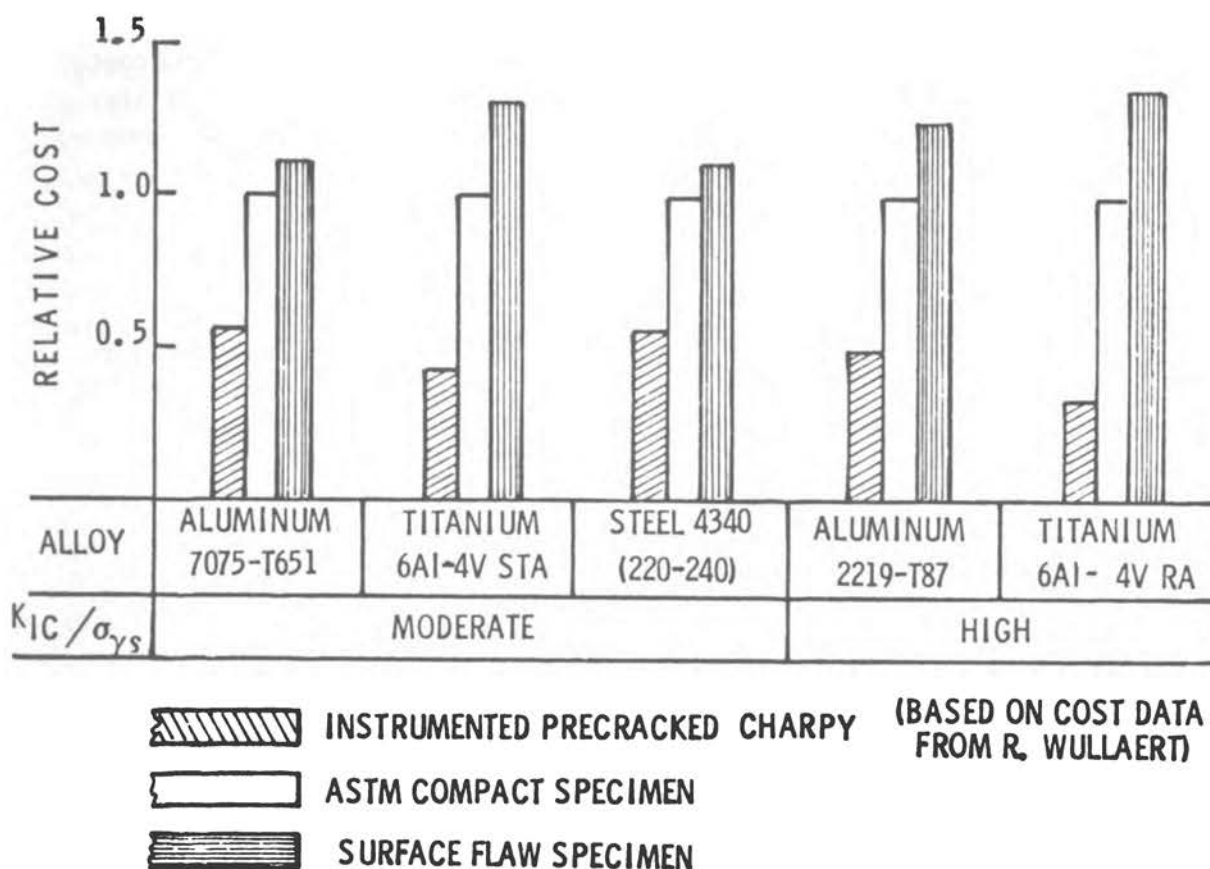
NOTE: Cost data for the compact and surface-flaw specimens were obtained from the Boeing Aerospace Company, Seattle, Washington. Cost data for the precracked Charpy tests were obtained from Effects Technology, Inc., Santa Barbara, California.

FIGURE C-21   Relative Cost Data.

that can be tested to two; namely, the L-S and T-S directions. For thick plates (> ≈ 2 in.), it might be possible to test the L-S and T-S directions in addition to the L-S and T-S directions. The short transverse directions could be tested only by attaching grips to a test section cut from the plate.

It is possible to test surface-flaw specimens at a wide range of loading rates and test temperatures in a fully equipped test laboratory. However, equipment needed for such tests normally would not be found in a quality-control laboratory.

From the standpoint of quality-control testing, prospects for improvement of SF specimens are not good. The most desirable improvements would be a significant decrease in size requirements and precracking costs. Decreases in size would lead to post-yield fractures that would have to be analyzed using a

post-yield analysis method such as the COD or J-integral methods. Other specimen types are better suited to such analyses methods. Precracking cost could be reduced relative to their present levels for specimens tested in large quantities. At best, however, precracking costs would equal or exceed those for ASTM compact specimens.

C.4.1 Summary

The surface flaw specimen has proven to be an excellent specimen for the development of design data and for use in failure analyses. From the standpoint of quality control testing of fracture resisting materials, however, high fabrication costs, large specimen size requirements, and inconsistent correlations with ASTM compact specimen fracture toughness data hinder the usefulness of the surface flaw specimen for quality control testing.

Recommendation -- It is recommended that no effort be devoted to improving the suitability of the surface-flaw specimen for use in quality-control testing.

C.4.2 Glossary of Terms

F_{tu} - Uniaxial tensile ultimate strength.

K_{IE} - Fracture toughness values obtained from surface flaw specimen tests using peak load and initial flaw dimensions.

σ_{ys}, F_{ty} - Uniaxial tensile yield strength.

C.5 EVALUATION OF TENSILE LOADED SPECIMENS

Tensile loaded tests can be considered as a rapid test for quality control when the relative strength ratio is the criterion. In essence, this approach is the notch ratio approach with fatigue cracked specimens. The compact, double cantilever and surface flaw specimens are prohibitive from a cost standpoint when compared to the cost of machining a notched round bar or double edge notched specimen. The latter two methods already are being used for notch ratio considerations. The DENF specimen per ASTM E338-68 and the NRB specimen are being considered by ASTM Task Groups E24.01.02 and E24.01.07, respectively.

Normally, notch ratio data are not reported as a correlation parameter to K_{Ic} but instead, as an alternate measurement, when the K_{Ic} test is found to be invalid. Therefore, correlation data are virtually nonexistent. Caution must be exercised when using this approach as a measure of fracture toughness because fracture toughness changes with temperature. A decrease in the ratio with temperature, as found with titanium alloys, might reflect only an increase in the yield strength while K_{Ic} remains constant.

The only correlation data is with aluminum alloys (section C.1) but these are for machined and not fatigue-cracked NRB specimens. The fatigue crack is the differentiation factor between notch yield ratio and specimen strength ratio. A machined notch would not be suitable for steel or titanium alloys. Neither would fatigue precracking a notched round bar be practical because of eccentric loading problems.

Thus, the tensile loaded specimens cannot compete as a low-cost quality-control approach compared to the precrack Charpy in slow-bend to measure $R_{sb\text{-}CV}$ except possibly for aluminum and magnesium alloys. However, the use of a notch-round bar in bending as the ultimate in a low-cost approach should be evaluated. It would combine both the minimum cost approach to machining (i.e., NRB) and the minimum cost approach to testing (i.e., bending). Use of a precrack would pose a major obstacle.

APPENDIX D

CHARPY-SIZE SPECIMEN

This appendix discusses the use of Charpy-size specimens to obtain fracture toughness information. The term "Charpy-size specimen" has specific connotations within the context of this report regarding specimen geometry, size, and mode of loading as follows:

a. The specimen blank is a rectangular bar with a 0.394 in. by 0.394 in. (10 mm by 10 mm) cross section and a 2.165 in. (55 mm) length.

b. There is a notch or precrack across one surface at specimen mid-length.

c. The specimen is loaded in simple three-point bending with the notch in tension.

For specific experimental purposes, one of the specimen dimensions (such as the thickness) may be varied. However, major changes in dimensions are not included under this designation of a "Charpy-size specimen" since the specimen would then become a size variation of another series such as the standard ASTM E399 bend specimen or the dynamic tear specimen.

Several testing methods using the basic Charpy-size specimen have evolved; they differ primarily in the following respects:

a. Notch Geometry and Severity -- For the results considered in this appendix, the notches are either the standard 0.010-in. root radius machined notch or a fatigue precracked notch.

b. Rate of Loading -- Either at impact rates or in slow bending.

c. Instrumentation -- With or without instrumentation to obtain load/time or load/displacement information.

d. Data Measured -- Either during the breaking of the specimen or on the broken specimen.

104

Various combinations of these features result in the several different methods of testing Charpy specimens which can be designated as:

a. Standard Charpy Impact Test

b. Instrumented Charpy Impact Test

c. Precracked Charpy Impact Test

d. Instrumented Precracked Charpy Impact Test

e. Precracked Charpy Slow-Bend Test

f. Instrumented Precracked Charpy Slow-Bend Test

The subsequent portions of this appendix first give some testing details about these methods followed by available information concerning their use to obtain linear elastic fracture mechanics (LEFM) toughness parameters. It will be pointed out that under certain circumstances, fracture toughness quantities K_{Ic} or K_{Id} (K_{Id} = dynamic fracture toughness measured at rapid loading rates) can be obtained from the measurements. In other cases, purely empirical correlations of some quantity measured on the specimen with K_{Ic} or K_{Id} are utilized. In addition, the use of test results from Charpy-type specimens to derive other toughness-related transition temperature parameters such as the nil-ductility transition temperature (NDT) and crack arrest temperature (CAT) are discussed.

D.1   TEST METHODS AND PROCEDURES

D.1.1 Standard Charpy Impact Test

This specimen and its testing procedure are covered by ASTM E23. In particular, all of the discussion herein relating to this test method is concerned with the V-notched geometry (Type A Charpy specimen in ASTM E23), often designated by the symbol C_V*.

As implied by the designation, the standard Charpy impact test is conducted at impact loading rates and the quantity most commonly measured is the total energy (e.g., ft-lb) absorbed in breaking the specimen. Other quantities such as the appearance of the fracture (percent fibrous or ductile mode) and the amount of deformation (lateral expansion of the compression side) also can be measured on the broken specimen. In certain classes of materials, particularly the low- and medium-strength steels, these quantities are strongly dependent on test temperature. This behavior is used to denote a transition temperature (TT)

---

* Terms are defined at the end of the appendix.

for these materials. Examples include the temperature to attain some arbitrary level of energy (e.g., 30 ft-lb TT), a given proportion of fracture appearance (e.g., 50 percent fibrous FATT) or some specific level of deformation (e.g., 15 mils lateral expansion).

Also, some materials exhibit a loading rate sensitivity in their fracture behavior, particularly the low- and medium-strength steels and many titanium alloys. Therefore, the implications arising from the fact that the results obtained in the standard Charpy impact test pertain only to the loading rate of the test must be recognized.

D.1.2 Instrumented Standard Charpy Impact Test

As implied, this test augments the ordinary Charpy test by adding some type of instrumentation to obtain a load-time and/or load-displacement record of the specimen during the impact loading and fracturing sequence. The most common arrangement uses strain gauges on the striking tup to sense the load versus time. An example of such a record in idealized form is shown in Figure D-1. The overall form of the curve depends on the notch toughness and fracture characteristics of the material. For a very brittle material, fracture may occur prior to general yielding of the specimen ($P_F < P_{GY}$) and the curve would essentially have a sharp "spike" form. At the other extreme of a very ductile material, the curve would be of a "roundhouse" shape with a continuous decrease to zero load after reaching maximum load. Figure D-1 illustrates an intermediate situation between these two extremes.
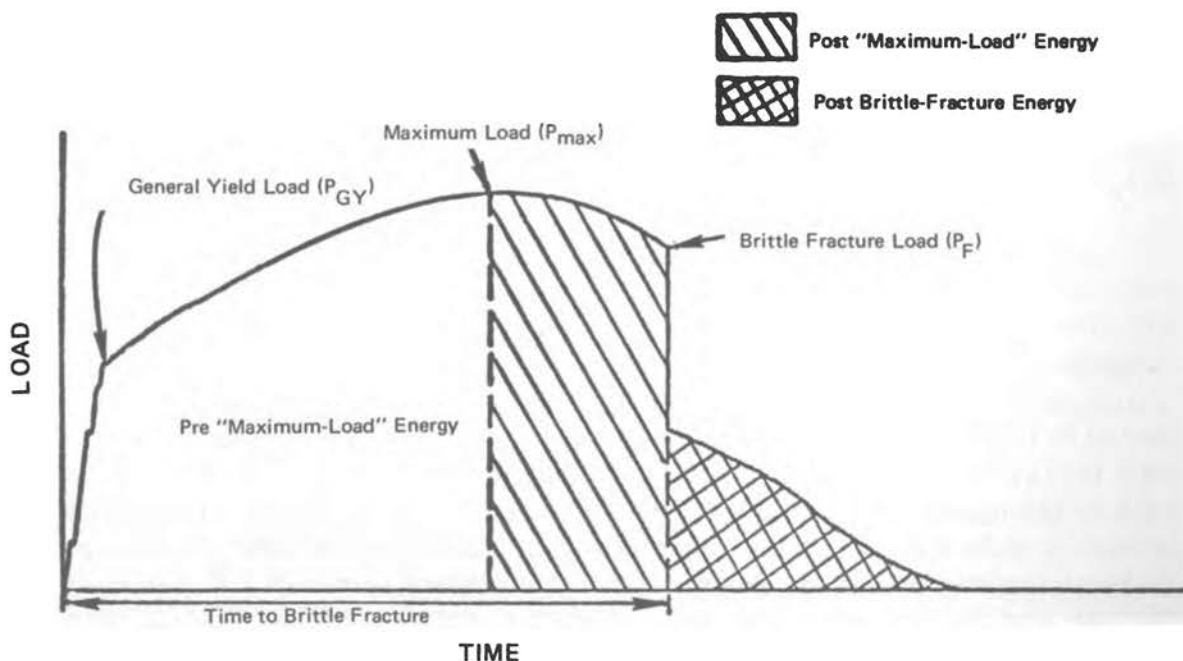
FIGURE D-1 An Idealized Load-Time History for a Charpy Impact Test.

Careful procedures and attention to detail are necessary to obtain unambiguous load-time records. Experimental problems arise because the time duration of the events of interest in a C_V impact test generally occur in the 0.1 to several millisecond range. False load signals may be obtained from the tup strain gauges due to:

a. Inertial effects from the tup specimen impact.

b. Oscillations, vibrations, and elastic deformations in various parts of the testing machine.

c. Vibration and stress wave reflections in the specimen.

d. Electronic noise and frequency limitations in the sensing, amplification, and recording system.

The details of these problem areas, their analysis, and procedures for minimizing them have been described (Venzi et al., 1970; Turner, 1970; Saxton et al., 1973; and Ireland, 1973). Conducting the test at several impact velocities was recommended as one means of separating some of these effects, especially the inertial effects, in the early part of the record.

The load-time curve when converted to load-displacement can be integrated to obtain energies up to various characteristic points on the curve as illustrated in Figure D-1. This provides a separation of the total absorbed energy into the major constituent portions and can improve the understanding of the conventional C_V impact test results.

D.1.3 Precracked Charpy Specimen Tests

The basic specimen feature difference between the standard C_V and the precracked specimen is the introduction of a fatigue crack at the tip of the V-notch. There are two reasons for testing a precracked specimen. First, the fracture behavior of many materials is sensitive to notch acuity and a fatigue precrack is the most severe notch that can be obtained reproducibly in a test specimen. Second, precracked Charpy test results are apt to correlate better with ASTM E399 fracture toughness values (K_{Ic}) that utilize a fatigue precracked specimen.

The precracked Charpy specimen can be tested in impact similarly to the standard specimen without or with instrumentation for load versus time information. Without instrumentation, the energy absorbed is the usual quantity measured that often is converted to energy per unit area as discussed later in this appendix. With instrumentation, the maximum load often is used to derive an approximate value of K_{Id}. The precracked Charpy impact test is not presently a standardized ASTM test but Task Group E24.03.03 of ASTM Committee E24 is in the process of developing a proposed standard.

The precracked Charpy specimen also has been tested in the slow bend mode, again, with or without instrumentation. The instrumented version can be tested as an ASTM E399 fracture toughness specimen to obtain appropriate secant offset fracture loads as well as the maximum load, crack opening displacement, and energy absorption values for analysis and correlation. Without instrumentation, the maximum load is the only measurement obtained. Within the specified limits, the ASTM E399 test method can include slow-bend testing of a precracked Charpy specimen.

D.2   CORRELATION OF STANDARD CHARPY IMPACT TESTS

Since none of the quantities measured in the standard Charpy impact test is related directly to K_{Ic}, all correlations between C_V test results and K_{Ic} are empirical. The simplest correlation is a plot of K_{Ic} versus C_V energy. Other correlations involve an estimate or prediction of the temperature dependence of K_{Ic} through the use of one of the transition temperatures obtainable from C_V versus temperature data. Still other empirical correlations involve K_{Id} on the basis that the C_V impact test involves a fast loading situation.

Most of the effort in developing correlations between Charpy (V-notch) impact properties and K_{Ic} values has been on steels. This effort included the whole range from low-strength carbon steel grades to ultra-high-strength alloy grades and maraging steels. The reason is that the Charpy test has a wide and long background of usage in characterizing the toughness properties of steels. In contrast, efforts to seek correlations for aluminum and titanium alloys have been very limited and the information available to examine the usefulness of any correlation is extremely scarce.

D.2.1 Steels in the Charpy Upper Shelf Region

These correlations apply in the temperature range where the Charpy energy of the steel has reached the maximum or shelf values. The first correlation for these conditions proposed by the following relation (Rolfe and Novak, 1970):

$$(K_{Ic}/\sigma_Y)^2 = 5\,(CVN/\sigma_Y - 0.05), \qquad (Eq.\ D\text{-}1)$$

where K_{Ic} is expressed in ksi $\sqrt{in.}$, σ_Y is 0.2 percent yield strength (ksi), and CVN is Charpy energy (ft-lb). (The constants in Eq. D-1 apply only with these units.) Not all of the K_{Ic} values used to initially develop this relation were valid values per ASTM E399. Subsequently, valid K_{Ic} data for 9-4-25 steel (Wessel, 1968; Wessel et al., 1966), for 9-4-20 steel (Ault, 1968), and for turbine rotor forging steels (Begley and Toolin, 1973) indicated a general usefulness of the relation. Figure D-2 shows this relation and the supporting valid K_{Ic} data.
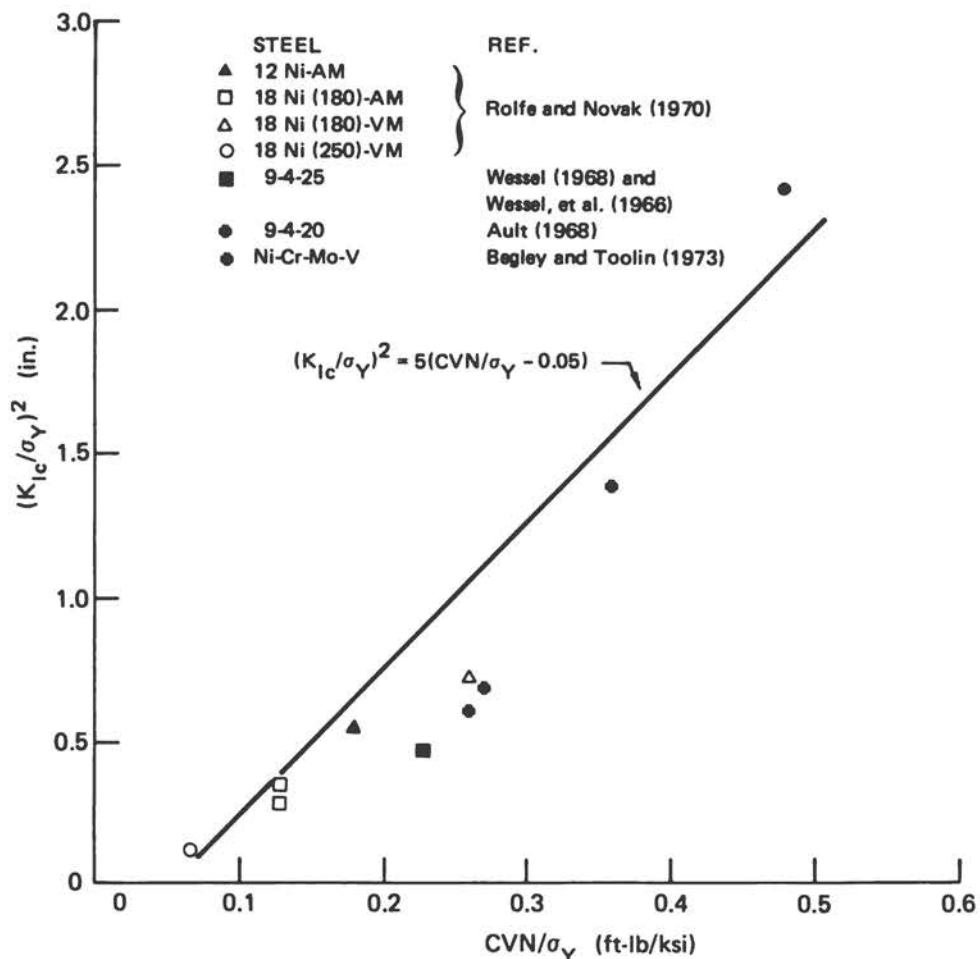
FIGURE D-2 Correlation of Valid K_{Ic} with Charpy Upper Shelf Energy (CVN) for Several Steels and the Rolfe-Novak Correlation Equation (Tetelman et al., 1974).

The ranges of material properties included in this figure are: RT yield strength = 130 to 250 ksi, K_{Ic} = 87 to 200 ksi $\sqrt{in}$., and CVN = 16 to 60 ft-lb.

Other empirical correlations using data from a series of very-high-strength steels (NiCrMo + W, Si, V; 300M and 9-4-45) have been presented (Ault et al., 1971). The properties ranges included in this case were: yield strength = 234 to 287 ksi, K_{Ic} = 34 to 70 ksi $\sqrt{in}$., and CVN = 11 to 21 ft-lb. One of the correlation equations obtained (Ault et al., 1971) in the same form as the Rolfe-Novak relation (Eq. D-1) and using the same units as Eq. D-1 is:

$$\left(K_{Ic}/\sigma_Y\right)^2 = 1.37 \left(CVN/\sigma_Y\right) - 0.045 \qquad \text{(Eq. D-2)}$$

The reported standard error for Eq. D-2 within the correlation range is about $\pm$ 15 ksi $\sqrt{in}$.

Figure D-3 is a plot of Eq. D-2 with the supporting data. The Rolfe-Novak relation (Eq. D-1) also is shown and the difference is evident; however, the data in Figure D-3 cover only the extreme lower end of the Rolfe-Novak relation. (It is assumed that all of the data shown in Figure D-3 are valid K_{Ic} and the CVN values are in the upper shelf region but this was not verified.)

One of the problems in developing correlations of the type discussed above is the general trend of decreasing CVN shelf energy with increasing yield and tensile strengths. As a result, a simple plot of K_{Ic} against CVN often provides a relation nearly as useful as the more refined ones. This is illustrated
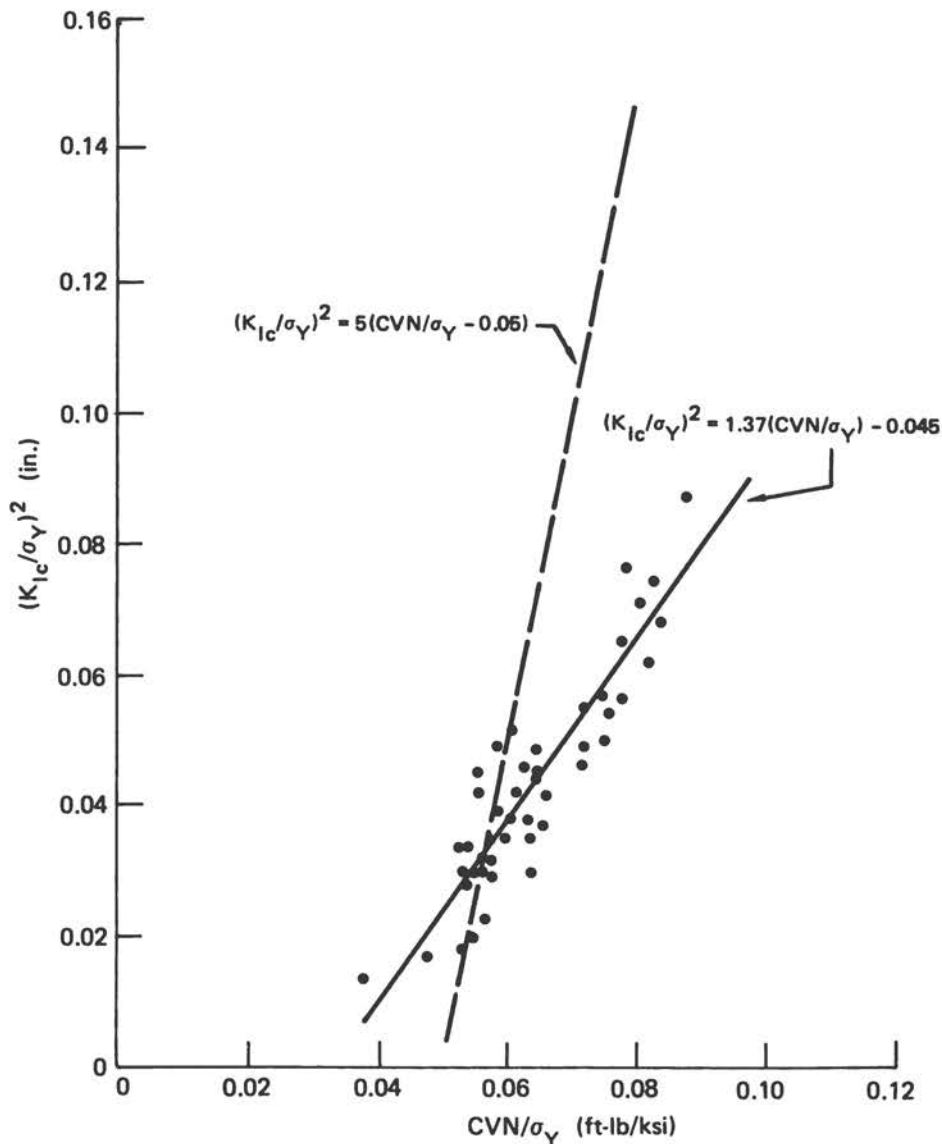
FIGURE D-3 Comparison of Two Correlation Equations between K_{Ic} and Charpy Upper Shelf Energy with Data of Ault et al. (1971) for Ultra-High Strength Steels.

in Figure D-4 using data previously shown in Figure D-2 and some of the data from Figure D-3. There is a suggestion of one relation for maraging steels and another for low-alloy steels.

In summary, relations such as Eq. D-1 or simple empirical correlations such as Figure D-4 can be useful as a general guide for estimating major differences in the fracture toughnesses. In this respect, the principal use might be in alloy development activities where a preliminary estimate of any large toughness differences is sought. It could be useful for K_{Ic} quality control purposes if sufficient data were generated for a specific alloy grade but even then, the limits of precision are apt to be fairly large. If used, the limitations of any empirical correlation plus the specific limitations (steels at upper shelf regions) of the equations and correlations must be kept in mind.
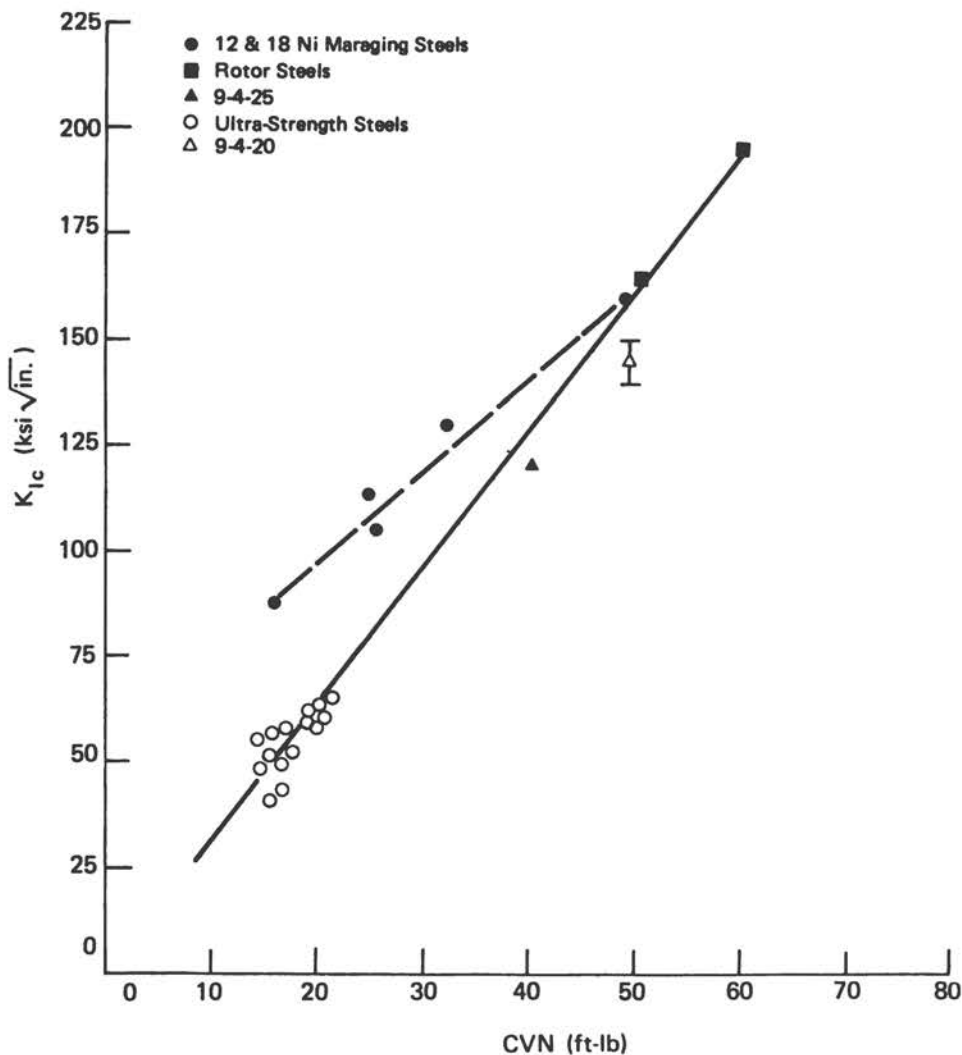
FIGURE D-4 K_{Ic} versus CVN for Several Steels at CVN Upper Shelf Conditions (Ault et al., 1971).

D.2.2 Steels in the Transition Temperation Region

When steels are Charpy tested at various temperatures, the results generally exhibit a transition behavior from low to high values with increasing temperature over a temperature interval specific to each steel. This transition temperature behavior is most pronounced in the low- and medium-strength grades.

Several methods and correlations have been proposed and used for estimating K_{Ic} from standard Charpy specimen data for steels in the transition temperature range. These are given below but it should be noted that all are empirical and generally do not have any theoretical basis.

One method described for turbine rotor steels (Brothers et al., 1965) involved correlating K_{Ic} from notched spin burst tests with temperature relative to the Charpy 50 percent fracture appearance transition temperature (FATT). Specifically, the correlation is a plot of K_{Ic} versus temperature minus FATT. Figure D-5 is a correlation plot of this type using compact specimen K_{Ic} data (Greenberg et al., 1970). Considerable scatter is evident but this method is useful in estimating K_{Ic} from Charpy tests for large steel forging in the 70 to 120 ksi yield strength range. In evaluating the scatter in an overall plot, such as Figure D-5, the variation in valid K_{Ic} among replicate tests should be recognized. One example from such data (Greenberg et al., 1970) illustrates this point. Five replicate tests on one rotor forging at the same test temperature gave K_{Ic} values ranging from 35 to 76 ksi $\sqrt{in}$.

A correlation similar in principle to Figure D-5 was used to correlate the temperature dependence of the fracture toughness of steels for nuclear reactor components. The differences in this case were the drop-weight test nil-ductility transition temperature as the indexing temperature and the correlation involved the dynamic and crack arrest fracture toughness properties of the steels.

Another simple method for the transition range is a direct plot of K_{Ic} against the Charpy energy value measured at the same test temperature as the K_{Ic} determination. An example of this correlation, including several steels having room temperature yield strengths ranging between 40 and 246 ksi, is shown in Figure D-6. A clear trend of increasing K_{Ic} with increasing Charpy ft-lb value for each of the steels individually is evident. It also is evident that a single correlation would not apply to all of the steels shown. Figure D-7 is a similar plot for a group of several grades of turbine rotor steels (Greenberg et al., 1970; Begley and Toolin, 1973). Again, a fair correlation is evident for any one grade but a separate correlation seems to exist for each specific grade.

Some representative indications of the spread in K_{Ic} and in Charpy energy values are shown in Figures D-6 and D-7. The scatter in both values can be large in some cases. This scatter is often a characteristic of steels in the transition range and creates difficulties in assessing the usefulness of any correlation.

Several empirical equations have been proposed to describe the relation between K_{Ic} and Charpy energy in the transition temperature range. One of
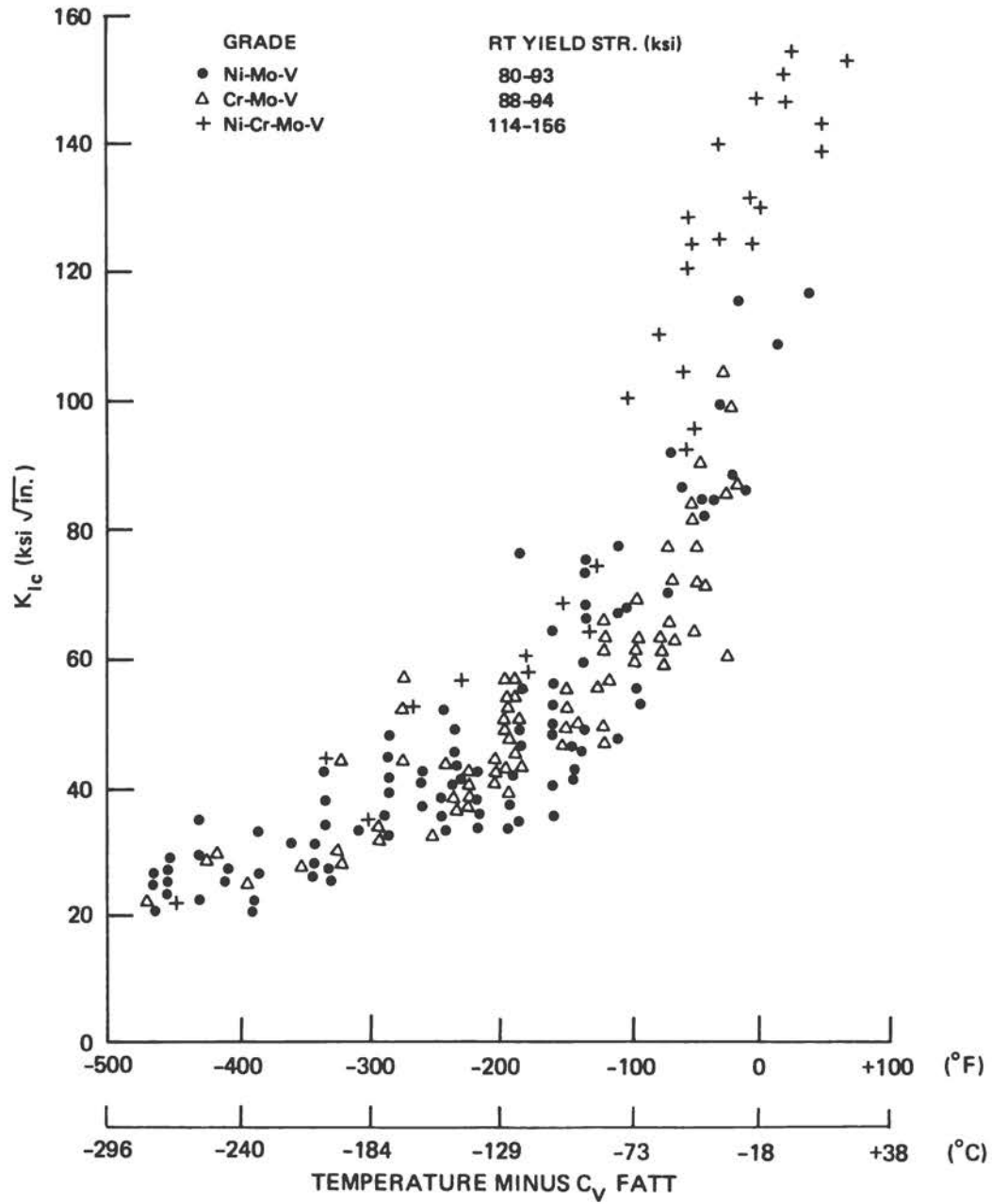
FIGURE D-5   Correlation of the Temperature Dependence of the K_{Ic} of Turbine Rotor Steels Using the C_V Fracture Appearance Transition Temperature (FATT).
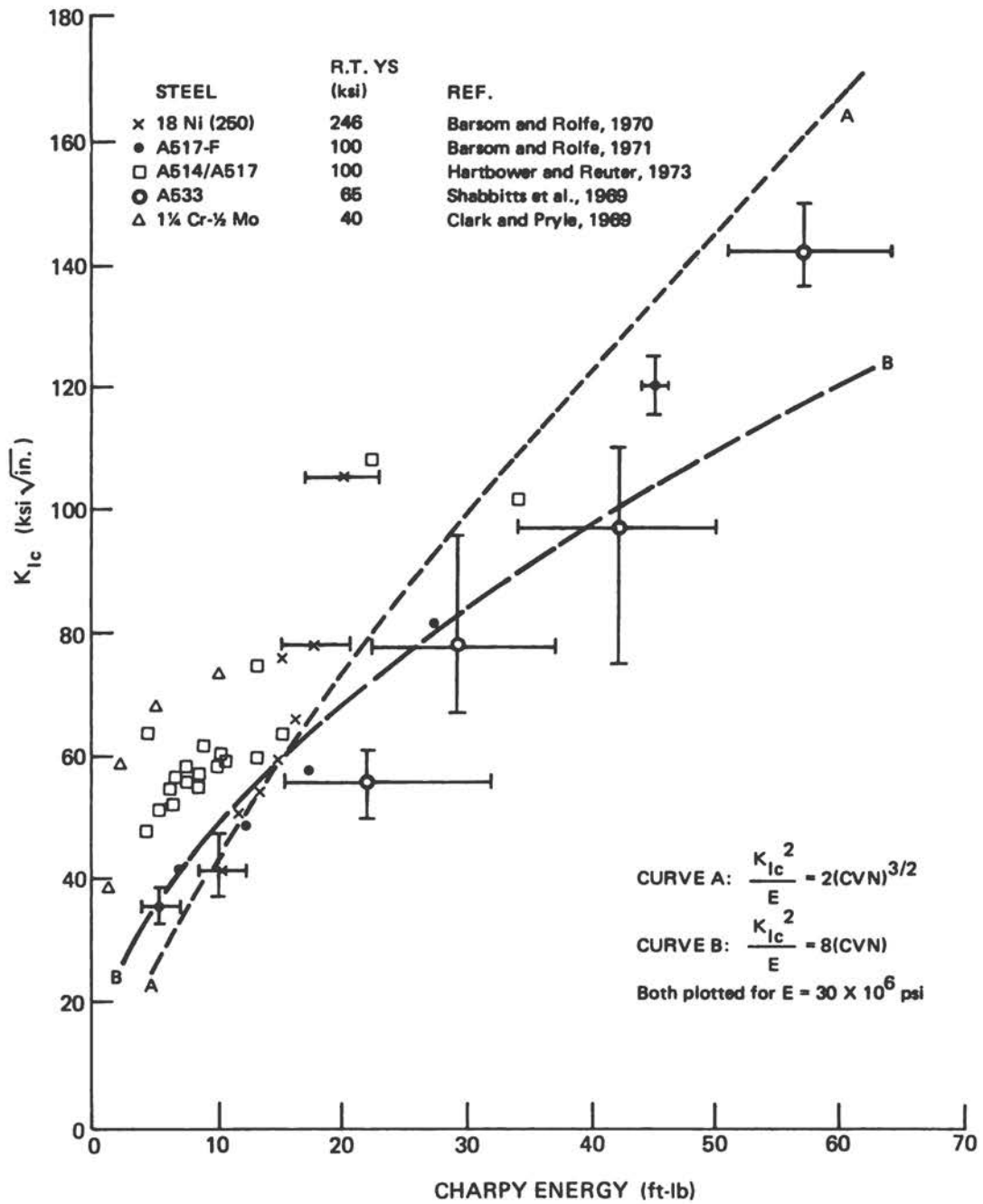
FIGURE D-6 Valid K_{Ic} versus V-Notch Charpy Impact Energy in the Transition Range for a Series of Steels.

these (Barsom and Rolfe, 1970) is based on data from low- and medium-strength steels including most of those considered in Figures D-6 and D-7. The equation is:

$$K_{Ic}^2/E = 2 (CVN)^{3/2} \qquad \text{(Eq. D-3)}$$
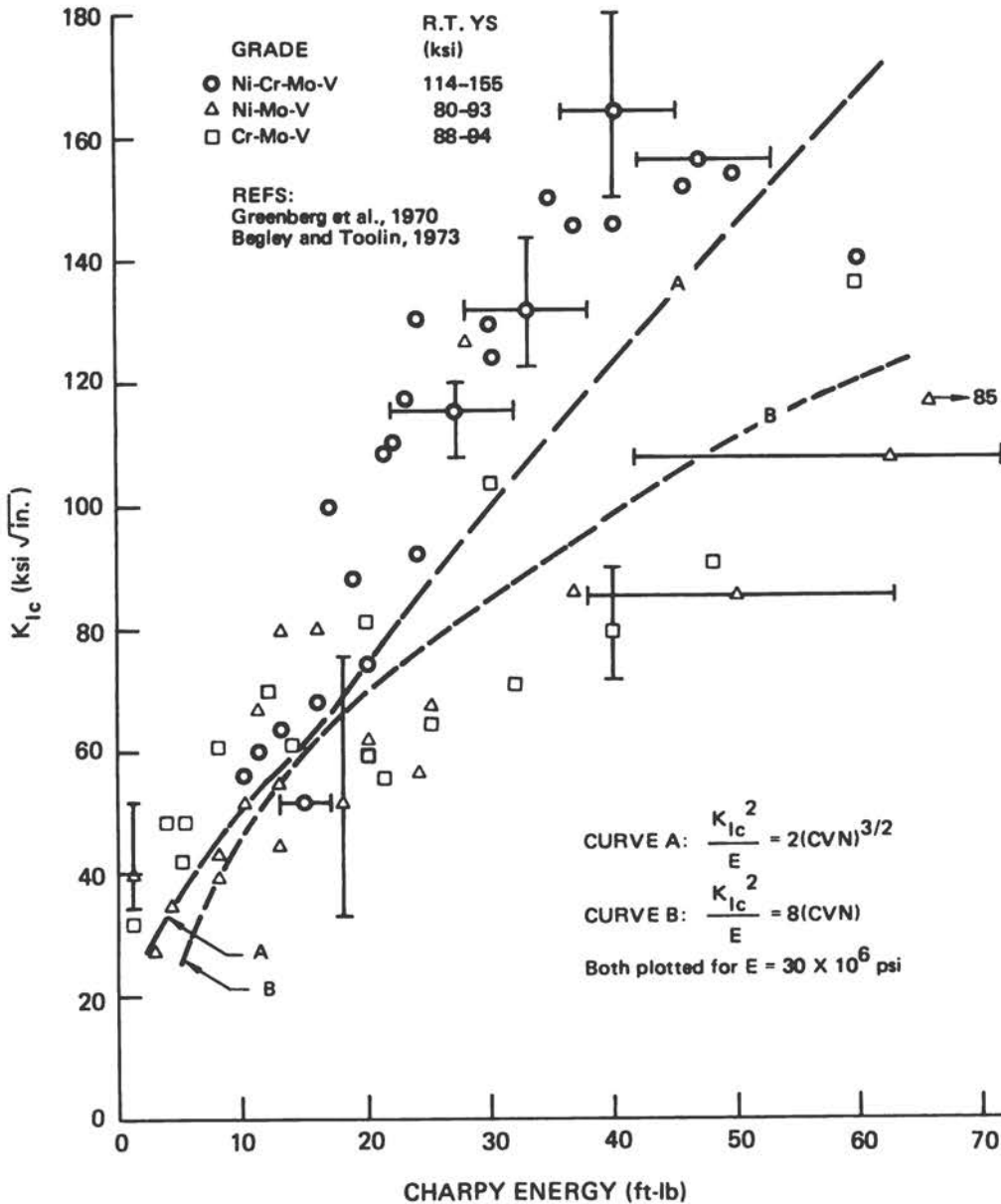
FIGURE D-7 Valid K_{Ic} versus V-Notch Charpy Impact Energy in the Transition Temperature Range for a Group of Turbine Rotor Steels.

where K_{Ic} is expressed in psi $\sqrt{in}$., E = elastic modulus (psi), and CVN is expressed in ft-lb. (Constants and exponents apply only with these units.)

For the examined data base, the spread in K_{Ic}^2/E was about ± 25 percent of Eq. D-3. Therefore, for a given modulus, E, the spread in K_{Ic} would be about ± 12 percent.

Another equation was derived based on data from a group of medium-

strength pressure vessel steels (Sailors and Corten, 1972). Here, the best fit equation for Charpy energy values between 5 and 50 ft-lb was:

$$K_{Ic}^{2}/E = 8(CVN) \qquad \text{(Eq. D-4)}$$

using the same units as Eq. D-3.

The K_{Ic} versus Charpy energy relation predicted by the above two empirical correlations are shown in Figures D-6 and D-7 for the value of E applicable to steels (30×10^{6} psi). Both correlations follow the general trend of the experimental data, but considerable variations between the predicted correlations and actual values can be noted. Thus, both of these empirical correlation equations should be considered only as approximate trend relations.

Also, a correlation between dynamic fracture toughness, K_{Id}, and Charpy energy for a group of low- and medium-strength steels was examined (Sailors and Corten, 1972). A reasonably good correlation fit was found for the data base examined.

Still another correlation method has been described (Begley and Logsdon, 1971). The steps in this method are illustrated in Figure D-8. Figure D-9 shows
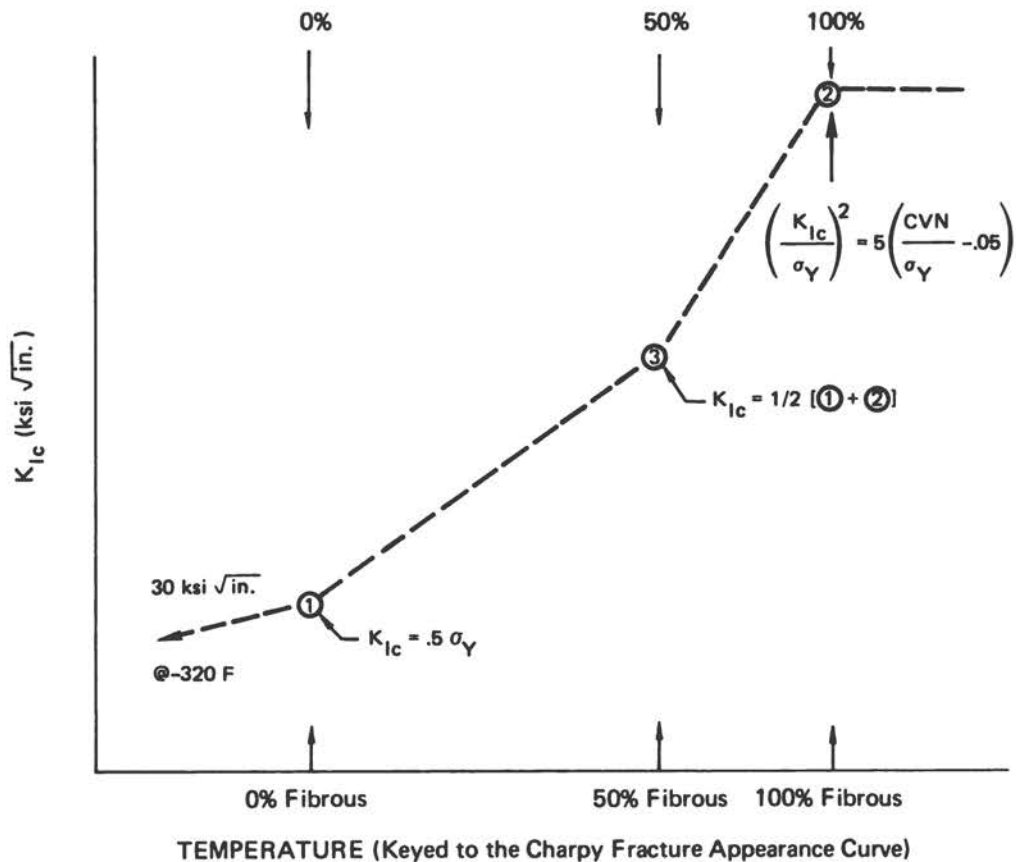
FIGURE D-8 Begley-Logsdon Method of Estimating K_{Ic} versus Temperature for Rotor Steels.

117
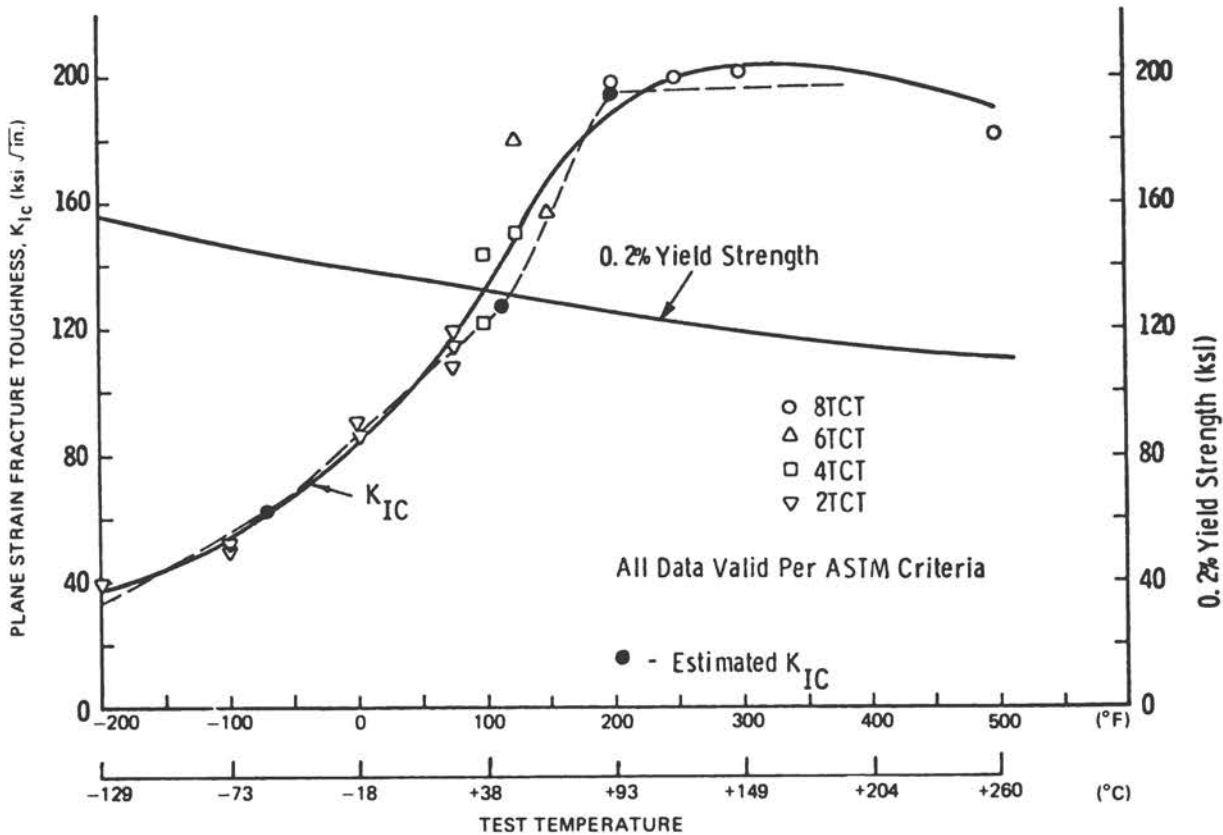
FIGURE D-9   Comparison of Estimated and Measured K_{Ic} versus Temperature for a Ni-Cr-Mo-V Steel (Begley and Logsdon, 1971).

the good agreement between predicted and measured K_{Ic} data for a turbine rotor steel. Figure D-10 shows the result when this method is applied to a pressure vessel steel using K_{Ic} data (Shabbits et al., 1969) and, here, the agreement between predicted and measured values is not as good. This correlation method assumes that the fracture properties are reasonably independent of strain rate effects. Other tests have shown that the fracture toughness behavior of the pressure vessel steel is sensitive to loading rate and, therefore, a good correlation would not be expected in this case.

Very recently, Barsom (1975) developed another correlation between K_{Ic} and V-notched Charpy specimen energy for steels in the transition temperature range. The form of the correlation equation is identical to Eq. D-4 but the numerical coefficient is different. The very important modification in the new proposed correlation is that the Charpy energy measured in a slow-bend test is correlated with K_{Ic}. The resulting correlation equation is:

$$K_{Ic}^2/E = 5(CVN) \qquad \text{(Eq. D-4a)}$$
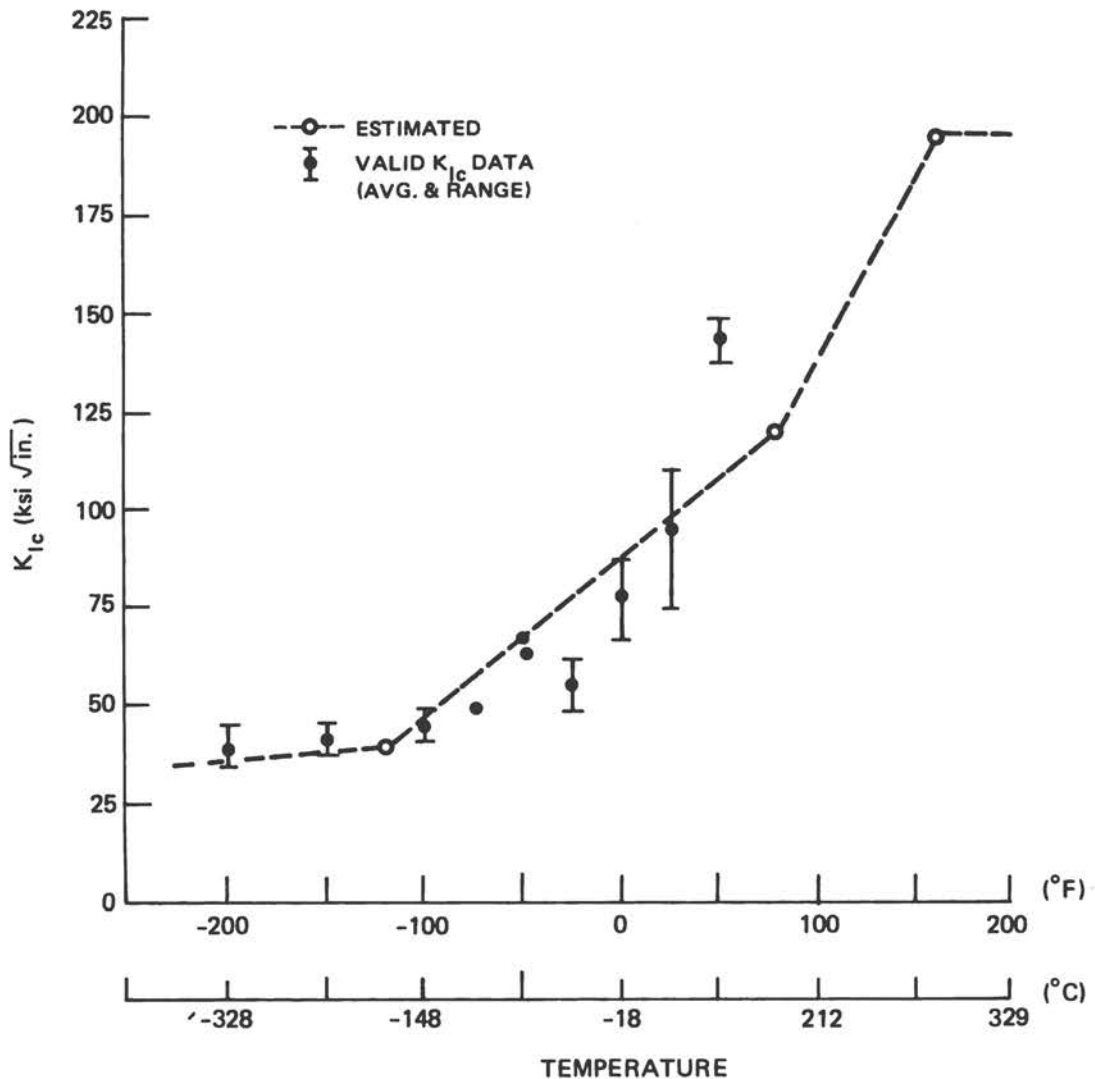
FIGURE D-10 Comparison of Estimated and Measured K_{Ic} for a Pressure Vessel Steel (A533, Grade B, Class 1).

where the units are the same as in Eqs. D-3 and D-4 and CVN is the slow-bend Charpy energy. The data for three tested steels show a spread of about ± 20 percent in K_{Ic}^2/E for CVN energies in the 10 to 35 ft-lb range and considerably larger percentage spread for Charpy energies less than 10 ft-lb. An equation identical to Eq. D-4a correlates dynamic fracture toughness, K_{Id}, and impact test Charpy energy. In short, it is suggested that correlations between fracture toughness and Charpy energy should be at similar loading rates (Barsom, 1975).

In summary, several empirical methods were used to correlate K_{Ic} with standard Charpy test data for steels in the transition temperature range but none appears to be generally applicable over a wide range of grades and strength levels. The main value of any one of them is for estimating K_{Ic} within the limits

of the specific category of steel for which it was derived. Usefulness for quality control of K_{Ic} must be established for each individual situation and even then, apparently, the acceptance/rejection limits might be large in some cases. Additionally, the complications inherent in these empirical correlations due to the notch acuity difference between the standard V-notch Charpy specimen and the sharp pre-crack of a K_{Ic} test specimen must be recognized.

D.2.3 Titanium Alloys

K_{Ic} versus CVN has been plotted for a series of titanium alloys (Freed, 1969). However, a number of these K_{Ic} data in the higher toughness region were invalid. Figure D-11 shows the K_{Ic} versus CVN relation for various sources of
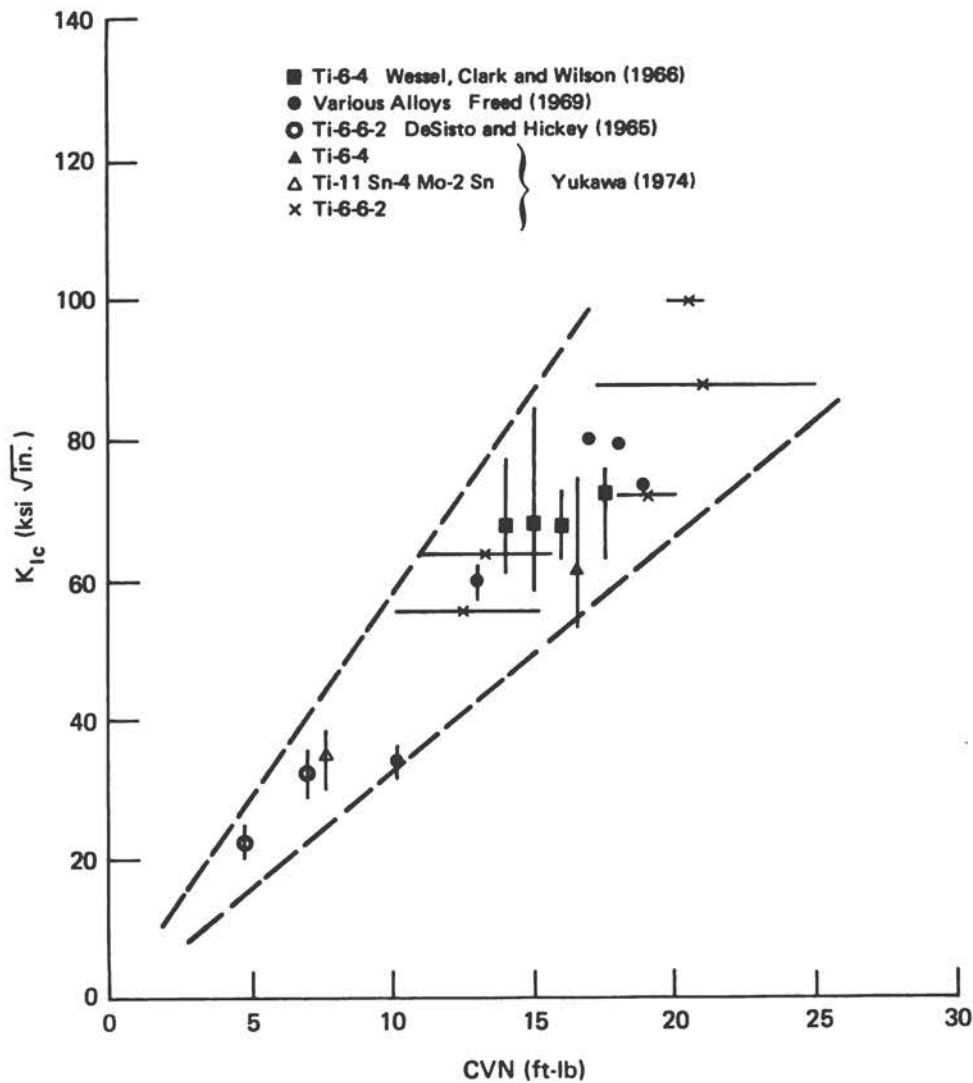
FIGURE D-11 K_{Ic} versus CVN for Titanium Alloys.

valid K_{Ic} data. A definite trend is noted, but considerable scatter is evident (approximately ± 25 percent). Due to the scatter and the limited amount of data, it does not seem fruitful to look for any relation other than simple correlation shown in Figure D-11. The data shown include several cases where tests were made at several temperatures on a single material and so the observed trend includes both the temperature effects as well as alloy variation effects.

The standard Charpy impact test might be useful as a rough screening test for titanium alloys but the available data does not indicate much promise for applications beyond this purpose.

D.2.4 Aluminum Alloys

The data available to evaluate any correlation is very limited. Figure D-12 shows the information available; no significant correlation is evident. The Charpy
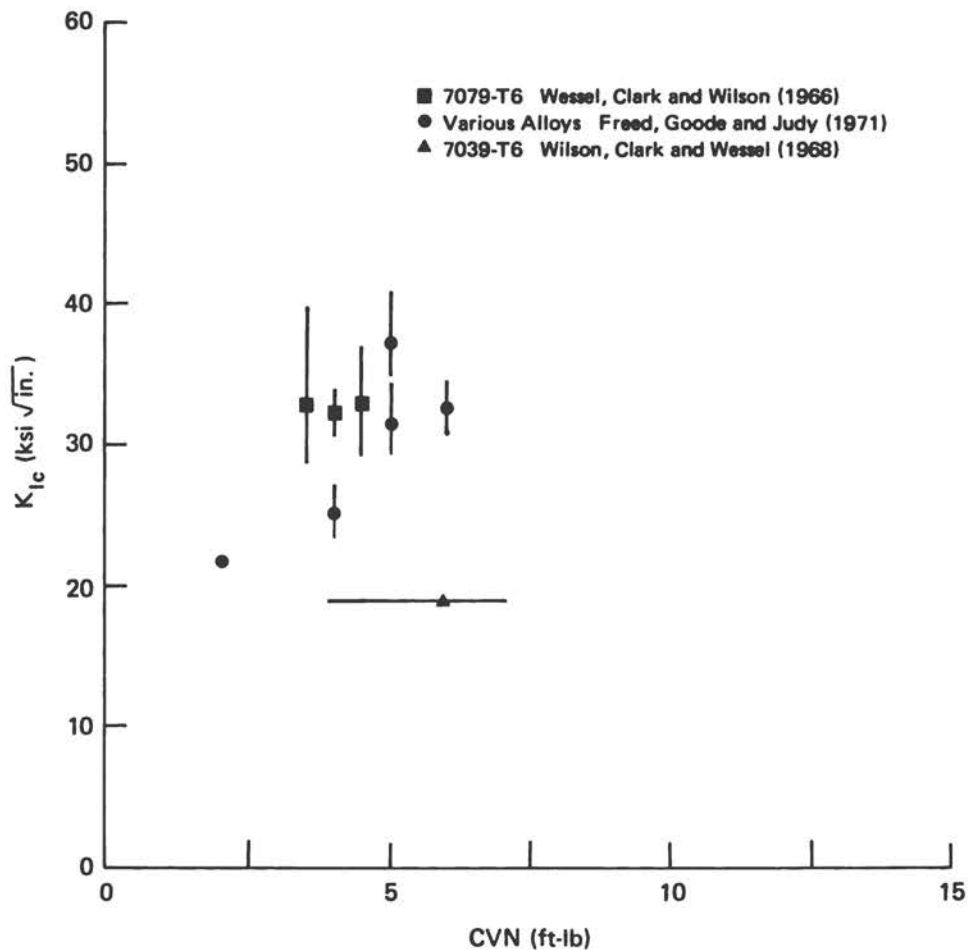
FIGURE D-12 K_{Ic} versus CVN for Several Aluminum Alloys.

values of aluminum alloys tend to be low and require a special impact tester to obtain better discrimination

D.3 CORRELATION OF INSTRUMENTED STANDARD CHARPY IMPACT TESTS

In recent years, efforts have been made to extract more information from conventional V-notch Charpy tests than simply the fracture energy (Wullaert, 1970; Tetelman et al., 1971). This was accomplished: (a) by instrumenting the tup and measuring the load-displacement or load-time record, and (b) by treating the Charpy specimen as a three-point bend fracture mechanics test piece. The main difficulty with this approach is that the relatively blunt 0.01-in. root radius of the standard V-notched Charpy specimen postpones the onset of crack extension to higher K values and general yielding intervenes before fracture. However, a method of treating the blunt root radius situation in terms of linear elastic fracture mechanics and extracting K_{Ic} or K_{Id} values has been proposed. The following reviews the method and the experimental support for correlation.

D.3.1 Interpreting the Load-Time Record

The typical character of a load-time record of a conventional Charpy test was described previously in connection with Figure D-1 (page 107). Referring to that figure, the following points are pertinent:

a. The quantity P_{GY}, the load corresponding to general yielding, is related to σ_{Yd}, the dynamic yield stress of the material corresponding to the mean or effective strain rate at the notch root.

b. The quantity P_F corresponds with a catastrophic loss of load-bearing capacity and is the load at which a relatively low toughness crack extends from the notch root. This can occur either before or after general yielding or after P_{max}. The quantity P_F can be related to the stress intensity at the notch root provided P_{GY} has not been exceeded.

c. Some workers believe that P_{max} corresponds to the onset of stable crack growth but this is not well documented.

d. Indications are that lateral contraction (through the thickness relaxation) develops rapidly when P_{GY} is exceeded. This suggests that plane-strain conditions are lost when $P > P_{GY}$ and raises questions about the interpretation of P_F values when $P_F > P_{GY}$ for the standard C_V specimen.

D.3.2 <u>Correlation between P_F and K_{Id} or K_{Ic}</u>

Essentially all the effort to extract fracture toughness values (K_{Ic} or K_{Id}) from instrumented standard C_V impact test information has been on low- to medium-strength steels. The analysis is limited to the case where $P_F < P_{GY}$ and, therefore, the correlation is restricted to lower temperatures where the toughness of these steels is low compared to their yield strengths at temperature.

Since the standard Charpy test is done at impact loading rates and these steels generally exhibit a loading rate effect, the best correlation should be with K_{Id}. The correlation analysis (details are given subsequently) results in an equation of the following form:

$$K_{Id} = \beta \, P_F. \tag{Eq. D-5}$$

For the steels investigated for this correlation, the average numerical value of β is:

$$\beta = 8.2 \text{ in.}^{-3/2},$$

for P_F = lbs. load and K_{Id} = psi $\sqrt{\text{in}}$.
One check on the validity and usefulness of Eq. D-5 is provided by data on an A533B steel tested at -112° F (-80° C) (Server, 1973):

Measured P_F, standard C_V -- 2,400 lb.

K_{Id} calculated from P_F -- (8.2)(2,400) = 19,800 psi $\sqrt{\text{in}}$.

K_{Id} from precracked C_V test -- 22,500 psi $\sqrt{\text{in}}$.

Comparisons of K_{Id} calculated from standard C_V test with measured K_{Id} also were examined at several temperatures for A212B and A302B steels (Tetelman et al., 1971); Figure D-13 shows the comparison for an A302B steel.

Although the correlations principally involve K_{Id}, a calculational method has been suggested (Tetelman et al., 1971) for predicting K_{Ic} from P_F. The method assumes that the critical fracture stress (for cleavage) is temperature and strain (loading) rate independent, whereas yield strength is a function of both of these parameters. By knowing or estimating the yield strength variation with loading rate at various temperatures, the relation between K_{Ic} and K_{Id} can be predicted and from this, K_{Ic} can be predicted from the P_F obtained in a standard C_V impact test. Figure D-13 also shows the comparison between predicted and measured K_{Ic} values using this approach.

The preceding results constitute about the sum total of data available on the method of predicting K_{Id} or K_{Ic} from instrumented standard C_V test data. For the results available, the comparison is good, generally within 10 to 20 percent.
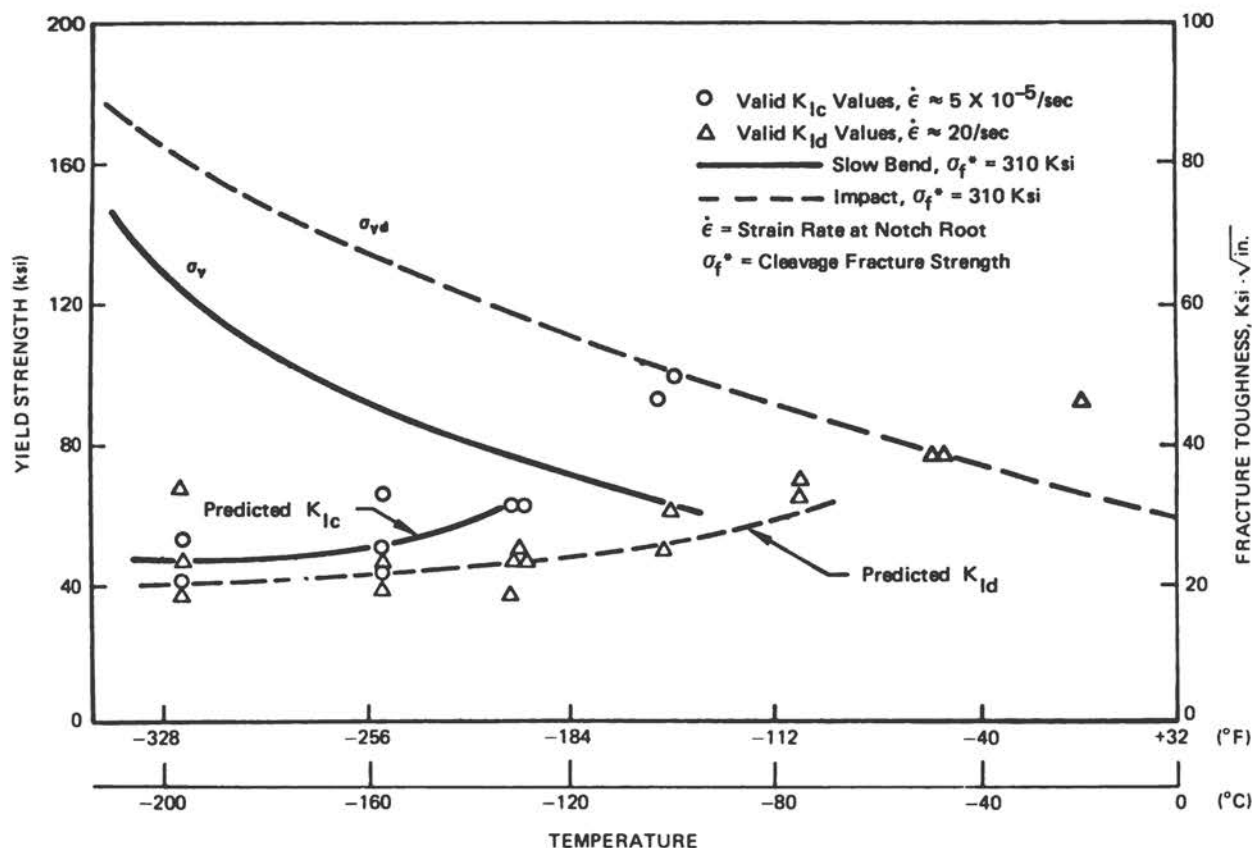
FIGURE D-13   Comparison of Predicted and Measured Values of the Critical
Stress Intensity Factor (K_{Ic}) as a Function of Temperature and
Strain Rate for A302B Steel (Tetelman et al., 1976; reprinted
with permission from Pergamon Press, Ltd.).

The very definite limitations of the analysis underlying the correlation must be
kept in mind. The strict application of the requirement that fracture (P_F) occurs
at less than general yielding (P_{GY}) means the following approximate upper limit
on the toughness measurement capability for the standard C_V specimen (notch
radius = 0.010 in.):

$$K_{Id}/\sigma_{Yd} \leq 0.25 \sqrt{in.}$$

In view of this measurement capacity limit, it does not seem fruitful to
pursue the use of instrumented standard C_V test to predict K_{Id} or K_{Ic} very
extensively. Instead, the precracked C_V permits measurements to similar or
higher toughness levels without the uncertainties of the blunt root radius
adjustment required on the standard C_V specimen.

D.3.3 Details of the Correlation Analysis

Considering the C_V test as a three-point bend fracture specimen and also assuming that the machined notch is a sharp crack, the K formula with the appropriate dimensions inserted (B = W = 0.394 in., a/W = 0.2, S/W = 4) becomes:

$$K_I = 19 \, P, \tag{Eq. D-6}$$

for the load, P, in pounds and K_I in psi $\sqrt{\text{in}}$.

The effect of notch root radius on the apparent value of K_{Ic} for slow loading fracture tests has been examined (Wilshaw et al., 1968; Hahn et al., 1974). Examples of the root radius effect from these two studies are shown in Figure D-14. The results generally follow the relation (Wilshaw et al., 1968) which can be expressed as:

$$K_{Ic \, (\rho)} = A \sqrt{\rho}, \tag{Eq. D-7}$$

where $K_{Ic \, (\rho)}$ is designated as the apparent K_{Ic} for a root radius, ρ. Also, below a certain radius, ρ_0, $K_{Ic \, (\rho)}$ becomes equal to and stays at a value equal to K_{Ic}. The quantity, A, in Eq. D-7 then can be defined as:

$$A = K_{Ic \, (\rho)} / \sqrt{\rho_0} \, . \tag{Eq. D-8}$$

Combining Eq. D-7 and Eq. D-8:

$$K_{Ic} = K_{Ic \, (\rho)} \sqrt{\rho_0 / \rho} \, . \tag{Eq. D-9}$$

From the value of $K_{Ic \, (\rho)}$ where $\rho = 0.01$ in. (root radius of C_V specimen) and K_{Ic} for cracked specimens, ρ_0 can be calculated. Also, the ratio $\sqrt{\rho_0 / \rho_{C_V}}$ where $\rho_{C_V} = 0.01$ in. can be determined. Table D-1 summarizes these data, which indicate an average value of 0.43 for $\sqrt{\rho_0 / \rho_{C_V}}$ for the steels listed.

For a dynamic loading situation, an equation similar to Eq. D-8 would be:

$$A = K_{Id \, (\rho)} \sqrt{\rho_0} \, . \tag{Eq. D-8a}$$

Test data suggest that A and K_{Ic} are approximately equal for a given material (Server, 1973; Tetelman et al., 1971). Combining Eq. D-7 and D-8a and assuming that the value of $0.43 = \sqrt{\rho_0 / \rho_{C_V}}$ also holds for the impact loading case,

$$K_{Id} = 0.43 \, K_{Id \, (C_V)}, \tag{Eq. D-10}$$
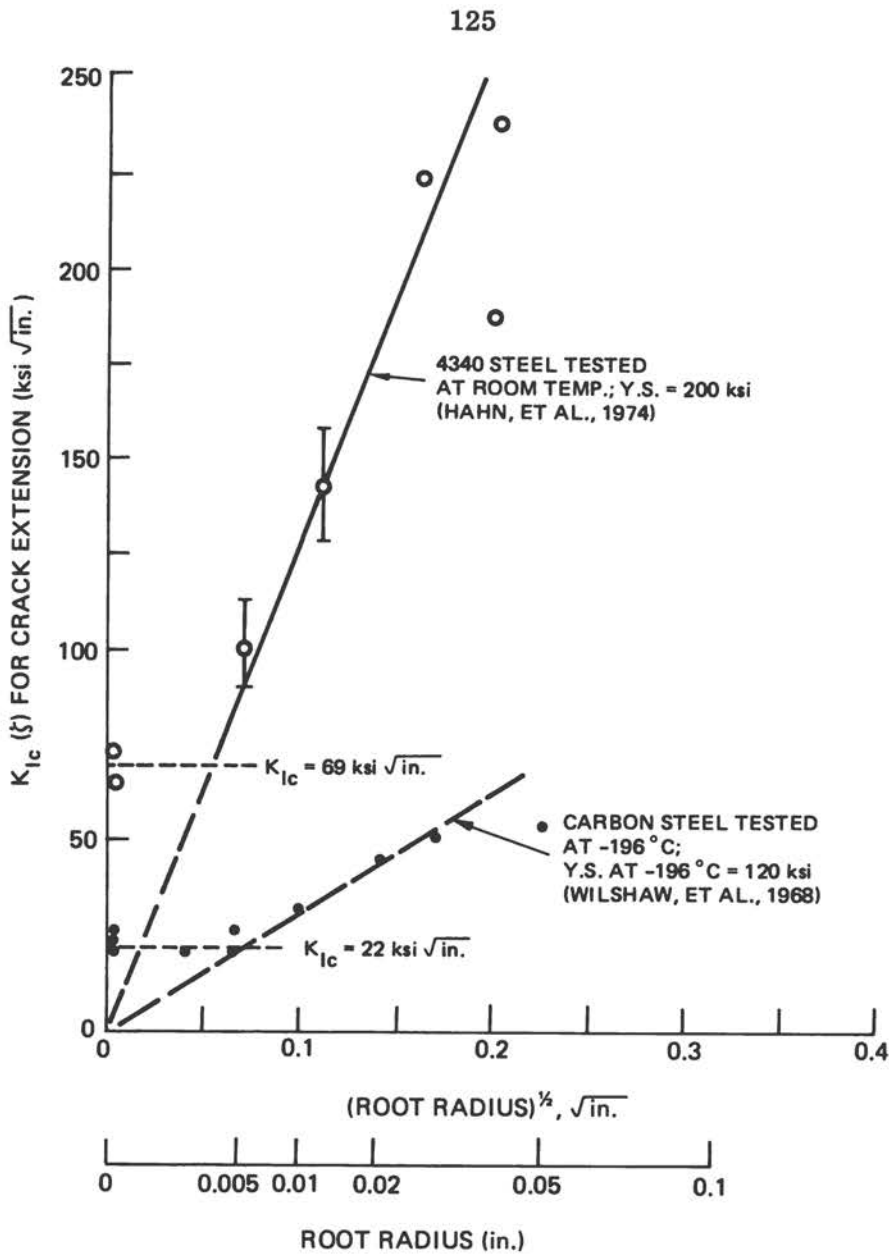
FIGURE D-14   Influence of the Root Radius on the Stress Intensity Factor, $K_{Ic\,(\mathcal{J})}$, for the Onset of Crack Extension.

where $K_{Id\,(C_V)}$ denotes the apparent value of K_{Id} measured from P_F in an instrumented standard C_V impact test. Referring back to Eq. D-6, the final result is:

$$K_{Id} = (0.43)(19)\,P_F = 8.2\,P_F \qquad \text{(Eq. D-11)}$$

for K_{Id} in psi $\sqrt{in}$. and P_F in pounds. Eq. D-11 gives the numerical value cited earlier in connection with Eq. D-5.

TABLE D-1 Tabulated Values of Static Fracture Toughness, Yield Stress, and Calculated Values of ρ_o and $\sqrt{\rho_o/\rho_{C_V}}$.

Steel	Ref.*	Temp. (°C)	K_{Iq} (ksi √in.) ($\rho = 0.01$ in.)	K_{Ic} (ksi √in.) (precracked)	σ_y (ksi)**	ρ_o (in.)	$\sqrt{\rho_o/\rho_{C_V}}$
A212B	(a)	-196	47	18	130	010015	0.38
A302B	(a)	-196	58	28	135	0.0023	0.48
A302B	(a, b)	-196	60	24	125	0.0016	0.40
ABSC	(a, b)	-196	46	20	115	0.0020	0.44
A517	(a, b)	-196	100	36	171	0.0013	0.36
4340 Q&T	(c)	RT	140	75	205	0.0027	<u>0.53</u>

Avg. 0.43

* <u>References</u>   ** Yield strength at test temperature.

 (a) Tetelman, Wullaert and Ireland (1971).
 (b) Shoemaker and Rolfe (1971).
 (c) Hahn, Hoagland and Rosenfield (1974).

The limitation that this procedure applies for P_F less than P_{GY} restricts the measurement capability. From relation (Green and Hundy, 1956) for a specimen of C_V dimensions:

$$P_{GY} = 0.03\, \sigma_Y \qquad\qquad \text{(Eq. D-12)}$$

for P_{GY} in pounds and σ_y, the yield strength, in psi units. For the dynamic case, $\sigma_y = \sigma_{Yd}$, the yield strength corresponding to the mean or effective strain rate at the notch root. Using Eq. D-11 and Eq. D-12, the measurement capability limit for $P_F = P_{GY}$ can be determined as:

$$\frac{K_{Id}}{\sigma_{Yd}} = (8.2)(0.03) = 0.25\, \sqrt{\text{in.}} \;. \qquad\qquad \text{(Eq. D-13)}$$

D.4 CORRELATION OF PRECRACK CHARPY W/A VALUES WITH K_{Ic} OR K_{Id}

The difference in notch acuity or severity between the 0.010-in. radius of a standard Charpy specimen and the sharp crack of linear elastic fracture mechanics test specimen places obvious shortcomings and limitations on correlations between the results from the two kinds of tests. The precracked Charpy specimen obviates this problem source in obtaining correlations.

The precracked C_V specimen can be tested in slow loading as a slow-bend test or in impact loading in a standard Charpy impact test machine. In this section, correlations based on energy absorption values obtained from precracked C_V tests are discussed. Correlations based on load data on precracked Charpy specimens are discussed in subsequent sections.

Energy values measured on precracked C_V specimens usually are expressed as W/A values where W = energy absorbed* and A = net (uncracked) section area. A typical unit for W/A is in.-lbs./in.² In a slow bend test, W/A is obtained from the load-displacement information. When tested in a standard Charpy machine, W is obtained from the dial reading. With an instrumented tup, W/A values up to various characteristic points on the load-time (displacement) record can be derived -- e.g., $(W/A)_m$ = W/A up to maximum load.

It should be emphasized that, in contrast to the standard Charpy impact tests, no standard procedure currently exists for precracked Charpy testing, particularly for determination of W in a slow-bend test. This lack of standardization can result in an undefined variability between the results obtained by different laboratories on the same test material. The W/A value derived from slow-bend precracked Charpy tests can depend on a number of factors including the manner in which the displacements are measured, the compliance of the testing machine, and the method of test record analysis (Succop et al., 1975). Under some conditions, these factors can have a large effect on the W/A values. For example, if the W/A value is based on a record cut-off at maximum load, the result can differ by a factor of 2 to 3 depending on whether the displacement measurement directly references the specimen or is related to the turns of the loading screws in the tensile machine.

For the instrumented precrack Charpy impact test, the literature does not define clearly the problems that must be solved before this test can be standardized. Also, the impact test with instrumentation is more complex than the slow-bend test and the records are often difficult to interpret.

In the initial studies on precracked Charpy W/A testing, it was presumed that a theoretical basis for a correlation with K_{Ic} (or K_{Id}) existed. However, the results showed that the basis of correlation are only empirical and do not follow the presumed theoretical relations. The problems with the presumed theoretical basis are described briefly following a presentation of the available data and empirical correlations.

---

* Note that W used in this context should not be confused with the use of W often used to designate a specimen dimension.

D.4.1 <u>Correlation Results</u>

An early work examined the correlation between precrack Charpy results and fracture toughness quantities (Orner and Hartbower, 1961a); however, this work principally concerned plane stress fracture toughness and good correlations were shown between W/A values and G_c for a number of higher strength sheet alloys. Another study examined a correlation between W/A values and plane-strain fracture toughness (Ronald et al., 1972). For a group of titanium alloys, aluminum alloys, and steels in the high-strength grades, the best correlation obtained was between the slow-bend precracked Charpy W/A values and K_{Ic}. The basis of the correlation was a presumed direct proportionality between the quantities K_{Ic}^2/E and W/A. Although a potentially useful correlation was observed, many of the K_{Ic} values used were not valid in terms of ASTM E399 requirements (Ronald et al., 1972).

More recently, a large amount of slow-bend precracked Charpy W/A data with matching valid K_{Ic} values have become available from several sources including the continuation of Ronald's work at the Air Force Materials Laboratory (Rich, 1973; Succop et al., 1975). Since these results are not available in the literature at this time, they are summarized in Table D-2 for convenient reference. As shown in the table, the materials tested include the 2,000, 6,000 and 7,000 series of aluminum alloys, a variety of high-strength steels (18 Ni maraging, 4340, D6AC, 4330M, 300M, PH 13 - 8 Mo and HP9-4-30) and two titanium alloys (Ti-6-4 and Ti-8-8-2-3). In several cases, variations in product form, heat treatment conditions, sample size, and test orientations are represented in these data.

Interestingly, the K_{Ic}/σ_y values in this data set range up to 0.75, 1.0, and 0.41 $\sqrt{in}$. for the aluminum, steel, and titanium alloys, respectively. (Table D-2 also lists the nominal strengths at maximum load obtained during the course of W/A testing; these results are discussed in a later section of this appendix.)

Figure D-15 plots K_{Ic}^2/E versus W/A derived from the data in Table D-2. Regression analyses using several possible functional relations between the two quantities were made treating all of the results as a single data set. In the analyses, W/A was considered the independent variable and K_{Ic}^2/E as the dependent one. The best correlation fit was obtained for a simple linear regression. This relation and the associated 95 percent confidence limits are shown in the figure. The linear regression equation obtained is:

$$K_{Ic}^2/E = 5.4 + 0.542 \, (W/A), \qquad \text{(Eq. D-14)}$$

where both quantities are expressed in units of in.-lbs./in.^{2}. The correlation coefficient, r, for the equation is 0.96. Since the constant in the equation is small, the regression analysis implies a direct proportionality between K_{Ic}^2/E and W/A.

TABLE D-2 Valid K_{Ic} and Slow-Bend Precracked Charpy Data.

Material	σ_Y (ksi)	σ_{UTS} (ksi)	K_{Ic} (ksi $\sqrt{in.}$)	W/A (in.-lbs./in.^{2})	σ_N (ksi)	Reference
Aluminum Alloys						
7075-T651, 1.4" plate	79	87	22.0	76	74	Succop et al., 1975
2.5" plate	74	86	24.8	84	85	
4" plate	61	71	19.0	36	60	
7075-T7351, 1.4" plate	63	74	31.4	246	102	Succop et al., 1975
7475-T7351, 1.8" plate, LT	62	73	46.5	574	123	Succop et al., 1975
TL	61	72	36.2	283	117	
2219-T851, 1.5" plate	51	67	32.8	136	89	Succop et al., 1975
2124-T851, 3" plate	64	70	31.4	181	103	Succop et al., 1975
265-L93, 3" plate	65	69	23.7	77	75	Succop et al., 1975
6061-T651, 2" plate	45	49	30.3	246	90	Succop et al., 1975
2020-T6	78.7	82.4	23.0	71	65	Ronald, 1974
7075-T73	60.4	71.6	32.0	284	91	Ronald, 1974
Titanium Alloys						
Ti-8Mo-8V-2Fe-3Al, aged 800° F	156	169	46	253	150	Succop et al., 1975
900° F	198	211	46	168	139	
1000° F	178	184	54	215	161	
1100° F	157	163	63	321	178	
Ti-6Al-4V, duplex annealed, long.	143	152	51.5	248	176	Ronald, 1974
trans.	141	149	50.5	215	166	
mill annealed, long.	140	147	51	335	190	
trans.	136	143	56	403	202	
Steels						
18 Ni, aged 700° F	173	192	(174)*	1897	373	Succop et al., 1975
725° F	190	206	147	1521	378	
750° F	203	218	133	1210	389	
775° F	213	227	116	886	381	
800° F	227	238	95	617	344	
850° F	253	263	76	553	287	
900° F	259	265	82	502	280	
950° F	252	261	85	508	277	
1000° F	232	242	87	439	285	
1050° F	204	218	106	603	320	
1100° F	180	198	147	1498	370	
4340, tempered 600° F	232	267	53	137	176	Succop et al., 1975
750° F	214	233	70	241	232	
850° F	198	212	88	483	289	
925° F	183	194	105	767	320	
4340	221	269	53	190	173	Ronald, 1974
D6AC	207	226	85	511	279	Ronald, 1974
4330 M	193	224	75	416	235	Ronald, 1974
HP-9-4-30	189	230	90	767	306	Ronald, 1974

* Not E399 valid.

TABLE D-2   Valid K_{Ic} and Slow-Bend Precracked Charpy Data (continued).

Material	σ_Y (ksi)	σ_{UTS} (ksi)	K_{Ic} (ksi $\sqrt{in.}$)	W/A (in.-lbs./in.^{2})	σ_N (ksi)	Reference
Steels (continued)						
Steel, 300 M forgings	254	296	51.0	167	185	Ronald, 1974
	254	296	58.6	152	194	
	252	296	65.5	164	171	
	249	287	58.6	223	210	
	252	295	59.1	167	195	
	254	299	59.0	178	197	
	249	295	54.4	178	179	
	261	300	49.1	130	173	
	255	293	59.6	171	199	
	254	295	58.9	156	202	
	254	295	60.7	171	198	
	254	296	55.3	164	181	
	254	296	55.1	181	184	
	252	296	59.1	208	192	
	255	298	51.0	186	176	
	254	301	57.7	171	175	
	252	295	58.5	214	181	
	254	299	55.6	178	183	
	249	295	61.8	235	193	
	261	300	48.3	162	167	
	255	293	58.0	204	185	
	254	295	54.6	192	178	
	251	300	64.1	214	187	
Al, 7075-T7351, plate	53	--	31.1	253	--	Rich, 1973
7050-T73651, plate	68	--	35.3	666	--	
2021-T81, plate	61	--	27.0	112	--	
Ti-6Al-4V, mill annealed	134	--	65.1	335	--	Rich, 1973
mill annealed	137	--	58.4	265	--	
vacuum formed	131	--	63.6	321	--	
S. T. and overaged	129	--	70.4	363	--	
recrys. annealed	131	--	57.5	421	--	
Steel, 300 M, plate	233	--	51.8	172	--	Rich, 1973
Steel, PH 13-8Mo, bar	205	--	101	973	--	Rich, 1973

NOTE: The K_{Ic} and W/A data from Rich and from Succop et al. are the averaged values from replicate tests (generally three to six) conducted on each material and condition. This is also the case for all of Ronald's data with the exception of the 300M steel results. The latter are for a single K_{Ic} determination and single or duplicate precracked Charpy test made on individual pieces from a group of forgings.
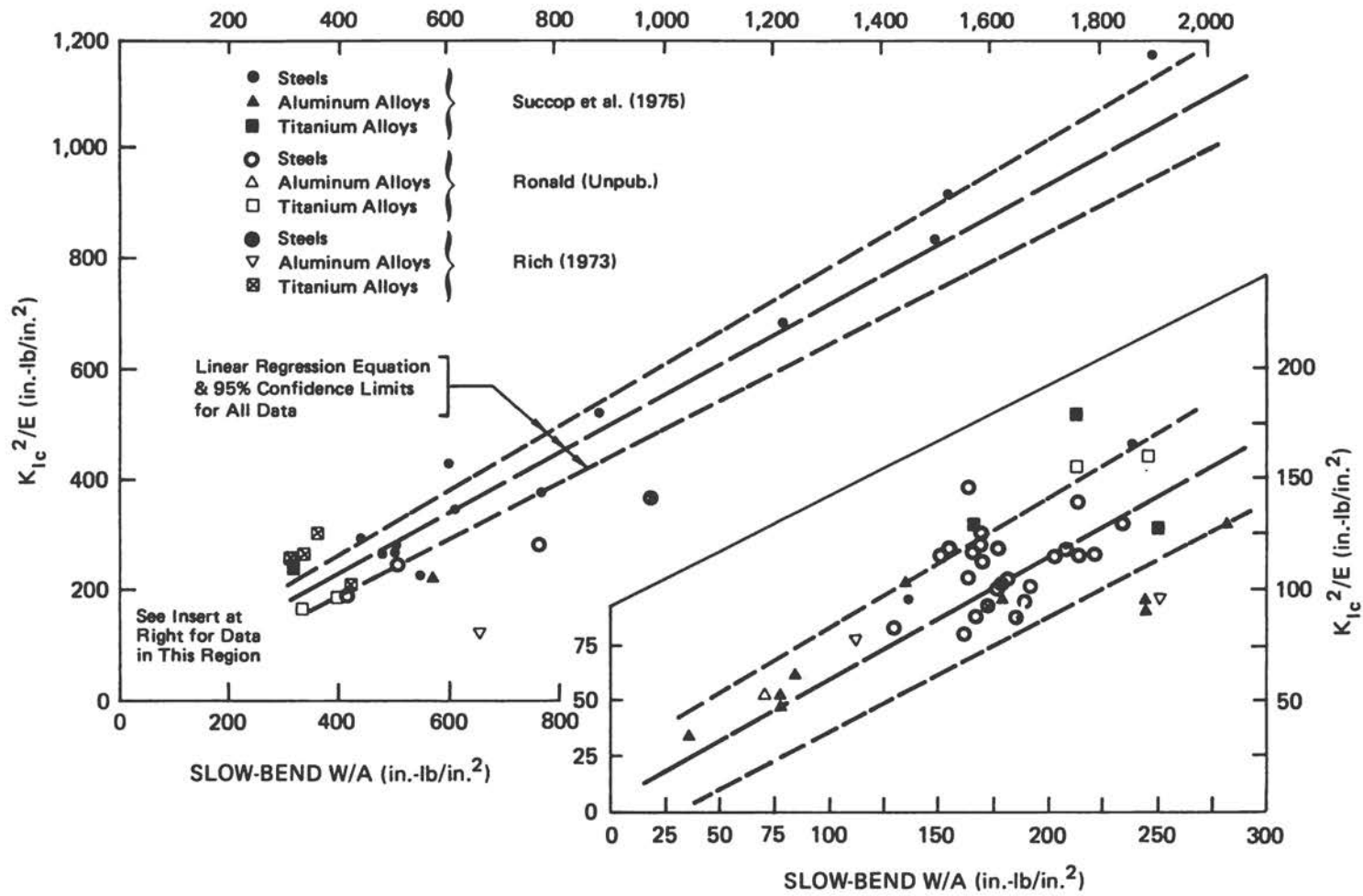
FIGURE D-15   Composite Plot of K_{Ic}^{2}/E versus Precracked Charpy Slow-Bend W/A Data.

Although the overall trend is evident in Figure D-15, occasional large deviations ranging up to about 50 percent in K_{Ic}^2/E from the regression line can be noted. However, most of the results fall within about ± 30 percent of the regression predictions. This is equivalent to about ± 15 percent spread in K_{Ic} for a given elastic modulus.

It also can be noted in Figure D-15 that individual alloy types do not necessarily follow the trend established by the total data set. This is illustrated in Figure D-16 for the aluminum alloy data only, and it is evident that a statistical analysis of this sub-set of the data would produce a different correlation line and confidence limits than those from the total data set. The existence of these differences for their results have been pointed out (Succop et al., 1975). Thus, apparently, correlations specific to alloy types and grades must be established for a tighter correlation for quality-control purposes.

Another indication of the situation likely to be encountered from a quality-control standpoint can be seen for the 300M steel (Rich, 1973). As mentioned earlier, these data were obtained on a number of forgings all heat
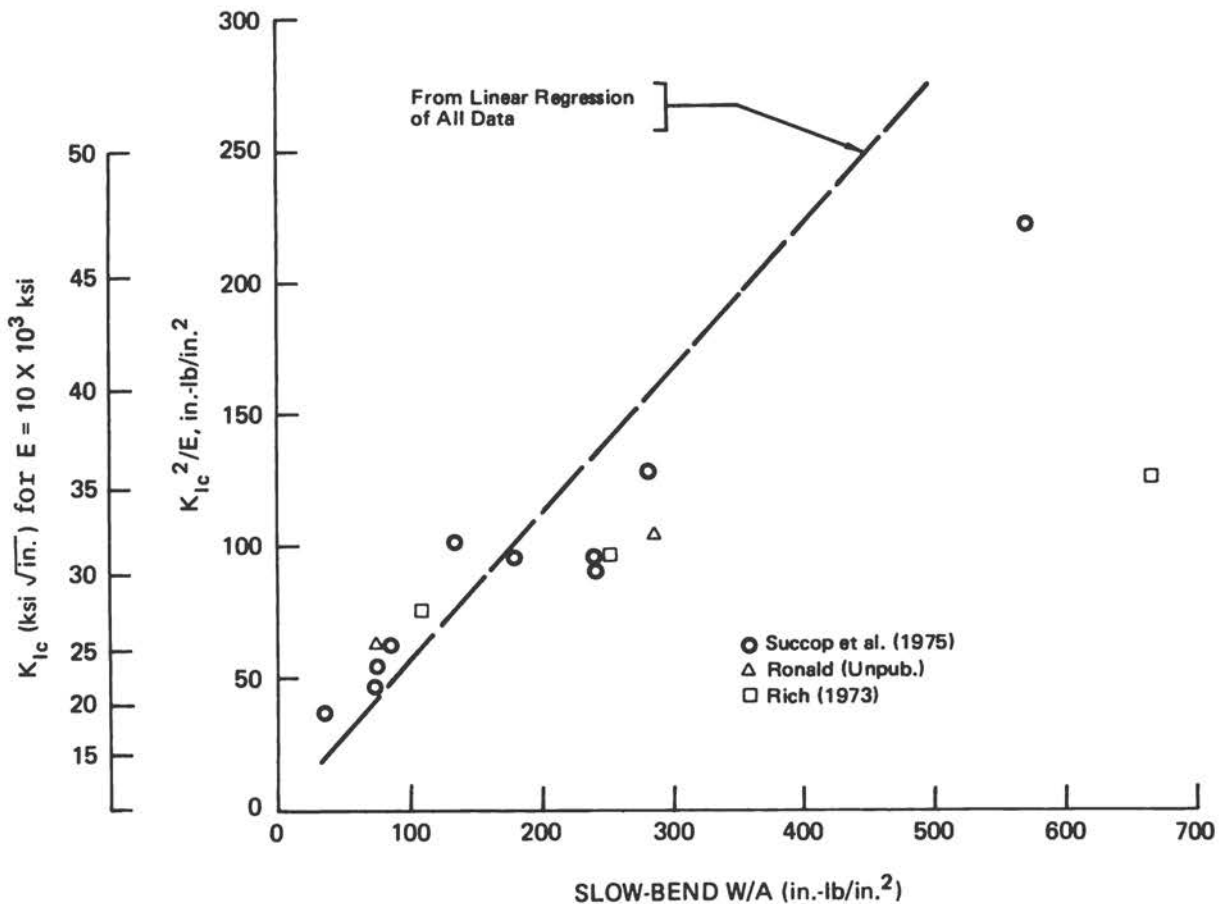
FIGURE D-16 K_{Ic}^2/E versus Precracked Charpy Slow-Bend W/A Data for Aluminum Alloys.

133

treated to a specified tensile strength range. Figure D-17 plots these data including the variations in W/A values where duplicate tests were made. In this case, the minus 95 percent confidence limit from the overall data correlation appears to be a possible quality-control working curve for the 300M steel results. However, a very different trend curve and confidence limits would result for the 300M data only.

A part of the problem in the scatter in the correlation may be due to differences in testing technique and test record analysis for W/A. However, the overall spread in Figure D-15 appears comparable to the spread within each data source. In spite of these problems, the results demonstrate that the precracked Charpy slow-bend W/A test offers good potential for correlation with K_{Ic} up to reasonably high relative toughnesses ($K_{Ic}/\sigma_y = 1\sqrt{in.}$). Future results for a wider data base should improve the correlation and also define the toughness limit of applicability.

Another way to test precracked C_V specimens is under impact loading conditions either with or without instrumentation. Several sources of data are available for examining a correlation between K_{Ic}^a/E and precracked C_V impact W/A values. A composite plot of the data is shown in Figure D-18, followed by a table of materials and references.
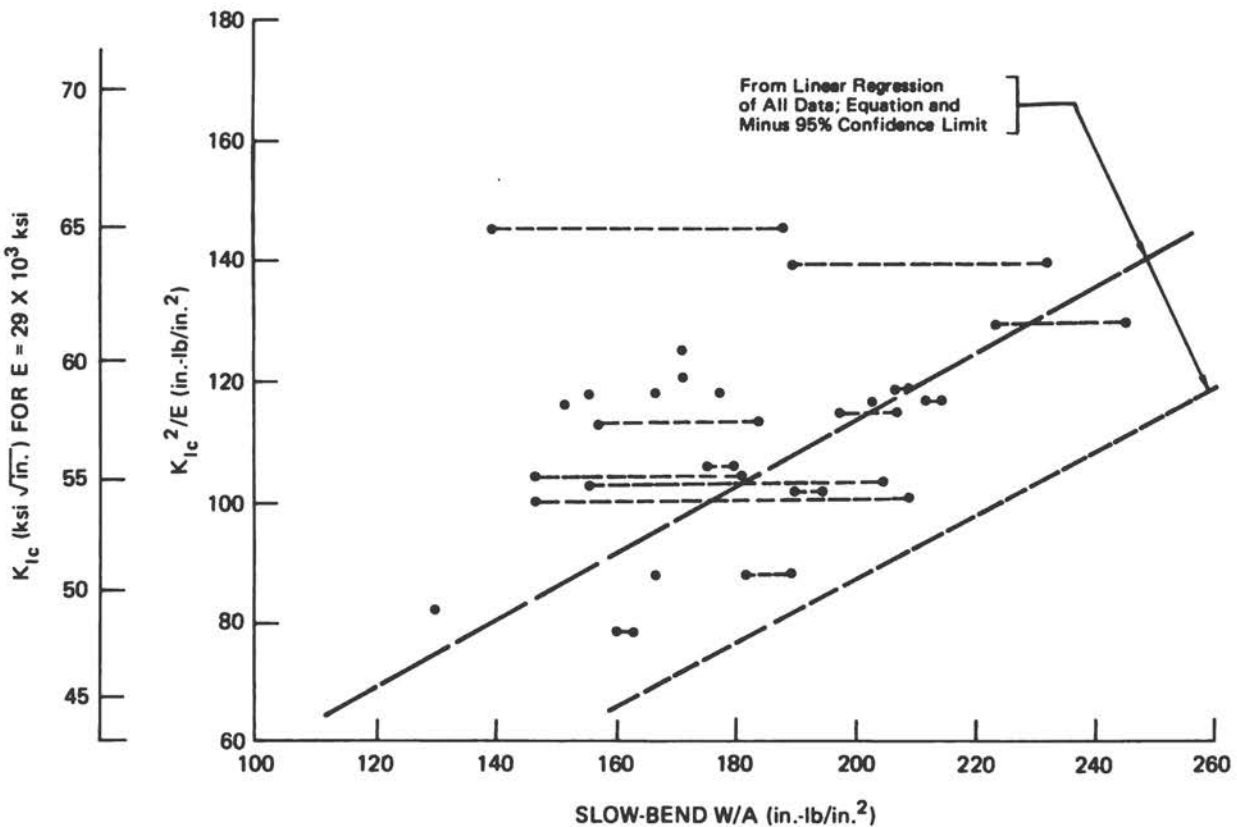
FIGURE D-17 K_{Ic}^a/E versus Precracked Charpy Slow-Bend W/A Data for a Group of 300M Steel Forgings (Ronald, 1974).
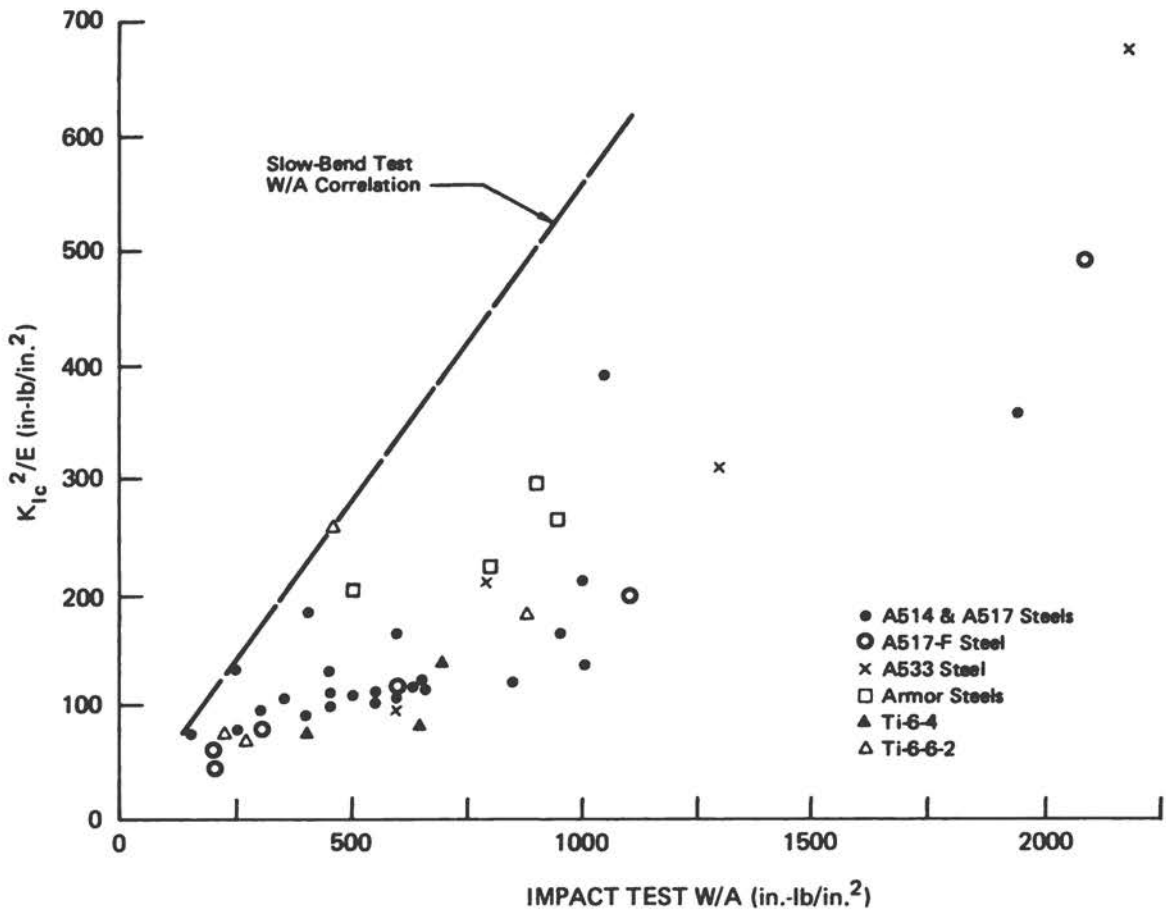
FIGURE D-18 Comparison of K_{Ic}^2/E with Precracked Charpy Impact Test W/A Values for Several Steels and Titanium Alloys.*

---

* Materials and References for Figure D-18 are given below:

Material	Room Temperature YS (ksi)	Reference
A533 Steel	65	K_{Ic} from Shabbits et al., 1969 W/A from Server and Tetelman, 1972
A517-F Steel	110	Barsom and Rolfe, 1971
A514 and A517 Steels	100 (minimum)	Hartbower and Reuter, 1973
Titanium-6-4	--	Ewing and Raymond, 1974
Titanium-6-6-2	--	Ewing and Raymond, 1974
Armor Steels	200-216	Hickey, 1974

Data on Ti-6-4 (Ewing and Raymond, 1974) included three combinations of heats and specimen orientations, all for the mill annealed condition. The Ti-6-6-2 data (Ewing and Raymond, 1974) included the several different heat treatment conditions on the same heat.

In Figure D-18, a very rough correlation between K_{Ic}^{2}/E and impact W/A exists but the scatter is large. The data along the very upper part of the scatter-band follows the trend line established by the slow-bend W/A correlation (i.e., Eq. D-14). However, the bulk of the data lies considerably below the slow-bend correlation trend.

The basic problem leading to much of scatter present in Figure D-18 is the loading rate sensitivity of the various materials. K_{Ic} is measured under relatively slow loading rate conditions but impact W/A obviously is measured under high loading rate conditions. Therefore, if any correlation is expected, it should be between dynamic fracture toughness, K_{Id}, and impact W/A. In studies on the titanium alloys, K_{Id} calculated from the instrumented precracked C_V load values were higher than the measured valid K_{Ic} values and tended to produce a reasonable correlation with impact W/A values (Ewing and Raymond, 1974).

Others also observed a poor correlation between K_{Ic} and impact pre-cracked C_V W/A, especially for Ti-6-4 samples (Ronald et al., 1972). Instances where impact W/A were higher or lower than the slow-bend W/A were observed in several titanium alloys and in D6AC steel (Hartbower, 1970). In low- and medium-strength steels, the K_{Id} values generally are lower than the K_{Ic} values with the difference depending on loading rate.

These instances of K_{Id} being greater or less than K_{Ic} mean that if Figure D-18 had been plotted using K_{Id} values (if available), an even greater scatter might be expected. This situation indicates the importance of consider-ing the rate-of-loading sensitivity in any attempts to correlate impact test values with K_{Ic} measured under slow loading conditions. One simple procedure for evaluating loading-rate sensitivity is to compare precracked C_V results in slow-bend and impact tests.

Another problem in trying to correlate LEFM fracture toughness quanti-ties with precrack C_V W/A values is that K_{Ic} pertains only to onset of fracture instability while W/A includes both the energy up to crack initiation plus the energy for propagation. Except for very-low-toughness conditions, the total W/A can be several times the W/A up to maximum load that can be taken as a crude approximation of crack initiation. For example, total W/A (two to five times W/A to maximum load) has been observed in precracked Charpy impact tests, even for relatively low-toughness, high-strength steels (Koppenal, 1973). Fracture initiation W/A may provide a better empirical basis for correlation with K_{Ic} (or K_{Id}).

Another experimental problem with impact W/A, especially at low values, is the extraneous energy losses in the specimen. The magnitude of this effect is appreciated when it is realized that 1 ft.-lb. approximately equals 100 in.-lbs./in.^{2} in the usual precracked C_V specimen.

In summary, the following observations pertain to correlations between precracked Charpy W/A values and K_{Ic} (or K_{Id}):

a. Most currently available data are for correlations of slow-bend W/A and K_{Ic}; these include results for aluminum, steel, and titanium alloys primarily in the higher strength grades. A good empirical correlation exists between K_{Ic}^2/E and W/A considering all results as single data set.

b. The overall correlation indicates that K_{Ic} can be predicted within about ± 15 percent from slow-bend W/A in most cases for materials with a toughness ratio, K_{Ic}/σ_y, approximately up to 1 $\sqrt{in}$. However, instances of deviations ranging up to about ± 25 percent are noted.

c. A more detailed analysis suggests that the relation between K_{Ic}^2/E and slow-bend W/A may vary for different material types and, therefore, its use for quality-control purposes should be verified by obtaining a sufficient data base for each specific alloy type and grade.

d. Impact test W/A values show poorer correlation with K_{Ic} on an overall basis probably because of variations in loading rate sensitivity of fracture toughness among the various materials. Thus, the slow-bend W/A test offers the best basis for correlation with K_{Ic}. Impact W/A may correlate with K_{Id} but the data are insufficient to permit evaluation of such a correlation.

e. A standardization of testing procedures is required to insure consistency of W/A determination.

D.4.2 Analysis of Relation between W/A and K_{Ic} or K_{Id}

One approach that has been used in attempting to derive a theoretical relation between W/A and K_{Ic} (or K_{Id}) assumes that the total energy (W) absorbed in the fracture process equals the product of $\mathcal{J}_{Ic}$ times the fracture area (A) -- i.e., $W = (\mathcal{J}_{Ic})(A)$. Combining this with the relation $K_I^2 = E\mathcal{J}_I$ (and ignoring the Poisson ratio factor), the result is:

$$K_{Ic}^2/E = W/A. \qquad \text{(Eq. D-15)}$$

Note that this equation differs from the empirical relation (Eq. D-14) obtained earlier from the regression analysis where the constant of proportionality was approximately 0.57 instead of unity. The problem with the derivation of Eq. D-15 is that $\mathcal{J}_{Ic}$ only characterizes the conditions at the onset of unstable fracture and has no direct connection to energy absorption during fracture propagation.

Another approach is to calculate the work performed on the specimen up to the load corresponding to K_{Ic} -- i.e., the area under the load-displacement curve. For a linear elastic load-displacement behavior up to fracture, the work performed can be calculated from load-displacement compliance relations. Such a calculation can be made for a three-point loaded beam specimen using a derived load-point displacement formula (Tada et al., 1973). The result for a Charpy-size specimen in the usual range of relative crack depths used in precracked Charpy testing (a/W = 0.3 to 0.5) is:

$$K_{Ic}^{2}/E \approx (2) (W/A). \qquad \text{(Eq. D-16)}$$

An identical relation is obtained via the J-integral approximation formula for a deep-notched bend specimen. Clearly, Eq. D-16 also does not agree with the empirical relation indicated by the experimental slow-bend W/A results.

The general problem in the derivation of either Eq. D-15 or Eq. D-16 is that K_{Ic} is defined by conditions existing at the point of very limited crack extension, whereas the W/A measurement involves the total fracture process. Thus, only an empirical relation can be expected between K_{Ic} and W/A.

D.5 K_{Ic} AND K_{Id} PREDICTED FROM PRECRACKED CHARPY LOAD AND DISPLACEMENT MEASUREMENTS

If the material is sufficiently brittle, K_{Ic} can be obtained directly from the fracture load in a test of a precracked C_V specimen. For strict adherence to ASTM E399 requirements, the following measurement capacities apply for a typical a/W of 0.25 (a = 0.1 in.) and the dimensions of a Charpy specimen:

$$K_{Ic}/\sigma_y \leq 0.4 \sqrt{in}. \text{ to meet thickness requirement}$$

$$\leq 0.2 \sqrt{in}. \text{ to meet crack length requirement}$$

Even if the crack length requirement is neglected, the measurement capacity is limited to a fairly low value.

A considerably more liberal requirement would be that fracture must occur before general yield. Using the relation (Green and Hundy, 1956) for an a/W of 0.25 and the K formula for a three-point bend specimen, the measurement capacity would become:

$$K_{Ic}/\sigma_y \leq 0.56 \sqrt{in}.$$

Note that this interpretation ignores any crack length requirement. Based on this approach plus the results of transverse contraction measurement that indicate that the central 90 percent of the Charpy specimen thickness is in plane

strain up to $K_I/\sigma_y = 0.5\sqrt{in}.$, researchers (Tetelman et al., 1974) have estimated K_{Ic} from the load provided that:

$$K_{Ic}/\sigma_y \le 0.5\sqrt{in}.$$

At this limit, the thickness, B, of the Charpy specimen (0.394 in.) corresponds to $B = 1.6 (K_{Ic}/\sigma_y)^2$ whereas ASTM E399 requires $B \ge 2.5 (K_{Ic}/\sigma_y)^2$.

If the fracture conditions exceed the above limit, then other methods based on elasto-plastic fracture mechanics (e.g., COD, J-integral, or equivalent energy) must be used to derive fracture toughness quantities from precracked C_V test records.

In the following review of applicable results, the cases of fracture before and after general yield (K_{Ic}/σ_y less than or greater than $0.5\sqrt{in}.$) will be treated separately.

D.5.1 Results for Fracture Initiation before General Yield

A comparison of K_Q determined from precracked C_V slow-bend load data against valid K_{Ic} for a group of materials has been made (Rich, 1973). The load used to calculate K_Q is the secant offset load (P_Q) obtained per ASTM E399 techniques. The results are shown in Figure D-19 and include K_{Ic}/σ_y values up to $0.59\sqrt{in}.$ for the 7075-T7351 aluminum material. A general correlation trend within an approximately ± 20 percent spread is evident.

Figure D-19 indicates that most of the Ti-6-4 precracked C_V K_Q is lower than the valid compact specimen K_{Ic}. This situation in Ti-6-4 was investigated further (Tetelman et al., 1974) and an R-curve effect was found for fully flat, plane-strain crack propagation in this material. The R curve defines the resistance to propagation during slow crack growth and, in the case of Ti-6-4, the resistance increases as the crack grows after initiation. In this case, K_Q measured at 5 percent compliance change on a small specimen will be less than K_Q on a larger specimen since a smaller absolute amount of crack growth will produce the 5 percent change in a small specimen. This would not explain the reverse situation such as the 7050 aluminum result in Figure D-19.

For the situation of slow crack growth and a rising R curve, a method was proposed for adjusting precracked C_V results to account for it (Tetelman et al., 1974a). The method requires a knowledge of the R versus Δa curve for the material. The precracked C_V K_Q value then is adjusted by a factor equal to the ratio of the amount of crack growth in the large and the precracked C_V specimen at the K_Q measurement point. The results of applying this technique on a group of Ti-6-4 samples in several material conditions are shown in Table D-3 (Tetelman et al., 1974). The largest discrepancy is noted in material No. 1, but the need for repeat tests was indicated prior to calculating the pre-cracked C_V K_Q. Material No. 6 shows the next largest difference but the
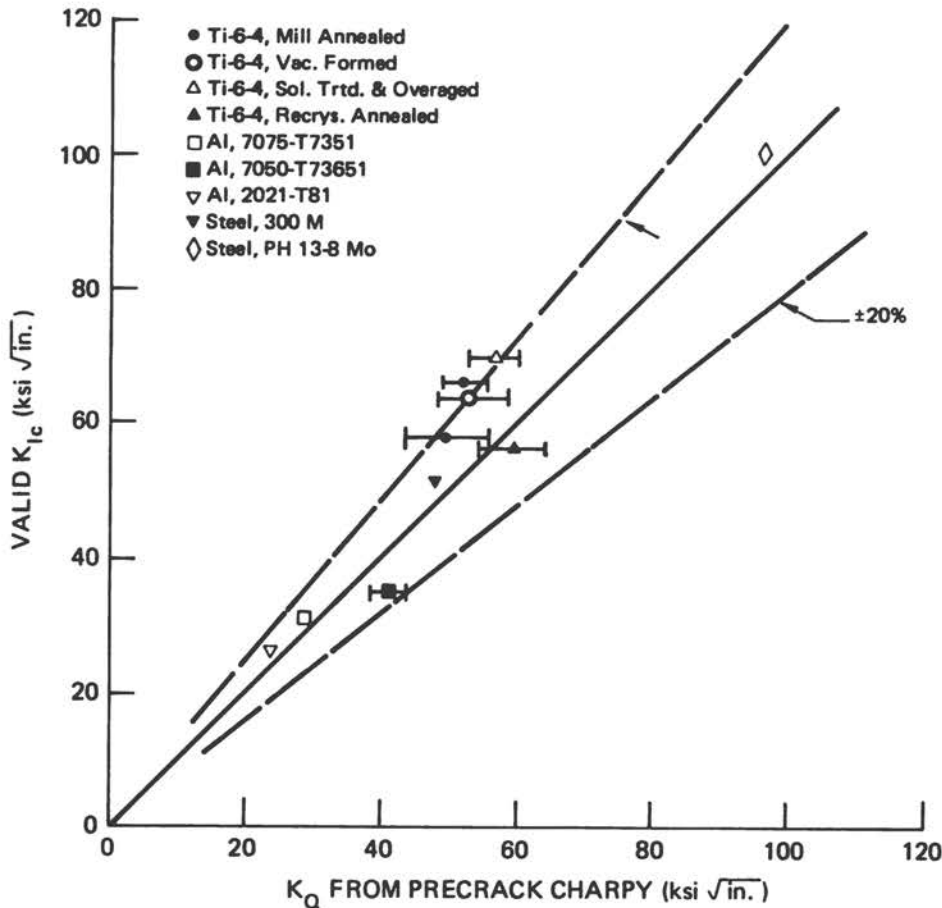
FIGURE D-19 Comparison of Valid K_{Ic} with K_Q Calculated from Precracked Charpy Slow-Bend Load-Deflection Data (Rich, 1973).

precracked C_V value is conservative. In other cases, the difference is within 10 percent. The specification minimum was 75 ksi √in. and the small specimen results correctly discriminate for acceptance/rejection in eight of the nine cases.

The preceding comparison has been for a slow-bend mode of loading the precracked C_V specimen. In principle, the method can be applied to impact testing of this type of specimen by using instrumentation and calculating K_Q from the load-time information. The pop-in or fracture load is used to calculate K_Q since the ASTM E399 type secant offset load cannot be measured in the precracked Charpy impact test. An example of such results for A533B steel (50,000 psi minimum yield strength at room temperature) is shown in Figure D-20 (Server and Tetelman, 1972). Each curve on the scatter band shown in the figure is based on 20 to 30 data points over the indicated temperature range. Considering that the toughness of this steel generally decreases with increasing loading rate, the K_{Id} versus temperature curves obtained from precracked C_V specimens agree with, and show the same trend with, the K_{Id} values from large specimens obtained (Shabbits, 1970).

TABLE D-3 Results of the K_{Ic} Measurements on 6-4 Titanium Samples.

Material Number	Yield Stress (ksi)	Precracked C_V Specimen Data			K_{Ic} from Material Suppliers (ksi $\sqrt{in.}$)
		Crack Growth (in.)	K for Indicated Amount of Crack Growth (ksi $\sqrt{in.}$)	K_{Ic} (for 0.023 in. Crack Growth) by R-Extrapolation (ksi $\sqrt{in.}$)	
1	123	0.002	62	84	62
2	122	0.004	74	97	93
3	122	0.005	68	88	86
4	120	0.002	62	84	77
5	130	0.012	54	62	59
6	121	0.010	66	79	92
7	124	0.011	62	72	73
8	125	0.008	53	65	61
9	118	0.008	69	85	82

NOTE: Data from Tetelman et al., 1974.
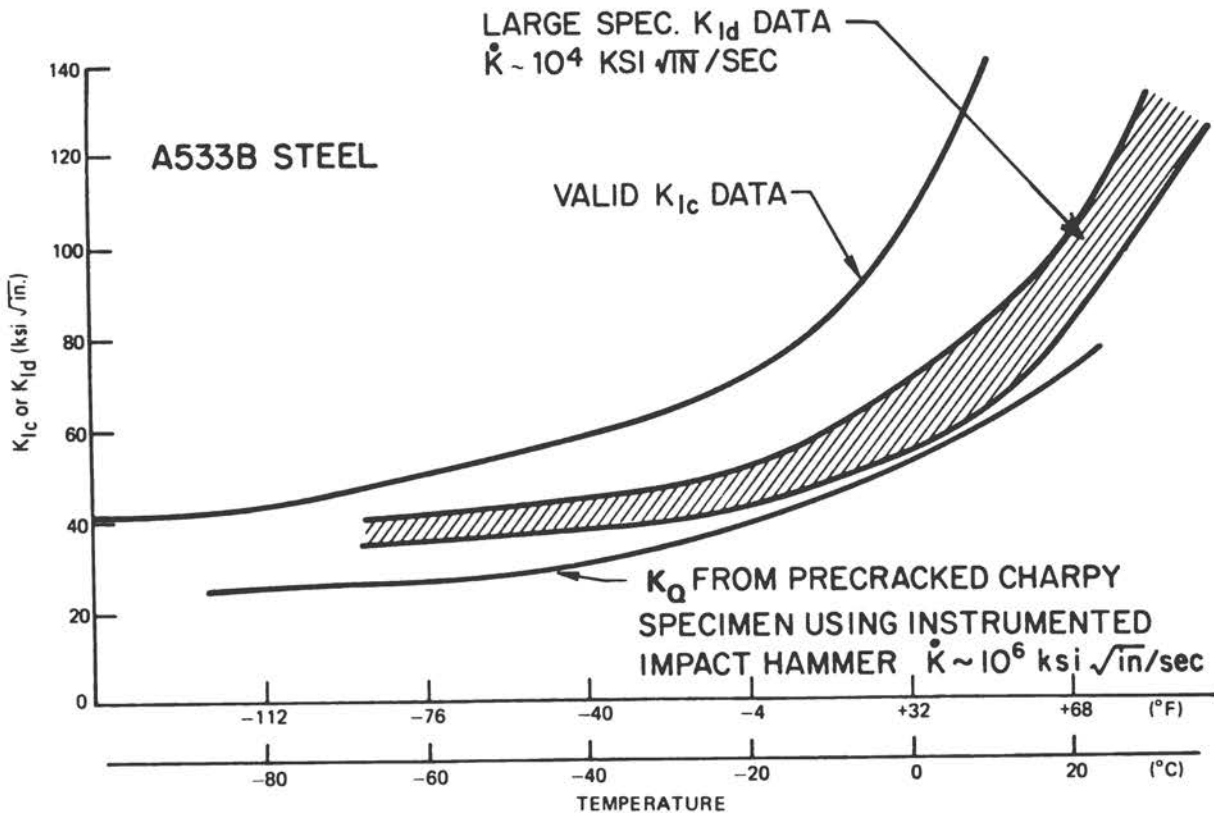
FIGURE D-20   Comparison of Static, Dynamic and Instrumented Precracked
Impact Fracture Toughness as a Function of Temperature
(Server and Tetelman, 1972, reprinted with permission from
Pergamon Press, Ltd., Engineering and Fracture Mechanics).

Although Figure D-20 indicates a reasonable correlation trend, extreme caution must be exercised in interpreting load-time data to derive K_Q and inferred K_{Id} values from precracked C_V impact tests. In particular, it must be ascertained that the load value from which K_Q is calculated does not involve slow crack growth and R-curve effects. This is not easy to discern in impact testing.

Another and a more general problem with impact test K_{Ic} (K_{Id}) results concerns the assumption that statically derived K expressions are valid under high-speed loading conditions. A study of this assumption is needed urgently.

The available data on the correlation of K_{Ic} or K_{Id} values with K_Q results calculated from load data in precracked C_V tests can be summarized as follows:

a.   The correlation is generally within ± 20 percent for cases where K_{Ic}/σ_Y (or $K_{Id}/\sigma_{Yd}) \leq 0.5\sqrt{in}$.; this measurement limit appears to be the useful upper limit of this method.

b. Slow crack growth and R-curve effects, if present, introduce difficulties and must be considered in calculating K_{Ic} or K_{Id} values from precracked C_V tests.

c. Slow bend, rather than impact, is the preferable method of testing for correlation with K_{Ic}.

D.5.2 Results for Fracture Initiation after General Yield

Calculation of toughness values on specimens fracturing in this regime requires elasto-plastic fracture mechanics methods (i.e., J-integral, equivalent energy, and crack opening displacement). This section discusses the results of the application of these methods to the precracked C_V specimen since this specimen is one of the possible geometries that can be utilized with these elasto-plastic methods. The COD method and results are described first.

The COD method was first proposed by Wells, and its basis is the following relation (Wells, 1961):

$$K = \sqrt{\frac{E\sigma_Y \cdot COD}{1 - \nu^2}} , \qquad \text{(Eq. D-17)}$$

where K = stress intensity factor, E = elastic modulus, σ_Y = yield strength, COD = crack opening displacement at the crack tip, and ν = Poisson's ratio. Experimental data in support of this relation are shown in Figure D-21 (Robinson and Tetelman, 1974a).

Since the crack tip COD is difficult to measure, two alternative measurements from which COD can be calculated for the precracked C_V specimen have been proposed. These are the use of on-load clip gauge displacement or the off-load notch root contraction in the crack tip region (Tetelman et al., 1974). Numerical relations were presented by these investigations for making the calculations. For clip gauge displacement (CGD) measurements on precracked C_V specimens, the following is used:

$$B_0 + B_1 COD + B_2 COD^2 + B_3 COD^3 + B_4 COD^4 = 0, \qquad \text{(Eq. D-18)}$$

$B_0 = 0.04271 \, CGD,$

$B_1 = 0.09391 \, CGD \cdot \left(\frac{a+z}{W-a}\right) - 0.04271,$

$B_2 = -0.009313 \, CGD - 0.09391,$

$B_3 = 0.003678 \, CGD + 0.009313,$ and

$B_4 = -0.0003678$

where COD and CGD are in thousandths of an inch, and W = specimen width (0.394 in. for C_V specimen), a = crack depth, and z = height of knife edges above the specimen surface. Eq. D-18 is based on COD data in the range from 0.001 to 0.01 in.
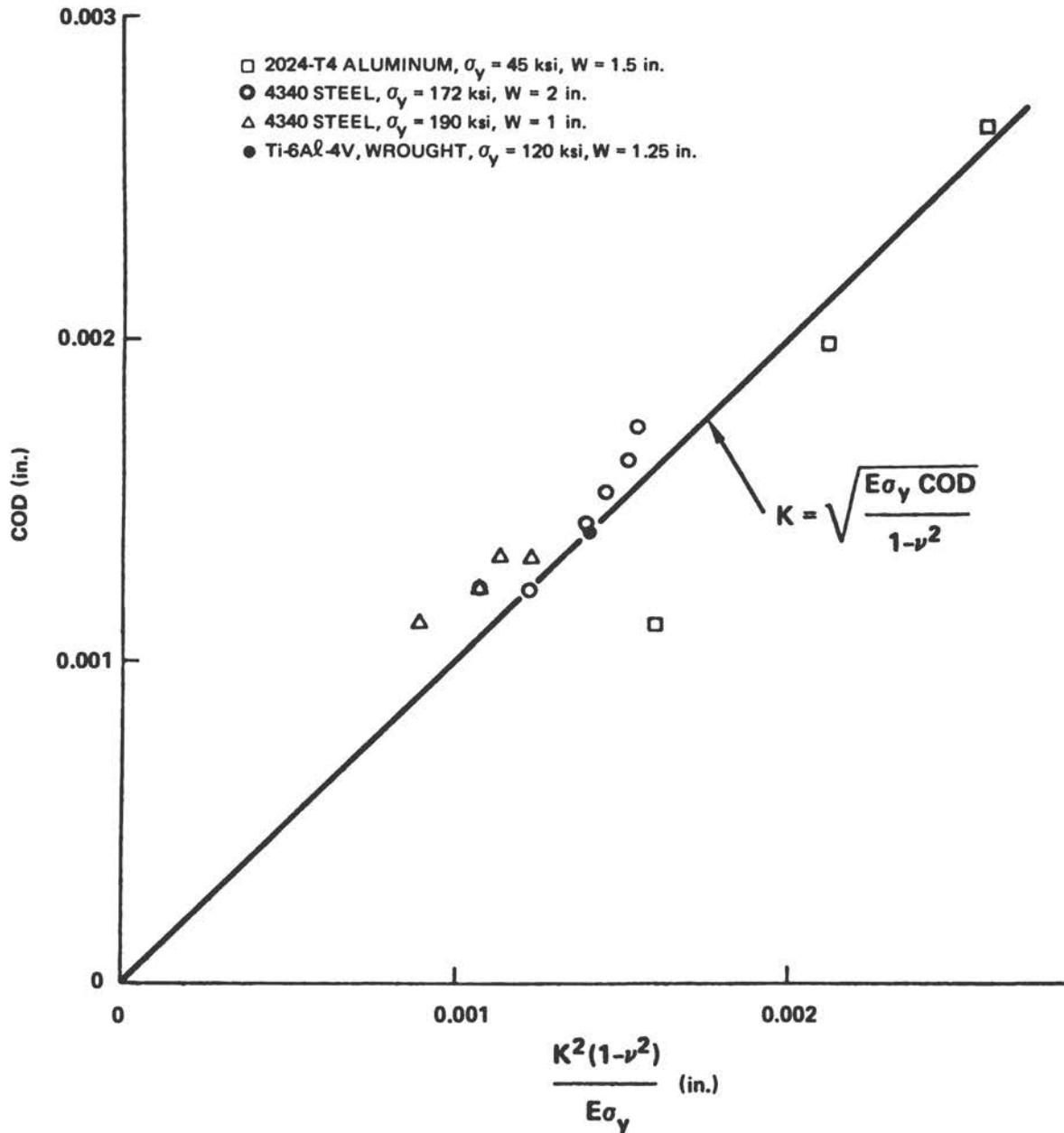
FIGURE D-21   Correlation between K and COD (Robinson and Tetelman, 1974).

The second technique of calculating COD in the precracked C_V specimen uses the following relation:

$$COD = 1.27 \, NRC_{off}, \qquad \text{(Eq. D-19)}$$

where NRC_{off} = notch root contraction in the off-load condition. The experimental procedure then involves determining the COD at fracture initiation and using Eq. D-17 to calculate a K_Q value for comparison to valid K_{Ic}.

Figs. D-22 and D-23 compare K_{Ic} predicted from the preceding COD method against valid K_{Ic} data for A533B and 4340 steels, respectively (Robinson and Tetelman, 1974a). The agreement is very good and indicates the potential of this method in predicting K_{Ic} in the elasto-plastic regime with small specimens.

METHOD OF DETERMINATION OF $(COD)_{Ic}$

● DOUBLE BEND
○ CRACK PROFILE
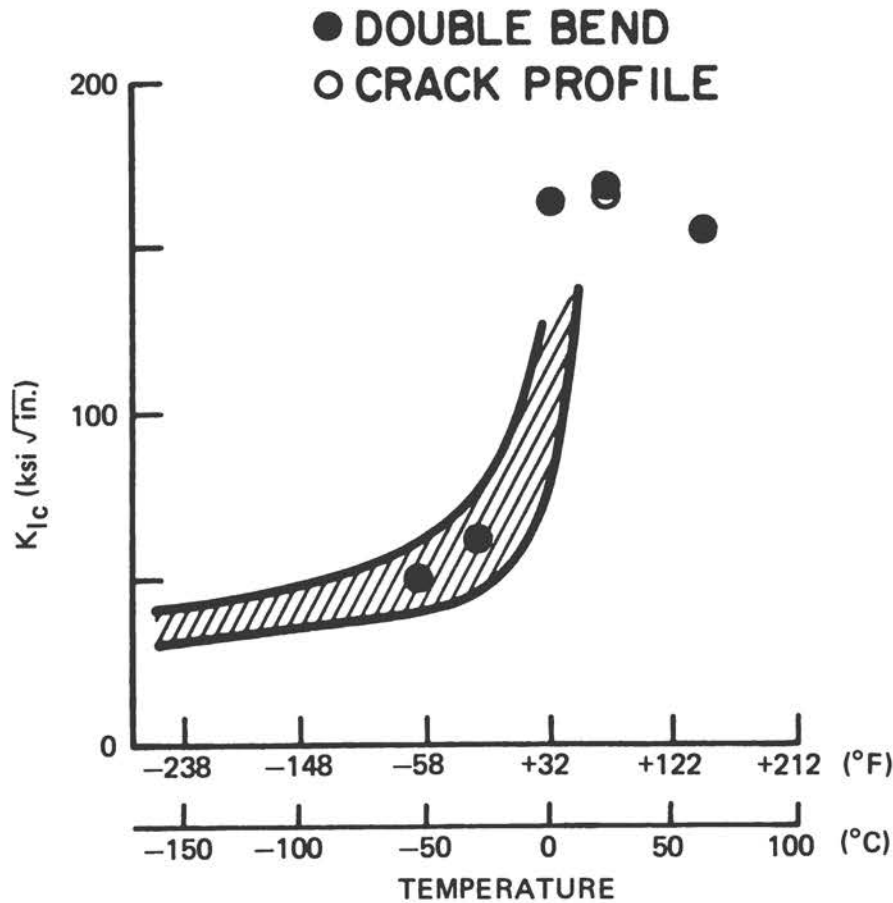
FIGURE D-22 K_{Ic} Calculated from $(COD)_{Ic}$ for A533B Steel Superimposed on the Scatter Band for HSST Valid K_{Ic} Results (shaded area) (Robinson and Tetelman, 1974).
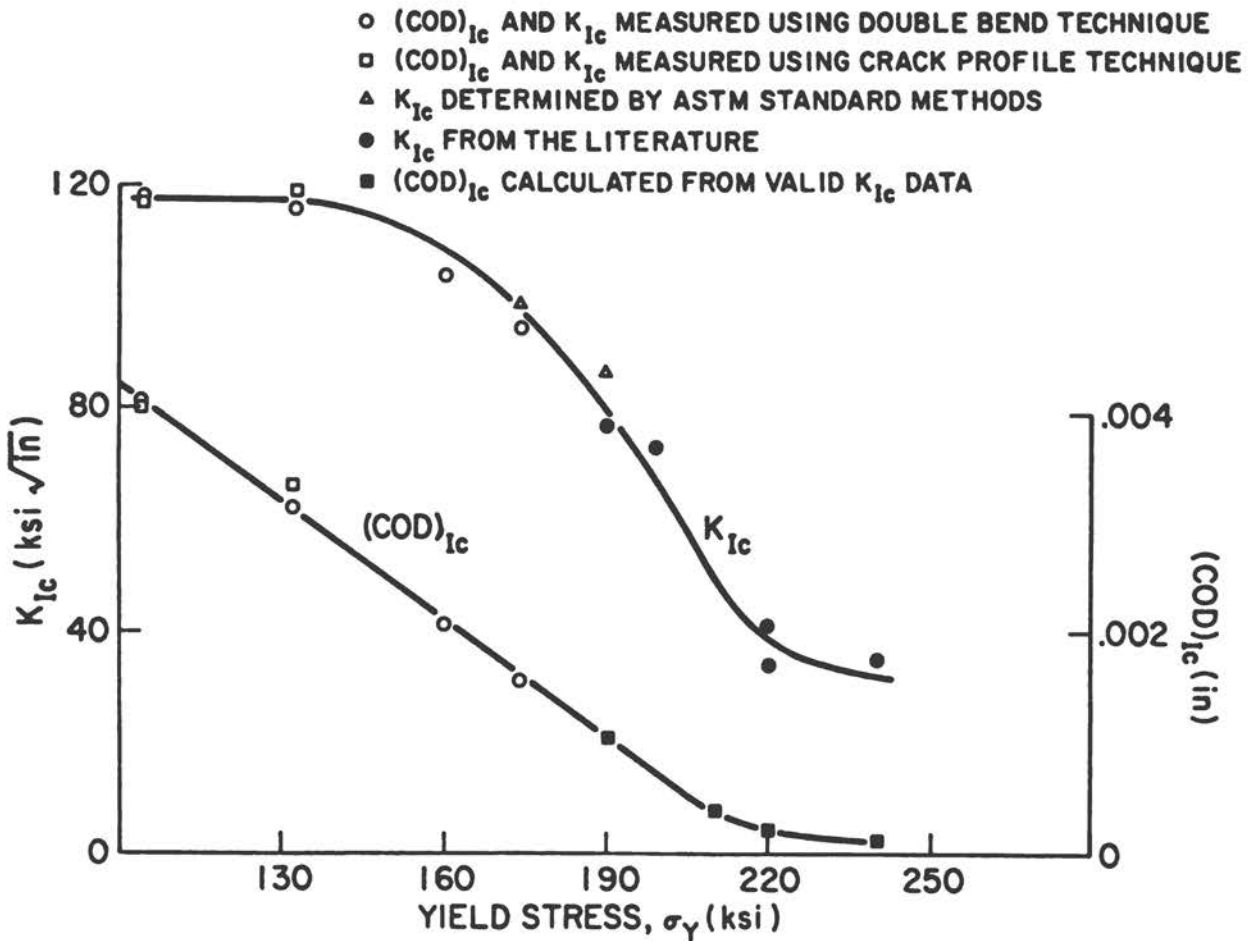
FIGURE D-23 Variation of $(COD)_{Ic}$ and K_{Ic} with Yield Stress for Quenched and Tempered 4340 Steel (Robinson and Tetelman, 1974).

The major problems with COD or any of the other approaches for the elasto-plastic regime are determining precisely the fracture initiation point if slow crack growth occurs and accounting for the R-curve effect in comparing small specimen results to K_{Ic} or K_{Id}. For slow loading tests, several experimental techniques are possible and have been used with varying degrees of success for solving these problems. However, for rapid or impact loading, there is no suitable technique at present. An arbitrary procedure such as using the maximum load may or may not be meaningful.

The J-integral and the equivalent energy methods are other possible approaches in precracked C_V specimen testing. The general concepts and analysis procedures of the J-integral method are described elsewhere in this report. With respect to the equivalent energy method, it has been shown to be identical to the J-integral for the case of bend type specimen such as the precracked C_V (Begley and Landes, 1973). The results for comparing K_{Ic} values

from slow-bend J-integral testing of precracked C_V specimens with valid K_{Ic} were found in only one research paper (Robinson and Tetelman, 1974b). Testing was on 4340 steel with 174 ksi yield strength with the following results:

Valid K_{Ic} -- 99 ksi $\sqrt{in}$.

J-Integral K_{Ic} -- 83-104 ksi $\sqrt{in}$.

The agreement is good and indicates the potential of precracked C_V specimens for use in this method of testing.

K_{Ic} values obtained via the J-integral method in instrumented impact precracked C_V tests for several high-strength steels have been reported (Iyer and Miclot, 1973). The maximum load was used as the criterion for J calculations. This procedure could be criticized as a very arbitrary definition of the fracture initiation point. However, a good correlation was observed with estimated valid K_{Ic} properties of the steels tested.

In summary, there currently is considerable activity in the general area of elasto-plastic fracture. With respect to its application to precracked C_V testing, the following points summarize the current status when fracture initiation occurs after general yield:

a. Slow-bend testing and the use of the COD concept show good correlation potential.

b. Methods based on the J-integral concept are an alternative and also would be useful if the validity of simplified testing and analysis procedures were established.

D.6   CORRELATION OF K_{Ic} WITH PRECRACKED CHARPY SPECIMEN STRENGTH RATIO

The definition of, and the calculational method for, obtaining the specimen strength ratio (R_S) are given in ASTM E399-74. It is the ratio of the nominal stress, σ_N, at maximum load to the material yield strength, σ_Y (i.e., $R_S = \sigma_N/\sigma_Y$). For a fatigue-cracked bend specimen, this ratio is additionally designated as R_{sb}. For purposes of clarity in this report, the ratio will be given the specific designation R_{sb-CV} when obtained from a fatigue-cracked Charpy-size specimen.

The equation for calculation of σ_N for a three-point loaded bend specimen is:

$$\sigma_N = \frac{3 P_{max} S}{2 B(W - a_o)^2} , \qquad \text{(Eq. D-20)}$$

where σ_N = nominal stress, P_{max} = maximum load, S = span, B = specimen thickness, W = specimen width, and a_o = initial crack depth (notch plus fatigue precrack). Note that σ_N as calculated from this equation is simply the nominal bending stress at maximum load based on the initial net section dimensions. Testing procedures are simple since maximum load and initial crack length are the only measurements required; displacement measurements are unnecessary if σ_N and R_{sb-CV} were the only quantities desired.

In general, the correlation between K_{Ic} and R_{sb-CV} would be empirical. However, in the lower toughness-to-yield-strength range, a theoretical basis for a correlation based on linear elastic fracture mechanics (LEFM) concepts can be formulated.

The primary data sources for examining a correlation between R_{sb-CV} values and matching valid K_{Ic} data were obtained during the course of slow-bend W/A testing (Succop et al., 1975; Ronald, 1974). Table D-3 (page 141) lists the σ_N values calculated from these data. As mentioned previously in the section on W/A correlations, the materials tested included aluminum, steel, and titanium alloys primarily in the higher-strength grades and conditions.

In addition, the following data sources also report information for calculating σ_N values along with valid K_{Ic} data:

Reference	Material	Remarks
DeSisto, 1973	Ti-6 Al-6 V-2 Sn	$K_{Ic}/\sigma_Y = 0.38\sqrt{in.}$
DeSisto, 1973	Ti-8 Mo-8 V-2 Fe-3 Al	$K_{Ic}/\sigma_Y = 0.23\sqrt{in.}$
DeSisto, 1973	Ti-11.5 Mo-6 Zr-4.5 Sn	$K_{Ic}/\sigma_Y = 0.32\sqrt{in.}$
Raymond, 1974	Al, 7075-T651	Tests in 5 different orientations; $K_{Ic}/\sigma_Y = 0.26$ to $0.33\sqrt{in.}$
Begley and Logsdon, 1971	NiMoV, CrMoV and NiCrMoV Rotor Steels	Tests at various temperatures; $K_{Ic}/\sigma_Y = 0.37$ to $1.28\sqrt{in.}$

In one instance, the σ_N values and, therefore, R_{sb-CV} only could be approximated since all of the requisite information is not included in the reference (Begley and Logsdon, 1971).

The results from these sources are shown in Figure D-24 in the form of K_{Ic}/σ_Y versus R_{sb-CV}. Up to R_{sb-CV} equal to approximately two, nearly all of the results fall within ± 20 percent of the linear relation indicated as the "LEFM relation."
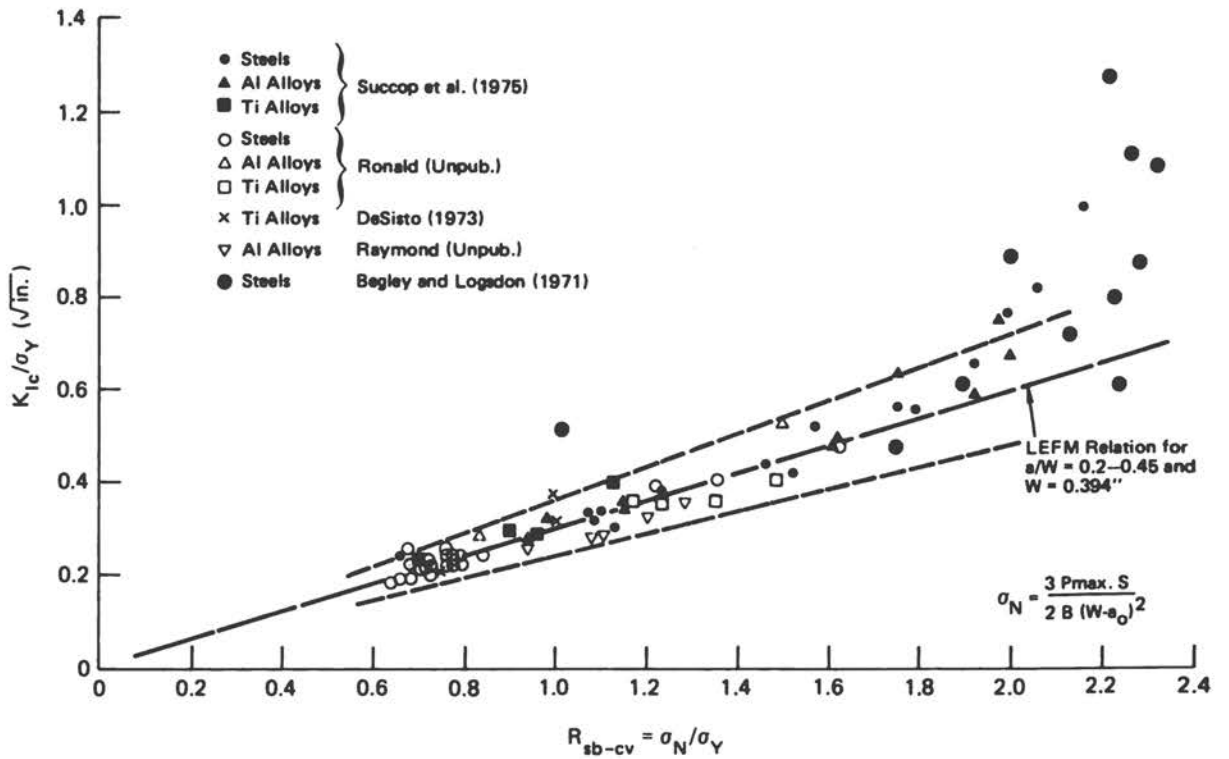
FIGURE D-24 Correlation of Valid K_{Ic} with Specimen Strength Ratio (R_{sb-CV}) in Precracked Charpy Slow-Bend Tests.

The LEFM relation is derived from the K_I formula for a three-point loaded bend specimen. Using one formula (Tada et al., 1973), K_I can be expressed in terms of σ_N as:

$$K_I = \sigma\sqrt{\pi W}\ Y(a/W), \qquad \text{(Eq. D-21)}$$

where W = specimen width, $Y(a/W)$ = function of relative crack depth, a/W, and S/W (S = span). For the specific dimension of a Charpy-size specimen (W = 0.394 in.) and S/W = 4, which is typical for slow-bend testing of precracked Charpy specimens, the relation between K_I and σ_N is as follows for several values of a/W:

a/W	K_I/σ_N
0.2	0.312
0.3	0.312
0.4	0.297
0.45	0.288
0.5	0.278

In the above tabulation, the numerical values for K_I/σ_N apply for K_I and σ_N expressed in units of ksi $\sqrt{in}$. (or psi $\sqrt{in}$.) and ksi (or psi), respectively. P_{max} and, therefore, σ_N, in a precracked Charpy test are assumed to correspond to the K_{Ic} measurement point, which means ignoring all thickness, crack size, P_{max}/P_Q and slow crack growth requirements of E399. The above tabulations show that in the range a/W = 0.2 to 0.45, K_{Ic} = 0.3 σ_N within a few percent. Dividing by σ_Y,

$$K_{Ic}/\sigma_Y = 0.3 R_{sb-CV} \quad , \qquad \text{(Eq. D-22)}$$

(for K_{Ic}/σ_Y in $\sqrt{in}$. units). Eq. D-22 is the "LEFM relation" shown in Figure D-24. The a/W values for virtually all of the precracked Charpy data shown in the figure were in the 0.3 to 0.45 range.

A distinct departure of the results from the LEFM relation can be seen in Figure D-24 beginning at about R_{sb-CV} = 2. The reason is that P_{max} exceeds the general yielding condition and approaches the limit load condition as K_{Ic}/σ_Y increases. The calculated lower bound of the general yield conditions (Green and Hundy, 1956) analysis would correspond to R_{sb-CV} of approximately two. Inserting this value of R_{sb-CV} in Eq. D-22, K_{Ic}/σ_Y is implied to be linearly proportional to R_{sb-CV} up to a relative toughness of K_{Ic}/σ_Y = 0.6 $\sqrt{in}$. This proportionality represents a slight extension of a conclusion discussed earlier in this appendix (Robinson et al., 1974).

The limit load in a three-point bend specimen appears to correlate best with the ultimate tensile strength of the observed material (Bucci et al., 1972). These results plus an earlier analysis (Green and Hundy, 1956) indicate that the limit load corresponds to σ_N/σ_{UTS} = 2.18 where σ_{UTS} = ultimate tensile strength. For most of the materials considered in Figure D-24, the ratio of ultimate-tensile-to-yield strengths are in the range 1.1 to 1.2. Therefore, for these materials, σ_N/σ_Y = 2.6 would represent the approximate upper bound for limit load conditions. The actual limit loads will vary depending on the strain hardening and the slow crack growth characteristics of each material.

The general yielding and limit load behavior places a limitation on the usefulness of the R_{sb-CV} as a correlation parameter at higher relative toughnesses. R_{sb-CV} will become a less sensitive index of K_{Ic} and the correlation will be strictly empirical specific to each alloy type and grade. However, the available data indicates a good potential for precracked Charpy slow-bend P_{max} as a quality-control test for materials with a relative toughness up to about K_{Ic}/σ_Y = 0.75 $\sqrt{in}$. Figure D-25 is a replot of the data in Figure D-24 in the form of K_{Ic} versus σ_N of the results within this somewhat arbitrary relative toughness limit. As with Figure D-24, the spread from the LEFM relation is approximately ± 20 percent.

Interestingly, a correlation of K_{Ic} with σ_N is basically an extension of the method discussed earlier in section D.5.1. There, the procedure was to use the load, P_Q, measured in the ASTM E399 sense (e.g., 5 percent secant offset) on a precracked Charpy specimen to obtain K_Q which then was compared with valid
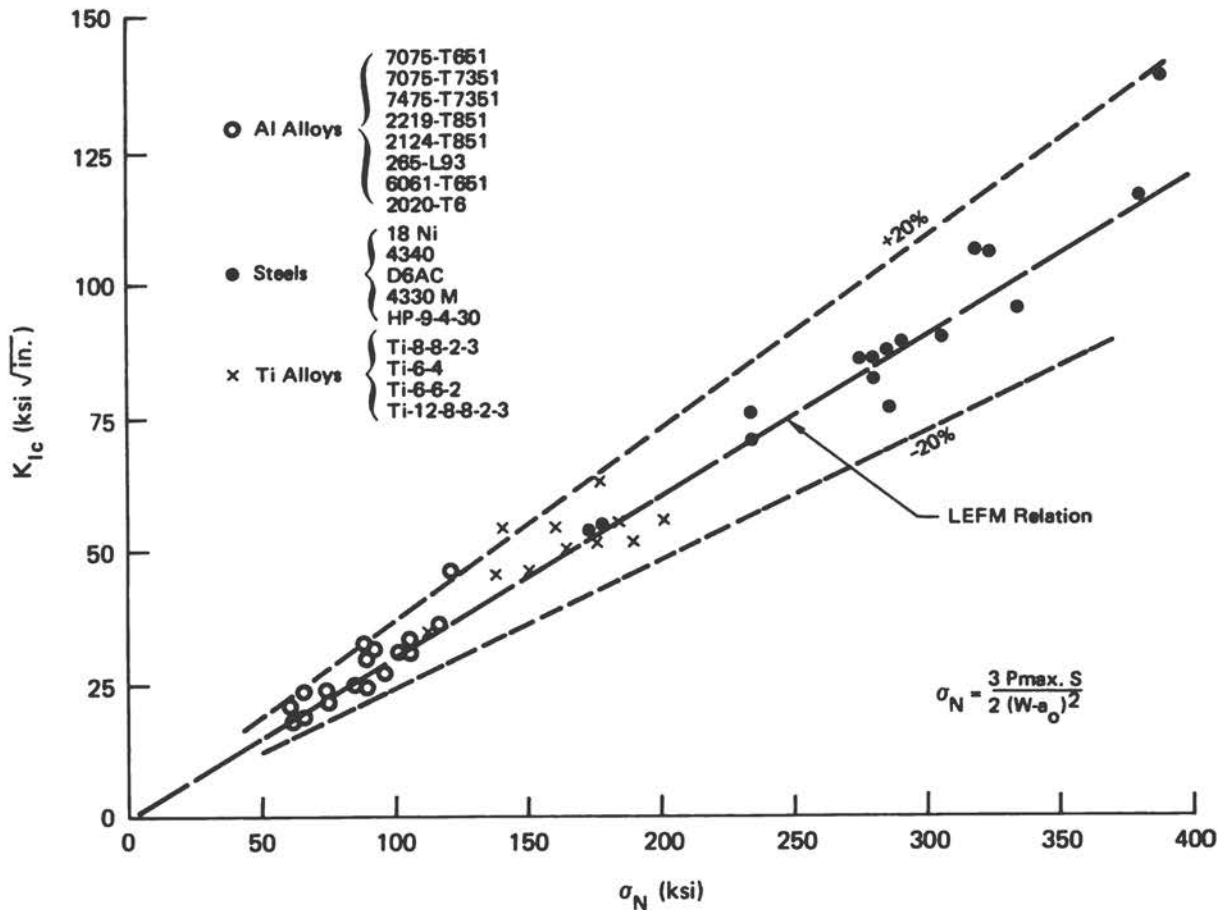
FIGURE D-25 Comparison of Valid K_{Ic} Data with Precracked Charpy Slow-Bend σ_N Values for $K_{Ic}/\sigma_N \leq 0.75 \sqrt{in.}$

K_{Ic}. For cases where P_Q is identical to P_{max}, the correlation of K_{Ic} with σ_N is the same as estimating K_{Ic} from K_Q. As shown in Figure D-19 (page 140), the correlation of K_Q with K_{Ic} was also within a scatter of about ± 20 percent.

Although Figure D-25 shows a generally good correlation when all materials are considered, examination of the results for a specific group (e.g., titanium alloys) could result in a correlation different from the LEFM relation. This indicates that, although the LEFM relation can be a useful guide, application in quality control should be based on empirical correlations for each specific material.

Some indication of the considerations that arise in quality-control applications is illustrated in Figure D-26 for results on 300M steel that were not included in Figure D-25. Although the LEFM relation provides a useful guide to a correlation, it probably is not the best correlation if analyzed statistically. Nevertheless, Figure D-25 shows that a large majority of the results are encompassed by a scatterband of ± 10 percent from the LEFM relation. The problem of occasional large variations in duplicate precracked Charpy test results can be noted.
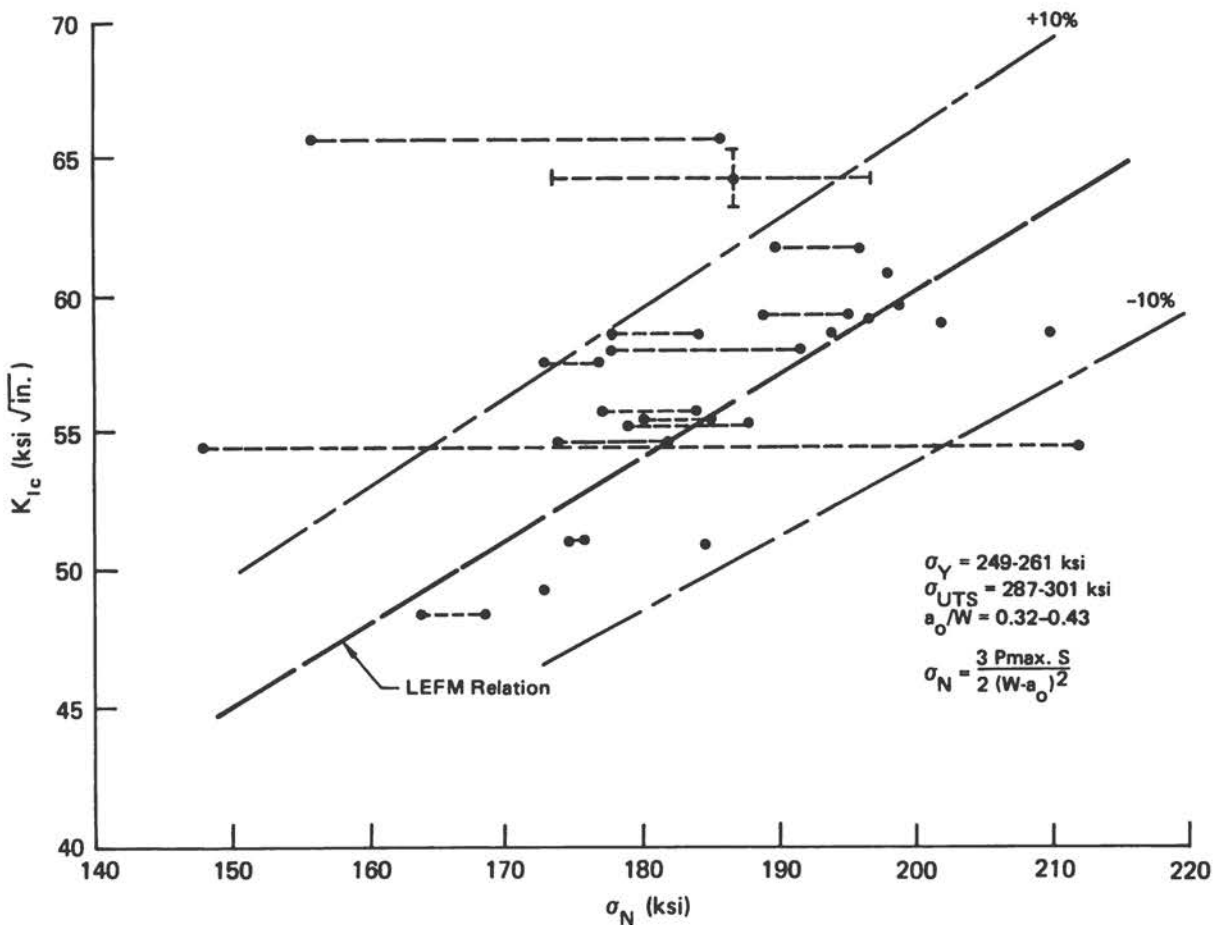
FIGURE D-26 Valid K_{Ic} versus Precracked Charpy Slow-Bend σ_N for Samples from 300M Steel Forgings (Ronald, 1974).

Comparing the merits of a correlation based on R_{sb-CV} relative to that based on W/A, the spread in K_{Ic} prediction is about the same. However, as noted above, the correlations with R_{sb-CV} become curvilinear at high relative toughness, whereas W/A results indicate a linear relation with K_{Ic}^2/E up to relatively high toughnesses. Thus, the W/A correlation might have a wider range of applicability. The strength ratio, R_{sb-CV}, has the virtue of being a much simpler experimental quantity to measure.

The following observations and conclusions can be derived from an evaluation of the currently available data concerning the use of the strength ratio, R_{sb-CV}, obtained from a precracked Charpy slow-bend test for correlation with K_{Ic}:

a. The fact that maximum load and initial crack length are the only measurements required makes the R_{sb-CV} parameter very attractive for quality-control testing.

b. The available results indicate that K_{Ic} can be predicted from R_{sb-CV} (or more simply from nominal strength, σ_N) within about ± 20 percent for relative toughnesses up to $K_{Ic}/\sigma_Y = 0.75 \sqrt{in}$.

c. Up to approximately $K_{Ic}/\sigma_Y = 0.75 \sqrt{in}$., the correlation between σ_N and K_{Ic} generally follows a relation derived from linear elastic fracture mechanics (LEFM).

d. Analysis of the data suggests that improved correlations with less spread might be obtained if only one specific alloy type grade were considered. These correlations would be empirical and a larger data base is required to evaluate their usefulness.

e. The R_{sb-CV} parameter loses its usefulness as a correlation basis at higher relative toughness ($K_{Ic}/\sigma_Y > 0.75 \sqrt{in}$.) because the nominal strength of the precracked Charpy size specimen approaches limit load condition. The exact limit of usefulness will have to be determined by additional experimental studies.

f. Potentially, R_{sb-CV} obtained from a precracked Charpy impact test could be correlated with dynamic toughness, K_{Id}; however, no attempts at such a correlation have been made yet.

D.7 PRECRACK CHARPY FOR TRANSITION TEMPERATURE DETERMINATION

Discussion thus far in this appendix focused on correlations of C_V specimen results with K_{Ic}. However, in the case of the lower- and medium-strength steels used in structural application, fracture control and, therefore, fracture toughness requirements were based on the transition temperature (TT) approach. This approach resulted because the fracture toughness properties of these materials exhibit a strong temperature dependence. The approach utilizes a transition temperature determined by one of several test methods as an indexing or reference temperature where the change in fracture toughness is most pronounced.

Some of the more common tests and transition temperatures that evolved are:

a. Standard V-notch Charpy specimen impact test --

   (1) Temperature for some specific energy level such as 15 or 30 ft-lb TT.

   (2) Temperature at 50 percent shear fracture (FATT).

   (3) Temperature for 15-mil lateral expansion (15-mil TT).

b. Nil-ductility transition temperature from a drop-weight test specimen (ASTM E208).

c. Crack arrest transition (CAT) curve that gives the temperature at which a running crack is arrested as a function of applied stresses; a wide-plate-type test specimen generally is used to determine this curve.

Each of these TTs is different and an enormous effort was expended in an attempt to find a general relationship between them for a range of steel types and grades. Also, the problem of the lowest allowable service temperature with respect to any one of the TTs still requires much judgment based on the grade of steel and service loadings in the structure.

Due to its small size and convenience in testing, TTs derived from the standard C_V impact test are used widely. However, the criticism has been made that the 0.010-in. radius notch does not always give the best or the most sensitive measure of the TT characteristics of a steel. The precracked C_V specimen was used to improve on this aspect of the standard C_V specimen.

The precracked C_V generally results in the transition behavior shifted upwards in temperature with respect to the standard C_V. The shift can be slight or rather large depending on steel grade and often differs from heat-to-heat within a given grade. In Figure D-27, the upward shift is substantial.

Precrack C_V impact energy versus temperature often exhibits a marked inflection at a temperature between the lower shelf and the transition range. This inflection temperature (e.g., -20° F in Figure D-27) provides a good estimate of the drop-weight test nil-ductility transition temperature in many instances (Orner and Hartbower, 1958; Wessel, 1960; Orner and Hartbower, 1961b). However, in other instances, the results indicate poor correspondence. Figure D-28 shows precracked C_V energy curves versus temperature for four steels (Gross, 1969) along with the drop-weight nil-ductility transition temperature for each. In the case of the A517-F steel, the nil-ductility transition temperature occurs at a considerably higher temperature than any noticeable inflection point of the precracked C_V curve.

The nil-ductility transition temperature is important as a useful guide to estimating the CAT curve; above it, the CAT curve rises sharply. Experience with service failures has shown that the nil-ductility transition temperature + 30° F provides reasonable assurance of crack arrest in structural carbon steels for stresses up to about one-half of the yield strength and the nil-ductility transition temperature + 60° F for stresses up to about the yield strength.

In a number of cases, the standard C_V energy was very high at the nil-ductility transition temperature or where service failures have occurred in spite of relatively high standard C_V energy at the failure temperature. A detailed discussion of these cases will not be given here; however, in many, the precracked C_V revealed a lower fracture toughness than that indicated by the standard C_V results.
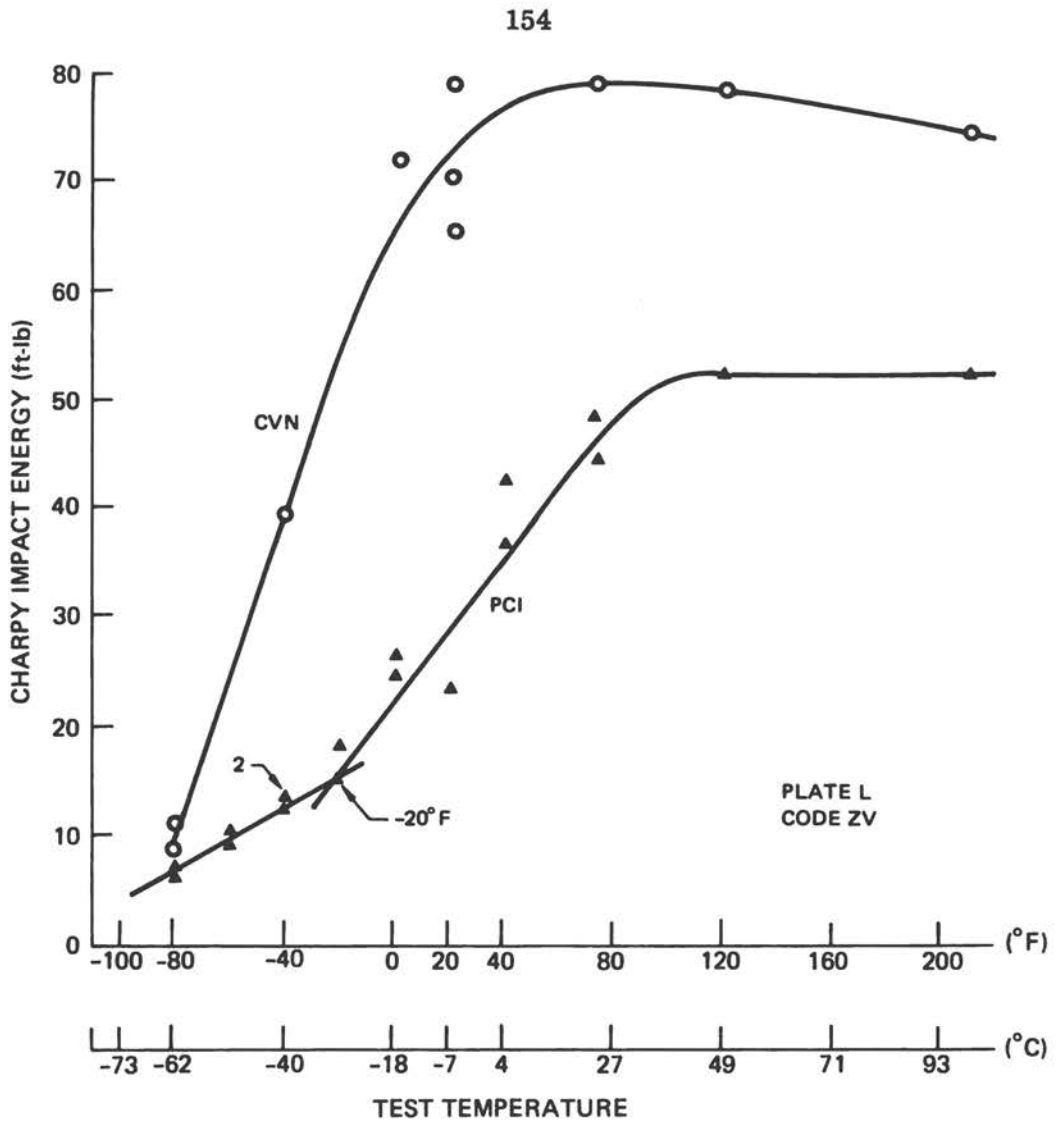
FIGURE D-27 Standard (CVN) and Precrack Charpy Impact (PCI) Transition
Curves for an A514F Steel Plate (Hartbower and Reuter, 1973).

In summary, the precracked C_V can be used as an alternate method to
ASTM E208 for determining the nil-ductility transition temperature of structural
grades of steels. The two methods generally give nearly identical measures of
the nil-ductility transition temperature; however, exceptions have been
observed and must be recognized if the precracked C_V is used as an alternate
to ASTM E208.
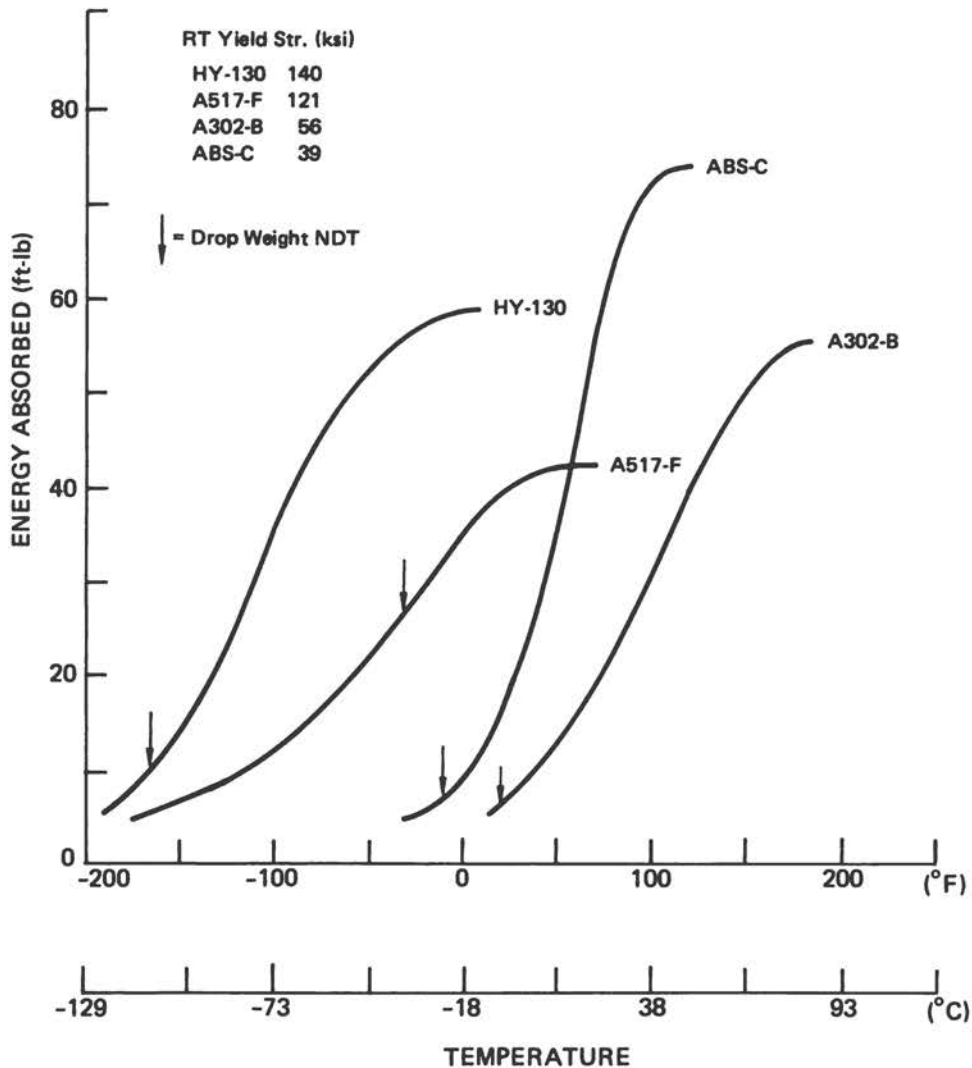
FIGURE D-28   Precracked Charpy Impact Test Transition Curves and Drop-
Weight Test Nil-Ductility Temperatures of Four Steels (Gross,
1969, by permission of the American Welding Society).

D.8   OTHER EVALUATION CONSIDERATIONS

D.8.1   Cost

The cost summary given elsewhere in this report indicates that the cost
of preparing and testing a standard C_V impact specimen is approximately the
same as the cost of an ordinary tensile test. The cost of precracked C_V testing
depends on the degree of instrumentation and data reduction as shown by the
following:

Test	Cost (Tensile Test = 100%)
Precracked, Ordinary Impact	250%
Precracked, Slow Bend, Maximum Load Only	250%
Precracked, Slow Bend, Load Displacement	300%
Precracked, Instrumented Impact	400%

The cost summary also shows that precracked C_V test ranges between about 20 percent to about 35 percent of the cost of preparing and performing the standard ASTM E399 compact specimen K_{Ic} test.

D.8.2 Specimen Size and Orientation Flexibility

The Charpy specimen is the smallest specimen in terms of material volume of all of the specimens considered in this report; thus, it has the following advantageous features:

a. Small test material requirements.

b. Replicate testing with minimum material volume removal.

c. Flexibility in multiple location sampling.

d. Excellent orientation capability (by using electron beam welded extensions, stock down to about 1/2 in. thickness can be tested in the short transverse orientation).

e. Small testing machine load requirements.

f. Small specimen space requirements for application such as in-reactor surveillance monitoring for radiation damage.

The small size results in some inherent disadvantages in that it limits the measurement capacity (toughness-to-strength ratio) when fracture mechanics test methods are used on the specimens and tends to produce greater sensitivity to local inhomogeneity in the material.

D.8.3 Complexity

Complexity varies with the specific C_V specimen test. The conventional C_V impact test is simple. Careful attention to the recording system and to the analysis of the load-time record is necessary for an instrumented impact test. Other variations are between these two extremes in complexity. Only the standard C_V impact currently is covered by an ASTM test specification. The ASTM E399 specification also would apply to the precracked C_V slow-bend test if the validity criteria are met.

D.8.4 Experience

The standard C_V impact test is well known and has been used for many years throughout the world. The precracked and instrumented versions are limited to laboratory investigations with virtually no current experience in routine quality-control testing.

D.8.5 Strain Rate Variation Capability

A wide variation from slow to impact loading rates is possible and is used. In the intermediate to high (impact) range, the usual procedure is to vary the striking velocity by releasing the striken pendulum from intermediate positions less than the full height.

D.8.6 Test Temperature Range Capability

Due to its small size, the C_V specimen can be tested easily at almost any temperature of interest. Tests have been conducted from cryogenic temperatures to over 1500° F.

D.8.7 Prospects for Improvement

Aside from the need to acquire more data for specific materials, grades, etc., to verify or improve the validity of the several correlation methods described, the major prospects for improvement are in the area of standardizing the test procedures for the precracked version of the C_V specimen test. Items within this area include:

   a. Optimum precracking conditions (stress level, initial notch sharpness and final depth).

b. Method of obtaining energy values from load-displacement record.

c. Operational definition of crack initiation in elasto-plastic fractures.

d. Validity of the static-stress intensity factor (K_I) calibration equations under impact loading conditions.

D.9 SUMMARY

The relatively small size of a Charpy test specimen offers several advantages in terms of material requirements, orientation flexibility, and testing convenience as a simple and inexpensive method of obtaining fracture toughness information. The standard 0.010-in. root radius V-notched Charpy specimen has a wide background of usage, particularly in the steel industry. In recent years, there has been considerable developmental activity on the precracked version of this specimen.

On the basis of information available and the degree of correlation plus testing requirement factors, slow-bend testing of precracked specimens is judged to be the most suitable among the various methods of testing Charpy-size specimens for correlation with static plane-strain fracture toughness, K_{Ic}. Suitable correlation indices derived from this test are the strength ratio (R_{sb-CV}) and the energy per unit area (W/A).

Other methods of testing either the standard or the precracked specimens are judged to be of lesser usefulness because of factors such as testing complexity, measurement interpretation, insufficient data for correlation or the specific and limited nature of the correlation.

D.10 GLOSSARY OF TERMS

a	- crack depth
A	- fracture area
a_o	- initial crack depth (notch plus fatigue precrack)
B	- specimen thickness
CAT	- crack arrest transition temperature
CGD	- clip gauge displacement
COD	- crack opening displacement
C_V	- V-notch Charpy specimen
CVN	- Charpy energy
E	- elastic modulus

FATT	- fracture appearance transition temperature
K	- stress intensity factor
K_{Ic}	- slow load (static) plane strain fracture toughness
$K_{Ic(y)}$	- stress intensity factor
$K_{Ic(\rho)}$	- apparent K_{Ic} for a root radius, ρ
K_{Id}	- dynamic fracture toughness measured at rapid loading rates
LEFM	- linear elastic fracture mechanics
NDT	- nil-ductility transition temperature
NRC	- notch root contraction
NRC_{off}	- notch root contraction in the off-load condition
PCI	- precrack Charpy impact
P_F	- corresponds with a catastrophic loss of load-bearing capacity and the load at which a relatively low toughness crack extends from the notch root
P_{GY}	- load corresponding to general yielding
P_{max}	- maximum load
R_s	- specimen strength ratio
S	- span
TT	- transition temperature
W	- specimen width
W/A	- energy absorbed divided by net (uncracked) section area -- measurement of energy value on precracked C_V specimen
z	- height of knife edges above specimen surface
ν	- Poisson's ratio
σ_N	- nominal stress; nominal strength
σ_{UTS}	- ultimate tensile strength
σ_Y	- yield strength
σ_{Yd}	- dynamic yield stress
ρ	- root radius

APPENDIX E

DYNAMIC TEAR TEST

The dynamic tear (DT)* test was evolved by the U.S. Navy in 1960 for the characterization of fracture toughness properties of ferrous and nonferrous structural metals. The initial version of the DT test featured a composite specimen utilizing a brittle cast bar welded to the tension edge of a three-point bend specimen of test material (Pellini et al., 1965). The composite specimens were fractured with a drop-weight machine of the type used for drop-weight nil-ductility transition temperature tests (ASTM E208) and the test was called the drop-weight-tear test (DWTT)**. Several specimens were required to establish the "fracture energy" of the test material for a specific temperature (i.e., via bracketing techniques). In 1963, an improved specimen design was evolved featuring an integral brittle weld for initiation of a sharp crack under impact loading. The crack starter weld was an electron beam weld embrittled by diffusing into it an embrittling element (e.g., titanium wire into steel) during the welding process. Also, in 1963 a large pendulum impact machine with direct energy readout was developed for testing 1-in.-thick DT specimens. These improvements simplified the test procedure and reduced the cost of testing by making it possible to determine the fracture toughness of material using one specimen for each temperature and metallurgical condition. In 1967, the procedure was renamed the dynamic tear test to reflect these improvements.

Since the 1-in. DT specimen required more metal than often was available in research studies or was practical for characterization for routine quality-control and specification requirements, a smaller 5/8-in.-thick DT specimen was developed about 1966 (Cooley and Lange, 1967). However, to permit using the test method by all research and engineering laboratories, the electron beam crack starter weld was replaced by a sharpened deep-machined notch. In addition,

---

* Terms are defined at the end of the appendix.

** Not to be confused with ASTM E436, "Standard Method for Drop-Weight Tear Tests of Ferritic Steels," which is a test for determining temperature transition characteristics based on fracture appearance, not on energy for fracture.

single- and double-pendulum (shock free) machines of 2,000-ft-lb capacity were designed, and the drop-weight machine was modified to provide for fracture energy measurements from single specimens.

Since the mid-1960s, the DT test has been used extensively by the Navy to characterize fracture resistance of low- to high-strength steels, titanium alloys, and aluminum alloys; in 1970, the DT test began replacing the Charpy V-notch test (C_V) as the basic fracture toughness test for characterizations, specification, and quality control of Navy ship and submarine hull materials. The DT test, based on the 5/8-in. DT specimen, was adopted as a Navy standard test method in 1973 (MIL-STD 1601[SHIPS]). In 1974, the ASTM E-24 Committee on Fracture Toughness Testing for Metallic Materials approved the DT test for publication in the 1975 ASTM Annual Standards' gray pages for information purposes.

Navy research in the late 1940s and early 1950s documented the failure of the C_V to provide an invariant method for characterization of the true transition temperature range features for a number of low- to high-strength steels. This led to the development and validation by 1953 of the drop-weight test (DWT) (Pellini, 1969 -- see appendix F). The DWT was designed specifically for the determination of the critical temperature below which the steel is brittle and above which the steel shifts to high levels of fracture toughness (high shelf) as a result of a change from brittle to ductile microfracturing mode (cleavage to microvoid coalescence). By 1962, it became evident that a new test was required for characterizing the properties of steels featuring low-shelf fracture toughness (i.e., low crack ductility due to mixed-mode microfracture processes). These include the high- and ultra-high-strength steels and steels of intermediate strength levels that featured pronounced "weak" fracture orientations. The dynamic tear test was developed initially to fill this need, and was extended quickly to titanium alloys and aluminum alloys when they became candidate hull materials, particularly for deep-diving submersibles. For these materials, in addition to the variant nature of the C_V test for defining fracture toughness with temperature, it was found that:

a. The fracture mode under impact loading was always ductile (micro-void coalescence) so that no abrupt rise in fracture toughness occurred over a small range of increase of temperature. The DWT-NDT test (ASTM E208) was not appropriate since the nil-ductility transition temperature is based on a change from brittle to ductile microfracture mode.

b. The C_V results did not correlate with results obtained in explosion tear test behavior of large plates containing through cracks of length twice the plate thickness; in fact, the difference between C_V values was small for large differences in fracture toughness performance obtained in the explosion tests (Goode and Huber, 1965; Pellini et al., 1965).

Structural metals exhibit a variety of fracture modes from plane strain (flat break), to elastic-plastic (mixed-mode), to full plastic (full slant), depending on the intrinsic fracture toughness of the material and severity of the imposed mechanical constraint. The DT test was developed as an engineering method to characterize the fracture resistance of metals for the full range of fracture modes. Conceptually, the DT test measures the total energy to fracture a specified cross-sectional area of metal for limit severity test conditions, and determines the characteristic fracture propagation mode. The energy expended in crack initiation from a sharp notch or brittle crack starter weld is small compared to the propagation energy for the elastic-plastic and full-plastic case. Limit severity conditions are imposed by incorporating into the DT specimen a sharp crack or notch of sufficient length to maximize the mechanical constraint for the thickness involved and the dynamic loading. In effect, the energy measured to fracture the specimen represents a definable lower limit of fracture toughness for the given specimen thickness, i.e., it cannot be less than that indicated for the limit conditions.

The DT test has been used primarily by the Navy for materials featuring elastic-plastic and plastic fracture properties. The engineering implications of the test data are translated to structural performance by analyzing the data in terms of fracture analysis diagram (FAD) procedures for the temperature transition steels, and ratio analysis diagram (RAD) procedures for the high-strength steels, titanium alloys, and aluminum. The RAD procedure for the high-strength materials was established in the late 1960s and early 1970s by the development of DT-K_{IC} test data correlations. This appendix is focused only on the DT test for the plane-strain condition. As such, this appendix generally relates to low- and intermediate-strength steels at temperatures below the nil-ductility transition temperature and for high-strength steels, titanium alloys, and aluminum alloys above 150, 120, and 40 ksi yield strength, respectively, depending on metal quality.

E.1   TEST SPECIMENS AND EQUIPMENT

A broad range of section thicknesses, 5/8 to 12 in., was investigated in full-thickness DT tests to provide an analysis for size effect since specimens more than 1 in. thick are not considered practical for general engineering use. The dimensions for the various DT specimen sizes tested are listed in Table E-1 for steels. For titanium and aluminum alloys, DT specimens up to 3 in. thick were tested.

The DT specimen contains a sharp notch or brittle crack starter weld of a depth considered adequate to provide maximum constraint at the notch or crack tip for specimens up to 3 in. thick. The specimen is impact-loaded in three-point bending at a velocity between 16-28 ft/sec. An important aspect of the test is that sufficient fracture length (W-a) is provided to permit the propagating crack to develop the characteristic fracture mode for the material.

TABLE E-1   Dimensions and Weights of Various Steel Specimens Used in the Dynamic Tear Test.

Specimen Designation	Thickness, B (in.)	Depth, W (in.)	Length, L (in.)	Span between Supports, S (in.)	Width** W-a (in.)	Weight (lb.)
5/8-in. DT*	0.625	1.62	7	6.5	1.125	2
1 in.	1	4.75	18	16	3.00	24
2 in.	2	8	28	26	5.00	127
3 in.	3	8	28	26	5.00	190
6 in.	6	12	62	58	9.00	1,220
12 in.	12	15	90	84	12.00	4,580

NOTE: Data from Pellini, 1969.

* Deep-machined notch having tip sharpened by pressed knife edge.
** Net cross section (fracture length).

The 5/8-in. DT specimen provides the same characterization capability as the 1-in. specimen for both the sharpened deep-machined notch as well as electron beam crack starter weld. However, to provide for general engineering usage of the DT method, the ASTM practice relates to the sharpened deep-machined notch configuration, limiting the hardness of the material that can be tested to Rockwell C 36 (HR_c 36) or less. The limitation is due to the inability of a notch-sharpening knife-edge blade of HR_c 60 to press the notch root. The Navy specification standard encompasses both the notch and electron beam embrittled weld method; it is not limited in this way.

Correlations of the 5/8-in. DT with the 1-in. DT test are shown for low- to ultrahigh-strength steels in Figure E-1 and for aluminum alloys in Figure E-2. Similar correlation attempts for titanium alloys (Figure E-3) indicate that correspondence of the 5/8- and 1-in. DT tests may depend on the specific alloy (Judy and Goode, 1973).

Pendulum and drop-weight test machines basically provide the impact loading to the DT specimen. The pendulum-type machines consist of a single pendulum and stationary specimen anvil, similar to a Charpy machine, or two opposed pendulums (swinging tup and swinging anvil) matched for centers of percussion to eliminate the shock transmitted to the base mounting. DT energy is determined with the pendulum machines by computing the potential energy associated with the initial and final pendulum positions (similar to C_V). A digital readout system also can be added to indicate fracture energy directly.

SYMBOL	MATERIAL	YIELD STRENGTH (ksi)
○	A201B	48
□	A302B	56
△	A515 GRADE 55	32
▽	A515 GRADE 60	47
⬦	A533B CLASS 2	80
◊	A542 CLASS 2	84
⊙	HY-80 (VAC.)	82
○	HY-130(E.F.-AIR)	136
⬠	HY-130 (VIM)	146
⊖	A533B HSST 1	70

SYMBOL	MATERIAL	YIELD STRENGTH (ksi)
◆	9 Ni-4 Co-0.25C	180
■	9 Ni-4 Co-0.20C	183
⬤	9 Ni-4 Co-WELD	192
✳	9 Ni-4 Co-WELD	179
✺	9 Ni-4 Co-WELD	188
▲	9 Ni-4 Co-WELD	165
⬥	9 Ni-4 Co-WELD	181
▼	9 Ni-4 Co-WELD	175
●	10 Ni-8 Co-Cr-Mo	181
◆	10 Ni-8 Co-Cr-Mo	181
●	18 Ni-MARAGE	221
✳	18 Ni-MARAGE	249
●	18 Ni-MARAGE	260
+	18 Ni-MARAGE	260

FIGURE E-1   Relationship between 5/8- and 1-in. Dynamic Tear Tests for High- and Ultrahigh-Strength Steels (Judy and Goode, 1973).

For the vertical drop-weight machine, DT energy is obtained by use of calibrated absorption blocks to measure the residual energy of the weight after specimen fracture. However, a strain-gauged tup coupled with suitable instrumentation also is used to obtain a force-time record from which DT energy can be determined (Lange and Loss, 1966).
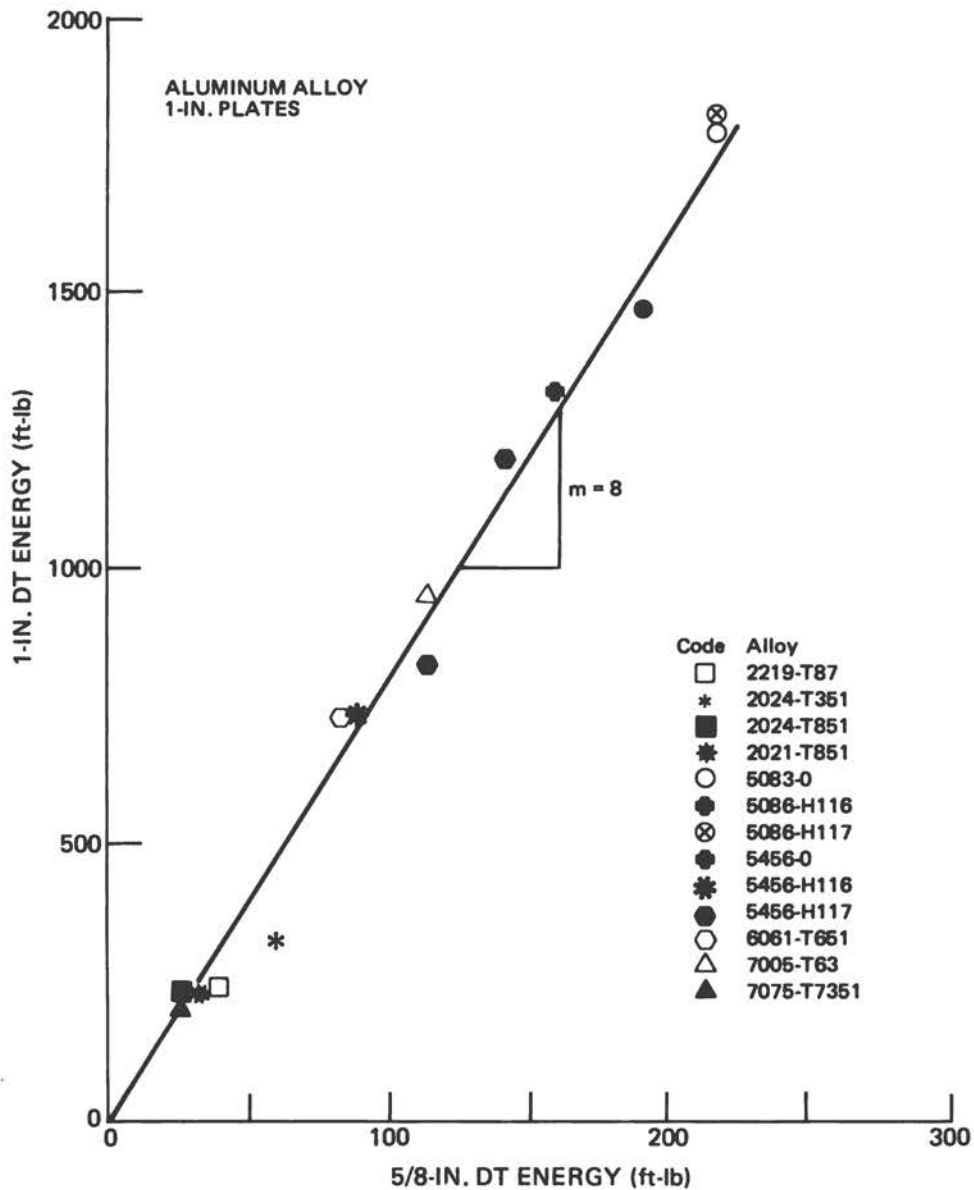
FIGURE E-2 Relationship between 5/8- and 1-in. Dynamic Tear Tests for High-Strength Aluminum Alloys (Judy and Goode, 1972).

For 1-in. DT specimens, a capacity of 10,000 ft-lb is adequate for evaluating the full range of fracture resistance of all metals. Single-pendulum machines and drop-weight machines are used for tests of these larger specimens. For specimens larger than 1 in., impact machines with very high capacities are required; for specimens 3 in. to 12 in. thick, drop-weight machines of 40,000 and 800,000 ft-lb capacity, respectively, have been used.
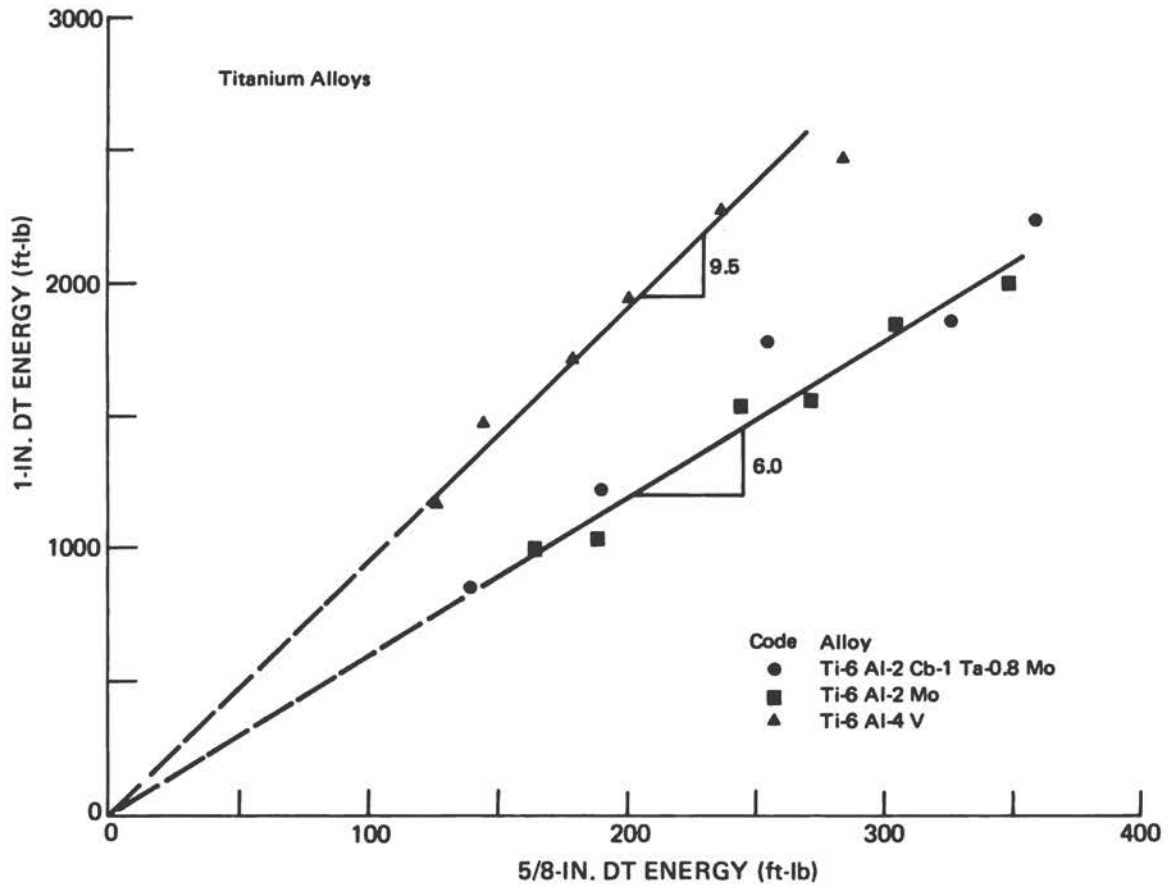
FIGURE E-3   Relationships between 5/8- and 1-in. Dynamic Tear Tests for
Specific High-Strength Titanium Alloys (Judy and Goode, 1973).

E.2   PARAMETERS DERIVED FROM THE DYNAMIC TEAR TEST

The basic parameter obtained in the DT test is the total energy required
to fracture the net cross section (width minus crack depth, W-a) of the DT
specimen. The tests are run over a range of temperatures to define DT tempera-
ture transition characteristics, particularly for low- and intermediate-strength
steels or at a single temperature (minimum service temperature), a procedure
more commonly used for high-strength steels and titanium and aluminum alloys.
Secondary parameters that can be determined as desired are the macroscopic
fracture appearance, percent slant versus flat fracture, and percent contraction
or lateral expansion.

E.3   CORRELATIONS OF DYNAMIC TEAR WITH K_{Ic} VALUES

E.3.1 Steels

The DT indexing to K_{Ic} was initiated for steels in 1967 (Goode et al., 1967) and reported in 1969 (Freed and Goode, 1969) per ASTM E399. Single-edge notched (SEN) tensile specimens were used to determine the K_{Ic} values. The SEN specimens and experimental compliance calibration for calculation of K_{Ic} were modeled on Sullivan's work (Sullivan, 1964). In both the DT and K_{Ic} tests, the specimens were 1 in. thick. The K_{Ic} specimens had a/W = 0.32 and W = 5.0 in. and were side-grooved to a depth of 5 percent of the thickness on each side for all but the highest strength (lowest toughness) materials. The yield strength and fracture toughness properties of the high-strength steels are shown in Table E-2.

The correlation of K_{Ic} with DT test energy that was obtained for steels is shown in Figure E-4. Among the criteria used to determine the validity of the K_{Ic} values was the requirement that the specimen thickness, $B \geq 2.5(K_{Ic}/\sigma_{YS})^2$. On this basis alone, the data points corresponding to K_{Ic} values of 100 ksi $\sqrt{in}$. and below are valid. Consideration of E399-70T and later procedures with respect to the four data points in the valid region (Figure E-4) indicate that they still should be valid.

No direct correlation of DT with K_{Ic} for high- or ultrahigh-strength steels thicker than 1 in. has been conducted.

The DT-K_{Ic} correlation for a variety of high-strength steel cast material (Steel Foundry Facts, 1973) using the deep-notched 5/8-in. DT specimen for the lower strength steels and a fatigue crack starter for those above 150 ksi yield strength is shown in Figure E-5. Superimposed on the data points is the DT-K_{Ic} relation of Figure E-4, corrected for the 5/8-in. thickness. The K_{Ic} tests involved 3-in. compact tension specimens and were conducted in conformance with ASTM E399-70T procedures. Each data point represents one K_{Ic} test and duplicate DT tests. Only point no. 3 was considered invalid according to the above ASTM E399 procedure; however, points 25 and 33 obviously need verification. Material for duplicate K_{Ic} tests was not available.

E.3.2 Titanium Alloys

The DT-K_{Ic} relationship has been established for high-strength titanium alloys for section sizes up to 3 in. (Judy et al., 1973). The K_{Ic} specimens were three-point edge-notched bend specimens of B = 3 in., and the 1-in. DT specimens were cut from surface and centerline locations in the plate. An electron beam crack starter weld, embrittled by the diffusion of iron into the weld during welding, provided the deep sharp crack in the DT specimen. The mechanical property data for the 3-in.-thick plane-strain material are given in Table E-3. The K_{Ic} values were determined by averaging the results from two to four specimens and are valid according to ASTM E399-70T procedures.

TABLE E-2 Plane-Strain Fracture Toughness Data for High-Strength Steels Derived from Single-Edge-Notched Specimens.

Alloy Designation	Fracture Direction	YS (ksi)	Dynamic Tear Test Energy (ft-lb)	Number of Specimens	K_{Ic} Range (ksi $\sqrt{in}$.)	Average K_{Ic} (ksi $\sqrt{in}$.)
9-4-0.25C	RW	180.0	1,844	2	158-165	158
	WR	180.3	1,295	2	137-138	135
	RW	--	1,996	2	155-156	151
	WR	183.2	2,000	2	152-155	149
12Ni - MA	RW	--	--	1	166	161
	WR	185.3	--	2	116-124	118
	WR	176.3	--	3	131-143	134
	RW	178.6	--	1	153	148
	WR	--	--	2	119-130	124
	WR	178.0	--	3	131-137	132
	WR	171.2	744	2	100	98
	WR	180.7	1,630	2	125-126	123
9-4-0.25C	WR	176.3	2,112	3	163-166	160
		186.1	1,280	4	150-156	149
12Ni - MA	WR	176.8	--	3	198-206	192
		174.9	4,340	1	(252)	(235)
		177.3	3,251	3	201-213	197
		171.1	3,538	1	211	200
		185.5	2,271	1	155	150
		189.4	2,176	2	184-192	182
9-4-0.25C	WR	179.2	1,996	2	158-169	158
		169.7	2,026	3	167-175	165
		180.2	1,692	3	159-166	158
		168.3	2,186	3	164-176	161
H-57	WR	176.6	593	3	89-91	88
D-63A	RW	229.5	400-500	1	70	69
D-63B	RW	234.5	400-500	2	75-79	76
D6AC	--	212*	--	1	96	95
J-79	WR	144	--	2	252	233

NOTE: Data from Goode, 1974.   * This value represents WR fracture direction.
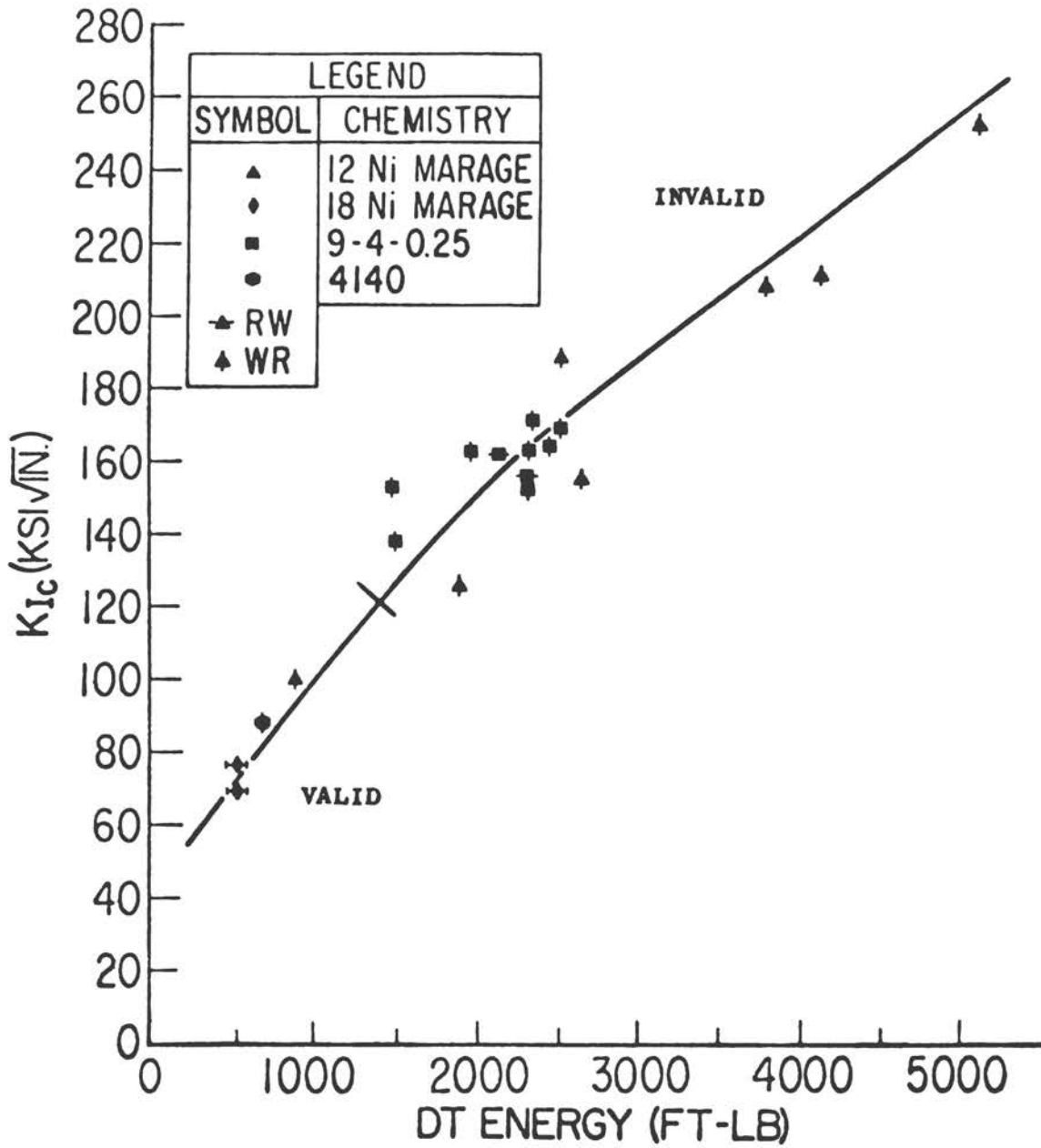
FIGURE E-4 DT-K_{Ic} Relationship for High- and Ultrahigh-Strength Steel
Plate (Goode, 1974).

TABLE E-3 Mechanical Properties of 3-in.-thick Titanium Alloy Plates --
Plane Strain.

| Nominal Composition | Fracture Resistance | | | | | | Tensile Yield Strength (ksi) | | |
| | 1-in. DT Energy (ft-lb) | | | Avg. K_{Ic} (ksi $\sqrt{in.}$) | K_{Ic} Range (ksi $\sqrt{in.}$) | Number of Specimens | Surface | Center | Average |
	Surface	Center	Average						
Ti-6Al-4V-2Mo	472	714	593	69	66-71	3	151.7	139.9	147.8
Ti-6Al-4V	587	699	643	89	88-91	3	136.1	130.4	134.2
Ti-6Al-4V	986	1,120	1,053	100	96-103	4	112.7	112.6	112.7
Ti-6Al-4V	836	1,205	1,020	101	99-105	4	125.6	122.2	124.4
Ti-6Al-2Mo	1,166	1,320	1,243	110	107-114	2	113.3	115.0	113.9
Ti-6Al-4V-1Mo	1,033	1,349	1,191	117	111-118	4	113.1	112.1	112.8
Ti-5Al-2V-2Mo-2Sn	1,250	1,330	1,267	117	116-118	4	115.4	111.3	114.0
Ti-6Al-2Cb-1Ta-1.2Mo	1,352	1,534	1,443	123	115-131	3	114.8	114.5	114.7
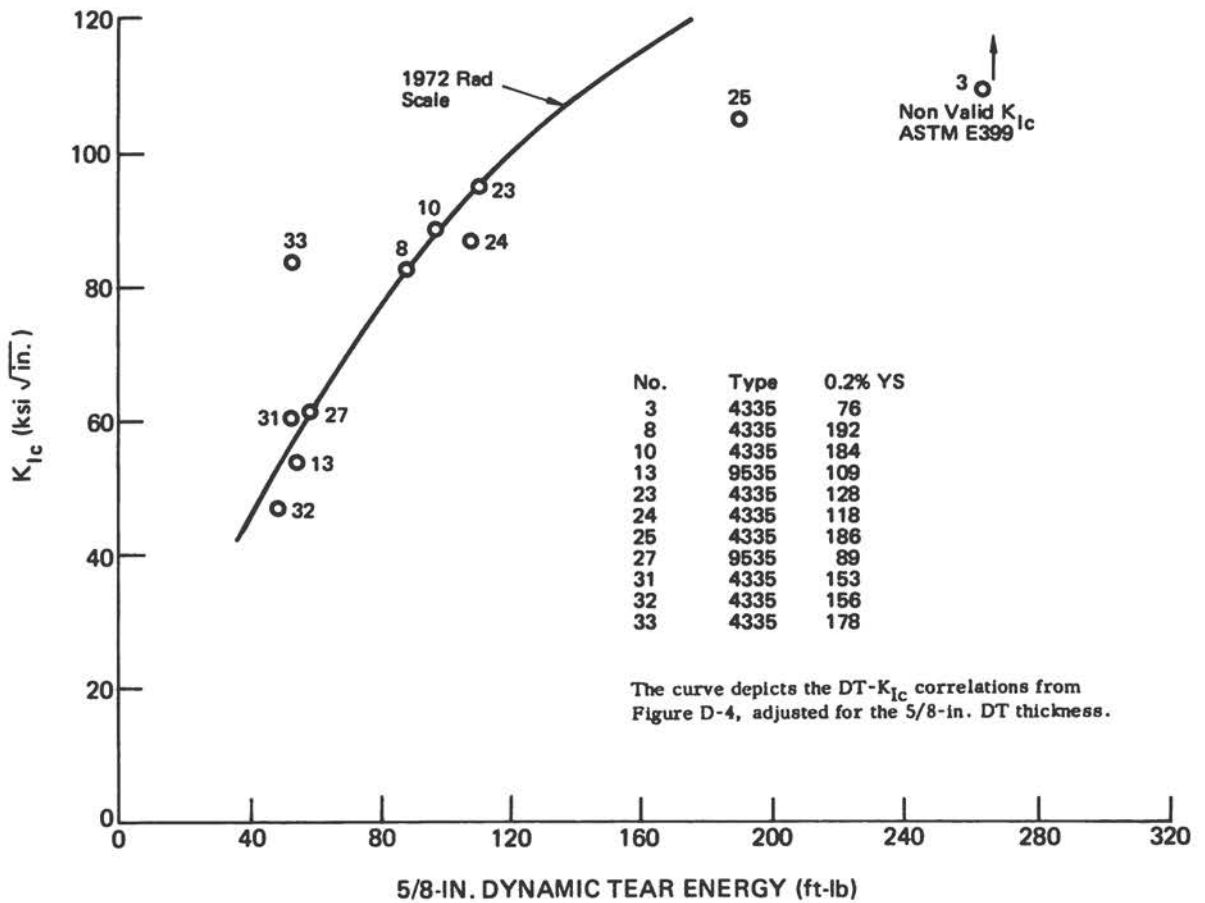
FIGURE E-5 DT-K_{Ic} Correlation for High-Strength Steel Castings (Goode, 1974).

The DT-K_{Ic} correlation for high-strength titanium alloys is shown in Figure E-6. Included on the plot are data points for 1-in.-thick K_{Ic} tests involving SEN and four-point notch bend specimens (Freed and Goode, 1969). For the four-point notch bend specimen, the parameters were W = 2.5 in., B = 1 in., with S_1 = 20 in. (notch edge), and S_2 = 5 in. centered on the plane of the notch. The notch depth was 0.50 in. with a further extension of 0.10 in. by fatigue. The mechanical property data for these earlier studies are given in Table E-4. Much of the data scatter is attributed to the variability of properties from point to point in the plate material and to through-thickness gradients in fracture properties (see Table E-3).
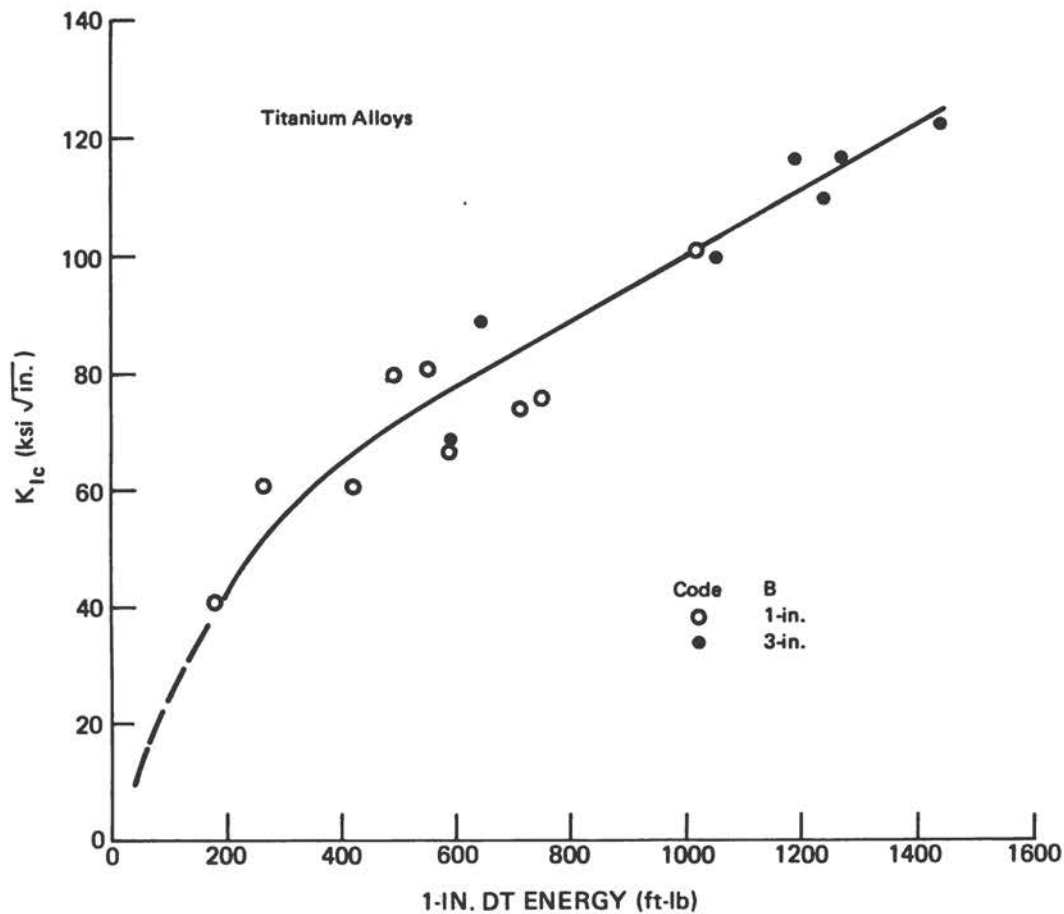
FIGURE E-6 DT-K_{Ic} Relationship between Dynamic Tear Tests and Full-Thickness K_{Ic} Tests for 1- and 3-in.-thick Plate (Judy et al., 1973).

TABLE E-4 Plane-Strain Toughness Data for Titanium Alloys.

Alloy Designation	Fracture Direction	Types of Specimens	Number of Specimens	YS (ksi)	K_{Ic}* Range (ksi √in.)	Avg.* K_{Ic} (ksi √in.)
T-20 (Ti-6Al-4Sn-1V)	RW	SEN	6	127.3	77-92	85
T-21 (Ti-6Al-6V-2.5Sn)	WR	SEN	2	152.0	59-63	61
T-21A (Ti-6Al-6V-2.5Sn)	RW	SEN	2	166.5	57-62	60
T-21B (Ti-6Al-6V-2.5Sn)	RW	SEN	1	129.7	81	81
	WR	SEN	1	135.6	76	76
T-21C (Ti-6Al-6V-2.5Sn)	RW	SEN	1	137.2	80	80
	WR	SEN	2	137.2	74	74
T-21D (Ti-6Al-6V-2.5Sn)	RW	SEN	2	186.0	32-35	34
T-23 (Ti-8Al-2Cb-1Ta)	RW	SEN**	--	112.0	--	115
T-27A (Ti-6Al-4V)	RW	SEN	8	132.5	101-112	108
	WR	SEN	4	140.1	104-114	106
T-36 Ti-6.5Al-5Zr-1V)	WR	SEN	3	124.5	91-100	96
T-55A (Ti-6Al-4Zr-2Mo)	WR	SEN	3			
		NB	2	135.7	98-121	113
T-55B (Ti-6Al-4Zr-2Mo)	WR	SEN	4	132.0	92-102	97
		NB	2			
T-67 (Ti-6Al-4V-2Sn)	RW	SEN	4	115.8	98-106	101
T-67A (Ti-6Al-4V-2Sn)	RW	SEN	4	129.8	71-90	82
		NB	1			
T-67B (Ti-6Al-4V-2Sn)	RW	SEN	4	122.0	95-112	101
		NB	1			
T-68A (Ti-6Al-4Zr-2Sn-0.5Mo-0.5V)	RW	SEN	4	117.5	117-124	119
T-68B (Ti-6Al-4Zr-2Sn-0.5Mo-0.5V)	RW	SEN	4	119.2	100-116	110
T-68D (Ti-6Al-4Zr-2Sn-0.5Mo-0.5V)	RW	SEN	3	121.3	124-131	126
T-68E (Ti-6Al-4Zr-2Sn-0.5Mo-0.5V)	RW	SEN	1	121.5	121	121

NOTE: Data from Goode, 1974.

* Calculated without plastic-zone correction factor.

** Specimens of dimensions 1.5 by 0.25 by 3.3 in. (width by thickness by length) were tested by Dr. J. Krafft, Mechanics Division, Naval Research Laboratories.

E.3.3 Aluminum Alloys

The determination of the relation of DT to K_{Ic} for aluminum alloys was initiated in 1968 (Freed et al., 1971). The K_{Ic} values were determined using the single-edge-notch tension specimen configuration described above. The specimens were nominally 1 in. thick and represented the full-plate thickness. A three-point and a four-point bend specimen of square cross section were used to provide additional data for each alloy. The 1 in. DT specimen contained an electron beam crack starter weld embrittled by diffusion of bronze during welding. The fracture toughness data are shown in Table E-5.

The DT-K_{Ic} correlation for aluminum alloys of 1-in. section size is shown in Figure E-7. An additional data point for K_{Ic} tests of 3-in.-thick three-point bend specimens of 7005-T6351 (Nelson and Kaufman, 1972) and a 1-in. DT cut from the 3-in. section also are included. This point meets ASTM E399-72 requirements for validity and tends to confirm the DT-K_{Ic} relationship established for the 1-in. K_{Ic} data.
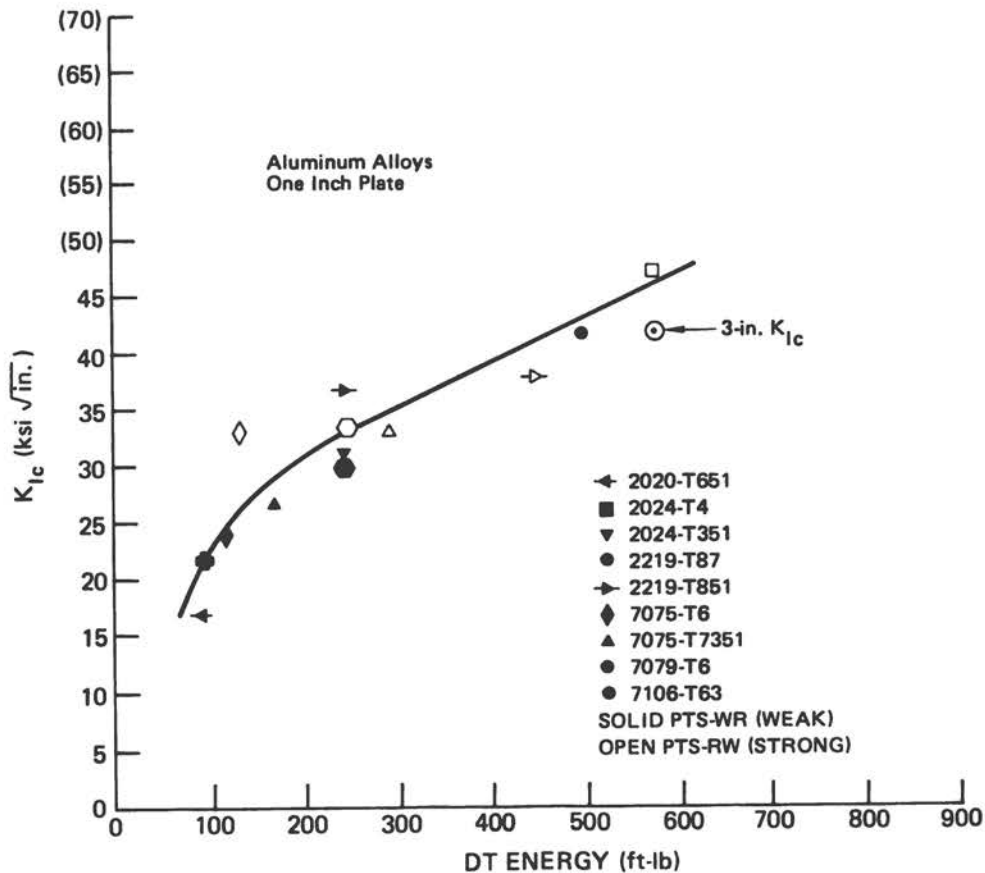
FIGURE E-7   DT-K_{Ic} Relationship between 1-in. Dynamic Tear Tests and Full-Thickness K_{Ic} Tests of 1- and 3-in.-thick Plate (Goode, 1974).

TABLE E-5 Plane-Strain Fracture Toughness Data.

Alloy	Fracture Direction	Types of Specimens	Number of Specimens	YS (ksi)	K_{Ic} Range (ksi $\sqrt{in.}$)	Avg. K_{Ic} (ksi $\sqrt{in.}$)
2020-T651	WR	SEN	1	76.3	16.4	16.4
2024-T4	RW	SEN	3	48.1	45.1-46.8	45.8
2024-T351	WR	SEN	4	43.9	30.2-30.7	30.5
2219-T87	RW	SEN	2	57.9	31.6-34.4	33.0
	WR	SEN	2	55.2	29.3-30.4	29.9
2219-T851	RW	SEN	4	59.3	34.9-37.2	36.0
		NB-3*	3		35.1-40.8	38.3
	WR	SEN	8	58.4	32.4-37.8	37.3
		NB-4*	4		35.2-35.9	35.5
7075-T6	RW	SEN	6	78.5	31.6-33.5	32.9
	WR	SEN	1	77.8	23.9	23.9
7075-T7351	RW	SEN	4	66.7	30.3-33.4	32.5
	WR	SEN	4	64.9	23.4-26.8	26.7
		NB-4*	4		25.1-27.2	26.1
7079-T6	WR	SEN	1	74.9	21.7	21.7
7106-T63	WR	SEN	3	52.5	40.3-41.6	40.8

NOTE: Data from Goode, 1974.

*NB-3, NB-4: NB specimens, three-point or four-point loaded.

E.3.4 Precision of Correlation

Predictions of K_{Ic} values from DT energy measurements can be made well within $\pm$ 15 ksi $\sqrt{in.}$ using the scales of the ratio analysis diagram (RAD) (Pellini, 1972; National Materials Advisory Board, 1973). An example of the significance of this degree of correspondence between DT energy and K_{Ic} values is depicted by the example in Figure E-8 comparing the DT and K_{Ic} data on the titanium RAD for a 3-in. section. The plane-strain limit $[B \geq 2.5 (K_{Ic}/\sigma_{ys})^2]$ and general yield limit $[B \geq 1.0 (K_{Ic}/\sigma_{ys})^2]$ are indicated.
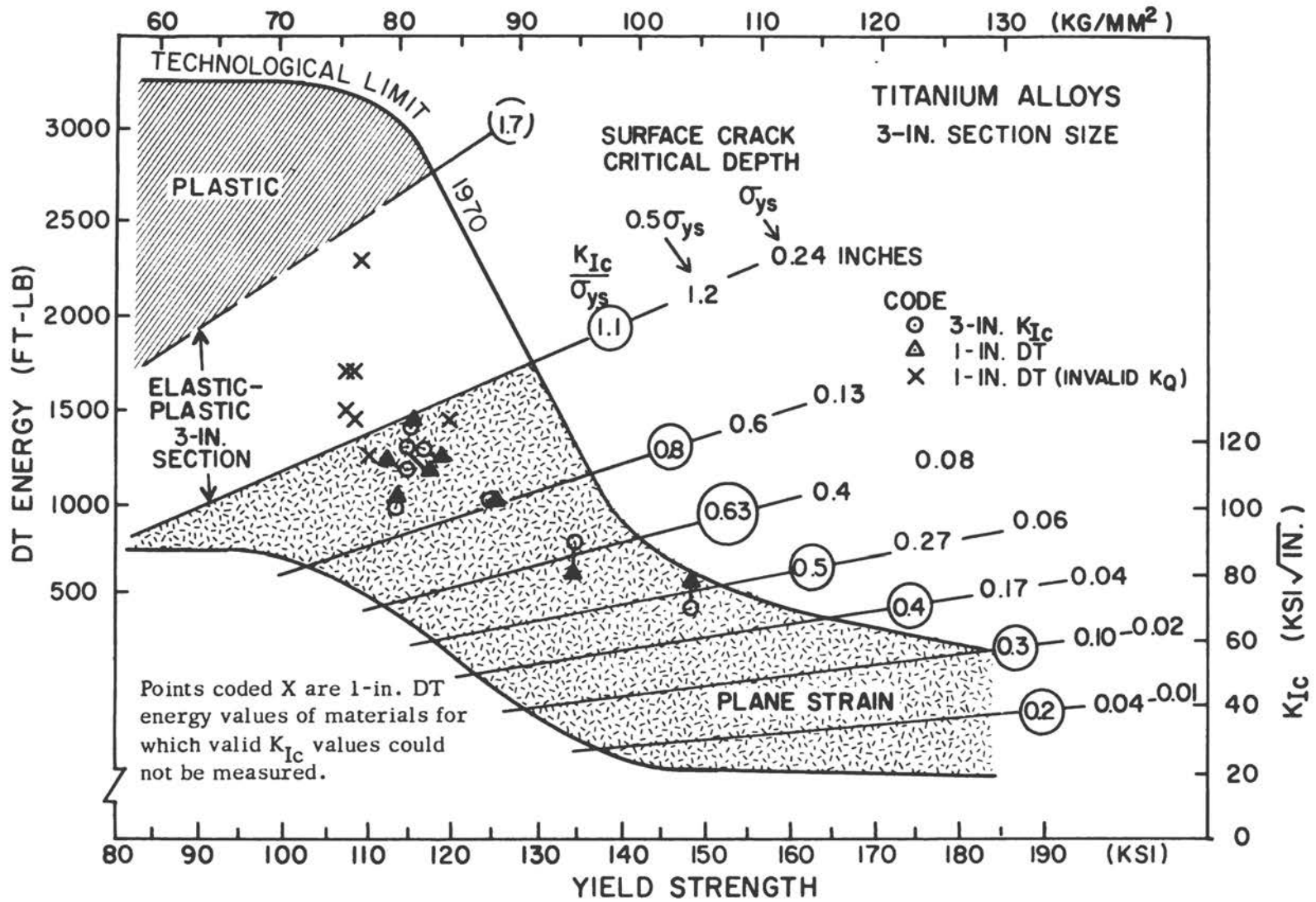
FIGURE E-8   Illustration of K_{Ic} Indexing Capability of the Dynamic Tear Test (Judy et al., 1973).

The closeness of the K_{Ic} and DT data within the plane-strain region is sufficient to predict from DT energy values K_{Ic}/σ_{ys} ratio values to within about ± 0.05 ratio. For DT data falling close to the plane-strain limit line (1.1 K_{Ic}/σ_{ys} ratio for a 3-in. section), the B thickness requirement for plane strain is met, but invalid K_{Ic} test results may result due to secondary considerations (e.g., not meeting the $P_{max}/P_Q \leq 1.10$ load requirement of ASTM E399-72 (ASTM, 1973).

E.4 RELATION OF DYNAMIC TEAR TO NIL-DUCTILITY TRANSITION TEMPERATURE FOR LOW- AND INTERMEDIATE-STRENGTH STEELS

The rise of the DT energy curve with temperature is relatable to the nil-ductility transition temperature (NDT) and to the Robertson crack arrest temperature (CAT) curve for low- and intermediate-strength steels (Pellini et al., 1965; Pellini and Loss, 1969; Hawthorne and Loss, 1974). The nil-ductility transition temperature, determined by ASTM E208-69 (ASTM 1973) has been shown to correspond to the transition of brittle (cleavage) to mixed mode (cleavage and microvoid coalescence) fracture which always is located at the toe region of the DT versus temperature curves. Examples are shown in Figure E-9 for an A201B steel, in Figure E-10 for a series of quench and tempered steels and a carbon steel, and in Figure E-11 for 2-1/4 percent chromium-1 percent molybdenum steel, for which a comparison of dynamic tear and nil-ductility transition temperature to C_V energy is provided. To date, there are no instances of the DT transition occurring at temperatures below that indicated by NDT procedures.

Considerable work has been done at the Naval Research Laboratory concerning the relationships for temperature transition curves established using K_{Ic} (slow and fast loading) and DT test methods. Although the maximum constraint conditions are imposed for the section size of all specimens, the K_{Ic} transition curves occur at lower temperatures compared to NDT and DT transition due to loading rate effects. The Naval Research Laboratory references cover in detail the relationship between K_{Ic}, K_{Id}, NDT, and DT energy transitions for steels and their relationships to NDT and the fracture analysis diagram (FAD) (Goode, 1972, 1974; Goode and Huber, 1965; Goode et al., 1967; Judy and Goode, April 1973, November 1973; Judy et al., 1973; Pellini, 1967, 1968, 1969, 1973; Pellini et al., 1965; Pellini and Puzak, 1963, 1964).

E.5 OTHER FACTORS

E.5.1 Cost and Complexity

The cost of preparing 5/8-in. DT specimens is equivalent to the cost of preparing C_V specimens (ASTM E23-72). The dimensional tolerances are such that standard machine shop practices can be used; if careful cutting of the
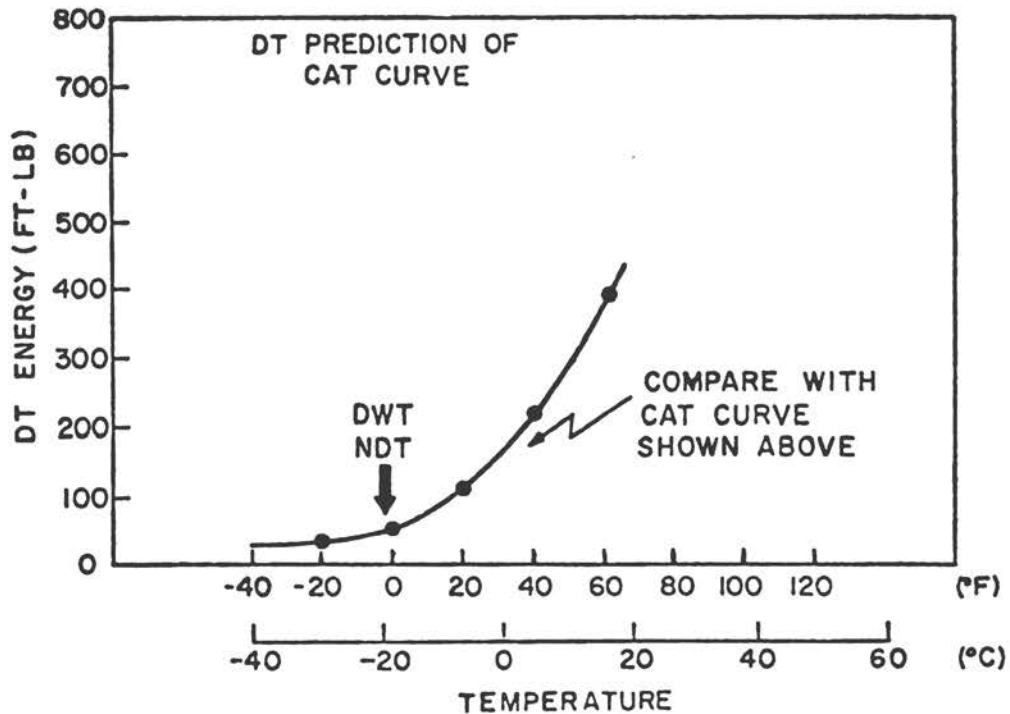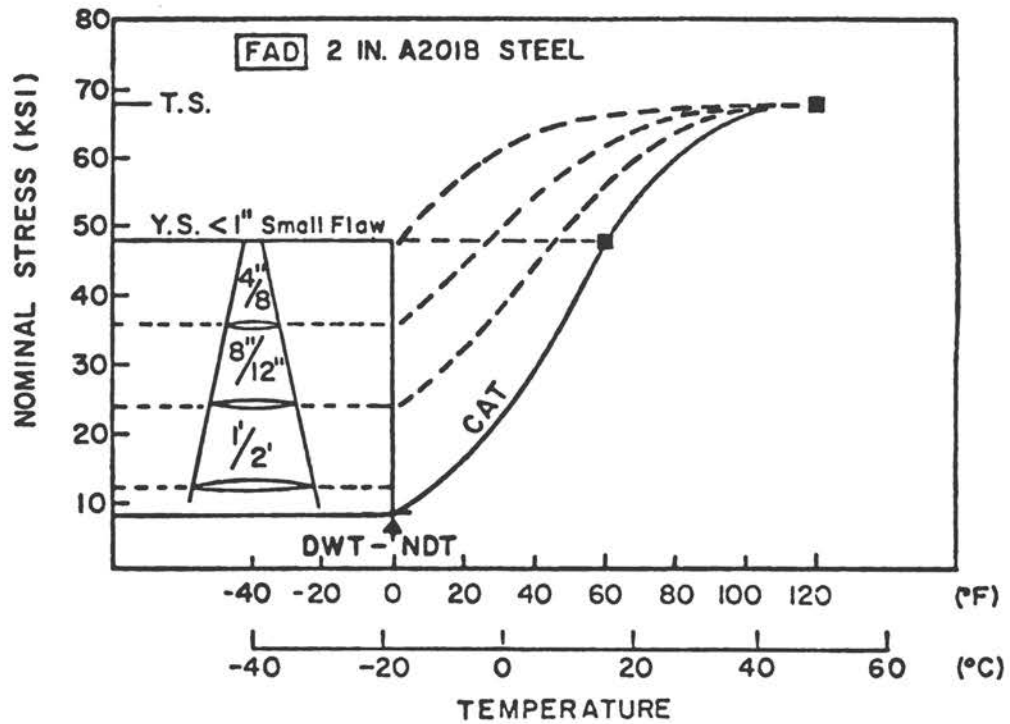
NOTE: DT energy rise corresponds to the crack-arrest temperature curve defined by the fracture analysis diagram.

FIGURE E-9   Illustration of Nil-Ductility Transition Temperature Indexed to Toe of 0.625-in. Dynamic Tear Temperature Transition Curve for a 2-in.-thick A201B Steel (Goode, 1974).
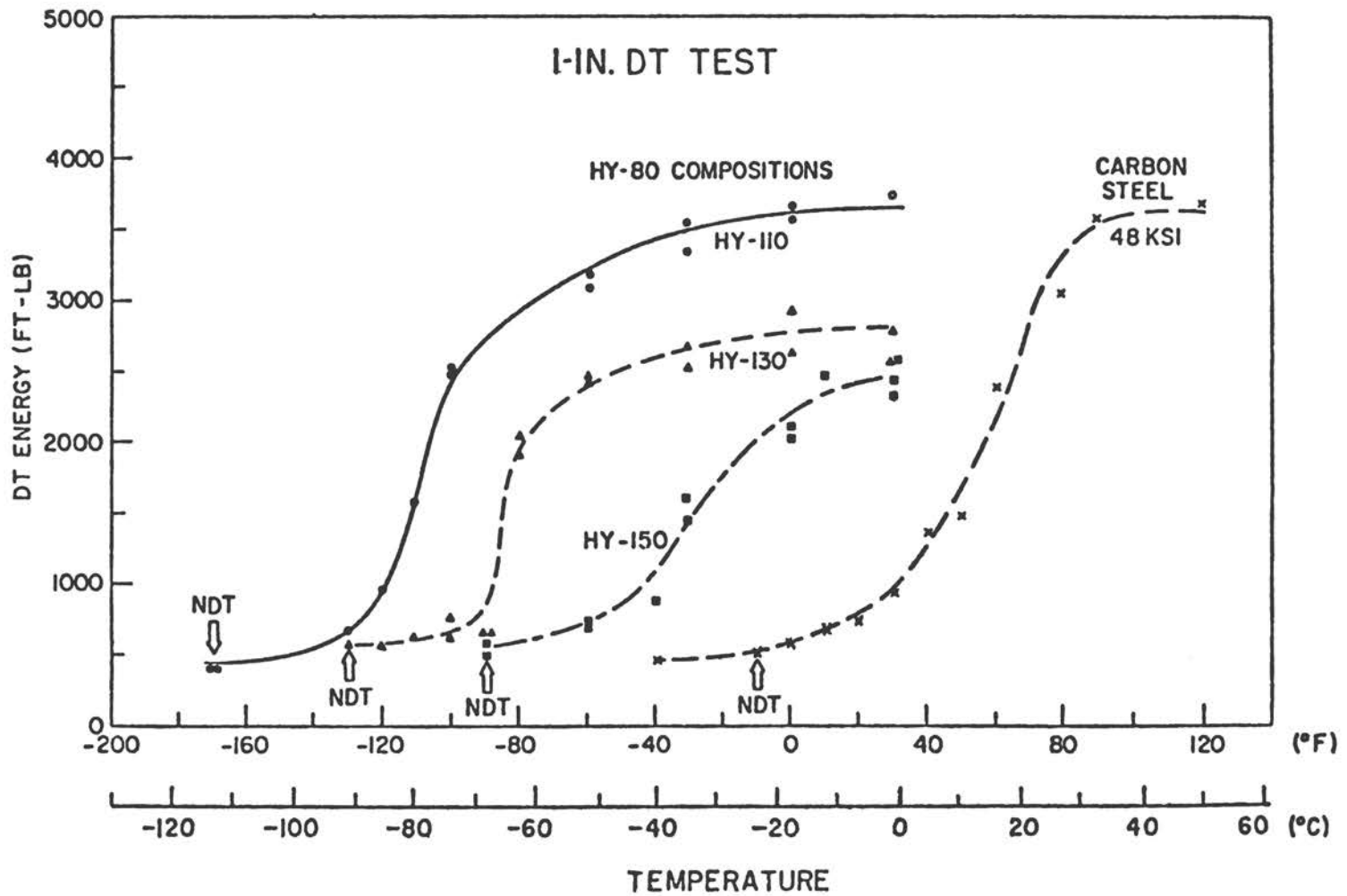
NOTE: DT energy transition curves showing DWT-NDT temperatures are always located at the toe of the respective DT curves.

FIGURE E-10   Representative DT Energy Transition Curves Showing DWT-NDT Temperatures (Goode, 1974).
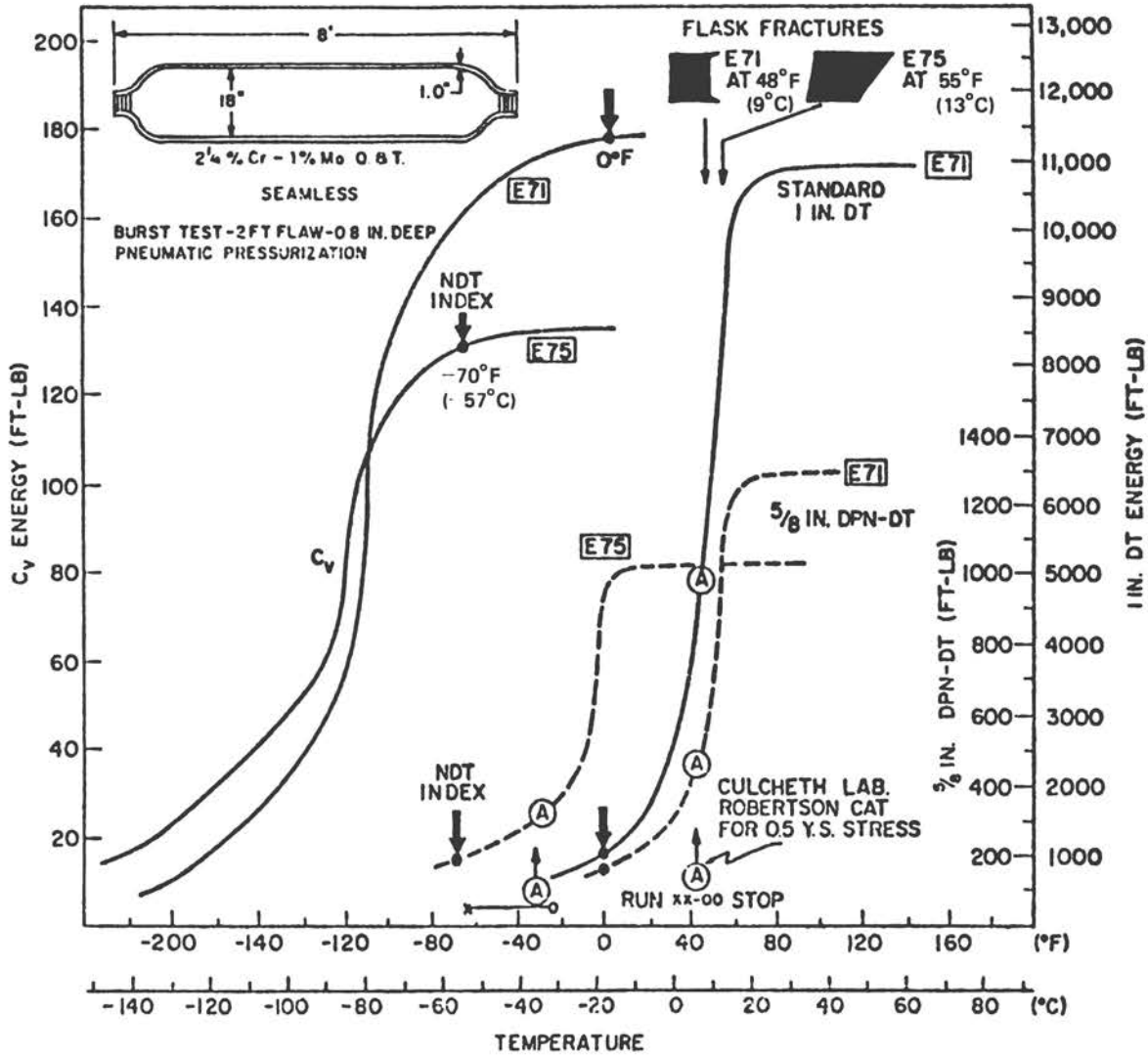
NOTE: This illustration shows complete lack of C_V correspondence to NDT and DT characterization for this steel.

FIGURE E-11   Example of DT Energy Transition Curves for 2-1/4 Percent Chromium-1 Percent Molybdenum Quenched and Tempered Steel Showing DWT-NDT Indexing to Toe of Transition Curves (Pellini, 1968).

specimen blanks is exercised, only machining of the notch is required. The greater depth of the notch and sharper notch root radius (0.005-in. maximum), compared to the C_V specimen, represents a greater portion of the specimen preparation costs. Sharpening of the machined notch tips requires only a sharp hardened steel blade pressed into the notch tip a controlled amount, normally 0.009 in., with a standard metallographic press.

The electron beam embrittled crack starter weld for both 5/8-in. and 1-in. DT specimens represents a cost savings over a fatigue-cracked notch, particularly for the larger specimens. However, the high capital investment cost for an electron beam welder generally makes this approach prohibitive.

Equipment and controls for heating or cooling specimens to specified test temperatures are similar to that for C_V specimens. Since the DT specimen involves a larger mass of material, slightly longer times are required for equalization of specimen temperature.

The cost of basic DT test machines can vary widely depending on whether purchased from commercial sources or fabricated by the user. Commercial drop-weight machines designed for 5/8-in. DT testing cost approximately two to three times that of a standard Charpy impact machine. Drop-weight machines for testing of the 1-in. DT specimen generally are not available from commercial sources. The double-pendulum machines for 5/8-in. DT testing are approximately four times costlier than standard Charpy machines if purchased commercially; single-pendulum machines for both 5/8-in. and 1-in. DT tests are not generally available commercially, but detailed engineering drawings that permit fabrication by the user are available at no cost from the Naval Research Laboratory.

E.5.2 Experience with the Dynamic Tear Test

In addition to being the principal characterization, specification, and quality-control test for advanced Navy hull and hydrofoil materials programs, the DT test also has been used for characterization and failure analysis purposes in connection with bridge, pressure vessel (nuclear and non-nuclear), aircraft, ship (ABS grades), and rotor steels as well as in titanium and aluminum alloy development programs for aircraft applications.

Without exception, the DT test faithfully reproduces the characteristic fracture mode and has predicted accurately the performance (percent surface strain) experienced in a large number of explosion bulge and explosion tear tests of cracked plates and welds, as well as service failures of large structures.

E.5.3 Orientation Capability

The DT test can be used for all fracture orientations (Goode, 1972) with the specific orientations limited according to the following minimum plate (or weld) thickness:

Orientation	Thickness (in.)
T-L and L-T	5/8
T-S and L-S	1-5/8
S-L and S-T	2 to 3*

E-6 Conclusion and Recommendations

Conclusion -- For some materials, a relationship exists between the K_{Ic} and DT test methods. Although these relationships for steels, titanium, and aluminum initially were evolved using nonstandard K_{Ic} methods as defined by ASTM E399, validation with standard K_{Ic} tests and analysis of service failures have shown them to be sufficiently accurate for engineering analysis of flaw size/stress level requirements for fracture in terms of RAD procedures (Pellini, 1972; National Materials Advisory Board, 1973). In this respect, the DT test appears to be a promising candidate method as a rapid, inexpensive quality control test for aircraft metals.

Recommendations -- To firmly establish the applicability of using the DT test for assuring adequate screening of material featuring K_{Ic} values lower than a specified minimum, the following should be resolved:

1. A more complete validation of the accuracy of the DT-K_{Ic} correlations is required, particularly for steels and aluminum alloys of high K_{Ic} properties requiring B = 3 in. Judicious selection of materials covering the strength (i.e., K_{Ic} range of interest) would obviate the need for large numbers of tests. The validation should be based on MIL-STD 1601 or proposed ASTM 5/8-in. DT test to conform to Standard Practice requirements.

2. The precision of the DT-K_{Ic} correlations for predicting K_{Ic} values from DT energy measurements requires finer definition to establish the probability (statistical) of screening out acceptable material. This aspect could be combined with the research directed to the previous recommendation.

---

* Requires use of extension tabs welded to test sample to provide for test span length, otherwise, 7-in. thickness is required.

3. A procedure for initiating a crack in the DT specimen must be developed for testing those materials of hardness greater than $HR_c = 36$. The use of the sharpened machined notch for the crack initiation in the DT specimen has not posed difficulties for the nonferrous metal alloys; however, its use is restricted to steels of hardness below HR_c 36. The brittle electron beam crack starter weld has no material limitation but the welding method is not available for general use. The use of fatigue-cracked specimens (as mentioned earlier for the cast steels) following ASTM E399 procedures for producing the fatigue cracks is feasible but increases the overall cost of the DT test; this increase in cost could be minimized by "gang" fatiguing a number of DT specimens using a multispecimen fatigue-cracking machine (Krafft and Gray, 1971) of which a version is commercially available for fatiguing C_V specimens.

E.7 SUMMARY

The dynamic tear test was developed by the U.S. Navy for characterizing the fracture resistance of steels, titanium alloys, and aluminum alloys for the full range of strength level and fracture toughness. Correlations of DT energy values with K_{Ic} results have been established for these materials in the high-strength range; however, these correlations, developed during the late 1960s, are based primarily on K_{Ic} data obtained with single-edge-notch tension specimens that do not conform to current ASTM standard K_{Ic} test methods and 1-in. DT test results. More recent results (of limited number) using ASTM standard K_{Ic} methods generally confirm the accuracy of the earlier results for thicknesses up to 3 inches.

The 5/8-in. DT test is covered by a military specification (MIL-STD-1601) and a Proposed Method has been published in the 1975 Annual ASTM Standards, part 10.

The DT test appears promising as a rapid, inexpensive quality-control test for aircraft-grade metal alloys. To this end, this appendix discussed further research needed to (a) verify the accuracy of the DT-K_{Ic} correlations and establish more exactly the precision for predicting K_{Ic} values from 5/8-in. DT test results, and (b) develop a practical method for introducing a fatigue crack into DT specimens of hardness greater than HR_c of 36.

E.8   GLOSSARY OF TERMS

B   - specimen thickness

C_V - Charpy V-notch test

DT   - dynamic tear

DWT   - drop-weight test

DWTT   - drop-weight tear test

FAD   - fracture analysis diagram

HR_c - Rockwell hardness number, scale c

K_{Ic} - slow load (static) plane strain fracture toughness

NB   - notch-bend specimen

NDT   - nil-ductility transition obtained by drop-weight test

P_{max} - maximum load specimen sustains

P_Q - load determined by 5 percent secant offset method on load-deflection trace for K_{Ic} test

RAD   - ratio analysis diagram

SEN   - single-edge-notch tension specimen

S_1 - loading point span for notch edge of four-point single-edge notch specimen

S_2 - loading point span for edge opposite notch for four-point single-edge notch specimen

(W-a)   - net cross section (fracture length)

2T   - through crack of length twice plate thickness

σ_{ys} - yield strength

APPENDIX F

DROP-WEIGHT (NIL-DUCTILITY TRANSITION TEMPERATURE) TEST

The drop-weight test (DWT)* was developed at the Naval Research
Laboratory in 1952 to investigate the conditions required to initiate brittle
fractures in structural steels. Specifically, the test is designed to determine
the nil-ductility transition temperature, above which transition from brittle-to-
ductile fracture occurs, and permits the ability of the steel to withstand yield-
point loading in the presence of a small flaw to be evaluated. The nil-ductility
transition temperature (NDT) is related to specific flaw size/stress level condi-
tions for initiation of brittle fracture by a generalized fracture analysis diagram
(FAD) relating to flaw size, nominal stress, and temperature.

The DWT was adopted by the Navy as a standard test method (NAVSHIPS
250-634.3) in 1962 (U.S. Navy, 1962) and by ASTM as a tentative test method in
1963. It became a full ASTM standard test method (ASTM E208-69) in 1969
(ASTM, 1974). It is the most widely used modern fracture toughness test (sharp
crack test) for failure analysis research, alloy development, specification, and
quality control for structural steels.

F.1 PHYSICAL DESCRIPTION OF THE DROP-WEIGHT TEST

The DWT employs simple beam specimens prepared to create a sharp,
thumbnail-size crack in test material at an early stage in the loading process.
The specimen is impact loaded in three-point bending to a fixed deflection
provided by stops. The stops prevent the specimen from deflecting more than a
few tenths of an inch. The deflection corresponds to yield-point loading in the
presence of a small crack that is initiated in a 2.5 by 0.5-in. notched, brittle
weld centrally located on the as-fabricated tension surface of the specimen and
propagated into the test material at elastic stress levels. Details of the specimen
size, support span and deflection stop dimensions, and drop-weight energy
requirements relative to specimen material yield strength, are given in Table F-1.

---

* Terms are defined at the end of the appendix.

TABLE F-1 Standard Drop-Weight Test Conditions

Type of Specimen	Specimen Size (in.)	Span (in.)	Deflection Stop (in.)	Yield Strength Level (ksi)	Drop-Weight Energy for Given Yield Strength Level	
					(ft-lb)	J
P-1	1 by 3-1/2 by 14	12.0	0.3	30 to 50	600	800
				50 to 70	800	1,100
				70 to 90	1,000	1,350
				90 to 110	1,200	1,650
P-2	3/4 by 2 by 5	4.0	0.06	30 to 60	250	350
				60 to 90	300	400
				90 to 120	350	450
				120 to 150	400	550
P-3	5/8 by 2 by 5	4.0	0.075	30 to 60	250	350
				60 to 90	300	400
				90 to 120	350	450
				120 to 150	400	550

NOTE: Data from American Society for Testing and Materials, 1974 (E208-69).

A drop-weight test machine is used to impact load the DWT specimen. The impact loading is provided by a guided, freely-falling weight of sufficient mass to attain 250 to 1,200 ft-lb of potential energy. The level of potential energy is controlled by the height above the specimen from which the weight falls.

In conducting the DWT, the selection of the test temperature range is determined with as few specimens as possible by finding the highest temperature where the specimen breaks and the lowest where it does not break. Within this temperature range, a series of specimens are tested at temperature intervals sufficient to establish the temperature limits for break and no-break performance to within 10° F. The nil-ductility transition temperature within this range is the highest temperature required for breaking the DWT specimen. A specimen is considered broken if fractured to one or both edges of the tension surface (i.e., complete separation of the specimen is not required).

Figure F-1a illustrates the general features of the DWT specimen and the effect of temperature on its fracture characteristics for a typical test series which defines the nil-ductility transition temperature as the highest temperature of nil-ductility break. The flat break signifies that fracture initiation due to the small flaw occurred prior to the development of significant plastic deformation. Figure F-1b
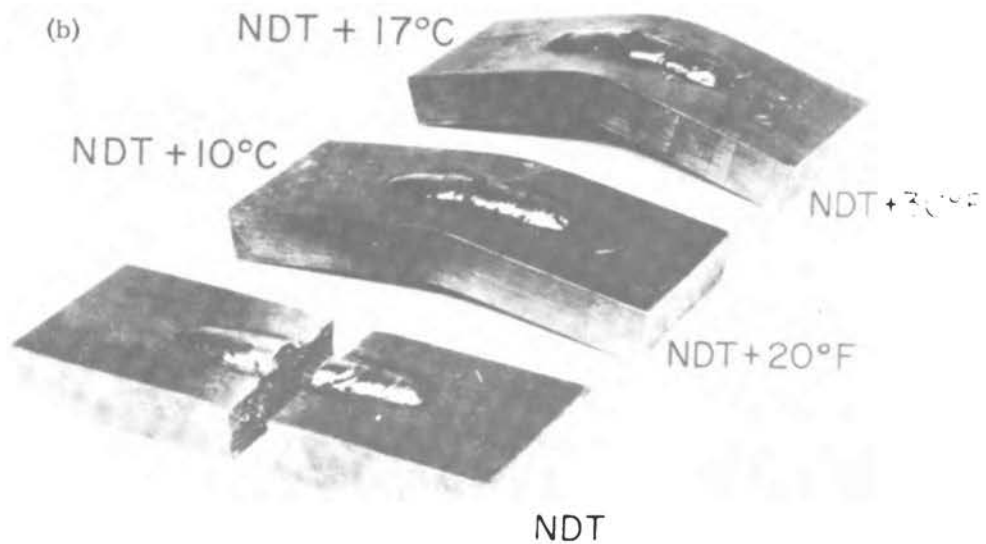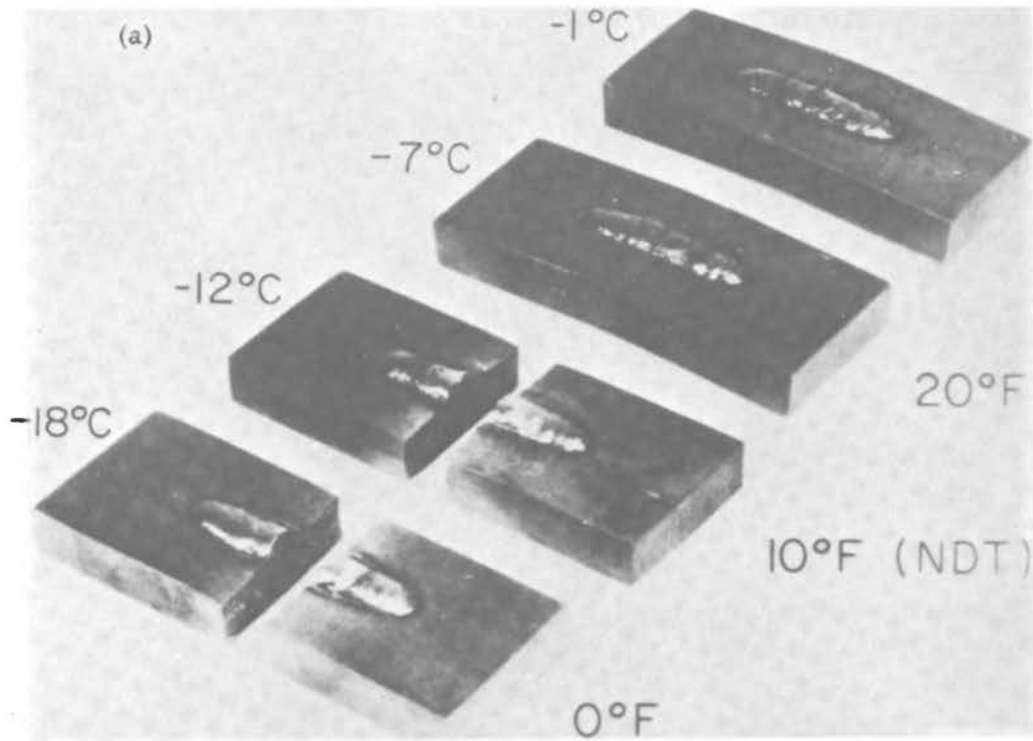
NOTE: The sharp increase in dynamic fracture toughness of the metal above the NDT temperature is illustrated (bottom) by the tolerance for plastic deformation for tests conducted in the absence of a deformation stop.

FIGURE F-1 DWT Test Series: (a) Typical Series Defining an NDT Temperature of 10° F (-12° C) and (b) Series Illustrating Tests Conducted without a Deflection Stop (Pellini, 1969).

illustrates tests conducted without a deflection stop. At NDT + 20° F and NDT + 30° F, the specimen is deformed plastically without causing fracture. This performance indicates clearly the sharp increase in dynamic fracture toughness developed above the NDT temperature.

The NDT temperature is not affected by orientation of the test specimen with respect to the rolling direction because brittle fractures are not influenced by the alignment of nonmetallic phases in structural steels.

F.2   PARAMETERS DERIVED FROM THE DROP-WEIGHT TEST

The only parameter derived from the DWT is the NDT temperature, the highest temperature (within the fracture range) at which a standard DWT specimen breaks. The significance of the DWT-NDT temperature is that is represents the highest temperature at which brittle fracture initiation and propagation can occur due to a small flaw (less than 1 in.) and yield-point loading.

The only standard test method for determining NDT temperature is the DWT according to ASTM E208 procedures. Other test methods for NDT temperature determination can be used only by correlation to DWT results.

F.3   DWT-NDT TEMPERATURE FOR SERVICE PERFORMANCE ANALYSIS

Interpretation of DWT-NDT temperature to conditions required for fracture initiation in steels is made by use of the generalized diagram shown in Figure F-2. This diagram, termed the fracture analysis diagram (FAD), was derived from a variety of fracture initiation and fracture arrest tests, as correlated with the NDT temperature established by the DWT test. The FAD has been validated in numerous analyses of service failures of pressure vessels, ships, and machinery components of forged and cast steel (Pellini and Puzak, 1963; 1964). The significance of the DWT-NDT temperature is its correspondence to the temperature at which the "small flaw" initiation curve of Figure F-2 falls to yield strength stress levels with decreasing temperature, noted as NDT in the figure.

The FAD provides a generalized definition of the flaw size, relative stress, and temperature relationships by a "Δt" or "temperature increment" reference to the NDT temperature. From determination of the NDT temperature, the location of the FAD to specific positions in the temperature scale can be made.

F.4   LIMITATIONS OF THE DROP-WEIGHT TEST

The DWT was designed only to determine the NDT temperature of steel featuring a rapid rise in fracture toughness with increasing temperature above the NDT temperature. Such behavior applies to ferritic steels and many quenched-and-tempered steels that exhibit a change in microfracturing mode from cleavage below NDT to mixed mode (cleavage plus microvoid coalescence) in the temperature transition region above NDT.
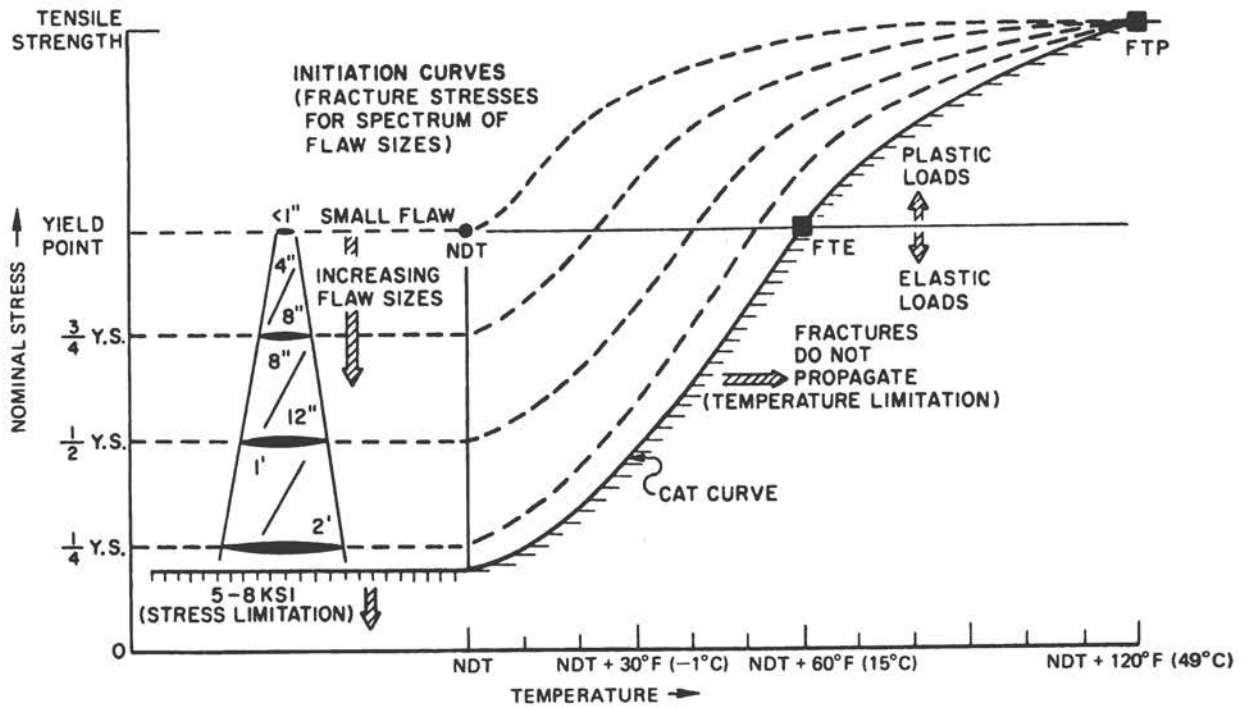
FIGURE F-2 Generalized Fracture Analysis Diagram as Referenced by the
Nil-Ductility Transition Temperature (Pellini and Puzak, 1963).

The DWT cannot be used for the nonferrous metals such as aluminum or titanium alloys since they do not display sharp transitions in fracture toughness with temperature. This lack of a sharp transition in these materials is a result of only a ductile (microvoid coalescence) microfracturing mode operating for fracture generated by impact loading over a wide range of temperature (-320 to +300° F) (Goode and Huber, 1965; Pellini, 1965). Other general limitations of the DWT-NDT procedure are:

    a.   The test is limited to section thicknesses of 0.62 in. and greater.

    b.   The test cannot be used where the heat-affected zone (HAZ) beneath the brittle crack starter weld is more fracture resisting than the unaffected test material. *

---

* This problem often is encountered in quenched-and-tempered steels of high hardness, usually obtained by tempering at low temperature, which often can be avoided by quench and tempering the specimen after the crack starter weld has been deposited.

F.5   COST AND COMPLEXITY

The cost of preparing the DWT specimens is usually less than that required for preparing C_V specimens. The specimen ends can be flame cut and the edges, saw cut. The tension surface is the as-fabricated surface unless otherwise specified. The brittle crack starter weld, specified in ASTM E208, is deposited using normal, manual, stick electrode welding practice.

The equipment and controls for heating and cooling specimens to specified test temperatures are similar to those for C_V specimens with only slightly longer times required for equilibration of specimen temperature due to the large mass of the DWT specimen. The drop-weight machine is of simple design and can be fabricated by the user from readily available structural steel products or purchased commercially at a cost equivalent to that of a C_V machine.

F.6   GLOSSARY OF TERMS

C_V - Charpy V-notch test as defined by ASTM E23-72

DWT   - drop-weight test as defined by ASTM E208-69

FAD   - fracture analysis diagram

NDT   - nil-ductility transition temperature

APPENDIX G

OTHER DUCTILITY TESTS

A number of attempts have been made to calculate K_{Ic} values from more easily measured mechanical properties, principally the elastic modulus, yield stress, strain-hardening index, and some measure of ductility derived from an unnotched test piece (Krafft, 1964; Hahn and Rosenfield, 1968; Barsom, 1971; Thomason, 1971; Weiss, 1971; Sailors, 1973; Hahn and Rosenfield, 1975; Hoagland et al., 1972; Ritchie et al., 1973). The calculations are based on analyses of flow and fracture at the crack tip and involve the following general concepts:

    a.   Crack extension in precracked specimens involves essentially the same plastic flow and fracture mechanisms that operate in unnotched test pieces.

    b.   The crack is basically a stress and strain concentrator. Peak stresses and strains generated in the vicinity of the crack tip and the sizes of the stressed and strained regions are a function of the K-level, elastic properties, and the resistance to plastic flow -- a function that can be derived from first principles (Rice and Rosengren, 1968; Hutchinson, 1968). The flow properties (yield stress and strain-hardening exponent) can be obtained from an ordinary tensile test.

    c.   Criteria exist for the onset of rupture locally and can be expressed in terms of a critical stress and/or strain applied to a microstructural element of finite dimensions. Actual values of the critical stress, strain, or element size depend on the fracture mode and material and can be inferred from tests of unnotched specimens.

The value of K for crack extension (the onset of rupture at the crack tip) is obtained by combining the description of stress and strain in terms of K described in item b with the appropriate critical stress/strain/element size described in item c. (Different formulations of K_{Ic} obtained in this way are listed in Table G-1.) A good example for the cleavage mode of fracture has been

190

TABLE G-1 Relationship between K_{Ic} and Material Flow Properties.

Final Expression	Relationship between K_{Ic} and Crack Tip Quantities	Length Parameter	Crack Tip Stress/Strain	Reference
1. $K_{Ic} = En\sqrt{2\pi d_T}$	$K_{Ic} = E\epsilon\sqrt{2\pi r}$	$r = d_T$	$\bar{\epsilon}_p = n$	(1) Krafft 1963
2. $K_{Ic} = \sqrt{\frac{2}{3} EY \epsilon_{ft} n^2}$	$\delta = \frac{Y}{2E}\left(\frac{K}{Y}\right)^2$	$\ell = n^2$	$\bar{\epsilon}_f = \frac{1}{3}\epsilon_{ft}$	(2) Hahn 1967
3. $K_{Ic} = A\sqrt{Y}\,\bar{\epsilon}_f^2$; $\bar{\epsilon}_f$ corresponding to $\alpha = \frac{1}{2}, \beta = 0$	$\delta = \frac{Y}{E}\left(\frac{K}{Y}\right)^2$	$\ell \propto (\delta)^m$	Measured	(3) Barsom 1971
4. $K_{Ic} C_1 \left\{ r\left[C_2 \frac{e^n - 1}{1-\nu^2} + C_3 \tan\left(\frac{\pi}{2}\left(1 - \frac{V_f}{0.09}\right)\right)\right]\right\}^{\frac{1}{2}}$	$\delta = \frac{(1-\nu^2)Y}{2E}\left(\frac{K}{Y}\right)^2$	$\ell \propto r_p$	$\bar{\epsilon}_f = f(V_f)$	(4) Thomason 1971
5. $K_{Ic} \simeq E\bar{\epsilon}_f \sqrt{\frac{SP^*}{1-\nu^2}}$	$K_{Ic} = \sqrt{\frac{G_{Ic}E}{1-\nu^2}}$	$\bar{\epsilon}_f = (0.279)^{1/n}\,\bar{\epsilon}_{f\alpha=1,\beta=0}$	ρ^*	(5,25) Weiss, et al.
6. $K_{Ic} = \sqrt{EYCH\delta_o \epsilon^{\bar{\epsilon}} P}$ $K_{Ic} \simeq 2CHY\sqrt{n\epsilon_{ftl}}$	$\delta = \frac{Y}{ECH}\left(\frac{K}{Y}\right)^2$ $C \simeq 1.3$ $H = \frac{1}{1+n}\left[\frac{\epsilon_{ft}}{0.002}\right]^n$ $\bar{\epsilon}_P = \ln\frac{\delta}{\delta_o}$	$\bar{\epsilon}_P \simeq 0.2\epsilon_{ftl}$	$\delta_o = 2D^*$ $\delta_o = 50(MFFP)^{**}$	(6) Sailors
7. $K_{Ic} = f_c^{-1/6}\sqrt{2YE\left(\frac{\pi}{6}\right)^{\frac{1}{2}} D}$	$\delta = \frac{0.5Y}{E}\left(\frac{K}{Y}\right)^2$	$\bar{\epsilon}_P \sim 1$	$\delta = \lambda c$	(7) Hahn and Rosenfield
8. $K_{ID} = \frac{w}{s}\sqrt{\frac{8}{\pi} YE\nu_L}$	$\delta = \frac{Y}{E}\left(\frac{K}{Y}\right)^2$	$\delta = \nu_L$	$\frac{w}{s}$	(8) Hoagland, et al.
9. $K_{Ic} = f(\sigma_f, Y, 2D)$	$\sigma_{YY}(r) = f(K,Y,n)$	$\sigma_{YY} = \sigma_F$	$r = 2D$	(9) Ritchie, et al.

NOTE: Terms are defined at the end of the appendix.

*ferritic-pearlitic steel
**martensitic steel

191

derived (Ritchie et al., 1973). The adopted criterion* was that cleavage occurs when: (a) the plastic zone extends over at least 2 grains and (b) the normal stress acting on the two grains exceeds the critical value for carbide-assisted, slip-induced cleavage crack initiation. The value of the critical normal stress was inferred from tests of unnotched bars. This approach permits the influence of temperature on K_{Ic} (Figure G-1) to be calculated and the effects of irradiation on K_{Ic} to be estimated (Rice, 1974).

The number of different expressions for K_{Ic} presented in Table G-1 is symptomatic of the difficulty of actually formulating a meaningful (local) fracture criterion. The problem is that both the cleavage and the fibrous modes of crack extension each involve the several competitive unit processes listed below:
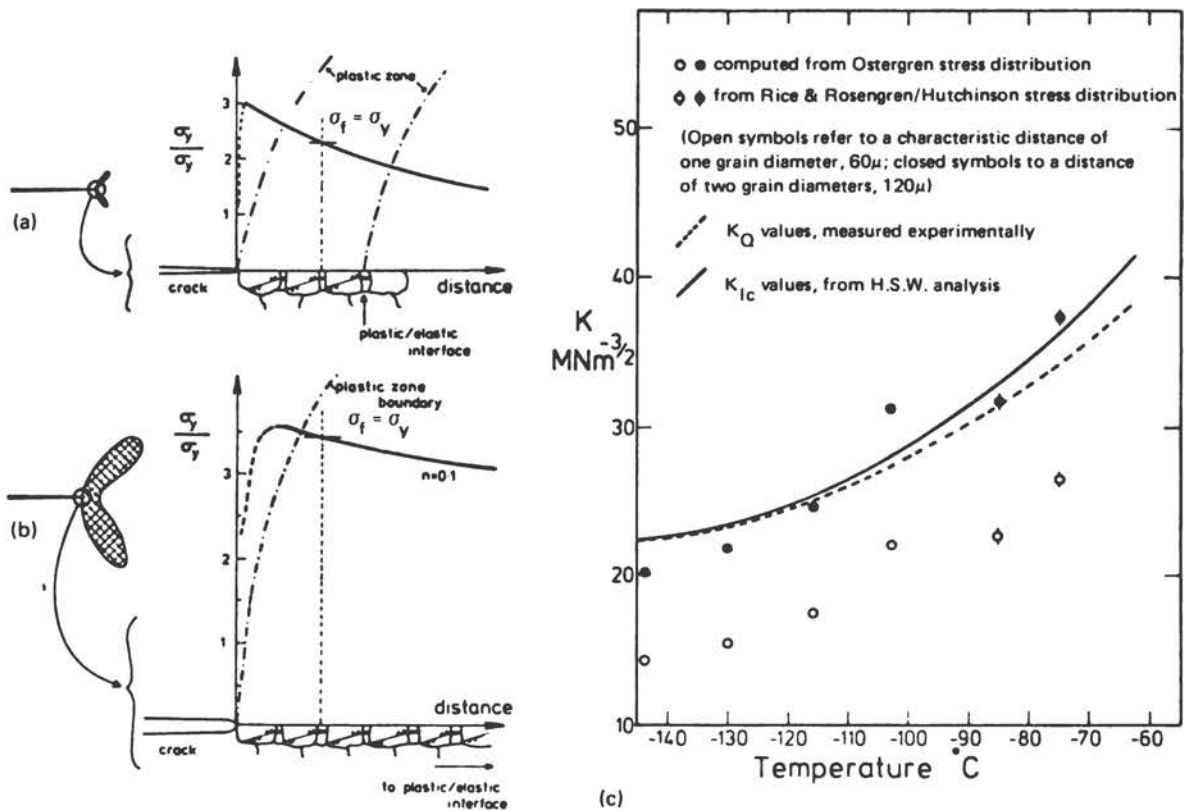
NOTE: (a) and (b) Crack tip stress and plastic zone conditions at onset of cracking at low and high temperature, respectively ($\sigma_y \gtrless \sigma_f$ and $r \geq 2$ grain diameters). (c) Comparison of measured and calculated K_{Ic} values.

FIGURE G-1   Crack Extension in Polycrystalline Steel by Microcrack Nucleation (Ritchie et al., 1973, reprinted with permission from Pergamon Press, Ltd., Journal of the Mechanics and Physics of Solids).

---

* Consistent with metallographic studies of cleavage in mild steels.

Cleavage	Fibrous
Slip-induced, carbide-assisted crack initiation	Particle-assisted void nucleation by particle cleavage
Associated tearing of ductile ligaments	Particle-assisted void nucleation by interface decohesion
	Void growth
	Void linking by coalescing
	Void linking by slip band decohesion

The relative contributions of these unit processes vary from one material (or testing temperature) to another. In principle, separate criteria must be formulated for each process. To make matters more complicated, these unit processes are more or less sensitive to the hydrostatic component of stress (particularly true of void nucleation and growth), and, as a result, the critical strain for fibrous rupture in a smooth bar (low triaxiality) tensile test may be ~ 20 times the value appropriate for the region of high triaxial tension ahead of a crack tip (Weiss, 1974; Sailors and Corten, 1973). Although progress is being made towards analyzing the effects of the hydrostatic tensile stress on void nucleation, growth, and the linking-up processes (McClintock, 1971; Argon et al., 1975; Cox and Low, 1973; Berg, 1970), the descriptions of K_{Ic} in Table G-1 are still limited in this respect. All of these formulations cannot be applicable generally, and not enough work has been done yet to establish even the limited ranges of applicability. This is a potentially fruitful area of research that deserves more attention in the future.

G.1   CORRELATIONS WITH SPECIAL DUCTILITY VALUES

As an alternative to analyzing effects of stress state on the criterion for fibrous fracture, a number of workers have attempted to measure the ductility (critical strain) using test pieces that more nearly reproduce the stress/strain states existing at the crack tip.

G.1.1   "Plane-Strain" Tension and Bend Specimens

A wide tensile specimen with a short gauge section (i.e., $B \geq 16A$ in Figure G-2b) has been employed (Clausing, 1970). The massive ends of this

test piece constrain deformation in the width or z-direction (Figure G-2b), reproducing the "plane-strain" strain state characteristic of the crack tip (Figure G-1a) but not the triaxial tensile stress state.* The "plane-strain" ductility

$$\overline{\epsilon}_{PS} \equiv \ell n\, \frac{A_o}{A_f} = \ell n\, \frac{\ell_f}{\ell_o}\,,$$

where A is the thickness of the gauge section and ℓ is the length of a small gauge mark oriented parallel to the y-direction (Figure G-1b). Since the dimension A

(a)

(c)

(b)

(d)
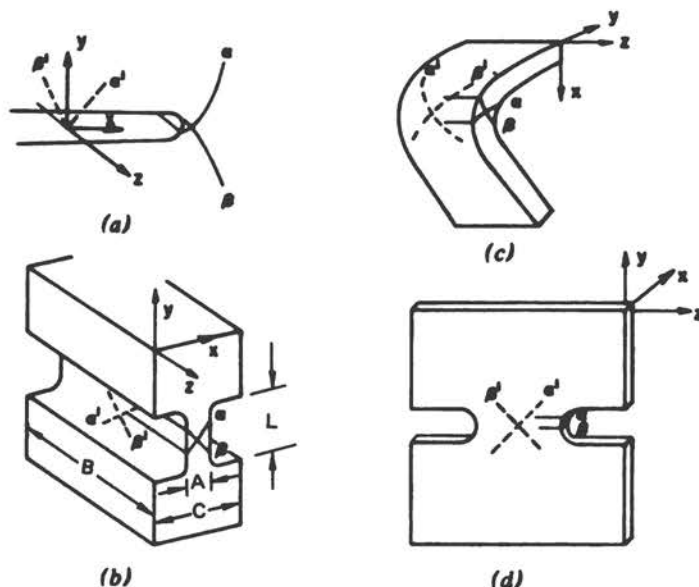
NOTE: "Plane-strain" deformation: (a) at the tip of a crack, (b) in the Clausing "plane-strain" tensile specimen, (c) in a plastically bent strip, and (d) in a "plane-strain" sheet coupon.

FIGURE G-2 Schematic Representation of "Plane-Strain" Deformation (Hahn and Rosenfield, 1975).

---

* "Plane-strain" biaxial loading is produced when plastic deformation in one of the principle directions is constrained as in the "plane-strain" tension, bend, and sheet coupons illustrated in Figures G-1a and -c. These produced a state of unbalanced biaxial tension and "plane strain": $\sigma_1 = 1/2\, \sigma_2$, $\sigma_3 = 0$; $\epsilon_1 = -\epsilon_3$, $\epsilon_2 = 0$ analogous to the state of stress at the root of a notch or crack (see Figure G-1a). They do not reproduce the high triaxial stress state characteristic of the plastic zone of a notch or crack at distance $\gtrsim 2$ root radii from the crack tip. For this reason, "plane strain" is written with quotation marks.

is necessarily small and the deformation is not uniformly distributed, thickness measurements are difficult and inaccurate. More accurate measurements can be made by vapor depositing a fine grid on the surface (Hahn and Rosenfield, 1975). The plane-strain tension specimen is bulky, requires large loads, and cannot be applied to sheet material. Efforts have been made to obtain "plane-strain" deformation with the analogous sheet coupon shown in Figure G-2d (Hahn and Rosenfield, 1975). The difficulty with this configuration is that strain concentrations form at the roots of the slot and tend to cause premature fracture there rather than in the center of the specimen where "plane strain" prevails.

A simpler method of reproducing the stress/strain conditions of the Clausing "plane-strain" tension specimen is by plastically bending a wide strip (Clausing, 1972; Hahn and Rosenfield, 1975; Hahn et al., 1975; Weiss and Sengupta, 1973; Weiss, 1972; Weiss et al., 1972 and 1973) as shown in Figure G-2c. Deformation in the width direction is constrained by the steep strain gradient (from tension to compression) in the thickness direction when the ratio of width to thickness > 8 (Weiss et al., 1972).

$$\bar{\epsilon}_{PS} \cong \ln \frac{\ell_f}{\ell_o} \quad ,$$

where ℓ is the length of a small gauge mark oriented parallel to the y-direction (Figure G-2c). Strain can be measured by depositing a fine grid on the tension surface. One difficulty is that cracks are relatively stable during plastic bending (i.e., they grow to the neutral axis and stop). An unstable arrangement can be produced by bending two ordinary bend coupons attached at their ends. In this case, the coupon on the tension side of the neutral axis remains under a net tension in excess of the yield stress and this favors unstable propagation of any crack nucleated on the tension surface as soon as it reaches critical size.

"Plane-strain" ductility values of a number of steels reflecting a wide range of strength levels with ordinary (axisymmetric) tensile values have been compared (Clausing, 1970; 1972). The ordinary ductility (true strain at fracture) of these steels was relatively high and independent of strength level, but the "plane-strain" ductility (and the ratio $\bar{\epsilon}_{PS}/\bar{\epsilon}_{AS}$) decreased systematically with strength level (Figure G-3a). A titanium and aluminum alloy behaved in the same way (Clausing, 1972). Since both the toughness and the "plane-strain" ductility decrease with strength level, it was reasoned that a connection existed between these two properties. To support this idea, the critical notch root strain at the onset of cracking of slow-bend, V-notch Charpy specimens from measurements of load-displacement curves and flow stress values was calculated (Clausing, 1970). As shown in Figure G-3b, the calculated critical notch root strain values nearly coincide with measured $\bar{\epsilon}_{PS}$ values.
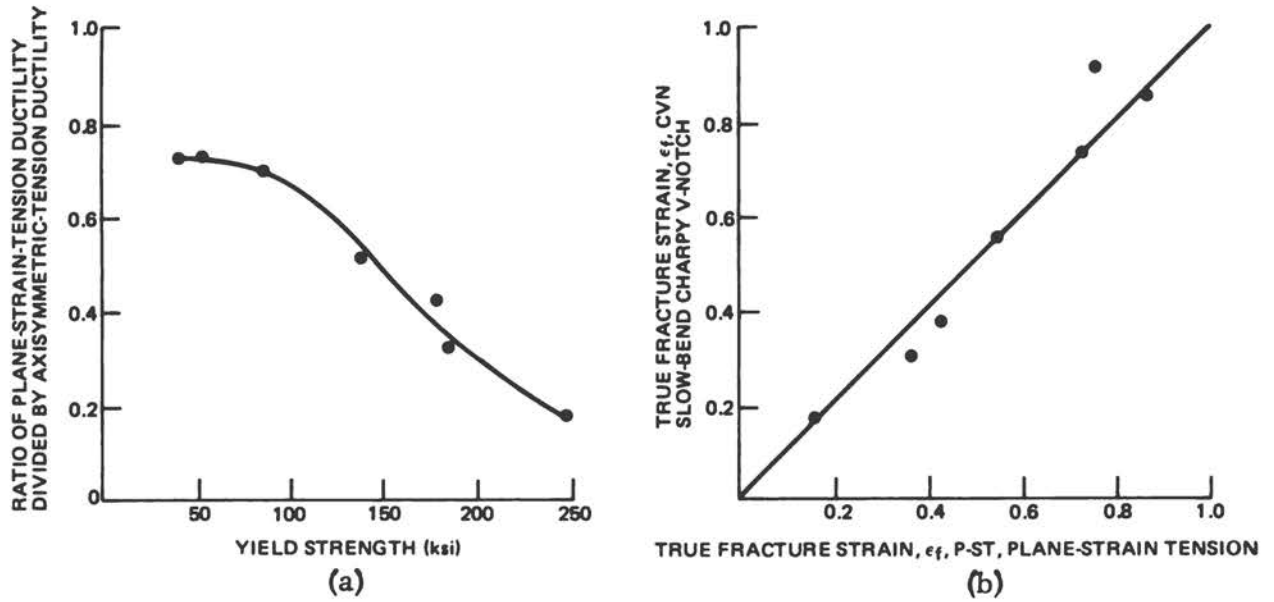
NOTE: (a) Effect of "plane strain" on ductility. (b) Charpy V-notch ductility versus "plane-strain" tension ductility.

FIGURE G-3   "Plane-Strain" Ductility Measurements of Steels (Clausing, 1970).

$\overline{\epsilon}_{PS}$ values have been measured using both simple "plane-strain" bend and $\overline{\epsilon}_{PS}$ values for 4340 steel correlate with K_{Ic} (Figure G-4) but a similar series of experiments with 250-grade maraging steel failed to support a correlation (Figure G-5).

G.1.2 Bulge Test Specimen

Weiss and coworkers have employed a bulge test that produced balanced biaxial tension to measure the ductility

$$\overline{\epsilon}_B \equiv ln\left(\frac{t_o}{t_f}\right)^*$$

(Weiss, 1972 and 1974; Weiss and Sengupta, 1973; Weiss et al., 1972 and 1973).

---

* It should also be noted that measurements of Weiss and coworkers (Figures G-6, G-7, and G-8) are presented in terms of the effective fracture strain,

$$\overline{\epsilon}_F = \left[\frac{2}{3}\left(\overline{\epsilon}_{1f}^2 + \overline{\epsilon}_{2f}^2 + \overline{\epsilon}_{3f}^2\right)\right]^{1/2} , \text{ so that } \overline{\epsilon}_F = \overline{\epsilon}_B, \quad \overline{\epsilon}_F = 1.15\,\overline{\epsilon}_{PS}.$$
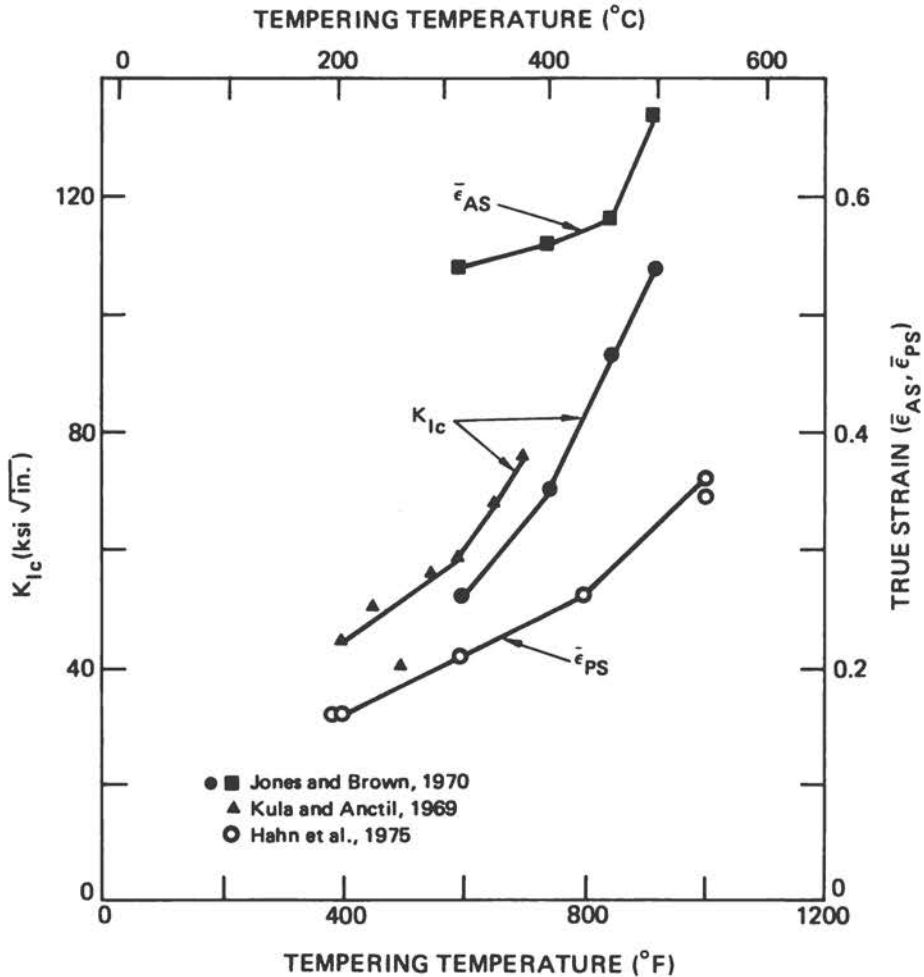
FIGURE G-4   Correlation between "Plane-Strain" Ductility and K_{Ic}.

"Plane-strain" and bulge ductility values also were measured for the same material using "plane-strain" tension, bend, and bulge tests. Some of the results, expressed in terms of $\bar{\epsilon}_F$, the effective fracture strain ($\bar{\epsilon}_B = \bar{\epsilon}_F$, $\bar{\epsilon}_{PS} = 0.86\,\bar{\epsilon}_F$), are reproduced in Figure G-6. In view of the above relations with $\bar{\epsilon}_F$, $\bar{\epsilon}_B$ and $\bar{\epsilon}_{PS}$ values appear to be comparable. The higher ductility values displayed by the hydraulic bulge specimens may be related to surface finish or the heat treatments given these specimens, but the discrepancy is not resolved. Thus, the existing measurements of $\bar{\epsilon}_B$ appear sensitive to the method of testing and cannot be regarded as an absolute measure of ductility. Figure G-7 shows the correlations that have been obtained between K_{Ic} values and $\bar{\epsilon}_B$ values for these materials (Weiss, 1974; Weiss et al., 1973).
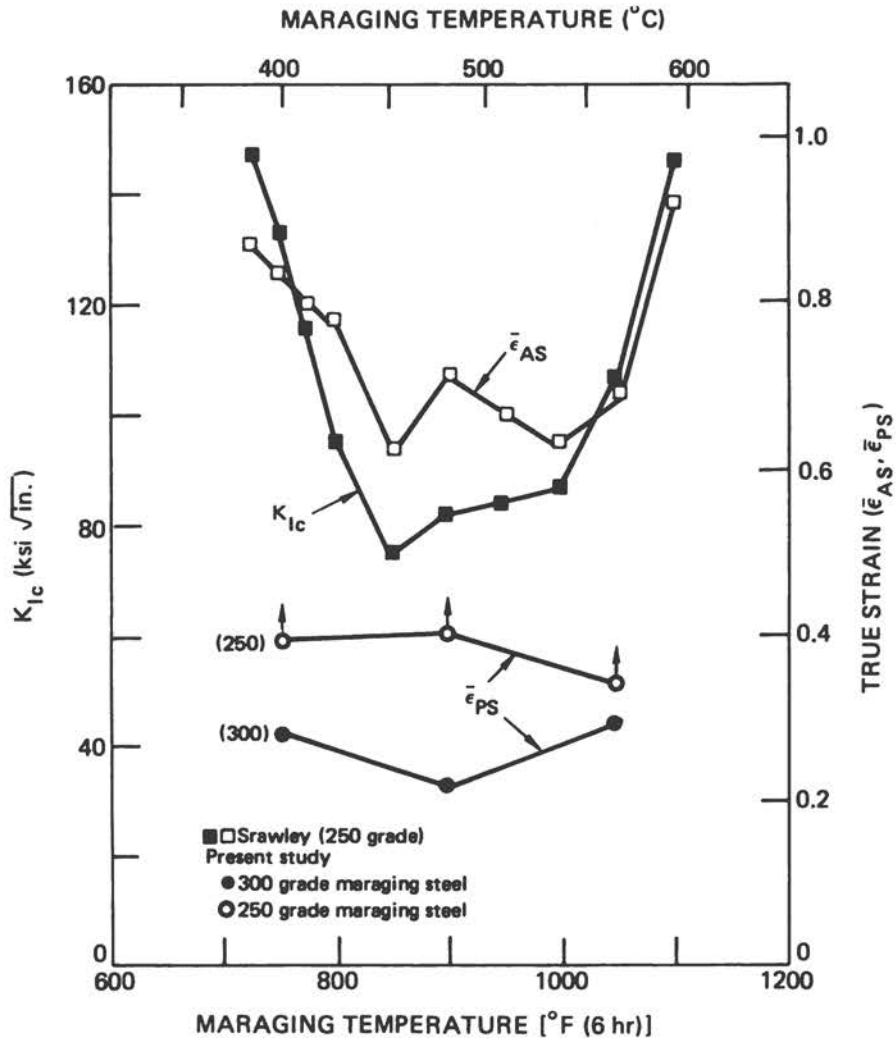
FIGURE G-5   Correlation between "Plane-Strain" Ductility and K_{Ic} (Srawley, 1969; Hahn et al., 1975).

G.1.3   Triaxial-Stress "Plane-Strain" Ductility Specimen

A triaxial-stress "plane-strain" ductility specimen (illustrated in Figure G-8) has been employed (Sailors and Corten, 1973). The fracture strain, $\bar{\epsilon}_f$, was measured by means of a strain gauge affixed to the root of the notch in line with the loading pinholes. In this way, the fracture strain at least could be bracketed between the strain required for a few voids to coalesce and the strain required to break the specimen into two pieces. Measurements on three different steels with yield strengths ranging from 41 ksi to 161 ksi showed that the ratio of triaxial-stress "plane-strain" fracture strain to the ordinary smooth
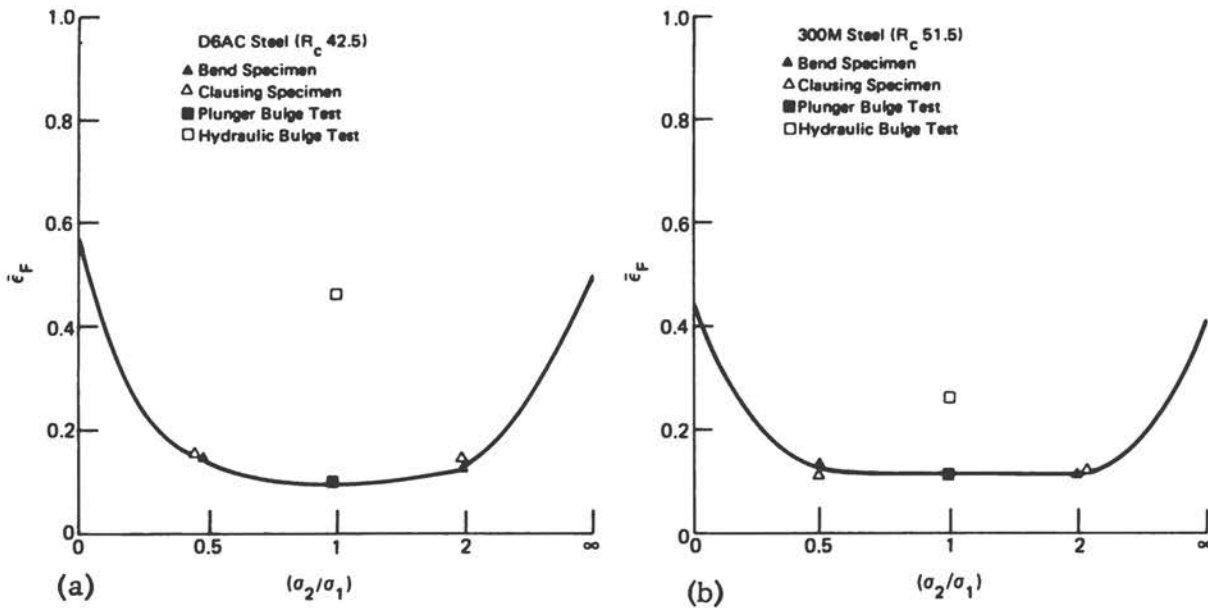
NOTE: (a) 0.145-in.-thick D6AC steel sheet. (b) 0.145-in.-thick 300M steel sheet.

FIGURE G-6   Effect of Stress State on Fracture Ductility for 0.145-in.-thick D6AC and 300M Steel Sheet (Weiss et al., 1972).

bar (axisymmetric) fracture strain $\bar{\epsilon}_f / \epsilon_{ft, I} \sim 0.04\text{-}0.05.$ * On the basis of this ratio, as well as the ratio $\bar{\epsilon}_f / \epsilon_{ft} = 0.25$ for the biaxial stress state at the crack root and some approximate (and questionable) descriptions of the strain distribution close to the crack tip, the expressions for K_{Ic} listed in Table G-1 were derived. As shown in Figure G-9, the calculated K_{Ic} values are in good agreement with measurements.

The correlations between K_{Ic} values and the "plane-strain" (or bulge) biaxial ductility values are surprising at first glance. These specimens do produce states of strain similar to those existing at the root of a notch or crack -- but they do not produce either the kind of strain gradients or the hydrostatic stress field generated in the plastic zone ~ 2 or more root radii ahead of the crack tip. Theory (McClintock, 1971; Argon et al., 1975) and experiment (Cox and Low, 1973) support the view that the triaxial tension greatly facilitates the void growth process by which the crack extends; therefore, it is difficult to understand how these tests can give a meaningful measure of toughness without the triaxial stress, but the two explanations described below have been advanced.

---

* For the onset of void linking up.
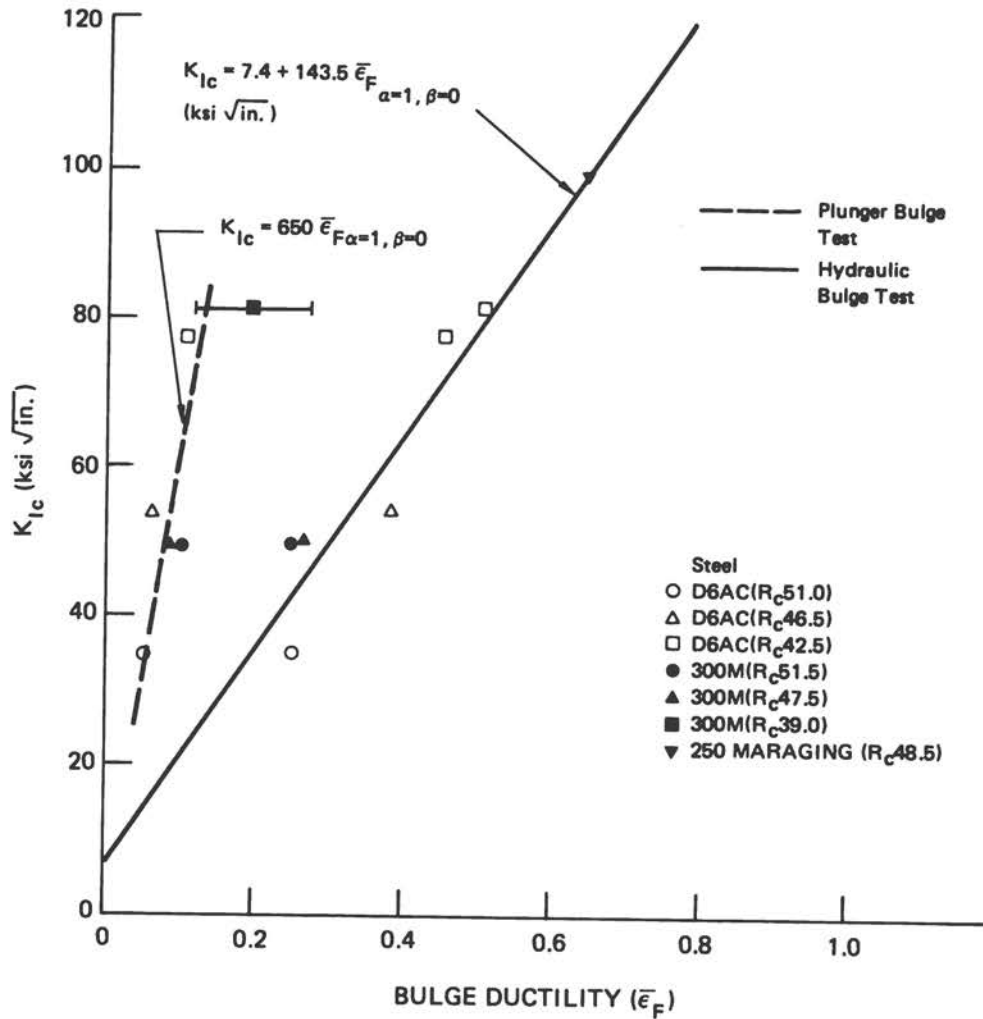
FIGURE G-7   Correlation between "Plane-Strain" Fracture Toughness and
Hydraulic Bulge Ductility for D6AC Steel, 300M Steel, and
250-Grade Maraging Steel (Weiss, 1974; Weiss et al., 1973).

G.1.3.1   Slip Localization.   Experimenters have shown that the
mechanism of failure of "plane-strain" tension and bend specimens of high-
strength alloys differs from that obtained with ordinary axisymmetric specimens
(Clausing, 1970; Hahn and Rosenfield, 1975; Hahn et al., 1975).   Under "plane-
strain" conditions, slip on the α' and β' set of slip systems (Figure G-2) is
precluded by the constraint.   As a result of this, slip probably tends to become
more localized and concentrated in the form of "superbands," which are
aggregations of slip bands of the α, β variety (Figure G-2), and this leads to
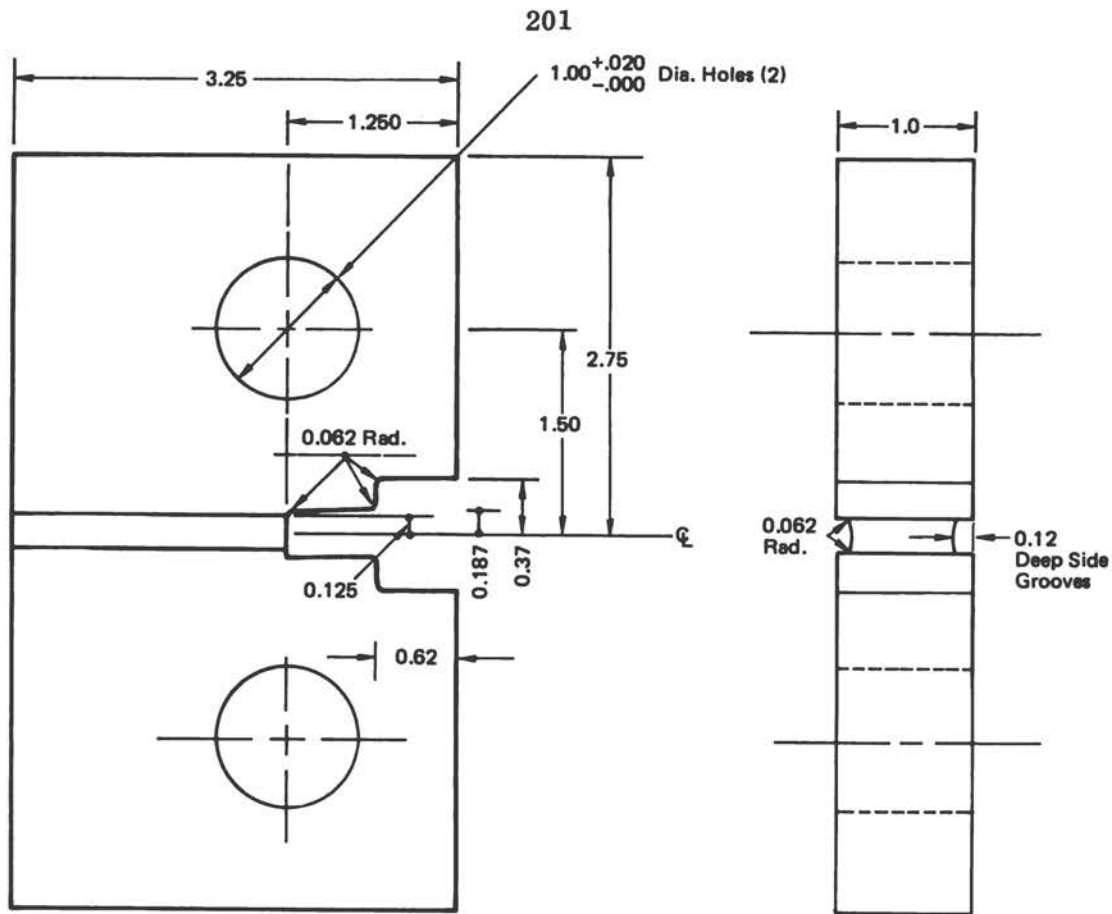
FIGURE G-8   Ductility Specimen -- Triaxial Stress "Plane Strain" (Sailors 1973).

premature cracking within the slip bands (Clausing, 1972; Hahn et al., 1975). It has been shown that the localization of slip contributes to the joining up of voids in 4340 steel, but not in a 200-grade maraging steel (Cox and Low, 1973). Viewed in this light, it is not unreasonable that "plane-strain" biaxial loading can give a measure of the tendency for slip localization that will correlate with toughness in alloys where the void joining-up-process dominates. By the same token, it is possible that "plane-strain" ductility values may not be sensitive to variations in K_{Ic} associated with the inclusion content. In that case, a valid measure of K_{Ic} might be obtained by combining the "plane strain" ductility with a measure of the inclusion content (Table G-1, Thomason, 1971).

G.1.3.2 Effects of the Hydrostatic Component. It has been argued that the effects of biaxial loading on ductility reflect the sensitivity of hole growth to the hydrostatic component and that this process can be represented by a critical volume strain criterion (Weiss, 1972 and 1974; Weiss and Sengupta, 1973; Weiss et al., 1972 and 1973). Such a criterion implies that fixed relations
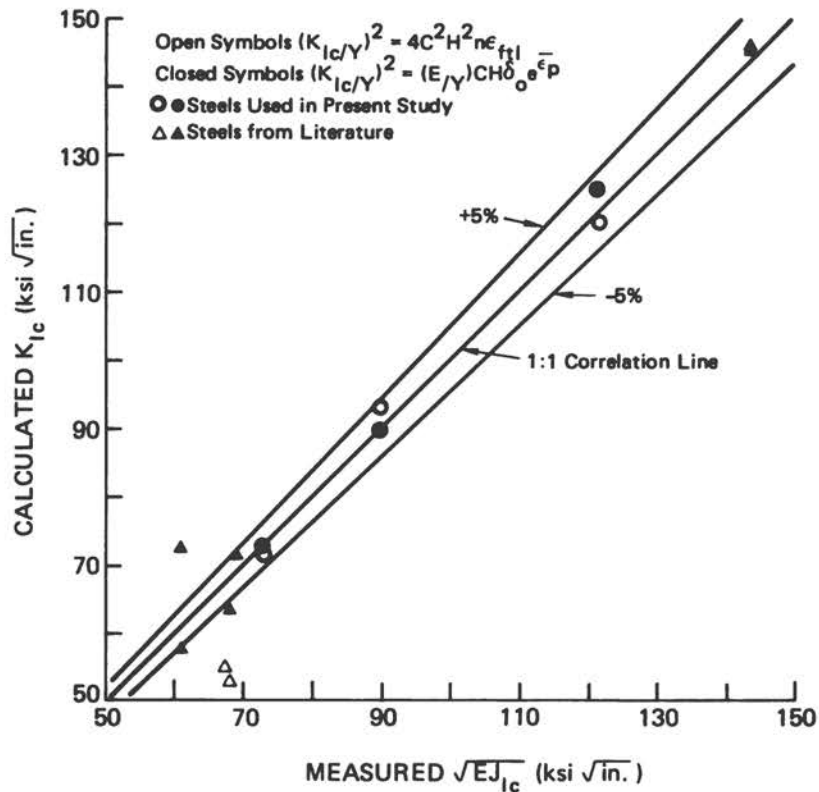
FIGURE G-9   Comparison of Calculated and Measured K_{Ic} Values (Sailors 1973).

exist between the strain-to-fracture at different states of stress -- e.g., $\bar{\epsilon}_f \alpha = 0.81$, $\beta = 0.61$, the critical strain corresponding to the fully constrained region ahead of the crack tip, and $\bar{\epsilon}_f \overbrace{\alpha = 1, \beta = 0,}^{t}$, the critical strain in the bulge:

$$\bar{\epsilon}_f \; \alpha = 0.81, \; \beta = 0.61 \; = (0.279)^{1/n} \; \bar{\epsilon}_f \; \alpha = 1, \; \beta = 0$$

where $\alpha = \dfrac{\sigma_2}{\sigma_1}$, $\beta = \dfrac{\sigma_3}{\sigma_1}$, and n is the strain hardening exponent.

Measurements of the bulge ductility, therefore, can be used to calculate the critical crack tip strain that appears in the Weiss expression, Equation 8, Table G-1. The problem is that two sets of bulge ductility values were reported (Figure G-7); consequently, it is not yet clear whether (a) one of these sets of measurements is incorrect; (b) the concept of well-defined relations between K_{Ic}, crack tip strain, and the bulge ductility is invalid; or (c) there is a

different explanation for the correlation. The bulge ductility values obtained from the plunger test appear more consistent with the plane-strain ductility values, $\overline{\epsilon}_{F, \alpha = 0.5}$, measured for these materials (Figure G-6), but the expected relation,

$$\overline{\epsilon}_F \text{ (plane strain, } \alpha = 0.5) = 1.2 \, \overline{\epsilon}_F \text{ (bulge, } \alpha = 1.0),$$

is not always observed (e.g., see Figure G-5b).

G.2 CONCLUSION AND RECOMMENDATION

<u>Conclusion</u> -- The various K_{Ic}-property relations and correlations mentioned in this appendix contain the germ of a number of possible quality-control procedures. The "plane-strain" tensile specimen and the "triaxial-stress/plane-strain" ductility specimen are impractical since they require nearly as much work as the standard fracture toughness specimen. A bend or bulge coupon, however, would be relatively cheap to produce and test, but it remains to be established whether these tests really reflect the kinds of K_{Ic} variations encountered in practice (particularly those associated with undesirable inclusions). Alternatively, the mechanical test could be combined with micro-structural analysis to give a more complete picture of toughness behavior.

<u>Recommendation</u> -- Further studies should be supported of the relations between K_{Ic} and other mechanical properties, such as yield stress, strain hardening, and ductility under multiaxial loading, that underly a number of potentially useful quality control methods.

G.3 GLOSSARY OF TERMS

A	- Thickness of gauge section of Clausing "plane-strain" tension specimen (see Figure G-2)
$\alpha, \beta, \alpha', \beta'$	- Identify operative slip systems
B	- Width of gauge section of Clausing "plane-strain" tension specimen (see Figure G-2)
C	- Coefficient that accounts for effect of plastic constraint on crack tip opening displacement
C_1, C_2, C_3, C_4	- Numerical coefficients
D	- Grain diameter

d_T	- Distance from crack tip to the point where ligaments begin to neck (process zone size)
δ	- Crack tip opening displacement
δ_o	- Characteristic length parameter
E	- Young's modulus
ϵ	- Strain
$\epsilon_1, \epsilon_2, \epsilon_3$	- Principal strains
$\bar{\epsilon}_{AS}$	- True diametrical strain at point of fracture in a round tensile bar; axisymmetry ductility
$\bar{\epsilon}_B$	- True strain at fracture in a bulge test (bulge ductility)
$\bar{\epsilon}_P$	- True plastic strain in y-direction for multiaxial stress state
$\bar{\epsilon}_{PS}$	- True strain at fracture under "plane-strain" biaxial loading ("plane-strain" ductility)
$\bar{\epsilon}_f$	- True strain at fracture (fracture strain) for multiaxial stress state
$\bar{\epsilon}_{ft}$	- True strain at fracture for uniaxial stress state
$\bar{\epsilon}_{ftI}$	- Uniaxial inhomogeneous true fracture strain
$\bar{\epsilon}_{f, \alpha, \beta}$	- True strain at fracture for the multiaxial stress state $\alpha = \dfrac{\sigma_2}{\sigma_1}$, $\beta = \dfrac{\sigma_3}{\sigma_1}$
F	- Thickness of grips of Clausing "plane-strain" tension specimen (see Figure G-2)
f_c	- Volume fraction of cavities or cracked particles
C	- Critical strain energy release rate (or fracture energy) for onset of crack extension under "plane strain"
H	- Coefficient that accounts for effect of strain hardening on crack tip opening displacement
K or K_I	- Stress intensity parameter (Mode I)
K_{Ic}	- Critical stress intensity parameter

L	- Gauge length of Clausing "plane-strain" tension specimen (see Figure G-2)
ℓ	- Characteristic microstructural length or length parameter
ℓ_o, ℓ_f	- Initial and final gauge length
λ_c	- Spacing of cracked particles
MFFP	- Mean free ferrite path
m	- Empirically derived exponent
n	- Strain hardening exponent
r	- Distance from crack tip
ρ^*	- Neuber micro-support effect constant
S	- Shape factor describing crack-tip strain distribution
s	- Spacing of ligaments
$\sigma_1, \sigma_2, \sigma_3$	- Principal stresses
σ_f	- Critical normal fracture stress for cleavage
σ_Y	- Normal stress perpendicular to crack plane
t_o, t_f	- Initial and final thickness
ν	- Poisson's ratio
v_L	- Maximum ligament stretch
w	- Ligament width
Y	- Yield stress

REFERENCES AND BIBLIOGRAPHY

Adachi, J. "Fracture Design Practices for Ordnance Structures." In Fracture --
An Advanced Treatise, edited by H. Liebowitz, vol. 5, pp. 287-381.
New York: Academic Press, 1969.

Aluminum Association. Adopted Aluminum Association Position on Fracture
Toughness Requirements and Quality Control Testing. New York: Aluminum
Association, 1972.

Army Materials and Mechanics Research Center. Size Requirements for Fatigue
Cracked Fracture Toughness Screening Specimens. AMMRC CTR-74-72.
Watertown, Mass.: AMMRC, 1974.

American Society for Testing and Materials. "Fracture Testing of High-Strength
Sheet Materials." ASTM Bulletin (January/February 1960).

_____. "Fracture Testing of High-Strength Sheet Materials." Third Report of
ASTM Special Committee on Fracture Testing of High-Strength Materials,
Materials Research and Standards. Philadelphia, Pa.: ASTM, 1961.

_____. 1973 Annual ASTM Standards. Philadelphia, Pa.: ASTM, 1973.
The following standard methods of test: E399-72, "Plane-Strain Fracture
Toughness of Metallic Materials;" E338-68, "Sharp-Notch Tension Testing of
High-Strength Sheet Materials;" E8-69, "Tension Testing of Metallic Materials."

_____. 1974 Annual ASTM Standards, Part 10. Philadelphia, Pa.: ASTM, 1974.
The following standard methods of test: E208-69, "Standard Method for Conducting
Drop-Weight Test to Determine Nil-Ductility Transition Temperature of Ferritic
Steels;" "Proposed Tentative Method for Sharp-Notch Testing of Thick High-
Strength Aluminum and Magnesium Alloy Products with Cylindrical Specimens."

Argon, A.S.; Im, J.; and Safoglu, R. "Cavity Formation from Inclusions in Ductile Fracture." Metallurgical Transactions A. 6A(April 1975): 825-37.

Ault, R.T. HP9-4-20 Steel Data. Massillon, Ohio: Republic Steel Research Center, 1968.

Ault, R.T.; Wald, G.M.; and Bertolo, R.B. Development of an Improved Ultra-High Strength Steel for Forged Aircraft Components. AFML-TR-71-27. Wright-Patterson Air Force Base, Ohio: Air Force Materials Laboratory, 1971.

Barsom, J.M. "Development of the AASHTO Fracture Toughness Requirements for Bridge Steels." Engineering Fracture Mechanics 7(1975): 605.

_____. "Relationship between Plane Strain Ductility and K_{Ic} for Various Steels." Paper No. 71-PVP-13, presented at the First National Congress on Pressure Vessels and Piping, San Francisco, May 1971.

Barsom, J.M. and Rolfe, S.T. Correlations between K_{Ic} and Charpy V-Notch Test Results in the Transition Temperature Range. ASTM STP-466, pp 281-302. Philadelphia, Pa.: ASTM, 1970.

_____. "K_{Ic} Transition Temperature Behavior of A517-F Steel." Engineering Fracture Mechanics 2(1971): 341-57.

Begley, J.A. and Landes, J.D. "J-Integral as a Fracture Criterion." Proceedings of the 1971 National Symposium on Fracture Mechanics, Part II, pp. 1-23. ASTM STP-514. Philadelphia, Pa.: ASTM, 1972.

_____. A Comparison of the J-Integral Fracture Criterion with the Equivalent Energy Concept, pp 246-63. ASTM STP-536. Philadelphia, Pa.: ASTM, 1973.

Begley, J.A. and Logsdon, W.A. Correlation of Fracture Toughness and Charpy Properties for Rotor Steels. WRL Scientific Paper 71-1E7-MSLRF-P1, presented at the Fifth National Symposium on Fracture Mechanics, Pittsburgh, 1971. Pittsburgh, Pa.: Westinghouse Research Laboratories, 1971.

Begley, J.A. and Toolin, P.R. "Fracture Toughness and Fatigue Crack Growth Rate Properties of a Ni-Cr-Mo-V Steel Sensitive to Temper Embrittlement." International Journal of Fracture 9(1973): 243-53.

Bentham, J.P. and Koiter, W.J. "Asymptotic Approximations to Crack Problems." In Methods of Analysis of Crack Problems, edited by G. C. Sih, Chpt. 3. Netherlands: Noordhoff International Publishing, 1972.

Berg, C.A. Inelastic Behavior of Solids, edited by M. F. Kanninen et al., p. 171. New York: McGraw-Hill, 1970.

Boyle, R.W., et al. "Determination of Plane Strain Fracture Toughness with Sharply Notched Sheets." Welding Journal, Research Supplement (September 1972).

British Standards Institution. Methods for Crack Opening Displacement (COD) Testing. Report No. DD 19. London, England: British Standards Institution, 1972.

Brothers, A.J.; Newhouse, D.L.; and Wundt, B.M. "Results of Bursting Tests of Alloy Steel Disks and Their Application to Design against Brittle Fracture." Paper presented at ASTM Meeting, June 1965.

Brown, W.F., Jr. The Circumferentially Notched Cylindrical Bar as a Fracture Toughness Test Specimen. NASA Document N74-23412/16A. Cleveland, Ohio: NASA-Lewis Research Center, 1974.

_____. "Interpretation of Notch-Yield and K_{Ic} Data from Kaufman." Private communication to NMAB committee, 1974.

Brown, W.F., Jr.; Lubahn, J.D.; and Ebert, L.J. "Effects of Section Size on the Static Notch Bar Tensile Properties of Mild Steel Plate." Welding Journal 26(1947): 554-9.

Brown, W. F., Jr. and Srawley, J. Plane Strain Crack Toughness Testing of High Strength Metallic Materials. ASTM STP-410. Philadelphia, Pa.: ASTM, 1966.

Brothers, A.J.; Newhouse, D.L.; and Wundt, B.M. "Results of Bursting Tests of Alloy Steel Disks and their Application to Design against Brittle Fracture." Paper presented at ASTM Meeting, June 1965.

Bucci, R.J.; Paris, P.C.; Landes, J.D.; and Rice, J.R. J-Integral Estimation Procedures. ASTM STP-514, pp 40-69. Philadelphia, Pa.: ASTM, 1972.

Budiansky, B. and Rice, J.R. "Conservation Laws and Energy Release Rates." Journal of Applied Mechanics 40(March 1973): 201-3.

Bueckner, H.F. Discussion on "Stress Analysis of Cracks," by P.C. Paris and G.C. Sih. ASTM STP-381, p. 82. Philadelphia, Pa.: ASTM, 1965.

_____. "Field Singularities and Related Integral Representations." In Methods of Analysis of Crack Problems, edited by G.C. Sih, Chpt 3. Netherlands: Noordhoff International Publishing, 1972.

Clark, W.G., Jr. and Pryle, W.H. Fracture Toughness and Fatigue Crack Growth Rate Properties of ASTM A356 Gr. 7 Cast Steel. WRL Report 69-1D9-NDTCU-R2. Pittsburgh, Pa.: Westinghouse Research Laboratories, 1969.

Clarke, G.A.; Andrews, W.R.; Paris, P.C.; and Schmidt, D. Proceedings of the 1974 National Symposium on Fracture Mechanics. Providence, R.I.: Brown University, 1974.

Clausing, D.P. "Effect of Plastic Strain State on Ductility and Toughness." International Journal of Fracture Mechanics 6(March 1970): 71-84.

_____. Comparison of Plane Strain and Axisymmetric Plastic Flow and Fracture. Technical Report on Project No. 35.066-001 (2). Monroeville, Pa.: U.S. Steel Research Laboratory, 1972.

Cooley, L.A. and Lange, E.A. "Fracture Development and Material Properties in PVRC-Penn State Pressure Vessel." Welding Research Council Bulletin. Ser. 126 (November 1967): 1-7.

Cox, T.B. and Low, J.R., Jr. An Investigation of the Plastic Fracture of High Strength Steels. NASA Document NASA CR138 162 TR-5. Cleveland, Ohio: NASA-Lewis Research Center, 1973.

Crosley, P.O. and Ripling, E.G. "Crack Arrest Toughness of Pressure Vessel Steels." Nuclear Engineering and Design 17(1971): 32-45.

Department of Defense. "Metallic Materials and Elements for Aerospace Vehicle Structure." Military Handbook MIL-HDBK-5B. Washington, D.C.: Department of Defense, 1966 (as amended).

DeSisto, T.S. Fracture Toughness Measurements of Three Titanium Alloy Extrusions. NTIS No. AD766682.* Watertown, Mass.: Army Materials and Mechanics Research Center, July 1973.

DeSisto, T.S. and Hickey, C.F. "Low-Temperature Mechanical Properties and Fracture Toughness of Ti-6Al-6V-2Sn." Proceedings of the ASTM 65(1965): 641.

Dugdale, D.S. "Yielding of Steel Sheets Containing Slits." Journal of the Mechanics and Physics of Solids 8(1960): 100-4.

---

* Publications with an NTIS number are available through the National Technical Information Service, 5285 Port Royal Road, Springfield, Virginia 22161.

Dull, D.L.; Buch, J.D.; and Raymond, L. "Compliance Calibrations of a Contoured and Face Grooved Double Cantilever Beam Specimen." Engineering Fracture Mechanics 4(1972): 523-31.

Ewing, A. and Raymond, L. Instrumented Impact Testing of Titanium Alloys. Masters Thesis, California State University. Long Beach, Calif.: California State University, 1974.

Fedderson, C.E.; Moon, D.P.; and Hyler, W.S. Crack Behavior in D6AC Steel. NTIS No. AD737779. Columbus, Ohio: Battelle-Columbus Laboratories, 1972.

Freed, C.N. "A Comparison of Fracture Toughness Parameters for Titanium Alloys." Engineering Fracture Mechanics 1(June 1968): 175-89.

Freed, C.N. and Goode, R.J. Correlation of Two Fracture Toughness Tests for Titanium and Ferrous Alloys. NRL Report 6740. Washington, D.C.: Naval Research Laboratory, 1969.

Freed, C.N.; Goode, R.J.; and Judy, R.W., Jr. "Comparison of Fracture Toughness Test Procedures for Aluminum Alloys." Engineering Fracture Mechanics 2(1971): 359-76.

_____. "Comparison of Fracture Toughness Test Procedures for Aluminum Alloys." Engineering Fracture Mechanics 2(1971): 359.

Freed, C.N. and Krafft, J.M. "Effect of Side Grooving on Measurements of Plane-Strain Fracture Toughness." Journal of Materials 1(December 1966): 770-90.

Gallagher, J.P. "Experimentally Determined Stress Intensity Factors for Several Contoured Double Cantilever Beam Specimens." Engineering Fracture Mechanics 3(1971): 27-43.

Gerberich, W.W. and Swedlow, J.L. "Plastic Strains and Energy Density in Cracked Plates, Part I -- Comparison with 'Elastic Theory'." Experimental Mechanics 4(November 1964): 335-44.

_____. "Plastic Strains and Energy Density in Cracked Plates, Part II." Experimental Mechanics 4(December 1964): 345-51.

Goode, R.J. "Identification of Fracture Plane Orientation." ASTM Materials Research and Standards 12(September 1972):31-2.

_____. Naval Research Laboratory, Washington, D.C., unpublished data, 1974.

Goode, R.J. and Huber, R.W. "Fracture Toughness Characteristics of Some Titanium Alloys for Deep-Diving Vehicles." Journal of Metals 17(August 1965): 841-6.

Goode, R.J.; Huber, R.W.; Howe, D.G.; Judy, R.W., Jr.; Crooker, T.W.; Lange, E.A.; Freed, C.N.; and Puzak, P.P. Metallurgical and Mechanical Characteristics of Ultra-High Strength Metals. NRL Report 6607. Washington, D.C.: Naval Research Laboratory, 1967.

Green, A.P. and Hundy, B.B. "Initial Plastic Yielding in Notch Bend Tests." Journal of the Mechanics and Physics of Solids 4(1956): 128-44.

Greenberg, H.D.; Wessel, E.T.; and Pryle, W.H. "Fracture Toughness of Turbine-Generator Rotor Forgings." Engineering Fracture Mechanics 1(1970): 653.

Griffith, A.A. "The Phenomena of Rupture and Flow in Solids." Philosophical Transactions of the Royal Society (London). Series A, 221(1920): 163-98.

Gross, J.H. "The Effect of Strength and Thickness and Notch Ductility." Welding Journal 48(October 1969): 441s-53s.

Hahn, G.T.; Barnes, C.R.; and Rosenfield, A.R. "Influence of Microstructure and Second Phases on Fracture Toughness." NTIS No. ADA017547. Columbus, Ohio: Battelle-Columbus Laboratories, 1975.

Hahn, G.T.; Hoagland, R.G.; Rosenfield, A.R.; and Sejnoha, R. "Rapid Crack Propagation in a High Strength Steel." Metallurgical Transactions 5(February 1974): 475-82.

Hahn, G.T. and Rosenfield, A.R. "Source of Fracture Toughness: The Relation between K_{Ic} and the Ordinary Tensile Properties of Metals." In Applications-Related Phenomena in Titanium Alloys, p. 5. ASTM STP-432. Philadelphia, Pa.: ASTM, 1968.

_____. "Metallurgical Factors Affecting Fracture Toughness of Aluminum Alloys." Metallurgical Transactions A 6A(April 1975): 653-68.

Hall, L.R. Influence of Specimen Design in Plane Strain Fracture Toughness Testing. ASTM STP-496. Philadelphia, Pa.: ASTM, 1971.

Hall, L.R. and Bixler, W.D. Subcritical Crack Growth of Selected Aerospace Pressure Vessel Materials. NASA CR-120834. Cleveland, Ohio: NASA-Lewis Research Center, 1972.

Hall, L.R.; Finger, R.W.; and Spurr, W.F. Corrosion Fatigue Crack Growth in Aircraft Structural Materials. AFML-TR-73-204. Wright-Patterson Air Force Base, Ohio: Air Force Materials Laboratory, 1973.

Hartbower, C.E. Materials Sensitive to Slow Rates of Straining. ASTM STP-466, pp 115-47. Philadelphia, Pa.: ASTM, 1970.

Hartbower, C.E. and Reuter, W.G. Fracture Toughness of High-Strength Steels for Bridge Construction. Report to California Department of Public Works, Division of Highways, January 1973.

Hawthorne, J.R. and Loss, F.J. Fracture Toughness Characterization of Shipbuilding Steels. NRL Report 7701. Washington, D.C.: Naval Research Laboratories, 1974.

Hickey, C.F. Toughness Data for Monolithic High-Hardness Armor Steel. ASTM STP-556, p. 55. Philadelphia, Pa.: ASTM, 1974.

Hoagland, R.G. "Use of the Double Cantilever Beam Specimen for Determining the Plane Strain Fracture Toughness of Metals." Journal of Basic Engineering 89D(Summer 1967): 525-32.

Hoagland, R.G.; Rosenfield, A.R.; and Hahn, G.T. "Mechanisms of Fast Fracture and Arrest in Steels." Metallurgical Transactions 3(January 1972): 123.

Hutchinson, J.W. "Singular Behavior at the End of a Tensile Crack in a Hardening Material." Journal of the Mechanics and Physics of Solids 16(January 1968): 13-31.

Hutchinson, J.W. "Plastic Stress and Strain Fields at a Crack Tip." Journal of the Mechanics and Physics of Solids 16(September 1968): 337-47, plate.

Ireland, D.R. "Procedures and Problems Associated with Reliable Control of the Instrumented Impact Test." Paper presented at the ASTM Symposium on Instrumented Impact Testing, ASTM Annual Meeting, June 1973.

Irwin, G.R. Onset of Fast Crack Propagation in High Strength Steel and Aluminum Alloys. Report No. NRL 4763. Washington, D.C.: Naval Research Laboratory, 1956.

_____. "Fracture." In Encyclopedia of Physics, vol. 6, edited by S. Flügge, pp. 551-90. New York: Springer-Verlag New York, Inc., 1957.

_____. "Plastic Zone Near a Crack and Fracture Toughness." Proceedings of the Seventh Sagamore Materials Research Conference. Syracuse, N.Y.: Syracuse University Research Institute, 1960.

Irwin, G.R. Department of Mechanical Engineering, University of Maryland. Supplement to notes for May 1961 ASTM meeting, unpublished, 1961.

_____. "The Slow Growth and Rapid Propagation of Cracks." Materials Research and Standards 1(May 1961).

_____. Analytical Aspects of Crack Stress Field Problems. Report No. 213. Urbana, Illinois: University of Illinois, Department of Theoretical and Applied Mechanics, 1962.

_____. "Crack Extension Force for a Part-through Crack in a Plate." Journal of Applied Mechanics 29(January 1970).

Iyer, K.R. and Miclot, R.B. "Instrumented Charpy Testing for the Determination of J-Integral." Paper presented at the ASTM Symposium on Instrumented Impact Testing, June 1973.

Jones, H.H. and Brown, W.F. Review of Developments in Plane Strain Fracture Toughness Testing. ASTM STP-463, p. 63. Philadelphia, Pa.: ASTM 1970.

Judy, R.W., Jr. and Goode, R.J. Ductile Fracture Equation for High-Strength Structural Metals. NRL Report 7557. Washington, D.C.: Naval Research Laboratory, 1973.

_____. "R-Curve Characterization and Analysis of Fractures in High-Strength Structural Metals." Metals Engineering Quarterly 13(November 1973): 27-34.

Judy, R.W., Jr.; Freed, C.N.; and Goode, R.J. "Characterization of the Fracture Resistance of Thick-Section Titanium Alloys." In Proceedings of the Second International Conference on Titanium Science and Technology, vol. 2, pp. 1393-1409, 1973.

Kaufman, J.G. Sharp-Notch Tension Testing of Thick Aluminum Alloy Plate with Cylindrical Specimens. ASTM STP-514, pp 82-97. Philadelphia, Pa.: ASTM, 1972.

_____. Notch-Yield Ratio as a Quality Control Index for Plane-Strain Fracture Toughness. ALCOA Report 9-73-20. New Kensington, Pa.: ALCOA Laboratories, 1973.

_____. "Compilation of Notch-Yield and K_{Ic} Data for Aluminum Alloys." ALCOA Center, Pa.: ALCOA, 1974, unpublished.

Kaufman, J.G. and Holt, M. Fracture Characteristics of Aluminum Alloys. ALCOA Report TR 18. New Kensington, Pa.: Alcoa Research Laboratories, 1965.

Kaufman, J.G.; Nelson, F.G., Jr.; and Holt, M. "Fracture Toughness of Aluminum Alloy Plate Determined with Center-Notch Tension, Single-Edge-Notch Tension and Notch-Bend Tests." Engineering Fracture Mechanics 1(August 1968): 259-74.

Kaufman, J.G.; Sha, G.T.; Kohm, R.F.; and Bucci, R.J. Notch-Yield Ratio as a Quality Control Index for Plane Strain Fracture Toughness. ALCOA Center, Pa.: ALCOA, 1975.

Kendall, D.P.; Underwood, J.H.; and Winters, D.C. Fracture Toughness and Crack Growth Measurements with "C" Shaped Specimens. NTIS No. AD769605. Watervliet, N.Y.: Watervliet Arsenal, Benet Weapons Laboratory, 1973.

Klier, E.P. and Weiss, V. "The Effect of Section Size on the Notch Strength and Fracture Development in Selected Structural Metals." In Proceedings of the ASTM 61(1961): 1307.

Koppenal, T.J. "Dynamic Fracture Toughness Measurements of High-Strength Steels Using Precracked Charpy Samples." Paper presented at the ASTM Symposium on Instrumented Impact Testing, June 1973.

Krafft, J.M. "Correlation of Plane Strain Crack Toughness with Strain Hardening Characteristics of Low, Medium, and High Strength Steel." Applied Materials Research 3(April 1964): 88-101.

Krafft, J.M. and Gray, R.A. "Effects of Neutron Irradiation on Bulk and Micro Flow-Fracture Behaviors of Pressure Vessel Steels." In Proceedings of the Institution of Mechanical Engineers -- Practical Application of Fracture Mechanics to Pressure Vessel Technology. London, England: Institution of Mechanical Engineers, 1971.

Kula, E.B. and Anctil, A.A. "Tempered Martensite Embrittlement and Fracture Toughness in SAE." Journal of Materials 4(December 1969): 817-41.

Landes, J.D. and Begley, J.A. "Effect of Specimen Geometry on J_{Ic}." In Proceedings of the 1971 National Symposium on Fracture Mechanics. ASTM STP-514, Part I, pp 24-39. Philadelphia, Pa.: ASTM, 1972.

_____. "Fracture Analysis, 11." In Proceedings of the 1973 National Symposium on Fracture Mechanics. ASTM STP-560, Part II, pp 170-85. Philadelphia, Pa.: ASTM, 1974.

Lange, E.A. Naval Research Laboratory, Washington, D.C. Private communication to the Committee, 1974.

Lange, E.A. and Loss, F.J. Dynamic Tear Energy -- A Practical Performance Criteria for Fracture Resistance. ASTM STP-466, pp 241-58. Philadelphia, Pa.: ASTM, 1970.

Logsdon, W.A. Proceedings of the 1974 National Symposium on Fracture Mechanics. Providence, R.I.: Brown University, 1974.

Lubahn, J.D. "Experimental Determination of Energy Release Rate for Notch Bending and Notch Tension. In Proceedings of the ASTM 59(1959): 885-915.

Malkin, J. and Tetelman, A.S. "Relation between K_{Ic} and Microscopic Strength for Low Alloy Steels." Engineering Fracture Mechanics 3(August 1971): 151-67.

Masters, J.N.; Bixler, W.D.; and Finger, R.W. Fracture Characteristics of Structural Aerospace Alloys Containing Deep Surface Flaws. NASA CR-134587. Cleveland, Ohio: NASA-Lewis Research Center, 1973.

May, M.J. In Review of Developments in Plane Strain Fracture Toughness Testing. ASTM STP 463, pp 42-62. Philadelphia, Pa.: ASTM, 1970.

McClintock, F.A. "Plasticity Aspects of Fracture." In Fracture -- An Advanced Treatise, edited by H. Liebowitz, vol. 3, pp 47-225. New York: Academic Press, 1971.

Mostovoy, S.; Crosley, P.B.; and Ripling, E.J. "Use of Crack-Line-Loaded Specimens for Measuring Plane Strain Fracture Toughness." Journal of Materials 2(September 1967): 661-81.

National Materials Advisory Board. Application of Fracture Prevention Principles to Aircraft. NTIS No. AD764513. Washington, D.C.: National Academy of Sciences, 1973.

Neuber, H. Theory of Notch Stresses. Ann Arbor, Michigan: Edwards Brothers, Inc., 1946.

Orner, G.M. and Hartbower, C.E. "The Low-Blow Transition Temperature." Proceedings of the ASTM 58(1958): 623-39.

_____. "Sheet Fracture Toughness Evaluated by Charpy Impact and Slow Bend." Welding Journal 40(September 1961): 405s-16s.

Orner, G.M. and Hartbower, C.E. "Transition-Temperature Correlations in Constructional Alloy Steels." Welding Journal 40(October 1961): 459s-67s.

Paris, P.C. and Sih, G.C. Stress Analysis of Cracks. ASTM STP-381, pp 30-83. Philadelphia, Pa.: ASTM, 1965.

Pellini, W.S. Advances in Fracture Toughness Characterization Procedures and in Quantitative Interpretations to Fracture-Safe Design for Structural Steels. NRL Report 6713. Washington, D.C.: Naval Research Laboratory, 1967.

_____. Evolution of Engineering Principles for Fracture-Safe Design of Steel Structures. NRL Report 6957. Washington, D.C.: Naval Research Laboratory, 1969.

_____. Criteria for Fracture Control Plans. NRL Report 7406. Washington, D.C.: Naval Research Laboratory, 1972.

_____. "Metal Improvement." In Application of Fracture Prevention Principles to Aircraft, pp 195-257. NTIS No. AD764513. Washington, D.C.: National Academy of Sciences, 1973.

Pellini, W.S.; Goode, R.J.; Puzak, P.P.; Lange, E.A.; and Huber, R.W. Review of Concepts and Status of Procedures for Fracture-Safe Design of Complex Welded Structures Involving Metals of Low to Ultra-High Strength Levels. NRL Report 6300. Washington, D.C.: Naval Research Laboratory, 1965.

Pellini, W.S. and Puzak, P.P. Fracture Analysis Diagram Procedures for the Fracture-Safe Engineering Design of Steel Structures. NRL Report 5920. Washington, D.C.: Naval Research Laboratory, 1963.

_____. "Practical Considerations in Applying Laboratory Fracture Test Criteria to the Fracture-Safe Design of Pressure Vessels." Journal of Engineering for Power, series A 86(October 1964).

Peterson, R.E. Stress Concentration Design Factors. New York: John Wiley and Sons, Inc., 1953.

Raymond, L., Aerospace Corporation, Los Angeles. Private communication to the Committee, 1974.

Raymond, L. and Usell, R.J., Jr. The Effect of N_2O_4 and UDMH on Subcritical Crack Growth of Various High-Toughness, Low-Strength Steels. NTIS No. AD726540. Los Angeles, Calif.: Aerospace Corporation, 1971.

Rice, J.R. Division of Engineering, Brown University. Private communication to the Committee, 1974.

_____ . "Path Independent Integral and the Approximate Analysis of Strain Concentration by Notches and Cracks." Journal of Applied Mechanics 35(June 1968): 379-86.

Rice, J.R.; Paris, P.C.; and Merkle, J.G. "Some Further Results of J-Integral Analysis and Estimates." In Proceedings of the 1972 National Symposium on Fracture Mechanics. ASTM STP-536, pp 231-45. Philadelphia, Pa.: ASTM, 1973.

Rice, J.R. and Rosengren, G.F. "Plane Strain Deformation Near Crack Tip in a Power Law Hardening Material." Journal of the Mechanics and Physics of Solids 16(January 1968): 1-12.

Rich, D.L. Evaluation of Slow Bend Test of Precracked Charpy Specimen for Fracture Toughness Determination. Report MDC A2210. St. Louis, Mo.: McDonnell Aircraft Company, 1973.

Ripling, E.J. and Falkenstein, E. "Measuring K_R-Curves for Thin Sheets. ASTM STP-527, pp 36-47. Philadelphia, Pa.: ASTM, 1973.

Ritchie, R.O.; Knott, J.F.; and Rice, J.R. "On the Relationship between Critical Tensile Stress and Fracture Toughness in Mild Steel." Pergamon Press, Ltd., Journal of the Mechanics and Physics of Solids 21(November 1973): 395-410. Reprinted with permission.

Robinson, J.N. and Tetelman, A.S. The Measurement of K_{Ic} on Small Specimens Using Critical Crack Tip Opening Displacement. ASTM STP-559, pp 139-58. Philadelphia, Pa.: ASTM, 1974.

Robinson, J.N. and Tetelman, A.S. Comparison of Various Methods of Measuring K_{Ic} on Small Precracked Bend Specimens that Fracture after General Yield. NTIS No. AD777009. Los Angeles, Calif.: University of California, 1974.

Rolfe, S.T. and Novak, S.R. Slow Bend K_{Ic} Testing of Medium Strength, High Toughness Steels. ASTM STP-463, p. 124. Philadelphia, Pa.: ASTM, 1970.

Ronald, T.M.F. Air Force Materials Laboratory, Wright-Patterson Air Force Base, Ohio. Unpublished data, 1974.

Ronald, T.M.F.; Hall, J.A.; and Pierce, C.M. "Usefulness of Precracked Charpy Specimens for Fracture Toughness Screening Tests of Titanium Alloys." Metallurgical Transactions 3(April 1972): 813-8.

Sachs, G.; Lubahn, J.D.; and Ebert, L.J. "Notch Bar Tensile Test Characteristics of Heat Treated Low Alloy Steels." Transactions of the ASTM 33(1944): 340-95.

_____. "The Effects of Notches of Varying Depth on the Strength of Heat Treated Low Alloy Steels." Transactions of the ASTM 34(1945): 505-16.

Sachs, G.; Ebert, L.J.; and Brown, W.F. Transactions of the AIME, p. 424. New York: AIME, 1948.

Sachs, G.; Weiss, V.; and Klier, E.P. "Effects of a Number of Heat Treating and Testing Variables on the Notch Strength of 4340 Steel." Proceedings of the ASTM 56(1956).

Sailors, R.H. Relationship between Tensile Properties and Microscopically Ductile Plane Strain Fracture Toughness. PhD Thesis (T&AM Report No. 367). Urbana, Ill.: University of Illinois, 1973.

Sailors, R.H. and Corten, H.T. Relationship between Material Fracture Toughness Using Fracture Mechanics and Transition Temperature Tests. ASTM STP-514, pp 164-91. Philadelphia, Pa.: ASTM, 1972.

Sanders, J.L. "On the Griffith-Irwin Fracture Theory." Journal of Applied Mechanics 27(1960): 352-3.

Saxton, H.J.; Ireland, D.R.; and Server, W.L. "Analysis and Control of Inertial Effects During Instrumented Impact Testing." Paper presented at the ASTM Symposium on Instrumented Impact Testing, June 1973.

Schaeffer, G.T. and Weiss, V. Effect of Section Size on Notch Tensile Strength. Interim Technical Report SURI MET-1078-664-I2. New York: Syracuse University, 1964.

Server, W.L. Dynamic Fracture Toughness Determination from Instrumented Pre-Crack Charpy Tests. Dyna Tup Report TR-73-28. Santa Barbara, Calif.: Effects Technology, Inc., 1973.

Server, W.L. and Tetelman, A.S. "The Use of Pre-Cracked Charpy Specimen to Determine Dynamic Fracture Toughness." Pergamon Press, Ltd., Engineering Fracture Mechanics 4(June 1972): 367-76. Reprinted by permission.

Shabbits, W.O. Dynamic Fracture Toughness Properties of Heavy Section A533, Grade B, Class 1 Steel Plate. HSST TR-13 (Oak Ridge National Laboratories). Pittsburgh, Pa.: Westinghouse Research Laboratories, 1970.

Shabbits, W.O.; Pryle, W.H.; and Wessel, E.T. Heavy Section Fracture Toughness Properties of A533, Grade B, Class 1 Steel Plate and Submerged Arc Weldment. Westinghouse Report WCAP-7414. Pittsburgh, Pa.: Westinghouse Research Laboratories, 1969.

Shah, R.C. and Kobayashi, A.S. "On the Surface Flaw Problem." In Proceedings of the Symposium on the Surface Crack: Physical Problems and Computational Solutions. New York: ASME, 1972.

Shoemaker, A.K. and Rolfe, S.T. "The Static and Dynamic Low-Temperature, Crack-Toughness Performance of Seven Structural Steels." Engineering Fracture Mechanics 2(June 1971): 319-39.

Srawley, J.E., NASA-Lewis Research Center, Cleveland. Unpublished data, 1975.

_____. "Plane Strain Fracture Toughness Tests on Two-Inch-Thick Maraging Steel Plate at Various Strength Levels." In Fracture 1969: Proceedings of the Second International Conference on Fracture, edited by P. L. Pratt, p. 131. London, England: Chapman and Hall, Ltd., 1969.

Srawley, J.E. and Gross, B. "Stress Intensity Factors for Crackline-Loaded Edge-Crack Specimens." Materials Research and Standards 7(1967).

Srawley, J.E.; Swedlow, J.L.; and Roberts, E., Jr. "Response: Discussion of 'On the Sharpness of Cracks Compared with Wells' COD' by A.A. Wells, F.M. Burdekin, and L.P. Pook." Journal of Fracture Mechanics 7(1971): 242-6.

Steel Foundry Facts, No. 308, March 1973.

Succop, G.; Jones, M.H.; and Brown, W.F., Jr. Effect of Some Testing Variables on the Results from Slow Bend Precrack Charpy Tests. Cleveland, Ohio: NASA-Lewis Research Laboratories, 1975.

Tada, H; Paris, P.; and Irwin, G. The Stress Analysis of Cracks Handbook, pp 2.6-2.7. Hellertown, Pa.: Del Research Corporation, 1973.

Tetelman, A. and McEvily, A.J., Jr. Fracture of Structural Materials. New York: John Wiley and Sons, 1967.

Tetelman, A.S.; Robinson, J.N. and Roman, I. "The Use of Small Precracked Bend Specimens to Measure Fracture Toughness for Quality Control Purposes." In Prospects of Fracture Mechanics, p. 563. Netherlands: Noordhoff International Publishers, 1974.

Tetelman, A.S.; Wullaert, R.A.; and Ireland, D. "Prediction of Variation in Fracture Toughness K_{IC} from Small Specimen Tests." Pergamon Press, Ltd., Engineering Fracture Mechanics 8(1976): 301-13. Reprinted by permission.

Thomason, P.F. "A Theoretical Relation between K_{IC} and Basic Material Properties in Ductile Metals." International Journal of Fracture Mechanics 7(December 1971): 409-20.

Tiffany, C.F. and Masters, J.N. Applied Fracture Mechanics. ASTM STP-381. Philadelphia, Pa.: ASTM, 1965.

Turner, C.E. "Measurement of Fracture Toughness by Instrumented Impact Test." In Impact Testing of Metals, pp 93-114. ASTM STP-466. Philadelphia, Pa.: ASTM, 1970.

U.S. Navy. Method for Conducting Drop-Weight Test to Determine Nil-Ductility Transition Temperature of Ferritic Steels. NAVSHIPS-250-634-3. Washington, D.C.: U.S. Navy, 1962.

_____. Method for 5/8 Inch Dynamic Tear Testing of Metallic Materials. MIL-STD-1601. Washington, D.C.: U.S. Navy, May 1973.

Van der Sluys, W.A. "Mechanisms of Environment Induced Subcritical Flaw Growth in AISI 4340 Steel." Engineering Fracture Mechanics 1(April 1969): 447-62.

Venzi, S.; Priest, A.H.; and May, M.J. "Influence of Inertial Load in Instrumented Impact Tests." In Impact Testing of Metals, pp 165-80. ASTM STP-466. Philadelphia, Pa.: ASTM, 1970.

Weiss, V. "Material Ductility and Fracture Toughness of Metals." In Mechanical Behavior of Materials: Proceedings of the International Conference on Mechanical Behavior of Materials, vol. I, pp 458-74. Kyoto, Japan, 1971.

_____. "Microstructural Aspects of Fracture Toughness-Ductility Relationships." Paper presented at 1974 ASM-AIME Material Science Symposium, Detroit, 1974.

Weiss, V. and Sengupta, M. "Correlation between the Fracture Toughness and Material Ductility." In Proceedings of the Third International Conference on Fracture, vol. 4, pp III-341. Düsseldorf, Germany: Verein Deutscher Eisenhüttenleute, 1973.

Weiss, V.; Sengupta, M.; and Lal, D. The Significance of Material Ductility to the Reliability and Load Carrying Capacity of Peak Performance Structures. NTIS No. AD741712. Syracuse, N.Y.: Syracuse University, 1972.

Weiss, V.; Sengupta, M.; and Sanford, W. The Significance of Material Ductility to the Reliability and Load Carrying Capacity of Peak Performance Structures. NTIS No. AD761217. Syracuse, N.Y.: Syracuse University, 1973.

Weiss, V.; Sessler, J.; Packman, P.; and Sachs, G. The Effect of Several Geometrical Variables on the Notch Tensile Strength of 4340 Steel Heat Treated to Three Strength Levels. Syracuse, N.Y.: Syracuse University, Department of Chemical Engineering and Materials Sciences, 1960.

Welding Research Council. "PVRC Recommendations on Toughness Requirements for Ferritic Materials." Welding Research Council Bulletin No. 175, August 1972.

Wells, A.A. "Unstable Crack Propagation in Metals -- Cleavage and Fast Fracture." In Proceedings of the Cranfield Crack Propagation Symposium, vol. 1, pp 210-30. Cranfield, England, 1961.

_____. "Application of Fracture Mechanics At and Beyond General Yielding." British Welding Journal 10(November 1963): 563-70.

_____. "Crack Opening Displacements from Elastic-Plastic Analyses of Externally Notched Tension Bars." Engineering Fracture Mechanics 1(April 1969): 399-410.

Wells, A.A. and Burdekin, F.M. "Discussion: J.E. Srawley, J.L. Swedlow, and E. Roberts, Jr., 'On the Sharpness of Cracks Compared with Wells' COD'." International Journal of Fracture Mechanics 7(1971): 233-41.

Wessel, E.T. "The influence of Pre-Existing Sharp Cracks on Brittle Fracture of a Ni-Mo-V Forging Steel." Transactions of the ASM 52(1960):277-306.

_____. "State of the Art of the WOL [wedge opening loading] Specimen for K_{Ic} Fracture Toughness Testing." Engineering Fracture Mechanics 1(1968): 77-103.

Wessel, E.T.; Clark, W.G., Jr.; and Wilson, W.K. Engineering Methods for the Design and Selection of Materials against Fracture. NTIS No. AD801005. Pittsburgh, Pa.: Westinghouse Research Laboratories, 1966.

Williams, M.L. "Some Observations Regarding the Stress Field Near the Point of a Crack." In Proceedings of the Cranfield Crack Propagation Symposium. Cranfield, England, 1961.

Wilshaw, T.R.; Rau, C.A.; and Tetelman, A.S. "General Model to Predict Elastic-Plastic Stress Distribution and Fracture Strength of Notched Bars in Plane Strain Bending." Engineering Fracture Mechanics 1(June 1968): 191-211.

Wilson, W.K.; Clark, W.G., Jr.; and Wessel, E.T. Fracture Mechanics Technology for Combined Loading and Low-to-Intermediate Strength Metals. NTIS No. AD682754. Pittsburgh, Pa.: Westinghouse Research Laboratories, 1968.

Wullaert, R.A. Applications of the Instrumented Charpy Impact Test. ASTM STP-466, pp 148-64. Philadelphia, Pa.: ASTM, 1970.

REPORT DOCUMENTATION PAGE		READ INSTRUCTIONS BEFORE COMPLETING FORM
1. REPORT NUMBER NMAB-328	2. GOVT ACCESSION NO.	3. RECIPIENT'S CATALOG NUMBER
4. TITLE (and Subtitle) Rapid Inexpensive Tests for Determining Fracture Toughness		5. TYPE OF REPORT & PERIOD COVERED Final Report
		6. PERFORMING ORG. REPORT NUMBER NMAB-328
7. AUTHOR(s) NMAB Committee on Rapid Inexpensive Tests for Determining Fracture Toughness		8. CONTRACT OR GRANT NUMBER(s) MDA-903-74-C-0167
9. PERFORMING ORGANIZATION NAME AND ADDRESS National Materials Advisory Board National Academy of Sciences 2101 Constitution Ave., N.W., Washington D.C. 20418		10. PROGRAM ELEMENT, PROJECT, TASK AREA & WORK UNIT NUMBERS
11. CONTROLLING OFFICE NAME AND ADDRESS Department of Defense -- ODDR&E Washington, D. C. 20301		12. REPORT DATE 1976
		13. NUMBER OF PAGES 248
14. MONITORING AGENCY NAME & ADDRESS(if different from Controlling Office)		15. SECURITY CLASS. (of this report) UNCLASSIFIED
		15a. DECLASSIFICATION/DOWNGRADING SCHEDULE

16. DISTRIBUTION STATEMENT (of this Report)

This report has been approved for public release and sale; its distribution is unlimited.

17. DISTRIBUTION STATEMENT (of the abstract entered in Block 20, if different from Report)

18. SUPPLEMENTARY NOTES

19. KEY WORDS (Continue on reverse side if necessary and identify by block number)

Bulge Test
Charpy Size Specimen
Ductility Test
Double Cantilever Beam Test
Double-Edge Notch Fatigue Test
Drop-Weight Test
Dynamic Tear Test

Fracture Toughness Testing
Nil-Ductility Transition Temperature
Nondestructive Testing
Notch-Round Test
Plane-Strain Fracture Toughness Test
Surface-Flaw Specimen Test
Tensile Test

20. ABSTRACT (Continue on reverse side if necessary and identify by block number)

　　　　All available, demonstrated correlations between the results of existing fracture test methods and valid plane-strain fracture toughness (K_{Ic}) measurements (made according to ASTM Standard Method of Test E399) have been assessed. The fracture toughness test methods considered include: standard and fatigue-precracked Charpy-size specimen tests; dynamic tear tests; unnotched, notched, and plane-strain tension tests; and bulge tests. The materials for which the correlations have been examined include aluminum and titanium alloys and steels of interest in aerospace, naval construction, army materiel, and nuclear pressure vessel applications.

　　　　In evaluating the various rapid, inexpensive test methods that have been proposed to measure fracture toughness, the Committee considered both the degree of correlation that could be demonstrated for a given test method and the complexity of the measurements to be made and their analysis, the probable capability of quality-control personnel to make and analyze such measurements, and the relative cost of preparing specimens and carrying out the tests.